INFORMATION TO USERS

This manuscript has been reproduced from the microfilm master. UMI films the text directly from the original or copy submitted. Thus, some thesis and dissertation copies are in typewriter face, while others may be from any type of computer printer.

The quality of this reproduction is dependent upon the quality of the copy submitted. Broken or indistinct print, colored or poor quality illustrations and photographs, print bleedthrough, substandard margins, and improper alignment can adversely affect reproduction.

In the unlikely event that the author did not send UMI a complete manuscript and there are missing pages, these will be noted. Also, if unauthorized copyright material had to be removed, a note will indicate the deletion.

Oversize materials (e.g., maps, drawings, charts) are reproduced by sectioning the original, beginning at the upper left-hand corner and continuing from left to right in equal sections with small overlaps.

Photographs included in the original manuscript have been reproduced xerographically in this copy. Higher quality 6" x 9" black and white photographic prints are available for any photographs or illustrations appearing in this copy for an additional charge. Contact UMI directly to order.

Bell & Howell Information and Learning
300 North Zeeb Road, Ann Arbor, MI 48106-1346 USA
800-521-0600

UMI®

DISSERTATION

PULMONARY TUBERCULOSIS: A COMPARATIVE IMMUNOPATHOLOGICAL INVESTIGATION

Submitted by

Oliver Christian Turner

Department of Microbiology

In partial fulfillment of the requirements

for the Degree of Doctor of Philosophy

Colorado State University

Fort Collins, Colorado

Spring 2002

ProQuest Information and Learning Company
300 North Zeeb Road
P.O. Box 1346
Ann Arbor, MI 48106-1346

COLORADO STATE UNIVERSITY

March 19 2002

WE HEREBY RECOMMEND THAT THE DISSERTATION PREPARED UNDER OUR SUPERVISION BY OLIVER CHRISTIAN TURNER ENTITLED PULMONARY TUBERCULOSIS: A COMPARATIVE IMMUNOPATHOLOGICAL INVESTIGATION BE ACCEPTED AS FULFILLING IN PART REQUIREMENTS FOR THE DEGREE OF DOCTOR OF PHILOSOPHY.

Committee on Graduate Work

Adviser

Co-Adviser

Department Head

ABSTRACT OF DISSERTATION

PULMONARY TUBERCULOSIS: A COMPARATIVE IMMUNOPATHOLOGICAL INVESTIGATION

Inhalation of *Mycobacterium tuberculosis* precipitates an elaborate cascade of immunopathological events within the lung. The prototypical lesion is the granuloma, marked by a zonal accumulation of epithelioid macrophages, necrosis, fibrosis and a varied lymphocyte population. The containment or progression of the disease is controlled by a multiplicity of factors, but principally by the macrophages and lymphocytes and the cytokines that they secrete. How these elements are arranged both temporally and spatially in the infected lung however is poorly understood.

In a series of *in vivo* experiments, inbred mice and outbred guinea pigs were experimentally incoulated with a low dose aerosol of *Mycobacterium tuberculosis*. We followed the growth of bacteria in the lungs alongside the development of the granulomas. Using histological, immunohistochemical, morphometric and flow cytometric analyses, special attention was paid to the arrangement of the lymphocyte subsets and the overall morphology of the lesion. This information was then applied to field studies, where pulmonary lesions of *M. bovis* infected European badgers, New Zealand brushtail possums and cattle were compared to each other and to the laboratory animals.

We found that the temporal and spatial arrangement of lymphocytes, in particular the $CD4^+$ and $CD8^+$ T cell subsets differed markedly both within and between species. The morphology of the granuloma was also similarly diverse.

Collectively, these data suggest that the immune response in the lungs to *Mycobacterium tuberculosis* infection depends not only on activation of specific immune cell populations, but also on the number and arrangement of primed T cells that reach the site of infection.

Oliver Christian Turner
Department of Microbiology
Colorado State University
Fort Collins
Colorado 80523
Spring 2002

ACKNOWLEDGEMENTS

I will always be extremely grateful to the myriad of people who have provided guidance, support, friendship and encouragement throughout my graduate education.

Above all, I appreciate the generosity of Dr. Ian Orme for inviting me to join his laboratory and for facilitating my academic growth. He has opened my eyes to some of the many exciting realms within the world of science and given me a wonderful passport to continue my explorations.

Other members of my committee also deserve great thanks. Dr. Tony Frank has consistently offered wise counsel and friendly advice that has helped me to see and focus on the big picture. Drs. Andrea Cooper and Joanne Turner have both been wonderful sources of scientific advice and honest criticism. In particular, Dr. Turner was a key factor in formatting the final draft of this dissertation. Her patience, insight and dedication to the cause were formidable. Dr. Patrick Brennan has served as a source of probing advice through the years and it has been an honor to interact with someone of his caliber. Dr. Greg Ogilvie has been a stalwart of support for my efforts. His kind, considerate and enthusiastic attitude have served as a breath of fresh air at many stages of this endeavor.

I thank friends in the Pathology department: Dr. Kevin Keane, for his assistance with imaging technology, Dr. Randall Basaraba for his help and advice with histopathology, and Dr. Dan Gould for his consistent encouragement and enthusiasm.

To members of the histotechnology department I extend a large thank you. In particular, I thank Frank Aquino, Robert Zinc, Bruce Cummings, Yang Sun Shin and Maryanna Tryjan. Without their expert skills much of my work would not have been possible.

Furthermore, I thank my friends and lab-colleagues in the Microbiology department, including Dr. Bridget Vesosky, Jenny Taylor, Ben Espinosa, Dr. Robert Keefe, Erik Rush, Dr. Mercedes Gonzalez-Juarrero, Dr. Tae Sun Shim, Marcus Lambert and Dr. Sarah Richart. It has been a great privilege to work and grow with them all.

I extend special thanks to Dr. Isamu Sugawara and Hiroyuki Yamada for their friendship, support and expert technical assistance in the field of electron microscopy.

In closing, I thank my family for their unconditional support and love through the years.

DEDICATION

I dedicate this dissertation to my fiancée, Wendy DeWall. Wendy has demonstrated amazing patience and kindness through the final months of my graduate work. Her support, her sacrifices and her love have made it possible to keep on track, to stay motivated and to realize this dream. How I look forward to sharing the rest of my life with this incredible lady.

TABLE OF CONTENTS

LIST OF TABLES

LIST OF FIGURES

Chapter One

'The study of the things caused, must precede the study of the causes of things'

J.Hughling Jackson

General Hypothesis

Based on the current concepts of pulmonary tuberculosis pathogenesis and the questions raised in the following literature review, I propose the following general hypothesis:

The immunopathology of pulmonary Mycobacterium tuberculosis infection varies both within and between different species of mammal. These differences are mediated by granuloma-specific events including the temporal and spatial arrangements of $CD4^+$ and $CD8^+$ T cells, the degree of fibrosis, necrosis and apoptosis, and the morphology of the granulomatous lesion as a whole. Attention to these factors allows for the prediction of variable disease progression in man.

Specific Aims

Aim 1: to perform a comprehensive histological, immunological and morphometric analysis of the events leading from initial aerosol infection through chronic disease, in inbred and gene knock-out strains of mice that differ in their ability to control bacterial load in the lung.

Aim 2: to perform similar studies in the guinea pig that either have or have not been vaccinated with *Mycobacterium bovis* BCG.

Aim 3: to contrast the histopathological disease in these experimental models with lesions found in wild animals and man.

Review of the Literature

Part I

The Bacillus and the Disease

Introduction

Genus Mycobacterium

The family of bacteria Mycobacteriaceae is currently classified within the taxonomic order Actinomycetales and suborder Corynebacterineae, sometimes called the Corynebacterium- Mycobacterium-Nocardia branch (169). The most medically important pathogens in this family are those of the genus *Mycobacterium.*

Characteristically mycobacteria are straight or slightly curved rods measuring in the range of 0.2-0.6μm x 1.0-10μm. They are aerobic, non-motile, and non-sporing, are catalase positive, and many form filaments that are rapidly fragmented (169). Typically, they have a high genome guanine and cytosine content of 62 -70 mol%. *Mycobacterium* is a geographically diverse genus with over 70 species that exhibit a spectrum of lifestyles including saprophytic, facultative intracellular, and obligate intracellular. The vast majority are saprophytic inhabitants of soil and water, degrade recalcitrant organic compounds such as vinyl chloride or phenanthrene, and produce secondary metabolites such as steroids and optically active oxides of lower alkenes. However, a few species have become intracellular pathogens of higher vertebrates, inflicting great suffering and death upon animals and humans.

Mycobacterium tuberculosis (*M. tuberculosis*), along with *M. bovis*, *M. africanum* and *M. microti*, can all cause the disease known as tuberculosis, and together form the 'Tuberculosis complex.' Each member of this complex is zoonotically pathogenic; however, *M. tuberculosis* usually causes disease in humans while *M. bovis* is primarily pathogenic for all other animals (234).

Tuberculosis complex organisms share several clinically important, biologic properties (169). They are obligate aerobes growing most successfully in tissues having the highest partial pressure of oxygen, such as lung apices. They are facultative intracellular pathogens preferentially utilizing mononuclear phagocytes as their habitats and only rarely, if at all, inhabiting nonprofessional phagocytes. They are slow growing with a generation time of 16 to 24 hours, which may account for the typical sub-acute to chronic evolution of tissue lesions. An unusually high lipid content to the cell wall makes the bacteria hydrophobic and creates a tendency for the bacillus to clump together. They stain poorly with Gram's stain but tuberculosis complex organisms are classified as acid-fast bacilli (AFB). This is because they retain carbol-fuchsin red dye after washing with acid, alcohol, or both (19). *M. tuberculosis* conforms to these general properties of the genus. It is a slow growing bacterium with an average generation time of 24 hours and grows optimally in a narrow range of slight acidity between pH6.5 to 7.0 (227). Following 10-20 days incubation at 37°C on 7H11 Middlebrook agar, individual 1-3mm diameter, dry, rough, yellow / tan colonies with irregular edges appear (229).

The shape-forming properties of the cell wall are attributable to peptidoglycan, the chemical structure of which in *M. tuberculosis* closely resembles that found in other bacteria (24). Attached to this by phosophodiester bonds is a branched-chain polysaccharide, the arabinogalactan, the distal ends of which are esterified with high-molecular-weight fatty acids (mycolic acids) of sizes and structures unique to mycobacteria. Mycolic acids are1-alkyl branched 2-hydroxy fatty acids, typically with 70 to 90 carbon atoms. The branch is commonly 24 carbon atoms long and is a simple alkyl chain, but the principal chain contains cyclopropyl, methoxyl or keto, and methyl groups. Peptidoglycan-arabinogalactan mycolate forms the cell wall skeleton, associated with which is a large variety of lipids and glycolipids (and some proteins). One possible mechanism for the particular virulence of *M. tuberculosis* is that the mycolic acids have been modified to provide greater resistance to host defense mechanisms by substitution of *cis*-double bonds found in the saprophytic *M. smegmatis*. These provide similar physiochemical properties to the lipid bi-layer of the cell wall, but afford greater resistance to oxidative stress (75, 137). Many other cell wall compounds have potent biologic activity when tested on eukaryotic cells in *in- vivo* systems, raising the possibility that they may also be important for pathogenesis.

Genetic considerations

In 1998 Cole et al. published the complete genome of *M. tuberculosis* strain H37Rv (37). This landmark event ushered in a new era of mycobacterial research, with new insight into the structure and function of the organism. The genome comprises 4, 411,529 base pairs and contains approximately 4000 genes. Recent progress translating the genome

information into proteins has yielded two-dimensional electrophoresis maps comprising more than 1500 distinct molecules and, to date, the identification of several-hundred proteins (98). Already, many potentially, clinically relevant areas of the genome have been identified. For example, approximately 9% of the *M. tuberculosis* genome consists of two related families of genes that have been named *PE* and *PPE* (37). These names describe the presence of conserved proline-glutamate (*PE*) or proline-proline-glutamate (*PPE*) residues near the N terminus of the predicted proteins of the family. One putative member of the *PPE* family of proteins (a gene that might be involved in the production of phthiocerol and phenolphthiocerol derivatives) has been shown to be essential for *in vivo* growth of *M. tuberculosis* (28).

The Clinical Disease

In order to understand the pathogenesis of *M. tuberculosis* infection on all levels, from the molecular to the holistic, it is essential to first understand the clinical behavior of this pathogen in humans.

Mode of transmission

Tuberculosis is predominantly an airborne disease (178) and the lung is its primary target organ. Bacilli may disseminate, however, to virtually any anatomical site after initial infection. Individuals with pulmonary tuberculosis may generate aerosols of bacilli by coughing, sneezing, speaking and singing, and infectious droplets can remain airborne for long periods of time. The droplet nuclei, which range in size between 1 and 10 μm, transport viable bacilli to the terminal bronchioles and alveolar spaces of the lung following inhalation (39). The infectious capability of droplet nuclei was formally

established by Wells (228) and Riley (173), who showed that the number of inflammatory foci in the lungs was equivalent to the number of live bacilli inhaled on droplet nuclei with a settling velocity of about 9mm/min. Infection can take place by ingestion of tubercle bacilli but is approximately 10,000-fold less effective than transmission via droplet inhalation, likely because tubercle bacilli are very sensitive to gastric acid (73).

Clinical signs

Spread of tuberculosis throughout the body may occur by one or more means, including local migration of infected cells, lymphatic and hematogenous spread, and spread along epithelial surfaces or within serous cavities (234). Either organ-specific or systemic illness may dominate the clinical picture. Tuberculosis may occur in any organ, but the most common form by far is pulmonary; a cough is thus the classic symptom of tuberculosis. Early in the course of illness the cough may be non-productive, but as inflammation and tissue necrosis ensue, sputum is usually produced. Fever, night sweats, malaise and cachexia often accompany pulmonary signs. Hemoptysis may also be a symptom. Inflammation of lung parenchyma adjacent to a pleural surface may cause pleuritic pain. Spontaneous pneumothorax may also occur, often causing chest pain and perhaps dyspnoea with possible respiratory failure (91).

The clinical spectrum of human pulmonary tuberculosis has been broadly categorized into primary and secondary disease (106). In primary disease, the most frequent sites of involvement are the apical and posterior segments of both right and left upper lung lobes.

A focal caseous and granulomatous parenchymal lesion known as a Gohn focus develops; along with lymphadenitis and lymphadenomegaly, it is called the Primary Complex (234). This may heal, leaving a scar in both lung and node with no viable organisms. Alternatively, it may become a latent infection with organisms remaining in a poorly defined 'dormant' state, or there may be fulminant progression of the disease. With progression, infected material may be spread via the airways into the lower portions of the lung, or to the contralateral lung. Erosion of a parenchymal focus of tuberculosis into a blood or lymph vessel may result in dissemination of the organism, resulting in a miliary pattern on chest radiographs, as well as other distant organs such as the spleen and liver (234).

Data from a variety of sources suggest that the lifetime risk of non-immunocompromised individuals developing clinically evident tuberculosis post-infection is approximately 10%, while 90% of infections either remain latent or resolve (39). Of the 10% of infected persons that manifest disease, approximately half will develop signs of progressive tuberculosis within three years. The other half develop recrudescing/reactivating tuberculosis after several decades, possibly as a consequence of an aging in cellular immunity to below an unknown threshold (19). Disease caused by *M. tuberculosis* is most commonly caused not by primary infection, but by reinfection (134) or reactivation of a dormant infection that the patient may have carried for many years (165).

Recrudescence/reactivation of the primary disease, and/or further inhalation of *M. tuberculosis*, results in secondary tuberculosis. In the latter case, a hypersensitivity type reaction to the inhaled second dose is characterized by tissue necrosis and the

formation of distinct, discrete inflammatory foci called tubercles, or granulomas. These may mineralize, liquefy and rupture into adjacent blood vessels and airways, producing a miliary lesion in multiple organs similar to that seen with the progression of primary tuberculosis. Secondary tuberculosis may be contained strictly within the lungs; however, in these cases there is usually severe, extensive, destructive, caseating lesions.

Epidemiological Considerations

The Global Burden

In 1993 the World Health Organization (WHO) declared a "Global Emergency" with regard to the rising mortality attributed to tuberculosis (Press Release: "WHO attacks global neglect of tuberculosis crisis. Millions dying from low priority disease"). In 1997, there was an estimated 7.96 million new cases, including 3.52 million cases of infectious pulmonary disease (smear-positive), and there were 16.2 million existing cases of disease(58, 128). An estimated 1.87 million people died of tuberculosis and the global case fatality rate was 23%, but exceed 50% in some African countries with high rates of Human Immunodeficiency Virus infection (HIV). The global prevalence of *M. tuberculosis* infection was estimated at 32%. Eighty percent of all incident *M. tuberculosis* cases were found in 22 countries, with more than half occurring in 5 Southeast Asian countries. Nine of the 10 countries with highest incidence rate per capita were in Africa. The 2002 WHO global tuberculosis control report indicates that these figures are still fairly indicative of the current problem (156). Tuberculosis thus remains, as it has been for centuries, the leading infectious cause of human death worldwide.

The consistent trend in developed countries over the last few decades has been a precipitous decline in tuberculosis rates (206), in large part due to socioeconomic development (135). Improvements in housing, ventilation and reduction of crowding have all served to dramatically reduce transmission rates. Effective chemotherapy and vaccines, segregation of infected peoples into sanatoria, the introduction of tuberculin testing of dairy herds and the pasteurization of milk are other important factors that have lead to the decline. However, it is now a reemergent problem in many industrialized countries, with rapid transportation, expanding trade and changing social and cultural patterns connecting even the most remote places on Earth. Evolution of *M. tuberculosis* infection is undoubtedly facilitated by the constant global movement of man, with concurrent selections for genetic mutation, adaptations and migrations increasing organism survival. One example of this may be the large, genetically related group of *M. tuberculosis* strains referred to as the W-Beijing family strains (16). Molecular epidemiological studies suggest that these strains are highly prevalent throughout Asia and the countries of the former Soviet Union, and they have also been reported in several other geographical regions including North America. Although the spread of W-Beijing family strains in diverse populations is well documented, the underlying host-pathogen factors accounting for their continued dissemination and burden of disease have yet to be determined (16).

The epidemic spread of tuberculosis in Russia during the 1990s after several decades of decline has also been a source of great concern (193). In this time, the notification rate of all new tuberculosis cases among permanent residents increased by 7.5% per year, and the death rate by 11% per year. Factors that may have helped to define the observed rise

in caseload include enhanced transmission due to the mixing of prison and civilian populations, an increase in susceptibility to disease, and changes in the proportion of cases detected by surveillance.

It is clear that tuberculosis has the most devastating effect in the developing world, where 95% of cases occur. Less than half of tuberculosis patients who start treatment become cured or complete their course of chemotherapy (199); worldwide, death may still be the most common way in which patients cease to be infectious to others. Poor treatment programs may worsen the situation by keeping infectious patients alive longer, thus prolonging the period of transmission (81). Given the on-going socioeconomic crises in many developing countries and the consequent deterioration of many tuberculosis control programs, infection rates often do not appear to have diminished at all.

Susceptibility factors

Disease due to tuberculosis is influenced by a number of identified factors, both host- and bacillus-related. These may include human genetic predisposition, race, age, immune status, nutritional status, previous exposure to mycobacteria, and mycobacterial virulence, strain, dose and predilection for specific tissues (12, 13, 76). Evidently, a very complex relationship between host and bacillus exists, that will ultimately determine the course of the disease.

The HIV / AIDS pandemic and tuberculosis

Several factors can increase the risk of an infected person developing tuberculosis, but over the last decade, infection with HIV has emerged as by far the most important of

these conditions. The intimate connection between tuberculosis and HIV infection was first demonstrated among both natives of sub-Saharan Africa and intravenous drug users in the United States (55,203). Co-infection with HIV and loss of immune control is thought to precipitate endogenous reactivation of latent *M. tuberculosis* infection that was acquired earlier in life. Worldwide, it has now become clear that mycobacteria, primarily *M. tuberculosis* and *M. avium*, are the most common opportunistic infections occurring in patients with Acquired Immune Deficiency Syndrome (AIDS). Of AIDS patients in Latin America, 20 to 30% have tuberculosis, and at least one third of all AIDS patients in African countries present with tuberculosis (81). In New York City in 1991, an estimated 46% of those 18-65 years of age who were hospitalized with newly diagnosed, previously untreated tuberculosis had clinical or serological evidence of HIV infection (188). It is clear that the *M. tuberculosis* situation is rapidly becoming desperate. To determine why, it is useful to first study the history of the disease.

A Brief History of Tuberculosis

Tuberculosis has had many aliases throughout history (234): The ancient Greeks called it phthisis (to waste). The swollen glands of the neck were termed 'scrofula.' In medieval times it became 'The Kings Evil' because newly crowned kings of England and France were believed to have powers to heal tuberculosis with their touch. Tuberculosis of the skin was known as lupus vulgaris. Tuberculosis of the bone, called Potts' Disease, resulted in characteristic vertebral fusion and deformity of the spine. The most familiar term for tuberculosis during the last few generations was consumption; this gave reference to the common course of the disease, whereby the body would be viewed as

wasting away or being consumed. Whatever mask it wore, tuberculosis accounted for 20% of deaths in1600s London, and over 30% of deaths in Paris in the1800s (57, 225).

M. bovis had been causing tuberculosis in the animal kingdom long before invading humanity. However, after the domestication of cattle between 8000-4000 BC, there is evidence of human infection by *M. bovis*, likely through milk ingestion (133). This coincides with archaeological evidence of spinal tuberculosis 5000-1000 BC, and *M. bovis* was the likely culprit. After 1000 BC, widespread pulmonary tuberculosis emerged; one theory is that *M. tuberculosis* may be an evolved, specialized form of *M. bovis* developed among milk-drinking Indo-Europeans, who then spread the disease during their migration into western Europe and Eurasia (50). By the first millennium BC, *M. tuberculosis* causing pulmonary disease had spread throughout the known world. The earliest tangible record of pulmonary tuberculosis arose between 668-626 BC (50), at which time the classic tuberculosis signs--cough, expectoration, hemoptysis, and wasting of the body, were well recognized. During that period, the earliest written evidence of pulmonary tuberculosis was found in the library of the Assyrian king Assurbanipal: "The patient coughs frequently, his sputum is thick and sometimes contains blood. His breathing is like a flute. His skin is cold, but his feet are hot. He sweats greatly and his heart is much disturbed. When the disease is extremely grave, he suffers from diarrhoea."

Exact pathological and anatomical descriptions of the disease began to appear in the seventeenth century (50). In his Opera Medica of 1679, Sylvius first identified actual tubercles as a consistent and characteristic change in the lungs and other areas of

consumptive patients. He also described their progression to abscesses and cavities. Manget described the pathological features of miliary tuberculosis in 1702. The earliest references to the infectious nature of tuberculosis appear in seventeenth century Italian medical literature. An edict issued by the Republic of Lucca in 1699 states that: "henceforth, human health should no longer be endangered by objects remaining after the death of a consumptive. The names of the deceased should be reported to the authorities, and measures undertaken for disinfection."

In 1720, English physician Benjamin Marten first conjectured that tuberculosis could be caused by "wonderfully minute living creatures," which, once they had gained a foothold in the body, could generate the lesions and symptoms of the disease (56). He stated, moreover, that "it may be therefore very likely that by an habitual lying in the same bed with a consumptive patient, constantly eating and drinking with him, or by very frequently conversing so nearly as to draw in part of the breath he emits from the lungs, a consumption may be caught by a sound person...I imagine that slightly conversing with consumptive patients is seldom or never sufficient to catch the disease." Dr. Marten's writings thus display a great degree of contemporary epidemiological insight. However, in contrast to this significant level of understanding about the etiology of consumption, which was already enabling prevention and a break in the chain of infection, those attempting to cure the disease were still groping in the dark.

During the first half of the 19th century, upwards of one-quarter of all deaths was due to tuberculosis (225). At this time, no one knew what caused this disease. Some doubted

that it was a single entity, so varied were its symptoms. Many people thought that it was an inherited disorder, as closely-housed family members of different generations would often develop the disease. It is interesting to consider that tuberculosis was also once viewed as a 'romantic disease' associated with creative genius. Tuberculosis killed St. Francis of Assisi, Federic Chopin, Charlotte Bronte, George Orwell, and Eleanor Roosevelt (50). Alexandre Dumas wrote in his time: "It was the fashion to suffer from the lungs; everybody was consumptive, poets especially; it was good form to spit blood after each emotion that was at all sensational, and to die before reaching the age of thirty" (Circa 1900).

Rene T.H. Laennec was a French physician who lived from 1781 to 1826, publishing lucid autopsy studies of tuberculosis which even today present examples of clear medical writing (68). Most importantly, Laennec's work firmly established that tuberculosis appearing in many forms and in many parts of the body did, indeed, represent a single disease, though the cause was yet unknown. In 1865, the French military doctor Jean-Antoine Villemin demonstrated that consumption could be passed from humans to cattle and from cattle to rabbits. On the basis of this revolutionary evidence, he postulated a specific microorganism as the cause of the disease, finally laying to rest the centuries-old belief that consumption arose spontaneously in each affected organism (132). It was left up to a German physician however, to first clearly describe the etiologic agent of tuberculosis.

By 1881 Heinrich Herrmann Robert Koch had established himself as a leading light in developing new methods in solid bacterial culture media, a crucial requirement if one is to grow pure strains of bacteria. In 1882, with Villemin's work as the starting point and using innovative staining techniques, he quickly demonstrated for the first time that the tubercle bacillus *Mycobacterium tuberculosis* is the cause of tuberculosis (107). His criteria for proof that the organism he discovered caused tuberculosis have been widely adopted and have become know as Koch's postulates. He specified that " it was necessary to isolate the bacilli from the body; to grow them in pure culture... and, by administering the isolated bacilli to animals, to reproduce the same morbid condition..." (107). The stage was thus set to begin more detailed and specific experiments on the pathogenesis of tuberculosis, in particular, work that would start to dissect out the immune response.

Early thoughts on immunity to tuberculosis

Further guinea pig studies by Koch clearly demonstrated acquired immunity following primary infection. For example, Koch noted that healthy guinea pigs inoculated cutaneously with tuberculosis bacilli healed the primary inoculation, only to die later of disseminated infection. However, a second inoculation of virulent organisms produced a very different result: the wound became indurated in 1 to 2 days and then ulcerated, but dissemination did not ensue. Additionally, when tuberculous guinea pigs were challenged cutaneously with a culture supernatant of *M. tuberculosis* (old tuberculin - OT) or with live organisms, there was necrosis both locally in the challenge site and at a distance in the preexisting tuberculous lesion, in a reaction now known as "the Koch phenomenon"(108). Koch was determined to develop an effective therapy for

tuberculosis; so impressed was he by his initial work with tuberculin that he proposed treating tuberculosis patients with it, a measure that eventually failed to have therapeutic benefit. Indeed, in some instances there were serious consequences - including death in a few unfortunate cases.

Although no therapeutic role for OT was ever found, an important and serendipitous finding did surface: such reactions were not seen in healthy people, and the diagnostic value of OT was quickly recognized. In 1907 it was demonstrated that reactions to OT could be initiated by intracutaneous administration in tuberculosis patients, who responded with local redness and measurable induration at the injection site. Manifestation of this so-called "delayed-type hypersensitivity" response is used to this day as the most widely used diagnostic tool for detecting tuberculosis in man and animal.

Diagnosis of Tuberculosis: PPD and DTH

In 1931, Florence Seibert began a series of studies designed to find "the active principle" of Koch's tuberculin (187). Her studies resulted in the preparation of a product drawn from tuberculin named 'purified protein derivative,' or PPD. While scarcely purified by modern chemical standards, and while containing many substances other than protein, PPD has since proven to be remarkably effective as a tuberculin skin test reagent. In 1941, Seibert and Glenn prepared a voluminous amount of PPD, half of which was set aside for research purposes, the other half of which was deposited with the United States Bureau of Standards and the World Health Organization (186). It serves to this day as the reference standard (PPD-S) against which all other subsequent batches of PPD, by all manufacturers, are calibrated.

Intradermal injection of PPD induces a classic delayed-type hypersensitivity (DTH), or a type-IV hypersensitivity response, in individuals previously exposed to *M. tuberculosis*, those vaccinated with BCG, or those exposed to other, similar mycobacteria. The reaction was determined to be mediated principally by antigen-specific, thymus-derived lymphocytes (T cells), since the response can also be seen in individuals who lack immunoglobulin and can be transferred between experimental animals by using pure T cells or cloned T -cell lines (96). PPD injection thus results in a red, indurated area of skin after a delay of some 48 to 72 hours and is used as one of the principal screening tests for *M. tuberculosis* infection. It has recently been speculated that the same reaction is thought to drive the development of pulmonary tuberculosis granulomas (159). Other important diagnostic tests include culturing, microscopic analysis and biochemical analysis of sputum samples, and radiography of the chest (19).

Treatment of Tuberculosis

Early therapies now seem highly fanciful and based more upon superstition than scientific fact. For example, common treatments included regular horseback riding, or eating the raw liver of a wolf (50). The fundamental and most widespread therapy for the treatment of tuberculosis during the late 19th and early 20th centuries consisted of prolonged bed rest in specially-designed sanatoria. Development of surgical techniques such as induced pneumonthorax and thoracoplasty ensued in the 1920s (50). Induced pneumothorax was used to treat some one hundred thousand patients with pulmonary tuberculosis (87), the primary concept being that collapse of the diseased lung would kill tissue-bound bacteria. Benefit was anecdotally described in many patients, but no rigorous study of the results was ever conducted. The procedure was furthermore quite

problematic, however, with side effects including inadvertent injection of air into a blood vessel, infection of the pleural space and hemorrhage. Alternatively, surgical reshaping of the chest by staged removal of ribs, or thoracoplasty, was first performed at the end of the 19th century by the Swiss surgeon De Cerenville (147). The aim was, as with induced pneumothorax, to collapse the diseased lung beneath. Other treatments included phrenic nerve crush and iatrogenic pneumoperitoneum, of course both aimed to promote healing in the diseased lung. Like bed rest, collapse therapies have now been consigned to history, having been displaced by far more effective, chemical treatments.

The chemotherapeutic era of tuberculosis treatment began in the 1940s with the discovery of para-amino-salicyclic acid (PAS) in 1943, and the subsequent discovery of streptomycin the following year (181), which was first administered to a human in 1944 (166). Not long after the initial use of these two drugs in humans, it was realized that using one drug at a time resulted in a decreased effectiveness due to bacterial resistance; subsequently, the effectiveness of combined streptomycin and PAS treatment (17) was described. In the early 1950s the drug isonicotinic hydrazide was discovered (175). Soon to be renamed isoniazid, or more simply, INH, it quickly became the cornerstone of treatment regimes. The combination of PAS and INH for eighteen to 24 months, complemented with streptomycin in the first two months, appeared to be 97% successful in curing clinical disease; however, decreased patient compliance within this regime resulted in the development of multi-drug-resistant tuberculosis (MDR-TB), usually to both INH and streptomycin (110). Many other chemotherapeutics have since been discovered and used as antituberculosis drugs, including rifampin, pyrazinamide,

ethambutol and thiacetozone; improvement over the earlier treatment regimes has, however, been limited.

MDR-TB has been an increasing problem ever since the1950s. Currently, some bacilli are resistant to both INH and rifampin, and cause an infection that is very difficult and expensive to treat, with a cure rate of less than 50% (20). Furthermore, although most industrialized countries successfully reduced the problem of MDR-TB in the 1950s and 1960s, fatal outbreaks of MDR-TB have occurred in the United States as recently as the last decade. (54,85). The incidence of MDR-TB remains high in developing countries, and where it is now complicated by the HIV epidemic, national tuberculosis control programs are being overburdened and the situation is rapidly becoming pandemic.

The 1970s saw the development of short-course chemotherapy (SCC), which lasts six to 8 months and ideally includes rifampin (47). In 1993, the World Health Organization recommended a drug regimen consisting of a two-month long intensive phase employing the drugs INH, rifampin, pyrazinamide and ethambutol, and a four-month long continuation phase utilizing isoniazid and rifampin (110). Due to the extended length and complexity of such a drug regimen, patient compliancy has again been poor, resulting in the development of the aforementioned multi-drug-resistant strains of *M. tuberculosis.* The development of the directly observed treatment, short-course (DOTS) therapy by the WHO has proved a very effective tool to increase compliancy and reduce disease levels (156). Recently, Stover et al (204) reported the development of a new anti-TB drug PA 824, which is effective against both replicating and dormant *M.tuberculosis.* PA-824 is

effective against MDR-TB, and shows definite potential for use in human clinical applications.

Prevention of Tuberculosis: The Search for a Vaccine

Beginning in 1908, Albert Calmette and Camille Guerin began to attenuate a strain of *M. bovis* isolated from a cow that had tuberculous mastitis (78) in the hope of succeeding where Koch had failed in developing a bacillus-derived treatment for tuberculosis. In the course of their work, the organism was subcultured on potato slices that had been soaked in sterile ox bile and 5% glycerol every three weeks for thirteen years. Eventually, after 233 subcultures, the organism was no longer virulent in animal models and was used to immunize a newborn at high risk of tuberculosis, whose mother had died of the disease and whose care-giving grandmother had active tuberculosis (19). The child lived a tuberculosis-free life. Subsequently, almost one thousand children were vaccinated that year, and only 3.9% of those children died of tuberculosis compared to the 32.6% of unvaccinated children who succumbed to the disease. However, since that initial triumph, bacille Calmette-Guerin (BCG) has had a chequered history. It is still considered the 'gold standard' of *M. tuberculosis* vaccines and is the most widely used vaccine worldwide, but it carries many liabilities as well as assets.

BCG is closely related to *M. tuberculosis* (>90% DNA homology), and recent data indicate that a large number of mutations have taken place during the long *in vitro* propagation of this strain (11,12,70). It is known that these mutations have resulted in the deletion of a great many open reading frames (ORFs: 16 deletions encoding 129 ORFs reported so far), encoding several important T-cell antigens such as the immunodominant

molecules ESAT-6 (Early Secretory Antigenic Target of 6KDa) and Culture-Filtrate Protein 10KDa (CFP10) (196). BCG provides a relatively high degree of protection in all animal models of tuberculosis infection; however, one of its greatest obstacles is that the efficacy has ranged so dramatically in various human trials around the world. Tests of the 1940s and 1950s in developed countries such as the United Kingdom, Denmark, Canada and North America demonstrated the vaccine to be highly efficient (70-80%). Conversely, more recent trials in developing countries (most notably the Chingleput trial of India) demonstrated no detectable protection against pulmonary tuberculosis; in fact, in some instances those vaccinated with BCG had a higher incidence of pulmonary tuberculosis compared to the placebo group (173,185).

Several explanations have been suggested for this variation in protective efficacy(64). These include: 1) interactions between the vaccine and environmental mycobacteria, frequent in tropical regions, 2) genetic variability in the populations studied, 3) differences in strains, doses and vaccination schedules, and 4) administration of the vaccine to individuals already infected. The hypothesis that has gained the most widespread acceptance attributes variation to higher levels of exposure to environmental mycobacteria in areas where the vaccine affords no protection. Experiments in animal models have supported this hypothesis, showing that prior contact with environmental mycobacteria interferes with the protection obtained by BCG vaccination (163); therefore, BCG may only achieve its full potential in situations where there is only a low level of exposure to environmental mycobacteria. It is thought that the positive protective action of BCG may be masked by environmental bacteria, or that the environmental bacteria may have a direct antagonistic influence and skew the immune

system towards a CD4 $^{+}$T helper 2 (Th2) direction (177). Andersen has also suggested that multiplication of BCG (needed for efficient protection) may be inhibited in animals sensitized with environmental mycobacteria (6). Nevetheless, BCG still has many advantages over other *M. tuberculosis* vaccines. It is inexpensive and stable (essential qualities for use in developing countries), a single vaccine produces relatively long-lasting sensitization, it can be given at any age (even at birth), and it provides a visible scar which is useful for epidemiological purposes.

Recently, the use of avirulent or saprophytic bacteria, auxotrophs, recombinants, DNA vaccines, subunit vaccines and a new generation of adjuvants has opened up novel areas of vaccine research (160). Each mode of vaccination has had a varied degree of success, but none have yet to truly challenge BCG as a replacement. A promising new area of investigation, however, was demonstrated by Brooks et al. where an Ag85 booster vaccine in aged mice (25) resulted in levels of protection in the lung comparable to those of young mice with minimal pathological damage. Boosting previously BCG vaccinated individuals may thus hold the key to future tuberculosis vaccination programs.

Part II

Pathology of Tuberculosis
(Biology of the Granuloma)

Introduction

The characteristic pathological feature of tuberculosis is the granuloma. There is some confusion in the literature as to what exactly constitutes a granuloma and its counterpart, granulomatous inflammation. In the strictest sense, granulomatous inflammation is defined as chronic inflammation with the presence of granulomas. However, over the years, significant liberty has been taken by pathologists in their classification of granulomatous inflammation, such that any chronic inflammatory infiltrate comprised predominantly of macrophages, has been so classified. Using either definition, it is the infiltration of activated macrophages with a modified epithelial-like (epithelioid) appearance that is critical for the definition of granulomatous inflammation (45).

The central role of granulomatous inflammation is to defend the host against persistent irritants, whether from endogenous or exogenous sources. If a particular irritant cannot be removed by typical acute and chronic inflammatory reactions, then an attempt is made to wall off, sequester, phagocytise, and destroy the inciting agent within the development of a discrete, unitized area of granulomatous inflammation, the granuloma (45).

Classically there are two types of granulomas, which differ in their pathogenesis. *Foreign body granulomas* are incited by relatively inert foreign materials such as talc, sutures or

other fibers large enough to preclude phagocytosis by a single macrophage. Epithelioid cells and giant cells are apposed to the surface and encompass the foreign body. *Immune granulomas* are caused by insoluble particles that are capable of inducing a cell-mediated response. This is typified not only by tuberculosis, but leprosy, syphilis and cat-scratch disease (45). The presence of Langhans - type giant cells and central caseous necrosis are the key diagnostic elements.

Some researchers divide granulomas into "high turnover" and "low turnover" granulomas (97). High turnover granulomas are characterized by significant macrophage death within the lesion and are usually seen when a hypersensitivity to the inciting agent is present. Recruitment of emigrating monocytes from the peripheral circulation as well as local mitotic division of macrophages within the granuloma replaces macrophages within these granulomas. These granulomas typically, but not always contain epithelioid macrophages, lymphocytes and mulitinucleate giant cells. The presence of the inciting agent is often scarce and difficult to find. Mycobacteria typically induce this type of granuloma. In contrast, low turnover granulomas have little macrophage death, and the macrophage infiltrate is generally maintained by longevity of the macrophage population rather than replacement by vascular emigration and cell division. Epithelioid macrophages may not be present, and the inciting agent is often found within the majority of the macrophages in the lesion. A hypersensitivity reaction is usually not a component; thus lymphocytes are uncommon. This type of granuloma is usually formed in response to agents that are inert, nontoxic, and fail to evoke an immune response.

A series of host responses occurs before the evolution of the granuloma. The initial response to the presence of *M.tuberculosis* in the human lung is an acute inflammatory reaction with an influx of neutrophils (234). These are ineffective and a progressive infiltration with macrophages occurs. Over time, the macrophages become 'epithelioid' and some fuse to become Langhans' giant cells. A zone of lymphocytes and occasional plasma cells surrounds this mass of cells and fibroblasts grow alongside. Within 2 weeks a firm, coagulative necrosis begins in the center. Histologically, the necrosis is structureless and eosinophilic. This type of appearance is called a 'productive' or 'proliferative' reaction because it is dominated by cells rather than fluid. An 'exudative' reaction in tuberculosis usually occurs in the serous cavities and is characterized by an outpouring of an inflammatory, fibrin-rich exudate which is infiltrated with lymphocytes and neutrophils. Epithelioid and Langhans' giant cells are scanty (234).

The granuloma may cease to progress and heal by fibrosis and eventually calcify. Alternatively, it may soften and enlarge, with individual necrotic foci tending to coalesce resulting in large areas of necrotic debris. Typically the necrosis at this time is of a caseous form. This reaction assists in localization of infection but also leads to tissue destruction. Liquefaction and accumulation of debris in large amounts can ultimately occur which may track to and rupture into a large airway and / or blood vessel. In human lungs, both 'productive' and 'exudative' lesions can occur and depending on the reaction of the tissue three pathological forms can be identified (234)

Acute caseous tuberculosis

This produces confluent caseation of much of the lung lobe (caseous bronchopneumonia). Large amounts of caseous debris in large bronchi occur (234).

Chronic tuberculosis

Caseous destruction occurs side by side with some healing by fibrosis. Three types of chronic tuberculosis are recognized depending on the degree of caseation or fibrosis: (a) caseous, (b) fibro-caseous, and (c) fibrotic. Bronchiectasis is a frequent complication of this type (234).

Non-reactive or anergic tuberculosis

Extensive necrosis teeming with mycobacteria occurs without any significant cellular reaction around them. This type of pathology is seen in the elderly (234) and in individuals with malnutrition, malignancies and immunosupression (e.g. HIV infection).

Immunopathology

One of the most characteristic and consistent features of tuberculosis is tissue necrosis. What is the mechanism of this necrosis and how does it differ from protective immunity? This question has been the subject of much debate since the "Koch Phenomenon" was first described (108).

Currently, there are three closely related and overlapping hypotheses as to the nature of the Koch phenomenon. Each draws from the Th1 and Th2 $CD4^+$ T cell paradigm, first

proposed by Mosmann (143). Some authors suggest that there is an imbalance between Th1 and proinflammatory cytokines. Thus too much tumor necrosis factor-alpha (TNF) could account for symptoms of tuberculosis, such as fever, weight loss and tissue damage. Evidence that these symptoms may indeed depend on TNF in human tuberculosis has come from experiments using thalidomide which decreases the half-life of the mRNA for this cytokine. Patients treated with thalidomide show rapid symptomatic relief and weight gain (100). There is therefore a paradox: TNF is essential for immunity, but may also be responsible for pathology.

The second hypothesis also involves TNF as a mediator of the damage, but suggests that this cytokine becomes damaging rather than protective, not because there is too much of it, but because it is being released into sites that contain a mixture of Th1 and Th2 cytokines. Although immunity to tuberculosis requires a Type 1 response, there is clear evidence in tuberculous mice that Type 2 cytokines are also expressed (78,143). The same is true in humans although this is less striking. The IL-4 gene is expressed in many patients' peripheral blood mononuclear cells (179, 182) while there is a deficit in IL-2 expression (182). This is supported by the fact that tuberculosis patients have elevated IgE antibody which is IL-4 dependent (182). Similarly, tuberculous granulomata can be shown to contain a Th0 (i.e. mixed Th1 and Th2) cytokine profile (15). Thus, although the Th1 component remains dominant (10), the data indicate the presence of an inappropriate Th2 component in disease. Even a small Th2 component leads to greatly enhanced susceptibility to tuberculosis and to TNF toxicity in mice (84). It appears to be a general rule, equally applicable in leishmaniasis and schistosomiasis, that there is

increased toxicity to TNF in sites of inflammation that contain a Th0 cytokine pattern (230).

The third hypothesis emphasizes the potential role of transforming growth factor beta (TGFβ), which can cause tissue damage and fibrosis, and can also inactivate the anti-mycobacterial functions of macrophages (215). However, TGFβ and the expression of other Th2 cytokines may simply be a natural part of disease progression; where there is a trigger of some sort to down-regulate the inflammatory response.These three hypotheses are not mutually exclusive, and they are probably all important components of the immunopathology.

The primary pulmonary immunological response to initial infection with *M.tuberculosis* restricts its replication and spread. If these mycobacteria continue to replicate, local dissemination via lymphatics and systemic spread throughout the body may occur via the blood stream creating new foci of infection. Both non-specific (innate) and specific (acquired) effector mechanisms play a role in immunity to tuberculosis

Non-specific (innate) immune effector mechanisms

- The role of macrophages

M. tuberculosis primarily infects macrophages. In contrast to other bacterial pathogens that avoid phagocytosis as a specific pathogenic strategy, *M. tuberculosis* is promiscuous in its use of multiple cell surface receptors to gain entry into the macrophage These receptors include the mannose receptors, complement receptors, and Fc receptors (1, 184,

185). *M. tuberculosis* bacilli enter the alveolar macrophage by means of conventional phagocytosis involving specific receptor-ligand interactions facilitated by surfactant apoprotein A (74). Complement receptors CR1 (CD35), CR3 (CD11b/CD18) and CR4 (CD11c/CD18), which are found on the surface of human monocytes and macrophages, have been shown to mediate phagocytosis of *M. tuberculosis* (183).

Ultimately, most mycobacteria are probably killed by macrophages activated by the various IFN-γ secreting cell types, although the final effector pathway is not known. In the mouse, IFN-γ activates macrophages so that they express enhanced capacity for production of oxygen reduction products such as superoxide anion and hydrogen peroxide, and also increased expression of the inducible form of nitric oxide synthase (iNOS: also known as Type II NOS)(33). The trigger that then causes nitric oxide (NO) production may be TNF. Treating mice with neutralizing anti-TNF antibodies has led to dissemination of BCG infection (104) and neutralizing antibodies or knock-out of the 55Kda TNFα receptor led to rapid death from *M.tuberculosis* (67). The NO released may have some intrinsic antimycobacterial activity (19,31) or it may interact with oxygen reduction products to yield peroxynitrites which may be the final effector molecules (211). However, it is not certain that the NO really is the relevant mycobactericidal pathway in the mouse and there is considerable debate as to whether this pathway is even possible in human macrophages, in which control of NO production is quite different. There is, however, a suggestive claim that high-output NO production is a property of alveolar macrophages from patients with tuberculosis (149).

-The role of other innate mechanisms

The recent discovery of the importance of the Toll-Like receptor (TLR) protein family in immune responses in insects, plants, and vertebrates has provided new insight into the link between innate and acquired immunity (220). It appears that distinct mycobacterial components may interact with different members of the TLR family (138). Specific intra-granulomatous TLRs may be expressed to sample mycobacterial components produced during persistent infection in order to maintain an effective antimycobcterial response, as hypothesized by Underhill (221). Demonstrating the significance of the various TLRs in host defense against *M. tuberculosis* awaits rigorous *in vivo* experimentation.

Mycobacterial factors

Mycobacteria employ various strategies to avoid being killed by phagocytes. They inhibit acidification of the phagosome (205), modify intracellular trafficking of vesicles (231) in particular the fusion of phagosome with lysosome (46) and cause quantities of lipoarabinomannan (LAM) to insert into glycosylphosphatidylinositol (GPI)-rich domains of the cell membrane (92). LAM is itself a GPI of unusual glycan structure, with the ability to modify numerous macrophage functions including the ability to respond to IFN-γ, and the ability to present antigen (32, 92). The last point may be relevant to the apparent inability of long-term mycobacterium-infected macrophages to present antigen to $CD4^+$ T cells (164).

M. tuberculosis has evolved strategies to avoid oxidative killing mechanisms. For example, complement receptors CR1 and CR3-dependent uptake does not trigger the

oxidative burst. *M. tuberculosis* also produces catalase and superoxide dismutase, two gene products capable of degrading reactive oxygen intermediates (ROI)(140). Deficiency in the *kat*G gene encoding the mycobacterial catalase results in increased susceptibility to peroxidative killing (232). LAM, mycobacterial sulfatides, and phenolic glycolipid-I (PGL-1) have all been shown to act as oxygen radical scavengers (19) decreasing the amount and toxicity of ROIs. LAM may serve a dual purpose in that it has also been reported to down regulate protein kinase-C and thereby inhibit the oxidative burst (32). LAM has also been shown to have immunogenic properties *in vitro*. It was found that LAM from the avirulent M. *tuberculosis* strain H37Ra, was 100-fold more potent at inducing tumor TNF secretion than LAM from the virulent Erdman strain (34). This lead to the hypothesis that the structure of LAM from a given mycobacterial isolate may directly influence its ability to elicit, or avoid, cytokine-mediated mechanisms of host resistance.

Recently, an entirely different type of anti-mycobacterial mechanism has been suggested. Certain signals that induce apoptosis of infected macrophages can lead to death of some of the contained mycobacteria. For instance, hydrogen peroxide simultaneously causes apoptosis, and reduced viability of phagocytosed *M. avium* in human monocytes (121). A similar effect can be induced by triggering apoptosis of human macrophages infected with *M.tuberculosis* via the purinergic receptors (89).

The recent discovery of the TACO (Tryptophan Aspartate-containing COat) protein provides the most succinct and direct mechanistic explanation for the inability of

mycobacteria-containing phagosomes to fuse with lysosomes (62). Analysis of the biochemical composition of mycobacterial phagosomes obtained by organelle electrophoresis of a microsomal fraction prepared from S-methionine / cysteine-labeled, BCG-infected macrophages has identified a 50-kDa host cell polypeptide specific for phagosomes containing live bacilli. This polypeptide was not detected in other subcellular fractions analyzed, including the phagosomes that contain dead BCG, nor was it present in metabolically labeled bacteria. By retaining TACO and thus intercepting the fusion of phagosome with lysosome, mycobacteria evade potent lysosomal antimicrobial functions of macrophages. It is important to remember that the specific bacterial proteins or cell envelope components that interact with the host cell to perturb these processes are completely unknown.

Mckinney et al. reported that persistence of *M. tuberculosis* in mice was facilitated by isocitrate lyase (ICL), an enzyme essential for the metabolism of fatty acids (136). Disruption of the *icl* gene attenuated bacterial persistence and virulence in immune-competent mice without affecting bacterial growth during the acute phase of infection. A link between the requirement for ICL and the immune status of the host was established by the restored virulence of delta *icl* bacteria in interferon-gamma knockout mice. This link was apparent at the level of the infected macrophage. Activation of infected macrophages increased expression of ICL, and the delta *icl* mutant was markedly attenuated for survival in activated but not resting macrophages. These data suggested that the metabolism of *M. tuberculosis* in vivo is profoundly influenced by the host

response to infection, an observation with important implications for the treatment of chronic tuberculosis.

Protective T-cell-mediated immunity

$CD4^+$ T cells

It is presently well known that acquired resistance against *M. tuberculosis* is mediated by cells rather than by humoral immunity. Work by Suter and Mackaness in the 1950s and 1960s (131, 209) and then by North in 1970s (150) demonstrated that T lymphocytes are the mediators of protection. In 1973, Lefford reported that adoptive transfer of thoracic duct lymphocytes in the rat model conferred immunity against tuberculosis (123). Orme and Collins went on to show that adoptive transfer of protective immunity could be achieved in T cell-deficient mice (157). Orme further identified different protective T cell subsets that emerge in mice infected intravenously with *M. tuberculosis.* It was also established that the $L3T4^+$ ($CD4^+$) T cells offered more protection than when compared to Lyt-2^+ ($CD8^+$) T cells. Moreover, Lyt-2^+ ($CD8^+$) T cells appeared to offer protection later in the infection, however, that infection was less than half of that offered by the $L3T4^+$ ($CD4^+$) T cells (158).

The accepted paradigm of immunity against *M. tuberculosis* is that Th1 $CD4^+$ T cells, recognizing mycobacterial peptides bound to class II major histocompatibility complex (MHC), secrete IFN-γ which in turn activates macrophages to kill bacilli as well as recruit monocytes for the initiation of granuloma formation (21, 158). In accordance with this paradigm, work from the Orme laboratory indicates that the kinetics of emergence

and loss of protective T cells that mediate immunity to tuberculosis in mice correlate strongly with the kinetics and emergence of IFN-γ (161, 162)

Where mycobacterial sensitization of the naïve $CD4^+$ T cells occurs is unclear, but bronchial-associated lymphoid tissues (BALT) are potential sites. In order for this sensitization to occur in mice, it is thought that antigen must be physically carried to the BALT due to the limited lymphatic drainage of murine alveoli. Gonzalez-Juarrero and Orme hypothesize that immature dendritic cells, which are distributed throughout the alveolar region, are responsible for capturing mycobacterial antigens and carrying them to lymphoid organs where they in their mature form present antigen to $CD4^+$T cells (77). In support of this hypothesis, dendritic cells isolated from murine lungs were capable of engulfing *M. tuberculosis*, which led to IL-12 secretion and the stimulation of $CD4^+$T cells to produce IFN-γ (77). The sensitized T cells then circulate and sample mycobacteria-infected lung tissue. It has been hypothesized that once the $CD4^+$T cells proliferate and secrete cytokines in response to mycobacterial antigen presented by infected macrophages, some remain in the infected area and are continually exposed to antigen. These short-lived cells are probably killed off by apoptosis in order to avoid local tissue damage caused by high concentrations of cytokines like IFN-γ, IL-2, and TNF. Some of the sensitized T cells leave the infected area through the blood or lymph and take on a memory phenotype (80).

Recent evidence for the protective role of $CD4^+$ type1 cytokines is strong. Disruption of the gene for IL-12 makes mice susceptible to tuberculosis (43, 44). Disruption of the

major histocompatability complex (MHC) Class II genes or of the gene for the β chain of the α/β receptor (117) resulting in deficiency of $CD4^+$ T cells, render mice susceptible even to the avirulent *M.bovis BCG* and so does disruption of the IFN-γ gene (39,62). IFN-γ is clearly also crucial for anti-mycobacterial immunity in humans, because children with defective genes for IFN-γ receptor die of BCG infection, and cannot be treated with conventional chemotherapy (148).

$CD8^+$ T cells

Immunity does not depend only on $CD4^+$ T cells. Mice with defective β-2 microglobulin genes, rendered unable to express normal quantities of Class I MHC products are very susceptible to *M.tuberculosis* (65). This may imply a role for $CD8^+$ cytolytic T-cells because such cytotoxicity could release organisms from macrophages that were failing to kill them and enable their uptake by fresh activated cells.

There are, however, other possible explanations for the effects of disrupting the gene for β-2 microglobulin because this associates not only with Class I MHC, but also with CD-1 (and other non-polymorphic MHC) (65), which is able to present a number of mycobacterial antigens to CD4-CD8- (double negative: (DN)) T-cells (11). The antigens recognized by these unusual lymphocytes include the mycolic acids and LAM (11,194). The role of these cells is unknown, but they appear to be cytotoxic, and to secrete the Th1 cytokine pattern, so they may well contribute to immunity (201) .

Early adoptive transfer studies showed that $CD8^+$T cells offer some protection against *M. tuberculosis*, possibly due to low-level secretion of IFN-γ (158). Enriched populations of immune $CD8^+$T cells transfer a small degree of resistance(158) and *in vivo* depletion of $CD8^+$T cells by intravenous injection of monoclonal antibody also diminishes resistance to a small degree (144). In a further study using antibody depletion (125) distinct pulmonary histopathologic differences were noticed between normal mice and those that had been depleted, suggesting a role for $CD8^+$T cells in the control of the immunopathology associated with tuberculosis. CD8 gene-disrupted mice have been shown to be able to control an aerosol infection with *M.tuberculosis* in a similar fashion to control mice for the first 55 days post infection. Thereafter, there is a slow rise in bacterial numbers above control for a total period of at least 150 days, suggesting a role for $CD8^+$T cells in chronic disease (218).

Whether $CD8^+$T cells act by cytolytic mechanisms in tuberculosis however, is unclear. One recent publication showed decreased survival of perforin gene knockout mice following intravenous infection (200), whereas in another study, perforin and granzyme gene knockout mice behaved the same way as control mice after aerosol infection. (41). It was speculated that that the protective role of $CD8^+$T cells was cytokine mediated, rather than lytic. In favour of this, it has been established that mycobacterial antigen-specific $CD8^+$T cells from mice and humans secrete IFN-γ after restimulation in vitro (118, 161, 190)

γδ T cells

There is also a large proportion of human peripheral blood γ/δ T-cells that will proliferate in response to mycobacteria (99). These cells recognize compounds containing 5' triphosphorylated thymidine (40), and also isopentenyl pyrophosphate and related prenyl pyrophosphate derivatives (214). Griffin and colleagues (79) demonstrated that γδ T cells do not accumulate any faster than αβ T cells in response to primary mycobacterial infection, and they failed to respond in an accelerated manner to reinfection. This thus suggested that γδ T cells were not involved in the memory response. This was in contrast to some earlier studies (94) where a preferential accumulation of γδ cells was observed in the peritoneal cavity of mice infected with *M. bovis BCG*. Studies using γδ T cell-receptor (TCR) knock-out (KO) mice showed that the size of the mycobacterial inoculum may determine whether γδ T cells contributed to a protective response. In the intravenous model a low-dose infection was contained but a high dose was not (115), and in the aerosol model there was no difference in the ability to contain growth of bacilli in the lungs (48). In this latter model, differences were seen however in the pulmonary granulomatous response. The γδ TCR KO mice manifested a more fulminant granulomatous response, characterized by many more polymorphonuclear cells (neutrophils). These findings suggested that γδ T cells play a protective anti-inflammatory role in the lungs, which may prevent immunopathologic inflammation. γδ T cells have been shown to secrete various cytokines. In particular the production of IL-12 and IFNγ by *Listeria moncytogenes* elicited peritoneal γδ T cells (195) suggests that they may be important in the formation of mycobacterial granulomas. Alveolar macrophages were found to serve as accessory cells for both resting and activated γδ T

cells in response to *M.tuberculosis* antigen. The specific role for the γδ T cell-receptor-bearing cell population in tuberculosis remains enigmatic.

NK1.1⁺ T cells

As mentioned, a population of mouse T cells DN for CD4 and CD8 surface antigens, has been discovered (70). Since then, a larger subset of DN T cells that express the natural killer (NK) cell surface receptor NK1.1⁺, TCR-αβ⁺,Ly6C and $CD44^{hi}$ have also been identified (210, 212). These cells have been shown to secrete cytokines *in vivo* including IL-4 and IFN-γ (14, 83). It is considered by some that another population of IFN-γ producing CD4⁺ NK1.1⁺ T cells may be contributors of initial or innate-like resistance against mycobacteria until mainstream CD4⁺ T cells enter the scene and take over the protective, IFN-γ secreting role (82).

Antibody responses

Prolific antibody responses to *M.tuberculosis* occur, but the role of these in protective immunity is unclear at present. Attempts at exploiting these responses for diagnostic purposes has not yet resulted in any serodiagnostic test useful in clinical practice. Based on serum passive transfer studies, the popular opinion is that antibodies play no role in protection (69). The role of B cells in the granuloma also remains enigmatic. It has been reported that granulomas in chronically infected B-cell-gene-disrupted mice are much smaller and there is less dissemination than in controls (22, 218), but neither study casts light on the reason why these cells are present in the first place.

Cytokines Controlling the Formation of Granulomas

It is now well established that a cascade of interacting extracellular signaling proteins orchestrates the trafficking of immune cells which set the stage for the formation of the pulmonary granulomatous lesions (127,129). Combining with relevant receptors on neighboring cells, cytokines regulate the expression of adhesion molecules on the vascular endothelium, within and around, the site of inflammation. This, in turn, favors the activation of inflammatory effector cells and modulates local survival and proliferation of different types of immune cells. If the inciting antigen(s) is removed, the inflammatory response generally resolves. However, in tuberculosis, the persistence of the mycobacteria and the imbalance of mechanisms for removal of inflammatory cells and their byproducts ultimately leads to a prolongation of inflammatory responses and the development of a granuloma.

In order to provide the appropriate clues to understanding the effect of the cytokine melieu at the core of the granuloma, in the next few paragraphs a brief description of the most relevant cytokines whose presence has been demonstrated at sites of ongoing inflammation will be provided.

Interleukin -1

Macrophages infiltrating tissues involved with hypersensitivity reactions produce detectable amounts of IL-1 (63). This cytokine may stimulate granuloma formation and fibrosis *per se* by inducing fibroblast proliferation and increasing collagen production.Sugawara et al. have shown that IL-1 type 1 receptor deficient mice develop

significantly larger granulomatous lesions with neutrophil infiltration in their lungs than wild-type mice after aerosol *M. tuberculosis* infection (207).

Interleukin -2

Actively released by T-cells, the role of IL-2 is to expand activated T-cell populations via the binding with its receptor IL2R, formed by three different chains: α (CD25), β(CD122), and γ(CD132) (96). IL-2 can act as a local growth factor for T lymphocytes infiltrating lung tissue and surrounding the granuloma (35). IL-2 receptor on alveolar macrophages has been shown to be significantly increased in tuberculosis as compared to healthy controls (93). Considering the fact that the addition of IL-2 to activated macrophages increases granulocyte-monocyte colony stimulating factor (GM-CSF) expression (146), it is likely that IL-2 could also be involved in the activation of some functional capabilities of macrophages participating in the development of the granulomatous structure.

Interleukin-4

This lymphokine, released by Th2 cells, is a cofactor for proliferation of multiple cell lineages. Th2 responses and in particular IL-4 in tuberculosis are subjects of some controversy. IL-4-deficient mice on a C57BL/6 background are resistant to *M. tuberculosis* infection (151). This however may be due to compensation by IL-5 and IL-13. Detection of IL-4 is variable, and although some reports have indicated that various Th2 responses exist in tuberculosis, it can be difficult to demonstrate. In human

studies, a depressed Th1 response but not an enhanced Th2 response was observed in peripheral blood mononuclear cells (PBMCs) from tuberculosis patients (126).

Interleukin- 6

This factor, which stimulates B-cell growth and T-cell proliferation, is produced by lung cells, macrophages, endothelial cells and fibroblasts. It causes fever and active synthesis of acute-phase proteins. This cytokine may have a role in the control of the *in situ* proliferation of fibroblasts in granulomas (189). Following low dose aerosol infection, early increases in lung burden, as well as decreased IFN-γ production, were observed in IL-6-/- mice, compared to control mice, suggesting that IL-6 is important in the initial innate response to the pathogen (180). Ladel has also shown that IL-6 deficiency can be lethal in the mouse model (116).

Interleukin-10

IL-10 exerts potent anti-inflammatory activities. It is produced by macrophages and T cells during *M. tuberculosis* infection and possesses macrophage deactivating properties, including down regulation of IL-12 production, which in turn decreases IFN-γ production by T cells. IL-10 directly inhibits $CD4^+$ T cell responses, as well as inhibiting APC function of cells infected with mycobacteria (176). Interestingly, Murray and Young demonstrated an increased antimycobacterial immunity in Interleukin-10-deficient mice (145). There are also data on its involvement in the pathophysiology of fibrosis in granulomas (88).

Interleukins -12 and 23

IL-12 has pro-inflammatory properties, is involved In Th1 responses and represents an integral component of innate immunity against a number of pathogens (26). Specifically, IL-12 induces the Th0 vs Th1 shift and stimulates the proliferation and the lytic activity of activated T-cells and NK cells. In synergy with IL-15, IL-12 favors contact between activated T-cells and APCs (103). Furthermore, it induces IFN-γ production by $CD4^+$ T-cells and NK cells. Its involvement in the development of tuberculosis granulomas has been shown (15). IL-12 is induced following phagocytosis of *M. tuberculosis* bacilli by macrophages and dendritic cells (43,77) which drives development of a Th1 response with production of IFN-γ. IL-12 enhances the IFN-γ response in antituberculous immunity. Convincing evidence of the importance of IL-12 in resistance to tuberculosis was provided by IL-12p40–gene deficient mice. These mice were moderately susceptible to infection and had a greatly increased bacterial burden, as well as decreased survival time, compared to control mice, probably due to the substantially reduced IFN-γ production in IL-12p40-/- mice (44). IL-12 receptor deficient humans have now been characterized and they exhibit impairment of mycobacterial immunity (5). Recent evidence further suggests that absence of the IL-12p40 subunit is more detrimental to the generation of protective responses than is the absence of the p35 subunit (43). The superior Ag-specific responses of the p35 gene-disrupted mice, when compared with the p40 gene-disrupted mice, suggested that the p40 subunit may act other than as a component of IL-12. A candidate molecule suggested as being capable of driving the protective responses in the p35 gene-disrupted mice is the novel cytokine IL-23. This cytokine is composed of the IL-12 p40 subunit and a p19 subunit (155). In support of a

role for this cytokine in protective responses to *M. tuberculosis*, it was shown that the p19 subunit is induced in the lungs of infected mice (43).

Interleukin-18

Previously known as IFN-γ-inducing factor (IGIF) IL-18 has similar activity to, although distinct from IL-1 (111). Mainly produce by monocytes and macrophages, it induces expression of IFN-γ and G-CSF, while it inhibits production of IL-10. Sugawara has shown that tuberculosis granulomatous lesion development by IL-18- deficient mice is inhibited significantly by treatment with exogenous recombinant IL-18, concluding that IL-18 is important for the generation of protective immunity to mycobacteria (208).

Interferon gamma (IFN-γ)

IFN-γ enhances the accessory function of APCs, increases the cytolytic function of macrophages and lymphocytes and regulates the secretion of other lymphokines. In addition, this cytokine activates macrophages to phagocytose intracellular organisms such as mycobacteria and listeria (29,224). IFN-γ is produced by $CD4^+$T cells and $CD8^+$T cells, NK cells and even the infected macrophage itself (61). The importance of IFN-γ is demonstrated by the high susceptibility to mycobacterial infections of patients with defective IFN-γ receptors (120). To date, IFN-γ knockout (GKO) mice are the most susceptible mice to virulent *M. tuberculosis* (42, 66).

Colony stimulating factors

GM-CSF, granulocyte-CSF (G-CSF), monocyte-CSF (M-CSF) and IL-3 are able to induce the growth and differentiation of myeloid progenitors in the bone marrow, facilitating the aggregation of monocyte-macrophages which form the central area of immune granulomas (170).

Chemokines

The superfamily of chemokines consists of an array of chemoattractant proteins which have been divided into three branches (C, C-C, C-X-C), according to variations in the shared cysteine motif (168). There are currently close to 50 related proteins. Structural variations of chemokines have been demonstrated to be associated with differences in their ability to regulate the trafficking of immune cells during inflammation, for example, the C-X-C family includes IL-8 and macrophage inflammatory protein (MIP) - 2, and the C-C family includes monocyte chemotactic protein (MIP) - 1 and monocyte inflammatory protein (MIP) - 1α -1β. Several lines of evidence now suggest that the C-X-C and C-C chemokines contribute to the progressive growth of immune granulomas and fibrosis development (198). Multiple chemokines have been implicated in the immune response to tuberculosis. Most recently, Orme and Cooper have discussed their role in delayed-type hypersensitivity (159).

Tumor Necrosis Factor alpha (TNF)

TNF is a pleiotropic factor predominantly produced by activated cells belonging to the monocyte-macrophage lineage which activates both neutrophils and macrophages,

leading to protease release, stimulation of the respiratory burst and induction of vascular adhesion molecule expression that is essential for cell recruitment to sites of inflammation (192).

M. tuberculosis induces TNF secretion by macrophages, dendritic cells, and T cells (216). In mice deficient in TNF or the 55-kDa TNF receptor, *M. tuberculosis* infection resulted in rapid death of the mice, with substantially higher bacterial burdens compared to control mice (67). TNF has an important role as a modulator of inflammation in this infection. Results of a recent study by Mohan et al (141) suggest that TNF plays an essential role in preventing reactivation of persistent tuberculosis, modulating the pulmonic expression of specific immunologic factors, and limiting the pathological response of the host. Turner et al demonstrated that the production of TNF is important and beneficial in limiting lesion development in the chronic stage of the disease (219).

Transforming Growth Factor beta (TGF-β)

This classic anti-inflammatory cytokine has been implicated in suppression of T cell responses in tuberculosis patients (85). The same author however, has also discussed the enhancement of intracellular growth of *M. tuberculosis* in human monocytes by TGF-β1 (86) . TGF-ß is present in the granulomatous lesions of tuberculosis patients (8) and is produced by human monocytes after stimulation with *M. tuberculosis* (217) or LAM (49).

Lymphotoxin - alpha (LTα)

Recently, Roach et al. have proposed that lymphotoxin - alpha (another TNF-alpha like molecule) is essential for the control of pulmonary tuberculosis, and its critical role lies not in the activation of T cells and macrophages per se but in the local organization of the granulomatous response (174).

Recently, granuloma-specific cytokine gene expression in mice has been investigated using laser capture microdissection, molecular beacon and realtime polymerase chain-reaction (PCR) technology (233). They reported that the relative levels of nitric oxide synthase 2 (NOS2), MCP-1, MIP-1α and Toll like receptor 2 (TLR2) RNA was higher in the granulomatous areas than that derived from total lung RNAs. In contrast, their preliminary results suggested that the relative levels of intra-granulomatous GM-CSF expression was lower than that determined using total lung tissues.

The Th1 / Th2 model in the development of granuloma

There are data in experimental and human granulomatous disorders suggesting that during the formation of the typical hypersensitivity granuloma, a Th1 $CD4^+$ T cell profile predominates (95), while Th2 type is associated with impaired granuloma formation and reduced resistance to intracellular pathogens. However, it is assumed that some granulomas may also be characterized by a Th2 pattern. For instance, T cells surrounding granulomas arising in response to parasitic ova chronically release Th2 cytokines while producing only small amounts of Th1 cytokines (222). Therefore, differences in the type of cytokines locally produced may have impact in determining the type of granuloma, its

intensity and the extent of the central necrosis. In particular, it is believed that the Th1 pattern provides the maximum protective immunity to invading intracellular pathogens while Th2 cytokines are required for the infiltration and activation of eosinophils, which contributes to the destruction of soluble, toxic antigens, as in the case of schistosomiasis. The Th1/ Th2 pattern also regulates the local fibrinogenic processes. It is thought for example that a switch to a Th2 T-cell pattern with concomitant release of IL-4 may lead to increased deposition of extracellular matrix components surrounding the granuloma (114).

Accumulation of Inflammatory Cells Sets the Stage for Granuloma Formation

Infiltration of T- cells

The concept that T-cell subset redistribution is important in the pathogenesis of granulomatous reactions comes from the comparison of the results obtained from the lymphocytic pattern in peripheral blood and at the sites of disease activity. For example, in sarcoid patients a peripheral CD4 lymphopenia is associated with a dramatic increase in memory CD4 T-cells in the lung, lymph nodes, liver and spleen (90). This finding substantiates the concept of T-cell compartmentalization, since it is presumable that the marked increase of CD4 cells at a site of involvement might lead to the consequent decrease in peripheral T lymphocytes. Macrophage cytokines (IL-1, TNF-α and IL-15) up-regulate expression of mRNA of adhesion molecules on endothelial cells (112). A probable scenario is thus that macrophages and other accessory cells (dendritic cells and endothelial cells) favor lymphocyte endothelium adhesion at sites of hypersensitivity reaction through cytokine release. Furthermore, some cytokines (IL-15 and RANTES

(Regulated and normal T cell expressed and secreted)) are likely to cooperate in the expansion of the CD4 T-cells within the granulomatous areas (2). The discovery that there is an increased number of T-cells expressing the cell-cycle related Ki67 antigen at sites of disease activity (38) indicates that they can proliferate *in situ*. This suggests that a second mechanism responsible for the accumulation of T-cell subsets in granulomatous tissues rests on an *in situ* IL-2 mediated proliferation. IL-2 has been shown to be important in supporting granuloma formation and accretion in response to mycobacteria (226).

Mechanisms leading to monocyte-macrophage recruitment

The cellular redistribution also involves the macrophagic component of the granuloma. Proofs supporting the concept of monocyte redistribution come from observations that macrophages involved with the hypersensitivity reactions show a monocyte-like phenotype pattern as well as reduced or missing activity of tartrate-resistant acid phosphatase, which is regarded as a marker of maturity for cells of the monocyte-macrophage lineage (113). Furthermore, macrophages in early sarcoid granulomatous lesions and around blood vessels in the intergranulomatous areas express the calcium binding protein calgranulin Mac387 (an antigen shared by granulocytes and circulating monocytes but only by a minimal proportion of tissue macrophages), thus confirming that the recruitment of adherent cells drives the development the core of the granuloma (36).

Most events responsible for the recruitment of monocytes from the bloodstream to sites of inflammation have been identified. They are attracted by relevant chemotactic stimuli

(MCP-1, TNF-α, RANTES and GM-CSF) and acquire the ability to release type IV collagenase, an enzyme which is capable of binding and degrading the major structural component of the basement membrane of vessel walls. By modifying the macromolecular organization of the basement membrane, this proteinase causes gaps or discontinuities through which circulating monocytes may enter peripheral tissues. Following the secretion of this enzyme, a heightened number of circulating monocytes enter the sites of inflammation and under the influence of macrophage derived cytokines (M-CSF and GM-CSF) (60) mature macrophages are generated, favoring the accumulation of mononuclear inflammatory cells releasing proinflammatory cytokines which, in turn, activate additional macrophages and surrounding T-cells. Evidence has also been accumulating which suggests that macrophages actively proliferate at the sites of inflammation (18). Macrophages isolated from the lung of patients with granulomatous pulmonary diseases, show an increased mitotic activity and form colonies when placed on soft agar and incubated *in vitro* (18). They also actively synthesize DNA, as demonstrated by the enhanced incorporation of 3H-thymidine (18, 154).

The central core of the granuloma is composed of macrophages at different stages of differentiation. There is a relationship between macrophage proliferation and fusion and subsequent formation of granuloma. The compartmentalization of different regulatory T-cells is likely to provide distinct effects on the evolution of the granuloma.

Local proliferation of activated T-cell clones favors the formation of granulomas

There is evidence that mycobacterial antigens induce expansion of an oligoclonal set of T-cells using particular Vβ regions. Different mechanisms could account for the limited usage of the TCR repertoire in patients with tuberculosis. One hypothesis is that the putative antigen(s) drives an oligoclonal expansion of T-cells using particular Vα or Vβ regions. Alternatively, the antigenic or superantigenic stimulation of T-cells might induce a preferential growth of cells with a limited TCR leading to an oligoclonal proliferation. In addition, the *in situ* release of cytokines likely plays a role in this phenomenon. It is thought that the antigen(s) involved in granulomatous lesions favor(s) the massive proliferation of a limited number of T-cell clones and an up-regulation of the physiological activation state of tissue T-lymphocytes.

Degeneration, Fibrosis and Chronic Disease

Alterations in mechanisms of apoptosis and necrosis affect the pathophysiology of granulomas

One of the major difficulties concerning the pathology of granuloma lies in the understanding of why the granulomatous lesion recovers in some patients whereas it persists in others. One theory claims that the persistent, exaggerated T-cell growth and the consequent continuous formation of immune granulomas are a reflection of dysregulations of the mechanisms which control local T-cell responses (191). The life and death of lymphocytes are tightly controlled by soluble factors and membrane receptors that activate either proliferative or apoptotic processes. Induction of apoptosis

assures rapid disappearance of the immune response upon antigenic clearance, avoiding the metabolic costs involved in sustaining a large number of effector cells. Furthermore, programmed cell death of antigen-specific T-cells prevents possible immune responses against self-antigens.

An oncogene, named *bcl-2*, which was first identified at the site of translocations common to follicular lymphoma, protects lymphoid cells from programmed cell death when certain growth factors, in particular IL-2, are withdrawn (4). Another system which is involved in the regulation of the T-cell inflammatory process is the Fas/Fas-L system (124). Both of these systems have been evaluated in patients with granulomatous disorders. Bcl and Fas molecules are expressed at higher levels on sarcoid T-lymphocytes than in normal T-cell populations, and it is believed that the imbalance of mechanisms for removal of inflammatory cells and/or the persistence of antigenic stimulation could lead to the maintenance of a local inflammatory response, setting the stage for the development of irreversible remodeling of the surrounding environment and, in some patients, the evolution toward tissue injury (3).

Apoptosis of alveolar macrophages (AMs) could be an effective weapon to kill or inhibit the growth of intracellular mycobacteria. Several findings suggest that AM apoptosis plays an important role in tuberculosis. Infection of human AMs with *M. tuberculosis* has been shown to induce apoptosis in vitro (102). Furthermore, extensive apoptosis (50–70%) was found within tuberculous granulomas in lungs of tuberculosis patients (102), and a significant increase in the number of apoptotic AMs was observed in

bronchoalveolar lavage fluid (BALF) from patients with active pulmonary tuberculosis(105, 167). Despite these observations, it is not clear which role AM apoptosis plays in the pathobiology of this disease and whether it increases or decreases the mycobacterial load in vivo. In vitro studies suggest that apoptosis may be a macrophage defense mechanism to infection by mycobacteria. Indeed, apoptosis of human monocytes limited the growth of *M.avium* (72) *M.bovis BCG* (142) and *M. tuberculosis* (153). However, *in vitro* studies are not adequate to determine the net effect of AM depletion on the host response to *M. tuberculosis.* AMs have important phagocytic and immune functions that could be disturbed by the apoptotic process.

Apoptosis or lysis of infected cells by $CD4^+$ T cells may also play a role in controlling infection (9); human $CD4^+$ T cells can produce perforin and granulysin, although these molecules did not seem to participate in bacterial killing. The effects of FasL- or TNF-induced apoptosis on *M. tuberculosis* viability in human and mouse macrophages is controversial; some studies report reduced bacterial numbers within macrophages after apoptosis (153), and others indicate this mechanism has little antimycobacterial effect (202).

From granuloma to fibrosis

Cells within an organ reside in a delicate framework of collagen and peptidoglycans, the extracellular matrix (ECM) that provides the complex anatomic structure needed for proper organ function. Repetitive or chronic injury results in the replacement of this highly organized supramolecular structure with dense collagen fibrils that may eventually impair organ function in a process called fibrosis. Granuloma collagen deposition is a

dynamic process. Major cytokine regulators of fibroblast function that are present in granulomatous inflammation include platelet derived growth factor (PDGF), IL-1, IL-4, IFN-γ, TNF-α and TGF-β (59). Buckley et al have recently proposed that fibroblasts are important sentinel cells in the immune system, playing a critical role in the switch from acute inflammation to acquired immunity and tissue repair (27). The possible role of the degredative enzymes such as matrix metalloproteinases (MMPs), is also an active area of mycobacterial research (171).

Memory

The finding in 1960 by Lambert (119) that mice infected with *M. tuberculosis* and then treated with isoniazid chemotherapy retain their capacity to strongly resist a second challenge infection, coupled with the work of Lefford and McGregor (122) who used a rat model, established the concept that chemotherapy of *M. tuberculosis*-infected animals, rather than leading to a decay of immunity, results in the retention by the animal of a state of immunologic memory. As required by the definition of immunologic memory first put forward by Celada (31) a heightened resistance to the specific infection long after cells that mediate the active immune response have disappeared is seen. With the advent of flow cytometric methods, antituberculosis memory T cells have been further characterized. Griffin and Orme (80) showed that $CD3^+$ T cells from the spleens of infected mice displayed a phenotype of $CD4^+CD44^+CD45RB^{hi}$ early in infection, a well recognized T cell activation phenotype. Over 2 to 3 weeks, a gradual decline in CD45RB expression resulted in predominantly $CD4^+CD44^{+hi}CD45RB^{lo/neg}$ cells, a phenotype associated with memory. Andersen confirmed that these cells are not truly resting, but they are arrested in the G1 phase of the cell cycle (7). Recently, Andersen has suggested

that there is an important role for memory cells that have reverted to a naïve phenotype in the long-term protection against *M. tuberculosis.* Thus, in contrast to the work of Griffin and Orme, $CD44^{lo}$ $CD45RB^{hi}$ are the important memory cells (7).

Latent vs Dynamic forces

M.tuberculosis is foremost amongst bacterial pathogens in its ability to establish and maintain latency, the period during which the infected person does not have clinically apparent tuberculosis, but harbors *M.tuberculosis* organisms able to reactivate at a later date. In latent infections, the state of the bacteria within the granuloma, or tubercle, is not known. The organism may be in a dormant non-replicating state, actively replicating but killed off by the immune response, or metabolically altered with limited or infrequent replicative cycles. Breakdown of immune responses designed to contain the infection can result in reactivation and replication of the bacilli, with necrosis and damage to lung tissue. Thus, a constant battle between the host and the mycobacterium is being waged, and the outcome depends on many factors. The balance between cell-mediated immunity and tissue damage throughout the course of this disease determines what form the disease takes and may not be dissimilar to the spectrum in leprosy that has been correlated to the balance of Th1 and Th2 lymphocyte subsets (223).

Part III

Comparative Immunopathology of Tuberculosis

Introduction

Researchers through the years have graded various responses to the tubercle bacillus in a variety of species. Perhaps the most comprehensive presentation of this was first put together by Francis (71) and modified only slightly since then by Karlson (101). Six groups of species were defined in relation to their cumulative score in each of the areas of sensitivity to tuberculin (allergy), number of bacilli per lesion, and presence of caseation, calcification, fibrosis and giant cells. Not included in Francis' work was the extent of liquefaction of solid caseous foci and cavity formation, which is the main mechanism by which tuberculosis is spread in humans (53). Their susceptibility to infection with *M. bovis*, *M. avium* and *M. tuberculosis* was assessed, as was the ease of spread between members of the same species and the most important route of infection. Francis used a simple 0-5 scale for each factor, but notes that differences in the response in the various species and within species may be very much larger than this simple linear scale suggests. However, although a somewhat arbitrary, subjective approximation, this study has proved a very useful tool to consider as a basis to comparative immunopathology of tuberculosis.

The first two groups in the Francis classification contain all the animals in which more or less typical tubercles are formed and the animals in these groups develop a high or fairly high degree of allergy.

Group 1: primitive man, monkeys, guinea-pigs, rabbits and voles

Group 2: urban man, elephants, cattle, buffaloes, goats, sheep, camels and pigs

Group one consists of highly susceptible species. There can be no doubt that monkeys in captivity, and primitive man subjected to civilization, are far more susceptible to fatal spontaneous infections than any other species of animal or bird. In both the main route of infection is by the respiratory tract; they develop a primary complex and, the histological reactions in both are similar. There is a tendency, even in monkeys, for secondary foci to produce only slight lesions in regional lymph-nodes. The main difference is that the monkey becomes less sensitive to tuberculin than man. The circulating transferrin is more saturated with iron in guinea pigs than in humans, cattle, mice and rabbits (109). Iron, which is needed for the growth of the bacillus, seems therefore to be more readily available in guinea pigs and may in part explain their susceptibility.

There is an essential similarity between the histological lesions of tuberculosis in man, cattle and monkeys. In all three species there is a central area of necrosis, caseation or cavitation surrounded by a zone in which epithelioid cells are usually infiltrated with neutrophils. The necrotic zone just inside the zone of viable cells is usually the richest in tubercle bacilli. Outside the layer of epithelioid cells there is usually a layer of macrophage cells and lymphocytes, and there is at least some attempt at encapsulation. Typical Langhan's giant cells are common in the three species, and there is a certain regularity about the lesions even in acute tuberculosis in the monkey. The tubercle is less well defined in the rabbit, guinea-pig and vole than in other species of the groups, but is

still clearly recognizable and contains the main elements: necrosis, caseation and calcification, epithelioid and giant cells, and some fibrosis. The animals in the second group are moderately susceptible to tuberculosis.

Group 3: fowls

Domestic fowl are on the whole very similar to those species in group two.

Group 4: horses, asses and mules

Necrosis and caseation may occur in the lesions of horses, but apart from the presence of giant cells , which may be numerous, the lesions are not typically tuberculous and have the appearance of chronic granulation tissue with regularly arranged macrophages and varying amounts of fibrosis. Mineralization is rarely observed. The animals in group four are considerably more resistant than those in group two.

Group 5 A: dogs

Group 5 B: cats, minks, ferrets

Group 5 C: hamsters

Group 5 D: mice, rats

Group 5 is not very homogeneous, in that dogs are as resistant as horses, and mice and rats much more so, whereas the other animals are highly susceptible: probably as susceptible as those in Group 1, however, although necrosis and liquefaction may occur,

there is no arrangement of tissues in to tubercles. In hamsters, mice and rats, caseation does not occur, necrosis is slight, giant cells rare, and of course there is no tubercle formation.

Group 6: chick embryo, tissue culture

It is salient to note that in the animals of Groups 1,2 and 3 typical tubercles develop and the animals become allergic. However, as the characteristic features of tuberculous lesions disappear in groups 4,5 and 6, so does the degree of allergy.

The Basis of Species Resistance to Tubercle Bacilli

The development of giant cells and fibrosis are often considered to be correlated with resistance (197) and this is probably true for animals in Groups 1 and 2. However, if one considers all the species on Francis' list, there is no constant histological feature associated with resistance. In fact, the most resistant animals, mice and rats, develop no tubercles. The only correlations which extend throughout all species are the absence of tubercles in species which do not become allergic, the inverse relationship between the number of bacilli in lesions and the degree of allergy; the balance which exists between these two factors and the amount of caseation which occurs. Studies in tissue culture do not indicate that cells from different normal animals vary greatly in their power to destroy tubercle bacilli.

Animal models

Despite these well documented species variations, the use of animal models is crucial for the further understanding of pathogenesis of tuberculosis in man. In particular, the correlation between growth of bacilli in the lungs and immunopathology is still poorly understood in the human lung. It is generally considered that those that cure the disease, completely clear the lung of mycobacteria, however, those that have reactivating disease presumably only arrest the growth and did not fully clear the infection. Those humans that have progressive disease and succumb to infection in only a few months to years, are thought to have a rising bacterial load from the outset. Animal models are invaluable to addressing this relationship.

Historically, the rabbit , guinea pig, and the mouse have been the most widely used. All three species cannot prevent inhaled fully virulent tubercle bacilli from establishing an infection, but they differ markedly in the type of disease produced once it is established. Using the rabbit model, Lurie was the first to propose that tubercle bacilli usually cause no detectable tissue damage until the host develops a strong local DTH response to their tuberculin-like products (130). Dannenberg has long suggested that the host develops tissue damaging DTH and cell-mediated immunity (CMI) after an initial period of logarithmic bacterial growth (51). Some investigators think these reactions are separate and dissociable phenomena, whereas others regard them as differing only in degree.

Dannenberg proposed a five-stage model of tuberculosis pathogenesis based on this rabbit model (52). Stage 1 is the ingestion of inhaled bacilli by pulmonary alveolar

macrophages. Stage 2 is the stage of logarithmic bacterial growth within non-activated macrophages. In this model, the presence of T cell subsets, neutrophils or the level of apoptosis is not addressed during these first two stages. In Stage 3 Dannenberg suggests that 'tissue damaging DTH apparently kills macrophages that harbor more than a few bacilli in their cytoplasm, thereby stopping their logarithmic intracellular growth and forming the tubercle's early caseous center'. It is this macrophage killing that is thought to be the key host event in controlling the number of viable bacteria in the host. Stages 4a and 4b have been developed from the work done by Lurie on susceptible and resistant rabbits respectively (130). In 4a, bacilli escape from the edge of the caseous center and again grow intracellularly within the poorly activated macrophages that surround the caseum (130). In 4b, bacilli escape from the edge of the caseous center, but cannot grow intracellularly within the highly activated macrophages that now surround the caseum. The final stage, Stage 5, is characterized by 'the liquefaction of the caseous center and growth of bacilli extracellularly. Bacterial numbers reach such high levels that the CMI of the resistant host is overwhelmed. With discharge of the granuloma core, bacteria are disseminated to other parts of the lung and the environment. In this model a well defined role for T cell immunity has never been addressed.

As information about the guinea pig accumulated, it became evident that it seemed to share several characteristics very similar to that seen in untreated human beings, particularly in terms of the morphology and necrotic degeneration of lung lesions as the disease process worsened. Because of this property, this animal is the definitive model

for the evaluation of new vaccines, which must possess the capacity to prevent this pathological process.

In contrast, common inbred mouse strains will generally arrest the growth of bacilli in the lungs and by some be termed 'resistant' animals (139). However, certain strains show evidence of bacterial regrowth of pulmonary tuberculosis after a period of apparent containment. Even here, however, this regrowth does not become evident until 200-250 days after aerosol infection, whereas guinea pigs succumb in about half this time (19). Certain strains, particularly those on the C57BL/6 background, can show evidence of a low-grade chronic lung disease for very considerable lengths of time, although this eventually degenerates. Rhoades proposed a five stage histomorphological model for this progression (172). As an extension of this, Cardona and his colleagues have recently proposed some modifications to this model. The Cardona model describes three forms of granuloma; primary, secondary and a tertiary form that is a combination of both (30).

Recently, Dannenberg has further discussed the differences in these three animal models. He proposes that progressive pulmonary tuberculosis is not due to increasing numbers of viable bacilli in rabbits, mice and guinea pigs, but is due to a continuous host response to mycobacterial products (54). In this light, he defines four basic concepts concerning the pathogenesis of tuberculosis. Firstly, initial inhibition and or killing of bacteria by the rabbit alveolar macrophage is more prominent with virulent *M. tuberculosis* than *M. bovis*, both of which are fatal to guinea pigs and mice. Secondly, in rabbits, mice and guinea pigs, an initial growth phase occurs, in which the bacilli multiply logarithmically

within the unactivated monocyte/macrophages that enter the developing pulmonary lesions (130). In the rabbit, the virulence of the bacilli and the innate resistance of the host have no marked effect on the *rate* of bacillary multiplication. In the mouse, however, attenuated strains will grow slower than virulent ones (152). The most virulent bacilli are apparently more resistant to the forces of acquired immunity, which end the initial logarithmic phase. The larger number of bacilli in a susceptible host perhaps provides a stronger antigenic stimulus to this host's relatively weak immune response. Alternatively, the rate at which the acquired immune response develops may be determined by the virulence of the infecting strain and may not be appreciably influenced by genetic differences among the hosts. Thirdly, after the rapid growth phase, there is a phase where the bacterial numbers in the lung become stationary. However, bacterial products are still being produced. Dannenberg proposes that the resistant host limits the accumulation of bacillary products better than does the susceptible host, so that the progress of the disease is slowed and in some cases is even arrested. Fourthly, the host's immune system cannot destroy tubercle bacilli growing extracellularly in liquefied caseum (19). Mice never form true cavities and guinea pigs rarely do.

In essence, Dannenberg theorizes that rabbits, mice, guinea pigs and humans use tissue-damaging DTH and CMI in differing proportions to control *M. tuberculosis*. Mice show little DTH and their lesions have little if any necrosis. Guinea pigs exhibit strong tissue-damaging DTH, but relatively weak CMI. Bacillary multiplication is controlled by this DTH, but caseous necrosis is extensive. Rabbits and modern humans develop a spectrum of disease that varies from that found in the mouse to that found in guinea pigs,

depending on the virulence of the bacilli and the native and acquired resistance expressed by the host. Both New Zealand white rabbits and immunocompetent adult human beings usually control the disease rather well due to an effective balance of tissue-damaging DTH and CMI (54). However, in both species, solid caseous tissue may liquefy and cavities may form. The bacilli may then multiply extracellularly, and may reach such large numbers that the strong immunity of the host cannot stop the fatal progression of the disease.

Other animal models are now being explored. For example, monkeys are used to a limited extent, and may be a necessity in the final evaluation stages of new tuberculosis vaccines. However, these animals are large and require sophisticated facilities, can be aggressive, can carry viruses fatal to humans, and present a perception problem for usage to the lay public.

Further models include the cow, which develops severe, multifocal, nodular calcified lesions in the lungs and head/neck lymph nodes after infection with *M.bovis*. Aquatic species such as goldfish and frogs have also been used (23, 213). These latter animals develop lesions after injection with the cold-adapted bacillus *M.marinum*; however while these models may provide some useful molecular genetic information the pathologic process is dissimilar to that seen in higher vertebrates and seems to have no acquired immunological basis.

In conclusion, understanding the host-mycobacteria relationship and pathogenesis is a formidable task with many controversies and uncertainties in the literature. The process of granulomagenesis in particular is an area of intense debate and these controversies can be found even within a single group of investigators. Currently, no single paradigm exists which completely explains the manifestation of pulmonary tuberculosis in mammals, however, it is reasonable to believe that continued accumulation of data, both *in vivo* and *in vitro*, will ultimately provide a comprehensive picture of tuberculosis.

References

1. **Aderem, A., and D. M. Underhill.** 1999. Mechanisms of phagocytosis in macrophages. Annu Rev Immunol. **17:**593-623.

2. **Agostini, C., L. Trentin, M. Facco, R. Sancetta, A. Cerutti, C. Tassinari, L. Cimarosto, F. Adami, A. Cipriani, R. Zambello, and G. Semenzato.** 1996. Role of IL-15, IL-2, and their receptors in the development of T cell alveolitis in pulmonary sarcoidosis. J Immunol. **157:**910-8.

3. **Agostini, C., R. Zambello, R. Sancetta, A. Cerutti, A. Milani, C. Tassinari, M. Facco, A. Cipriani, L. Trentin, and G. Semenzato.** 1996. Expression of tumor necrosis factor-receptor superfamily members by lung T lymphocytes in interstitial lung disease. Am J Respir Crit Care Med. **153:**1359-67.

4. **Akbar, A. N., M. Salmon, J. Savill, and G. Janossy.** 1993. A possible role for bcl-2 in regulating T-cell memory--a 'balancing act' between cell death and survival. Immunol Today. **14:**526-32.

5. **Altare, F., A. Durandy, D. Lammas, J. F. Emile, S. Lamhamedi, F. Le Deist, P. Drysdale, E. Jouanguy, R. Doffinger, F. Bernaudin, O. Jeppsson, J. A. Gollob, E. Meinl, A. W. Segal, A. Fischer, D. Kumararatne, and J. L. Casanova.** 1998. Impairment of mycobacterial immunity in human interleukin-12 receptor deficiency. Science. **280:**1432-5.

6. **Andersen, P.** 2001. TB vaccines: progress and problems. Trends Immunol. **22:**160-8.

7. **Andersen, P., A. Andersen, A. Sorenson, and S. Nagai.** 1995. Recall of long-lived immunity to *Mycobacterium tuberculosis* infection in mice. Journal of Immunology. **154:**3359-3372.

8. **Aung, H., Z. Toossi, S. M. McKenna, P. Gogate, J. Sierra, E. Sada, and E. A. Rich.** 2000. Expression of transforming growth factor-beta but not tumor necrosis factor-alpha, interferon-gamma, and interleukin-4 in granulomatous lung lesions in tuberculosis. Tuber Lung Dis. **80:**61-7.

9. **Balcewicz-Sablinska, M. K., J. Keane, H. Kornfeld, and H. G. Remold.** 1998. Pathogenic *Mycobacterium tuberculosis* evades apoptosis of host macrophages by release of TNF-R2, resulting in inactivation of TNF- alpha. J Immunol. **161:**2636-41.

10. **Barnes, P., S. Lu, J. Abrams, E. Wang, M. Yamamura, and R. Modlin.** 1993. Cytokine production at the site of disease in human tuberculosis. Infect. and Immunity. **61:**3482-3489.

11. **Beckman, E. M., S. A. Porcelli, C. T. Morita, S. M. Behar, S. T. Furlong, and M. B. Brenner.** 1994. Recognition of a lipid antigen by CD1-restricted alpha beta+ T cells. Nature. **372:**691-4.

12. **Bellamy, R., N. Beyers, K. P. McAdam, C. Ruwende, R. Gie, P. Samaai, D. Bester, M. Meyer, T. Corrah, M. Collin, D. R. Camidge, D. Wilkinson, E. Hoal-Van Helden, H. C. Whittle, W. Amos, P. van Helden, and A. V. Hill.** 2000. Genetic susceptibility to tuberculosis in Africans: a genome-wide scan. Proc Natl Acad Sci U S A. **97:**8005-9.

13. **Bellamy, R., and A. V. Hill.** 1998. Genetic susceptibility to mycobacteria and other infectious pathogens in humans. Curr Opin Immunol. **10:**483-7.

14. **Bendelac, A., N. Killeen, D. R. Littman, and R. H. Schwartz.** 1994. A subset of CD4+ thymocytes selected by MHC class I molecules. Science. **263:**1774-1778.

15. **Bergeron, A., M. Bonay, M. Kambouchner, D. Lecossier, M. Riquet, P. Soler, A. Hance, and A. Tazi.** 1997. Cytokine patterns in tuberculous and sarcoid granulomas: correlations with histopathologic features of the granulomatous response. J Immunol. **159:**3034-43.

16. **Bifani, P. J., B. Mathema, N. E. Kurepina, and B. N. Kreiswirth.** 2002. Global dissemination of the *Mycobacterium tuberculosis* W-Beijing family strains. Trends Microbiol. **10:**45-52.

17. **Birath, G.** 1969. Introduction of para-amino-salicylic acid and streptomycin in the treatment of tuberculosis. Recollections of the last 25 years. Scand J Respir Dis. **50:**204-9.

18. **Bitterman, P. B., L. E. Saltzman, S. Adelberg, V. J. Ferrans, and R. G. Crystal.** 1984. Alveolar macrophage replication. One mechanism for the expansion of the mononuclear phagocyte population in the chronically inflamed lung. J Clin Invest. **74:**460-9.

19. **Bloom, B. R. (ed.).** 1994. Tuberculosis. Pathogenesis, protection, and control, 1 ed, vol. 1. ASM Press, Washington, DC.

20. **Bloom, B. R., and J. D. McKinney.** 1999. The death and resurrection of tuberculosis. Nat Med. **5:**872-4.

21. **Boom, W. H., R. N. Husson, R. A. Young, J. R. David, and W. F. Piessens.** 1987. In vivo and in vitro characterization of murine T-cell clones reactive to *Mycobacterium tuberculosis*. Infect Immun. **55:**2223-9.

22. **Bosio, C. M., D. Gardner, and K. L. Elkins.** 2000. Infection of B cell-deficient mice with CDC 1551, a clinical isolate of *Mycobacterium tuberculosis*: delay in dissemination and development of lung pathology. J Immunol. **164:**6417-25.

23. **Bouley, D. M., N. Ghori, K. L. Mercer, S. Falkow, and L. Ramakrishnan.** 2001. Dynamic nature of host-pathogen interactions in *Mycobacterium marinum* granulomas. Infect Immun. **69:**7820-31.

24. **Brennan, P. J. a. D., D.** 1994. Ultrastructure of *Mycobacterium tuberculosis*, p. 271-284. *In* B. R. Bloom (ed.), Tuberculosis: pathogenesis, protection and control. ASM, New York.

25. **Brooks, J. V., A. A. Frank, M. A. Keen, J. T. Bellisle, and I. M. Orme.** 2001. Boosting vaccine for tuberculosis. Infect Immun. **69:**2714-7.

26. **Brunda, M. J.** 1994. Interleukin-12. J Leukoc Biol. **55:**280-8.

27. **Buckley, C. D., D. Pilling, J. M. Lord, A. N. Akbar, D. Scheel-Toellner, and M. Salmon.** 2001. Fibroblasts regulate the switch from acute resolving to chronic persistent inflammation. Trends Immunol. **22:**199-204.

28. **Camacho, L. R., D. Ensergueix, E. Perez, B. Gicquel, and C. Guilhot.** 1999. Identification of a virulence gene cluster of *Mycobacterium tuberculosis* by signature-tagged transposon mutagenesis. Mol Microbiol. **34:**257-67.

29. **Campbell, P. A.** 1994. Macrophage-Listeria interactions. Immunol Ser. **60:**313-28.

30. **Cardona, P. J., R. Llatjos, S. Gordillo, J. Diaz, I. Ojanguren, A. Ariza, and V. Ausina.** 2000. Evolution of granulomas in lungs of mice infected aerogenically with *Mycobacterium tuberculosis*. Scand J Immunol. **52:**156-63.

31. **Celada, F.** 1971. The cellular basis of immunologic memory. Prog Allergy. **15:**223-67.

32. **Chan, J., X. Fan, S. W. Hunter, P. J. Brennan, and B. R. Bloom.** 1991. Lipoarabinomannan, a possible virulence factor involved in the persistence of *Mycobacterium tuberculosis* within macrophages. Infect. Immunity. **59:**1755-1761.

33. **Chan, J., Y. Xing, R. S. Magliozzo, and B. R. Bloom.** 1992. Killing of virulent *Mycobacterium tuberculosis* by reactive nitrogen intermediates produced by activated murine macrophages. J Exp Med. **175:**1111-22.

34. **Chatterjee, D., A. D. Roberts, K. Lowell, P. J. Brennan, and I. M. Orme.** 1992. Structural basis of capacity of lipoarabinomannan to induce secretion of tumor necrosis factor. Infect Immunity. **60:**1249-53.

35. **Chensue, S. W., K. S. Warmington, J. H. Ruth, P. Lincoln, and S. L. Kunkel.** 1995. Cytokine function during mycobacterial and schistosomal antigen-induced pulmonary granuloma formation. Local and regional participation of IFN- gamma, IL-10, and TNF. J Immunol. **154:**5969-76.

36. **Chilosi, M., A. Mombello, M. Lestani, F. Menestrina, L. Fiore-Donati, A. Cipriani, R. Zambello, and G. Semenzato.** 1991. Immunohistochemical characterization of sarcoid granuloma: differentiation antigens and adhesion molecules. Sarcoidosis. **8:**171-2.

37. **Cole, S. T., R. Brosch, J. Parkhill, T. Garnier, C. Churcher, D. Harris, S. V. Gordon, K. Eiglmeier, S. Gas, C. E. Barry, 3rd, F. Tekaia, K. Badcock, D. Basham, D. Brown, T. Chillingworth, R. Connor, R. Davies, K. Devlin, T. Feltwell, S. Gentles, N. Hamlin, S. Holroyd, T. Hornsby, K. Jagels, B. G. Barrell, and et al.** 1998. Deciphering the biology of *Mycobacterium tuberculosis* from the complete genome sequence. Nature. **393:**537-44.

38. **Combadere, B., C. Blanc, T. Li, G. Carcelain, C. Delaugerre, V. Calvez, R. Tubiana, P. Debre, C. Katlama, and B. Autran.** 2000. CD4+Ki67+ lymphocytes in HIV-infected patients are effector T cells accumulated in the G1 phase of the cell cycle. Eur J Immunol. **30:**3598-603.

39. **Comstock, G. W.** 1982. Epidemiology of tuberculosis. Am Rev of Resp Dis. **125:**8-15.

40. **Constant, P., F. Davodeau, M. Peyrat, Y. Poquet, G. Puzo, M. Bonneville, and J. Fournie.** 1994. Stimulation of human gd T cells by no-peptidic mycobacterial ligands. Science. **264:**267-269.

41. **Cooper, A. M., C. D. D'Souza, A. A. Frank, and I. M. Orme.** 1997. The course of *Mycobacterium tuberculosis* infection in the lungs of mice lacking either perforin or granzyme mediated cytolytic mechanisms. Infect Immunity. **65:**1317-1320.

42. **Cooper, A. M., D. K. Dalton, T. A. Stewart, J. P. Griffin, D. G. Russell, and I. M. Orme.** 1993. Disseminated tuberculosis in interferon gamma gene-disrupted mice. J Exp Med. **178:**2243-7.

43. **Cooper, A. M., A. Kipnis, J. Turner, J. Magram, J. Ferrante, and I. M. Orme.** 2002. Mice Lacking Bioactive IL-12 Can Generate Protective, Antigen-Specific Cellular Responses to Mycobacterial Infection Only if the IL-12 p40 Subunit Is Present. J Immunol. **168:**1322-7.

44. **Cooper, A. M., J. Magram, J. Ferrante, and I. M. Orme.** 1997. IL-12 is crucial to the development of protective immunity in mice intravenously infected with *Mycobacterium tuberculosis*. Journal of Experimental Medicine. **186:**39-46.

45. **Cotran, R. S., Kumar, V and Collins T.** 1999. Robbins Pathologic Basis of Disease, Sixth ed. W.B Saunders Co, Philadelphia.

46. **D'Arcy Hart, P.** 1975. Response of macrophages to bacterial infection with special reference to their lysosomes. Pathol Biol (Paris). **23:**451-2.

47. **D'Esopo, N. D.** 1982. Clinical trials in pulmonary tuberculosis. Am Rev Respir Dis. **125:**85-93.

48. **D'Souza, C. D., A. M. Cooper, A. A. Frank, R. J. Mazzaccaro, B. R. Bloom, and I. M. Orme.** 1997. An anti-inflammatory role for gamma delta T lymphocytes in acquired immunity to *Mycobacterium tuberculosis.* J Immunol. **158:**1217-21.

49. **Dahl, K. E., H. Shiratsuchi, B. D. Hamilton, J. J. Ellner, and Z. Toossi.** 1996. Selective induction of transforming growth factor beta in human monocytes by lipoarabinomannan of *Mycobacterium tuberculosis.* Infect Immun. **64:**399-405.

50. **Daniel, T. M.** 1997. Captain of Death: The Story of Tuberculosis. University of Rochester Press, Rochester, NY.

51. **Dannenberg, A. M., Jr.** 1968. Cellular hypersensitivity and cellular immunity in the pathogensis of tuberculosis: specificity, systemic and local nature, and associated macrophage enzymes. Bacteriol Rev. **32:**85-102.

52. **Dannenberg, A. M., Jr.** 1991. Delayed-type hypersensitivity and cell-mediated immunity in the pathogenesis of tuberculosis. Immunol Today. **12:**228-33.

53. **Dannenberg, A. M.** 1984. Pathogenesis of tuberculosis: native and acquired resistance in animals and humans. ASM Press, Washington DC.

54. **Dannenberg, A. M., Jr., and F. M. Collins.** 2001. Progressive pulmonary tuberculosis is not due to increasing numbers of viable bacilli in rabbits, mice and guinea pigs, but is due to a continuous host response to mycobacterial products. Tuberculosis. **81:**229-42.

55. **De Cock, K. M., B. Soro, I. M. Coulibaly, and S. B. Lucas.** 1992. Tuberculosis and HIV infection in sub-Saharan Africa. Jama. **268:**1581-7.

56. **Doetsch, R. N.** 1978. Benjamin Marten and his "New Theory of Consumptions". Microbiol Rev. **42:**521-528.

57. **Dubos, R. a. D., J.** 1952. Tuberculosis, Man, and Society: The Whte Plague. Little, Brown and Co, Boston.

58. **Dye, C., S. Scheele, P. Dolin, V. Pathania, and M. C. Raviglione.** 1999. Consensus statement. Global burden of tuberculosis: estimated incidence, prevalence, and mortality by country. WHO Global Surveillance and Monitoring Project. JAMA. **282:**677-86.

59. **Elliot, D. E.** 1999. The Granulomatous Disorders. Coordinating ed., D. a. Z. Geraint James, A. Cambridge University Press, Cambridge.

60. **Enthammer, C., R. Zambello, L. Trentin, A. Cerutti, A. Milani, P. Bulian, A. Cipriani, S. Garbisa, C. Agostini, and G. Semenzato.** 1993. Synthesis and release of granulocyte--macrophage colony--stimulating factor by alveolar macrophages of patients with sarcoidosis. Sarcoidosis. **10:**147-8.

61. **Fenton, M. J., M. W. Vermeulen, S. Kim, M. Burdick, R. M. Strieter, and H. Kornfeld.** 1997. Induction of gamma interferon production in human alveolar macrophages by *Mycobacterium tuberculosis*. Infect Immun. **65:**5149-56.

62. **Ferrari, G., H. Langen, M. Naito, and J. Pieters.** 1999. A coat protein on phagosomes involved in the intracellular survival of mycobacteria. Cell. **97:**435-47.

63. **Ferreri, N. R., I. Millet, V. Paliwal, W. Herzog, D. Solomon, R. Ramabhadran, and P. W. Askenase.** 1991. Induction of macrophage TNF alpha, IL-1, IL-6, and PGE2 production by DTH-initiating factors. Cell Immunol. **137:**389-405.

64. **Fine, P. E.** 2001. BCG: the challenge continues. Scand J Infect Dis. **33:**243-5.

65. **Flynn, J. L., and J. Chan.** 2001. Immunology of tuberculosis. Annu Rev Immunol. **19:**93-129.

66. **Flynn, J. L., J. Chan, K. J. Triebold, D. K. Dalton, T. A. Stewart, and B. R. Bloom.** 1993. An essential role for interferon gamma in resistance to *Mycobacterium tuberculosis* infection. Journal of Experimental Medicine. **178:**2249-54.

67. **Flynn, J. L., M. M. Goldstein, J. Chan, K. J. Triebold, K. Pfeffer, C. J. Lowenstein, R. Schreiber, T. W. Mak, and B. R. Bloom.** 1995. Tumor necrosis factor-alpha is required in the protective immune response against *Mycobacterium tuberculosis* in mice. Immunity. **2:**561-72.

68. **Forbes, J.** 1962. Laennec R.T.H - A treatise on the disease of the chest (Translated by John Forbes). Hafner Publishing Company, New York. NY.

69. **Forget, A., J. C. Benoit, R. Turcotte, and N. Gusew-Chartrand.** 1976. Enhancement activity of anti-mycobacterial sera in experimental *Mycobacterium bovis* (BCG) infection in mice. Infect Immun. **13:**1301-6.

70. **Fowlkes, B. J., A. M. Kruisbeek, H. Ton-That, M. A. Weston, J. E. Coligan, R. H. Schwartz, and D. M. Pardoll.** 1987. A novel population of T-cell receptor alpha beta-bearing thymocytes which predominantly expresses a single V beta gene family. Nature. **329:**251-4.

71. **Francis, J.** 1958. Tuberculosis in Animals and Man: A study in Comparative Pathology. Cassell and co., London, England.

72. **Fratazzi, C., R. D. Arbeit, C. Carini, and H. G. Remold.** 1997. Programmed cell death of *Mycobacterium avium* serovar 4-infected human macrophages prevents the mycobacteria from spreading and induces mycobacterial growth inhibition by freshly added, uninfected macrophages. J Immunol. **158:**4320-7.

73. **Gaudier, B. a. G.-R.** 1962. Etude experimentale de la vitalite du B.C.G au cours de la traversee gastro-intestinale chez enfants non allergiques vaccines par voie digestive. Ann. Inst. Pasteur Lille. **13:**77-87.

74. **Gaynor, C. D., F. X. McCormack, D. R. Voelker, S. E. McGowan, and L. S. Schlesinger.** 1995. Pulmonary surfactant protein A mediates enhanced phagocytosis of *Mycobacterium tuberculosis* by a direct interaction with human macrophages. J Immunol. **155:**5343-51.

75. **George, K. M., Y. Yuan, D. R. Sherman, and C. E. Barry, 3rd.** 1995. The biosynthesis of cyclopropanated mycolic acids in *Mycobacterium tuberculosis*. Identification and functional analysis of CMAS-2. J Biol Chem. **270:**27292-8.

76. **Goldfeld, A. E., J. C. Delgado, S. Thim, M. V. Bozon, A. M. Uglialoro, D. Turbay, C. Cohen, and E. J. Yunis.** 1998. Association of an HLA-DQ allele with clinical tuberculosis. Jama. **279:**226-8.

77. **Gonzalez-Juarrero, M., and I. M. Orme.** 2001. Characterization of murine lung dendritic cells infected with *Mycobacterium tuberculosis*. Infect Immun. **69:**1127-33.

78. **Grange, J. M., J. Gibson, T. W. Osborn, C. H. Collins, and M. D. Yates.** 1983. What is BCG? Tubercle. **64:**129-39.

79. **Griffin, J. P., K. V. Harshan, W. K. Born, and I. M. Orme.** 1991. Kinetics of accumulation of gamma delta receptor-bearing T lymphocytes in mice infected with live mycobacteria. Infect. Immunity. **59:**4263-5.

80. **Griffin, J. P., and I. M. Orme.** 1994. Evolution of CD4 T-cell subsets following infection of naive and memory immune mice with *Mycobacterium tuberculosis*. Infect. Immunity. **62:**1683-90.

81. **Grzybowski, S.** 1991. Tuberculosis in the Third World. Thorax. **46:**689-91.

82. **Gumperz, J. E., and M. B. Brenner.** 2001. CD1-specific T cells in microbial immunity. Curr Opin Immunol. **13:**471-8.

83. **Hayakawa, K., B. T. Lin, and R. R. Hardy.** 1992. Murine thymic CD4+ T cell subsets: a subset (Thy0) that secretes diverse cytokines and overexpresses the V beta 8 T cell receptor gene family. J Exp Med. **176:**269-74.

84. **Hernandez-Pando, R., L. Pavon, K. Arriaga, H. Orozco, V. Madrid-Marina, and G. Rook.** 1997. Pathogenesis of tuberculosis in mice exposed to low and high doses of an environmental mycobacterial saprophyte before infection. Infect Immun. **65:**3317-27.

85. **Hirsch, C. S., J. J. Ellner, R. Blinkhorn, and Z. Toossi.** 1997. In vitro restoration of T cell responses in tuberculosis and augmentation of monocyte effector function against *Mycobacterium tuberculosis* by natural inhibitors of transforming growth factor beta. Proc Natl Acad Sci U S A. **94:**3926-31.

86. **Hirsch, C. S., T. Yoneda, L. Averill, J. J. Ellner, and Z. Toossi.** 1994. Enhancement of intracellular growth of *Mycobacterium tuberculosis* in human monocytes by transforming growth factor-β1. J Inf. Dis. **170:**1229-1237.

87. **Hochberg, L.** 1960. Thoracic surgery before the 20th century. Vantage Press, New York.

88. **Howard, M., and A. O'Garra.** 1992. Biological properties of interleukin 10. Immunol Today. **13:**198-200.

89. **Humphreys, B. D., J. Rice, S. B. Kertesy, and G. R. Dubyak.** 2000. Stress-activated protein kinase/JNK activation and apoptotic induction by the macrophage P2X7 nucleotide receptor. J Biol Chem. **275:**26792-8.

90. **Hunninghake, G. W., and R. G. Crystal.** 1981. Pulmonary sarcoidosis: a disorder mediated by excess helper T- lymphocyte activity at sites of disease activity. N Engl J Med. **305:**429-34.

91. **Huseby, J. S., and L. D. Hudson.** 1976. Miliary tuberculosis and adult respiratory distress syndrome. Ann Intern Med. **85:**609-11.

92. **Ilangumaran, S., S. Arni, M. Poincelet, J. M. Theler, P. J. Brennan, D. Nasir ud, and D. C. Hoessli.** 1995. Integration of mycobacterial lipoarabinomannans into glycosylphosphatidylinositol-rich domains of lymphomonocytic cell plasma membranes. J Immunol. **155:**1334-42.

93. **Ina, Y., K. Takada, A. Miyachi, M. Noda, T. Sato, H. Hashiba, S. Ito, N. Iijima, M. Yamamoto, M. Morishita, and et al.** 1991. [Interleukin-2 receptor expression in pulmonary granulomatous diseases]. Nihon Kyobu Shikkan Gakkai Zasshi. **29:**407-12.

94. **Inoue, T., Y. Yoshikai, G. Matsuzaki, and K. Nomoto.** 1991. Early appearing gamma/delta-bearing T cells during infection with Calmette Guerin bacillus. J Immunol. **146:**2754-62.

95. **James, D. G.** 1995. Granuloma formation signifies a Th1 cell profile. Sarcoidosis. **12:**95-7.

96. **Janeway, C. A., Travers, P., Walport, M and Capra, J.D.** 1999. Immunobiology. The Immune System in Health and Disease, Fourth ed. Current Biology Publications, London, UK.

97. **Jones, T. C., Hunt, R.D., King, N.W.** 1997. Veterinary Pathology, Sixth ed. Williams and Wilkins, Baltimore, MD.

98. **Jungblut, P. R., U. E. Schaible, H. J. Mollenkopf, U. Zimny-Arndt, B. Raupach, J. Mattow, P. Halada, S. Lamer, K. Hagens, and S. H. Kaufmann.** 1999. Comparative proteome analysis of *Mycobacterium tuberculosis* and *Mycobacterium bovis* BCG strains: towards functional genomics of microbial pathogens. Mol Microbiol. **33:**1103-17.

99. **Kabelitz, D., A. Bender, S. Schondelmaier, B. Schoel, and S. H. E. Kaufmann.** 1990. A large fraction of human peripheral blood γ/δ+ T cells is activated by *Mycobacterium tuberculosis* but not by its 65-kD heat shock protein. J.Exp.Med. **171:**667-679.

100. **Kaplan, G.** 1994. Cytokine regulation of disease progression in leprosy and tuberculosis. Immunobiology. **191:**564-8.

101. **Karlson, A. G.** 1960. Tubrculosis caused by human, bovine and avian tubercle bacilli in various animals. Proc. U.S. Livestock Sanitary Assoc. **64:**194-201.

102. **Keane, J., M. K. Balcewicz-Sablinska, H. G. Remold, G. L. Chupp, B. B. Meek, M. J. Fenton, and H. Kornfeld.** 1997. Infection by *Mycobacterium tuberculosis* promotes human alveolar macrophage apoptosis. Infect Immun. **65:**298-304.

103. **Kennedy, M. K., K. S. Picha, K. D. Shanebeck, D. M. Anderson, and K. H. Grabstein.** 1994. Interleukin-12 regulates the proliferation of Th1, but not Th2 or Th0, clones. Eur J Immunol. **24:**2271-8.

104. **Kindler, V., A.-P. Sappino, G. Grau, P.-F. Piguet, and P. Vassali.** 1989. The inducing role of tumor necrosis factor in the development of bacterial granulomas during BCG infection. Cell. **56:**731-740.

105. **Klingler, K., K. M. Tchou-Wong, O. Brandli, C. Aston, R. Kim, C. Chi, and W. N. Rom.** 1997. Effects of mycobacteria on regulation of apoptosis in mononuclear phagocytes. Infect Immun. **65:**5272-8.

106. **Kobzik, L.** 1999. The Lung, p. 697-755, Robbins Pathologic Basis of Disease, sixth ed. W.B Saunders Company, Philadelphia, PA.

107. **Koch, R.** 1882. Aeteologie der Tuberkulose. Berlin Klin Wochenchr. **19:**221-30.

108. **Koch, R.** 1891. Fortsetzung uber ein Heilmittel gegen Tuberculose. Dtsch. Med. Wochenschr. **17:**101-102.

109. **Kochan, I.** 1973. The role of iron in bacterial infections, with special consideration of host-tubercle bacillus interaction. Curr Top Microbiol Immunol. **60:**1-30.

110. **Kochi, A., B. Vareldzis, and K. Styblo.** 1993. Multidrug-resistant tuberculosis and its control. Res Microbiol. **144:**104-10.

111. **Kohno, K., J. Kataoka, T. Ohtsuki, Y. Suemoto, I. Okamoto, M. Usui, M. Ikeda, and M. Kurimoto.** 1997. IFN-gamma-inducing factor (IGIF) is a costimulatory factor on the activation of Th1 but not Th2 cells and exerts its effect independently of IL-12. J Immunol. **158:**1541-50.

112. **Krishnaswamy, G., J. Kelley, L. Yerra, J. K. Smith, and D. S. Chi.** 1999. Human endothelium as a source of multifunctional cytokines: molecular regulation and possible role in human disease. J Interferon Cytokine Res. **19:**91-104.

113. **Krombach, F., J. T. Gerlach, C. Padovan, A. Burges, J. Behr, T. Beinert, and C. Vogelmeier.** 1996. Characterization and quantification of alveolar monocyte-like cells in human chronic inflammatory lung disease. Eur Respir J. **9:**984-91.

114. **Kunkel, S. L., N. W. Lukacs, R. M. Strieter, and S. W. Chensue.** 1996. Th1 and Th2 responses regulate experimental lung granuloma development. Sarcoidosis Vasc Diffuse Lung Dis. **13:**120-8.

115. **Ladel, C. H., C. Blum, A. Dreher, K. Reifenberg, and S. H. Kaufmann.** 1995. Protective role of gamma/delta T cells and alpha/beta T cells in tuberculosis. Eur J Immunol. **25:**2877-81.

116. **Ladel, C. H., C. Blum, A. Dreher, K. Reifenberg, M. Kopf, and S. H. E. Kaufmann.** 1997. Lethal tuberculosis in interleukin-6-deficient mice. Infection and Immunity. **65:**4843-4849.

117. **Ladel, C. H., S. Daugelat, and S. H. Kaufmann.** 1995. Immune response to *Mycobacterium bovis* bacille Calmette Guerin infection in major histocompatibility complex class I- and II-deficient knock-out mice: contribution of CD4 and CD8 T cells to acquired resistance. Eur J Imm. **25:**377-84.

118. **Lalvani, A., R. Brookes, R. J. Wilkinson, A. S. Malin, A. A. Pathan, P. Andersen, H. Dockrell, G. Pasvol, and A. V. Hill.** 1998. Human cytolytic and interferon gamma-secreting CD8+ T lymphocytes specific for *Mycobacterium tuberculosis*. Proc Natl Acad Sci U S A. **95:**270-5.

119. **Lambert, H. P.** 1960. The influence of chemoprophylaxis on immunity in experimental tuberculosis. Am Rev. Respir Dis. **82:**619.

120. **Lamhamedi, S., E. Jouanguy, F. Altare, J. Roesler, and J. L. Casanova.** 1998. Interferon-gamma receptor deficiency: relationship between genotype, environment, and phenotype (Review). Int J Mol Med. **1:**415-8.

121. **Laochumroonvorapong, P., S. Paul, K. B. Elkon, and G. Kaplan.** 1996. H2O2 induces monocyte apoptosis and reduces viability of *Mycobacterium avium-M. intracellulare* within cultured human monocytes. Infect Immun. **64:**452-9.

122. **Lefford, M. J., and D. D. McGregor.** 1974. Immunological memory in tuberculosis. I. Influence of persisting organisms. Cell Immunol. **14:**417.

123. **Lefford, M. J., D. D. McGregor, and G. B. Mackaness.** 1973. Immune response to *Mycobacterium tuberculosis* in rats. Infect Immunity. **8:**182-189.

124. **Lenardo, M. J.** 1996. Fas and the art of lymphocyte maintenance. J Exp Med. **183:**721-4.

125. **Leveton, C., S. Barnass, B. Champion, S. Lucas, B. D. Souza, M. Nicol, D. Banerjee, and G. Rook.** 1989. T-cell-mediated protection of mice against virulent *Mycobacterium tuberculosis*. Infect. Immunity. **57:**390-395.

126. **Lin, Y., M. Zhang, F. M. Hofman, J. Gong, and P. F. Barnes.** 1996. Absence of a prominent Th2 cytokine response in human tuberculosis. Infect. Immunity. **64:**1351-6.

127. **Lipscomb, M. F., D. E. Bice, C. R. Lyons, M. R. Schuyler, and D. Wilkes.** 1995. The regulation of pulmonary immunity. Adv Immunol. **59:**369-455.

128. **Lopez, A. D., and C. C. Murray.** 1998. The global burden of disease, 1990-2020. Nat Med. **4:**1241-3.

129. **Lukacs, N. W., and P. A. Ward.** 1996. Inflammatory mediators, cytokines, and adhesion molecules in pulmonary inflammation and injury. Adv Immunol. **62:**257-304.

130. **Lurie, M. B.** 1964. Resistance to tuberculosis: Experimental studies in native and acquired defensive mechanisms. Harvard University Press, Cambridge, MA.

131. **Mackaness, G. B.** 1964. The influence of immunologically committed lymphoid cells on macrophage activity in vivo. J. Exp. Med. **129:**973-92.

132. **Major, R. H.** 1945. Classic Descriptions of Disease, Third ed. Charles C Thomas Publishing, Springfield, IL.

133. **Manchester, K.** 1984. Tuberculosis and leprosy in antiquity: An interpretation. Med Hist. **28:**162-173.

134. **Marchal, G.** 1997. Recently transmitted tuberculosis is more frequent than reactivation of latent infections. Int J Tuberc Lung Dis. **1:**192.

135. **McKeown, T.** 1979. The Role of Medicine: Dream, Mirage or Nemesis? Basil Blackwell, Oxford.

136. **McKinney, J. D., K. Honer zu Bentrup, E. J. Munoz-Elias, A. Miczak, B. Chen, W. T. Chan, D. Swenson, J. C. Sacchettini, W. R. Jacobs, Jr., and D. G. Russell.** 2000. Persistence of *Mycobacterium tuberculosis* in macrophages and mice requires the glyoxylate shunt enzyme isocitrate lyase. Nature. **406:**735-8.

137. **Mdluli, K., D. R. Sherman, M. J. Hickey, B. N. Kreiswirth, S. Morris, C. K. Stover, and C. E. Barry, 3rd.** 1996. Biochemical and genetic data suggest that InhA is not the primary target for activated isoniazid in *Mycobacterium tuberculosis*. J Infect Dis. **174:**1085-90.

138. **Means, T. K., S. Wang, E. Lien, A. Yoshimura, D. T. Golenbock, and M. J. Fenton.** 1999. Human toll-like receptors mediate cellular activation by *Mycobacterium tuberculosis*. J Immunol. **163:**3920-7.

139. **Medina, E., and R. J. North.** 1998. Resistance ranking of some common inbred mouse strains to *Mycobacterium tuberculosis* and relationship to major histocompatibility complex haplotype and Nramp1 genotype. Immunology. **93:**270-4.

140. **Middlebrook, G.** 1954. Isoniazid-resistance and catalase activity of tubercle bacilli. Am Rev Tuberc. **69:**471-472.

141. **Mohan, V. P., C. A. Scanga, K. Yu, H. M. Scott, K. E. Tanaka, E. Tsang, M. M. Tsai, J. L. Flynn, and J. Chan.** 2001. Effects of tumor necrosis factor alpha on host immune response in chronic persistent tuberculosis: possible role for limiting pathology. Infect Immun. **69:**1847-55.

142. **Molloy, A., P. Laochumroonvorapong, and G. Kaplan.** 1994. Apoptosis, but not necrosis, of infected monocytes is coupled with killing of intracellular Bacillus Calmette-Guerin. J Exp Med. **180:**1499-1509.

143. **Mosmann, T. R., H. Cherwinski, M. W. Bond, M. A. Giedlin, and R. L. Coffman.** 1986. Two types of murine helper T cell clone. I. Definition according to profiles of lymphokine activities and secreted proteins. J Immunol. **136:**2348-57.

144. **Muller, I., S. P. Cobbold, H. Waldmann, and S. H. Kaufmann.** 1987. Impaired resistance to *Mycobacterium tuberculosis* infection after selective in vivo depletion of L3T4+ and Lyt-2+ T cells. Infect Immun. **55:**2037-41.

145. **Murray, P. J., and R. A. Young.** 1999. Increased Antimycobacterial Immunity in Interleukin-10-Deficient Mice. Infect Immunity. **67:**3087-3095.

146. **Nacy, C. A., and M. S. Meltzer.** 1991. T-cell-mediated activation of macrophages. Curr Opin Immunol. **3:**330-5.

147. **Naef, A.** 1990. The story of thoracic surgery. Milestones and Pioneers. Hoegrefe and Huber Publishers, Toronto.

148. **Newport, M. J., C. M. Huxeley, S. Huston, B. A. Hawrylowicz, B. A. Oostra, R. Williamson, and M. Levin.** 1996. A mutation in the interferon-g receptor gene and susceptibility to mycobacterial infection. New Eng J Med. **335:**1941-1949.

149. **Nicholson, S., G. Bonecini-Almeida Mda, J. R. Lapa e Silva, C. Nathan, Q. W. Xie, R. Mumford, J. R. Weidner, J. Calaycay, J. Geng, N. Boechat, and et al.** 1996. Inducible nitric oxide synthase in pulmonary alveolar macrophages from patients with tuberculosis. J Exp Med. **183:**2293-302.

150. **North, R. J.** 1973. Importance of thymocyte-derived lymphocytes in cell-mediated immunity to infection. Cell Immunol. **7:**166-176.

151. **North, R. J.** 1998. Mice incapable of making IL-4 or IL-10 display normal resistance to infection with *Mycobacterium tuberculosis*. Clin Exp Immunol. **113:**55-8.

152. **North, R. J., and A. A. Izzo.** 1993. Mycobacterial virulence. Virulent strains of *Mycobacteria tuberculosis* have faster in vivo doubling times and are better equipped to resist growth-inhibiting functions of macrophages in the presence and absence of specific immunity. J Exp Med. **177:**1723-33.

153. **Oddo, M., T. Renno, A. Attinger, T. Bakker, H. R. MacDonald, and P. R. A. Meylan.** 1998. Fas ligand-induced apoptosis of infected human macrophages reduces the viability of intracellular *Mycobacterium tuberculosis.* J Immunol. **160:**5448-5454.

154. **Ohta, M., T. Okabe, K. Ozawa, A. Urabe, and F. Takaku.** 1986. In vitro formation of macrophage-epithelioid cells and multinucleated giant cells by 1 alpha,25-dihydroxyvitamin D3 from human circulating monocytes. Ann N Y Acad Sci. **465:**211-20.

155. **Oppmann, B., R. Lesley, B. Blom, J. C. Timans, Y. Xu, B. Hunte, F. Vega, N. Yu, J. Wang, K. Singh, F. Zonin, E. Vaisberg, T. Churakova, M. Liu, D. Gorman, J. Wagner, S. Zurawski, Y. Liu, J. S. Abrams, K. W. Moore, D. Rennick, R. de Waal-Malefyt, C. Hannum, J. F. Bazan, and R. A. Kastelein.** 2000. Novel p19 protein engages IL-12p40 to form a cytokine, IL-23, with biological activities similar as well as distinct from IL-12. Immunity. **13:**715-25.

156. **Organization, World Health.** 2002. WHO report 2002. Global Tuberculosis Control. Surveillance, Planning and Financing. World Health Organization.

157. **Orme, I., and F. Collins.** 1983. Protection against *Mycobacterium tuberculosis* infection by adoptive immunotherapy. Requirement for T cell-deficient recipients. J Exp Med. **158:**74-83.

158. **Orme, I. M.** 1987. The kinetics of emergence and loss of mediator T lymphocytes acquired in response to infection with *Mycobacterium tuberculosis.* J Immunol. **138:**293-8.

159. **Orme, I. M., and A. M. Cooper.** 1999. Cytokine/chemokine cascades in immunity to tuberculosis. Immunol Today. **20:**307-12.

160. **Orme, I. M., D. N. McMurray, and J. T. Belisle.** 2001. Tuberculosis vaccine development: recent progress. Trends Microbiol. **9:**115-8.

161. **Orme, I. M., E. S. Miller, A. D. Roberts, S. K. Furney, J. P. Griffin, K. M. Dobos, D. Chi, B. Rivoire, and P. J. Brennan.** 1992. T lymphocytes mediating protection and cellular cytolysis during the course of *Mycobacterium tuberculosis* infection. Evidence for different kinetics and recognition of a wide spectrum of protein antigens. Journal of Immunology. **148:**189-96.

162. **Orme, I. M., A. D. Roberts, J. P. Griffin, and J. S. Abrams.** 1993. Cytokine secretion by CD4 T lymphocytes acquired in response to *Mycobacterium tuberculosis* infection. J Immunol. **151:**518-25.

163. **Palmer, C. E., and M. W. Long.** 1966. Effects of infection with atypical mycobacteria on BCG vaccination and tuberculosis. Am Rev Respir Dis. **94:**553-68.

164. **Pancholi, P., A. Mirza, N. Bhardwaj, and R. M. Steinman.** 1993. Sequestration from the immune CD4+ T cells of mycobacteria growing in human macrophages. Science. **260:**984-986.

165. **Parrish, N. M., J. D. Dick, and W. R. Bishai.** 1998. Mechanisms of latency in *Mycobacterium tuberculosis*. Trends Microbiol. **6:**107-12.

166. **Pfuetze, K. H., Pyle, M.M., Hinshaw, H.C and Feldman, W.H.** 1955. The first clinical trial of streptomycin in human tuberculosis. Am. Rev. Tuberc. **71:**752-754.

167. **Placido, R., G. Mancino, A. Amendola, F. Mariani, S. Vendetti, M. Piacentini, A. Sanduzzi, M. L. Bocchino, M. Zembala, and V. Colizzi.** 1997. Apoptosis of human monocytes/macrophages in *Mycobacterium tuberculosis* infection. J Pathol. **181:**31-8.

168. **Premack, B. A., and T. J. Schall.** 1996. Chemokine receptors: Gateways to inflammation and infection. Nature Medicine. **2:**1174-1178.

169. **Prescott. L, H. J. a. K. D.** 1999. Microbiology, Fourth ed. WCB McGraw-Hill, New York.

170. **Prieditis, H., and I. Y. Adamson.** 1996. Alveolar macrophage kinetics and multinucleated giant cell formation after lung injury. J Leukoc Biol. **59:**534-8.

171. **Quiding-Jarbrink, M., D. A. Smith, and G. J. Bancroft.** 2001. Production of matrix metalloproteinases in response to mycobacterial infection. Infect Immun. **69:**5661-70.

172. **Rhoades, E. R., A. A. Frank, and I. M. Orme.** 1997. Progression of chronic pulmonary tuberculosis in mice aerogenically infected with virulent *Mycobacterium tuberculosis*. Tuber Lung Dis. **78:**57-66.

173. **Riley, R., and F. O'Grady.** 1961. Airborne infection:Transmission and control. The Macmillan Company, New York NY.

174. **Roach, D. R., H. Briscoe, B. Saunders, M. P. France, S. Riminton, and W. J. Britton.** 2001. Secreted lymphotoxin-alpha is essential for the control of an intracellular bacterial infection. J Exp Med. **193:**239-46.

175. **Robitzek, E. H. a. S., I.J.** 1952. Hyradzine derivatives of isonicotinic acid. Am. Rev. Tuberc. **65:**402-428.

176. **Rojas, M., M. Olivier, P. Gros, L. F. Barrera, and L. F. Garcia.** 1999. TNF-alpha and IL-10 modulate the induction of apoptosis by virulent *Mycobacterium tuberculosis* in murine macrophages. J Immunol. **162:**6122-31.

177. **Rook, G. A., G. M. Bahr, and J. L. Stanford.** 1981. The effect of two distinct forms of cell-mediated response to mycobacteria on the protective efficacy of BCG. Tubercle. **62:**63-8.

178. **Rouillon, A., S. Perdrizet, and R. Parrot.** 1976. Transmission of tubercle bacilli: The effects of chemotherapy. Tubercle. **57:**275-99.

179. **Sanchez, F. O., J. I. Rodriguez, G. Agudelo, and L. F. Garcia.** 1994. Immune responsiveness and lymphokine production in patients with tuberculosis and healthy controls. Infection & Immunity. **62:**5673-8.

180. **Saunders, B. M., A. A. Frank, I. M. Orme, and A. M. Cooper.** 2000. Interleukin-6 induces early gamma interferon production in the infected lung but is not required for generation of specific immunity to *Mycobacterium tuberculosis* infection. Infect Immun. **68:**3322-6.

181. **Schatz, A., Bugie, E and Waksman S.A.** 1944. Streptomycin, a substance exhibiting antibiotic activity against gram-positive and gram negative bacteria. Proc. Exptl Biol Med. **55:**66-69.

182. **Schauf, V., W. N. Rom, K. A. Smith, E. P. Sampaio, P. A. Meyn, J. M. Tramontana, Z. A. Cohn, and G. Kaplan.** 1993. Cytokine gene activation and modified responsiveness to interleukin-2 in the blood of tuberculosis patients. J Infect Dis. **168:**1056-9.

183. **Schlesinger, L., C. Bellinger-Kawahara, N. Payne, and e. al.** 1990. Phagocytosis of *Mycobacterium tuberculosis* is mediated by human monocyte complement receptors and complement component C3. J Immunol. **144:**2771-2780.

184. **Schlesinger, L. S.** 1993. Macrophage phagocytosis of virulent but not attenuated strains of *Mycobacterium tuberculosis* is mediated by mannose receptors in addition to complement receptors. Journal of Immunology. **150:**2920-2930.

185. **Schlesinger, L. S., S. R. Hull, and T. M. Kaufman.** 1994. Binding of the terminal mannosyl units of lipoarabinomannan from a virulent strain of *Mycobacterium tuberculosis* to human macrophages. Journal of Immunology. **152:**4070-4074.

186. **Seibert, F. B. a. G., J.T.** 1941. Tuberculin purified protein derivative:prepartion and analyses of a large quantity of standard. Am REv Tuberc. **44:**9-25.

187. **Seibert, F. B. a. M., B.** 1932. The chemical composition of the active principles of tuberculin. XV. A precipitated purified tuberculin protein suitable for the preparation of a standard tuberculin. Am Rev Tuberc. **25:**724-737.

188. **Shafer, R. W., K. D. Chirgwin, A. E. Glatt, M. A. Dahdouh, S. H. Landesman, and B. Suster.** 1991. HIV prevalence, immunosuppression, and drug resistance in patients with tuberculosis in an area endemic for AIDS. Aids. **5:**399-405.

189. **Shahar, I., E. Fireman, M. Topilsky, J. Grief, S. Kivity, Z. Spirer, and S. Ben Efraim.** 1996. Effect of IL-6 on alveolar fibroblast proliferation in interstitial lung diseases. Clin Immunol Immunopathol. **79:**244-51.

190. **Shams, H., B. Wizel, S. E. Weis, B. Samten, and P. F. Barnes.** 2001. Contribution of CD8(+) T cells to gamma interferon production in human tuberculosis. Infect Immun. **69:**3497-501.

191. **Shanklin, D. R., M. V. Stevens, M. F. Hall, and D. L. Smalley.** 2000. Environmental immunogens and T-cell-mediated responses in fibromyalgia: evidence for immune dysregulation and determinants of granuloma formation. Exp Mol Pathol. **69:**102-18.

192. **Shanley, T. P., R. L. Warner, and P. A. Ward.** 1995. The role of cytokines and adhesion molecules in the development of inflammatory injury. Mol Med Today. **1:**40-5.

193. **Shilova, M. V., and C. Dye.** 2001. The resurgence of tuberculosis in Russia. Philos Trans R Soc Lond B Biol Sci. **356:**1069-75.

194. **Sieling, P. A., D. Chatterjee, S. A. Porcelli, T. I. Prigozy, R. J. Mazzaccaro, T. Soriano, B. R. Bloom, M. B. Brenner, M. Kronenberg, P. J. Brennan, and et al.** 1995. CD1-restricted T cell recognition of microbial lipoglycan antigens. Science. **269:**227-30.

195. **Skeen, M. J., and H. K. Ziegler.** 1995. Activation of gamma delta T cells for production of IFN-gamma is mediated by bacteria via macrophage-derived cytokines IL-1 and IL-12. J Immunol. **154:**5832-41.

196. **Skjot, R. L., T. Oettinger, I. Rosenkrands, P. Ravn, I. Brock, S. Jacobsen, and P. Andersen.** 2000. Comparative evaluation of low-molecular-mass proteins from *Mycobacterium tuberculosis* identifies members of the ESAT-6 family as immunodominant T-cell antigens. Infect Immun. **68:**214-20.

197. **Smith.** 1917. In 'Tuberculosis in Animals and Man': A study in comparative pathology. Ed. Francis, J. Cassell and co., London, England

198. **Smith, R. E., R. M. Strieter, K. Zhang, S. H. Phan, T. J. Standiford, N. W. Lukacs, and S. L. Kunkel.** 1995. A role for C-C chemokines in fibrotic lung disease. J Leukoc Biol. **57:**782-7.

199. **Sneider, D. E.** 1993. Tuberculosis: the world situation. History of the disease and efforts to combat it. *In* K. McAdam (ed.), Tuberculosis: Back to the Future. John Wiley and Sons, Cichester, UK.

200. **Sousa, A. O., R. J. Mazzaccaro, R. G. Russell, F. K. Lee, O. C. Turner, S. Hong, L. Van Kaer, and B. R. Bloom.** 2000. Relative contributions of distinct MHC class I-dependent cell populations in protection to tuberculosis infection in mice. Proc Natl Acad Sci U S A. **97:**4204-8.

201. **Stenger, S.** 2001. Cytolytic T cells in the immune response to *mycobacterium tuberculosis*. Scand J Infect Dis. **33:**483-7.

202. **Stenger, S., R. J. Mazzaccaro, K. Uyemura, S. Cho, P. F. Barnes, J. P. Rosat, A. Sette, M. B. Brenner, S. A. Porcelli, B. R. Bloom, and R. L. Modlin.** 1997. Differential effects of cytolytic T cell subsets on intracellular infection. Science. **276:**1684-7.

203. **Stoneburner, R. L., D. C. Des Jarlais, D. Benezra, L. Gorelkin, J. L. Sotheran, S. R. Friedman, S. Schultz, M. Marmor, D. Mildvan, and R. Maslansky.** 1988. A larger spectrum of severe HIV-1--related disease in intravenous drug users in New York City. Science. **242:**916-9.

204. **Stover, C. K., P. Warrener, D. R. VanDevanter, D. R. Sherman, T. M. Arain, M. H. Langhorne, S. W. Anderson, J. A. Towell, Y. Yuan, D. N. McMurray, B. N. Kreiswirth, C. E. Barry, and W. R. Baker.** 2000. A small-molecule nitroimidazopyran drug candidate for the treatment of tuberculosis. Nature. **405:**962-6.

205. **Sturgill-Koszycki, S., P. Schlesinger, P. Chakraborty, and e. al.** 1994. Lack of acidification in Mycobacterium phagosomes produced by exclusion of the vesicular proton-ATPase. Science. **263:**678-681.

206. **Styblo, K.** 1989. Overview and epidemiologic assessment of the current global tuberculosis situation with an emphasis on control in developing countries. Rev Inf Diss. **11:**339-346.

207. **Sugawara, I., H. Yamada, S. Hua, and S. Mizuno.** 2001. Role of interleukin (IL)-1 type 1 receptor in mycobacterial infection. Microbiol Immunol. **45:**743-50.

208. **Sugawara, I., H. Yamada, H. Kaneko, S. Mizuno, K. Takeda, and S. Akira.** 1999. Role of interleukin-18 (IL-18) in mycobacterial infection in IL-18-gene- disrupted mice. Infect Immun. **67:**2585-9.

209. **Suter, E.** 1961. Passive transfer of acquired resistance to infection with *Mycobacterium tuberculosis* by means of cells. Am. Rev. Respir. Dis. **83:**535-543.

210. **Sykes, M.** 1990. Unusual T cell populations in adult murine bone marrow. Prevalence of CD3+CD4-CD8- and alpha beta TCR+NK1.1+ cells. J Immunol. **145:**3209-15.

211. **Szabo, C.** 1996. The pathophysiological role of peroxynitrite in shock, inflammation, and ischemia-reperfusion injury. Shock. **6:**79-88.

212. **Takahama, Y., A. Kosugi, and A. Singer.** 1991. Phenotype, ontogeny, and repertoire of CD4-CD8- T cell receptor alpha beta + thymocytes. Variable influence of self-antigens on T cell receptor V beta usage. J Immunol. **146:**1134-41.

213. **Talaat, A. M., R. Reimschuessel, S. S. Wasserman, and M. Trucksis.** 1998. Goldfish, Carassius auratus, a novel animal model for the study of *Mycobacterium marinum* pathogenesis. Infect Immun. **66:**2938-42.

214. **Tanaka, Y., S. Sano, E. Nieves, G. D. Libero, D. Rosa, R. L. Modlin, M. B. Brenner, B. R. Bloom, and C. T. Morita.** 1994. Nonpeptide ligands for human γδ T cells. PNAS, USA. **91:**8175-8179.

215. **Toossi, Z.** 1996. Cytokine circuits in tuberculosis. Infectious Agents and Disease. **5:**98-107.

216. **Toossi, Z.** 2000. The inflammatory response in *Mycobacterium tuberculosis* infection. Arch Immunol Ther Exp. **48:**513-9.

217. **Toossi, Z., T.-G. Young, L. E. Averill, B. D. Hamilton, H. Shiratsuchi, and J. J. Ellner.** 1995. Induction of transforming growth factor β1 by purified protein derivative of *Mycobacterium tuberculosis*. Infect. Immunity. **63:**224-228.

218. **Turner, J., C. D. D'Souza, J. E. Pearl, P. Marietta, M. Noel, A. A. Frank, R. Appelberg, I. M. Orme, and A. M. Cooper.** 2001. CD8- and CD95/95L-dependent mechanisms of resistance in mice with chronic pulmonary tuberculosis. Am J Respir Cell Mol Biol. **24:**203-9.

219. **Turner, J., A. A. Frank, J. V. Brooks, P. M. Marietta, and I. M. Orme.** 2001. Pentoxifylline treatment of mice with chronic pulmonary tuberculosis accelerates the development of destructive pathology. Immunology. **102:**248-53.

220. **Underhill, D. M., and A. Ozinsky.** 2002. Toll-like receptors: key mediators of microbe detection. Curr Opin Immunol. **14:**103-10.

221. **Underhill, D. M., A. Ozinsky, K. D. Smith, and A. Aderem.** 1999. Toll-like receptor-2 mediates mycobacteria-induced proinflammatory signaling in macrophages. Proc Natl Acad Sci U S A. **96:**14459-63.

222. **Vella, A. T., and E. J. Pearce.** 1992. CD4+ Th2 response induced by *Schistosoma mansoni* eggs develops rapidly, through an early, transient, Th0-like stage. J Immunol. **148:**2283-90.

223. **Verhagen, C. E., T. C. van der Pouw Kraan, A. A. Buffing, M. A. Chand, W. R. Faber, L. A. Aarden, and P. K. Das.** 1998. Type 1- and type 2-like lesional skin-derived *Mycobacterium leprae*- responsive T cell clones are characterized by coexpression of IFN- gamma/TNF-alpha and IL-4/IL-5/IL-13, respectively. J Immunol. **160:**2380-7.

224. **Virelizier, J. L., and F. Arenzana-Seisdedos.** 1985. Immunological functions of macrophages and their regulation by interferons. Med Biol. **63:**149-59.

225. **Waksman, S. A.** 1964. The Conquest of Tuberculosis. University of California Press, Berkely, CA.

226. **Wallis, R. S., and J. J. Ellner.** 1994. Cytokines and tuberculosis. J Leukoc Biol. **55:**676-81.

227. **Wayne, L. G.** 1976. Dynamics of submerged growth of *Mycobacterium tuberculosis* under aerobic and microaerophilic conditions. Am Rev Respir Dis. **114:**807-11.

228. **Wells, W. F.** 1955. Airbourne Contagion and Air Hygiene. Harvard University Press, Cambridge, Mass.

229. **Willet, H. P.** 1988. Mycobacterium, p. 423-48. *In* C. M. Wilfert (ed.), Zinsser Microbiology, 19 ed. Appleton and Lange, Connecticutt.

230. **Wynn, T. A., A. W. Cheever, D. Jankovic, R. W. Poindexter, P. Caspar, F. A. Lewis, and A. Sher.** 1995. An IL-12 vaccination method for preventing fibrosis induced by schistosome infection. Nature. **376:**594-596.

231. **Xu, S., A. M. Cooper, S. Sturgill-Koszycki, T. van Heyningen, D. Chaterjee, I. Orme, P. Allen, and D. G. Russell.** 1994. Intracellular trafficking in Mycobacterium and Mycobacterium-infected macrophages. J Immunol. **153:**2568-2578.

232. **Zhang, Y., B. Heym, B. Allen, D. Young, and S. Cole.** 1992. The catalase-peroxidase gene and isoniazid resistance of *Mycobacterium tuberculosis*. Nature. **358:**591-3.

233. **Zhu, G., Xiao, H, Tanaka, K, Tyagi, S, Salgame and Chan, J.** Granuloma - specific gene expression: The use of laser capture microdissection and the molecular beacon/realtime PCR technology. US-Japan Cooperative Medical Science Program: 36th Tuberculosis and Leprosy research Conference. 2001.

234. **Zumla, A. and Geraint James, D.** 1999. The Granulomatous Disorders, First ed. Chapter 10. Cambridge University Press, Cambridge.

Chapter Two

Immunopathology of Pulmonary Tuberculosis in C57BL/6 Mice

Abstract

The progression of the immune response in the lung after aerosol infection with *M. tuberculosis* is a complex cellular event dominated by macrophages and lymphocytes. Although the phenotype of the lymphocytes participating in the immune response is now generally accepted and characterized, the dynamic influx of these cell populations during the infection and their spatial arrangements within the lung tissue are still poorly understood. Similarly, the amount of necrosis and apoptosis of these lymphocytes and the overall architecture of the granuloma in terms of size and shape is yet to be fully described. Using the C57BL/6 mouse as a model of humans that arrest disease progression and then reactivate during chronic disease, significant changes in the lymphocyte populations within the lungs were observed. Between 10 and 30 days after aerosol infection with *M. tuberculosis*, initiation of granuloma development was heralded by a steady increase in the percentages of total $CD3^+$, $CD3^+/CD4^+$ and $CD3^+/CD8^+$ cells with consistently higher numbers of $CD3^+/ CD4^+$ cells as compared to $CD3^+/ CD8^+$ cells. As granuloma formation continued, the granuloma was found to consist of macrophages, $CD4^+$ and $CD8^+$ T cells, as well as significant numbers of $CD45R/B220^+$ B cells. $NK1.1^+$ T cells and γδ T cells were detected only in low numbers throughout the infection.

Whereas $CD4^+$ cells and B cells were found throughout the characteristic lymphocytic aggregates, many of the $CD8^+$ cells were seen only at the periphery. It is suggested that this may reflect a slower migration of $CD8^+$ T cells into the lesions and a role for this subset in perpetuating the chronic disease state. Individual granulomas developed with a predilection for sites that correlated with deep lymphatic and pleural lymphatic vessels and pleural vascular plexi. This indicted a possible important role for the murine pulmonary lymphatic system that has not been previously discussed.

Introduction

Acquired immunity generated against *M. tuberculosis* develops slowly in murine lungs (6, 7, 9, 17) with bacterial growth tending to stop as this immunity appears (11, 18). All mice ultimately succumb to infection, however, the terms 'resistant' and 'susceptible' are used to describe the length of time bacterial growth is controlled. Numerous studies using specific-gene-disrupted mice (8, 30), immune T cell transfer (19), and *in vitro* assays have demonstrated that immunity to *M. tuberculosis* infection is dependent on the emergence of specific sub-populations of T cells. It is well known that $CD4^+$ T cell populations are critical for survival of this infection (8, 21), but it is also becoming apparent that other cell populations such as $CD8^+$ T cells (30), $\gamma\delta$ T cells (3, 13) and NK and NKT (1) cells may also be important although their roles are less well characterized. What is clear, however, is that the host response to *M. tuberculosis* infection is dependent on production of IFN -γ by primed T cells (10,14,23) which in turn is dependent on IL-12 production from antigen presenting cells (macrophages and dendritic cells) (12). In the infected murine lung, these complex interactions take place in the context of a host remodeling response called granuloma formation, and it is the construction of these

structures that forms the hallmark of the disease. The C57BL/6 strain of mouse has been used as a model of an animal that is 'resistant' to infection (16). More accurately, it models the arrest and reactivation scenario in man (33). It is now clear that C57BL/6 mice develop a predictable and reproducible pulmonary inflammatory response in the lung after a low dose aerosol infection with *M.tuberculosis* infection that can be resolved in to distinct pathological stages (7, 27). The actual makeup of the granuloma, however, in terms of which T-cell subsets enter and where they are subsequently to be found has not been previously documented. Similarly, there is limited data on the amount of apoptosis within these lesions and even less on the specific size and shape of individual granulomas. How these factors may affect disease progression in this animal and whether they relate to the human condition is explored.

In this study, flow cytometry was used to define the early influx of $CD4^+$ and $CD8^+$ T cells into the lungs of C57BL/6 mice and immunohistochemistry was employed to define their relative distribution. Similar characterization of the $CD45R/B220^+$ B cell, $NK1.1^+$ T cell and γδ T cell populations was also attempted. The results obtained indicate that the two major T cell subsets occupy discrete and different patterns within the overall granuloma, which are presumably directly related to their function during the active and chronic phases of the disease process. B cells were prominent throughout the course of the disease but NK1.1 T cell and γδ T cell populations were rare. The presence of apoptotic cells was consistently low. Morphometric and detailed histopathological analysis helped redefine the previously published models of pathogenesis into a new five stage model. It is now clear that there is both temporal and spatial differences in the

arrangement of lymphocytes within C57BL/6 granulomas and this presumably is directly related to their different functions and the various phases of the disease process.

Materials and Methods

Mice

Specific-pathogen-free, female C57BL/6 mice of 6-8 weeks of age were purchased from the Jackson Laboratories (Bar Harbor, ME, USA). Infected and uninfected control mice were maintained in a biosafety level-3 facility at Colorado State University. All animals had free access to water and standard mouse chow. The specific-pathogen-free nature of the mouse colonies was demonstrated by testing sentinel animals. These were shown to be negative for 12 known mouse pathogens. In each experiment, 4 or 5 animals were used at each time point, with at least one uninfected control mouse. All animals were euthanized by carbon-dioxide asphyxiation.

Bacteria and infection

M. tuberculosis strain Erdman (TMCC #107) was grown from low passage seed lots in Proskauer-Beck liquid media containing 0.02% Tween 80 to mid-log phase and then aliquoted and frozen at -70^0C until use. Mice were infected via the aerosol route with a low dose of bacteria. Briefly, the nebulizer compartment of a Middlebrook airborne infection apparatus (Glas-col, Terre Haute, IN) was filled with 5 ml of H_2O containing a suspension of bacteria resulting in delivery of approximately 100 bacteria per lung during a 30 minutes exposure.

Enumeration of bacteria

At the times indicated, mice were euthanized by carbon-dioxide asphyxiation. Lungs were aseptically removed from the thoracic cavity and the number of viable bacteria in the lungs of the mice was determined by plating serial dilutions of either the left lung lobe or all lung lobes onto nutrient Middlebrook 7H11 agar. After three weeks incubation at 37^0C in humidified air, the number of bacterial colonies for each dilution were counted with a 4x magnification dissecting microscope. The data are representative of three experiments and are expressed as the log10 value of the mean number of colony forming units counted, with standard error of the mean indicated by vertical bars.

Histology

The lungs were removed from the thorax either as the entire pluck or as individual lobes. The tissue was then slowly infused with 10% neutral buffered formalin either through the trachea or at the hilus of individual lobes. The tissue was then submerged into formalin for a minimum of 72 hours. Tissues were prepared routinely and sectioned for light microscopy with lobe orientation designed to allow for the maximum surface area of each lobe to be seen. The standard hematoxylin and eosin stain was employed. Masson's trichrome and the Ziehl Neelson method were also used to detect type IV collagen and acid fast bacilli respectively. All tissue identification was masked and the order was randomized to preclude experimental group bias. Sections were examined at least three times to verify the reproducibility of the observations.

Criterion for assessment of pulmonary lesions

An assessment of all of the parenchymal and non-parenchymal tissue elements was performed in all sections, a minimum of three times. This included trachea, bronchi, bronchioles, alveoli, pleura and vasculature. In each case the presence and distribution of inflammatory cell types was noted. This included macrophages, mononuclear cells (lymphocytes and plasma cells), multinucleated giant cells and polymorphonuclear cells (neutrophils).

Morphometry

In an attempt to further classify the pulmonary lesions, the granuloma fraction was calculated from each of the hematoxylin and eosin stained histological slides. In brief, using Metamorph Image Analysis Software (Metamorph 4.5r5, Universal Imaging Corporation, Downington PA), images of individual lobes or all lobes were acquired. These were calibrated, measured and the perceived inflammatory area was defined and expressed as a percentage of the total lung area. This percentage of affected tissue was termed the granuloma fraction (24, 25).

To explore the shape of the granuloma, SURFdriver 3.5 software was employed (Kailua, HI). Ten 5μm sections at100μm apart were cut from the paraffin blocks and stained with hematoxylin and eosin. A representative granuloma was selected and imaged from each of the step-sections. All images were captured from the same position and at the same magnification. The series of images were then imported into the SURFdriver program

and stacked, and joined together to present a 3-D reconstruction. Only granulomas from chronic disease were examined in this fashion.

Immunohistochemistry

Purified rat anti-mouse monoclonal antibodies specific for mouse CD4 (L3T4 clone H129.19), CD8 (Ly-2 clone 53-6.7), CD45R/B220 (clone RA3-6B2), and Mac-3 (clone M3/84) and purified Armenian hamster anti-mouse monoclonal antibody specific for mouse γδ TCR (clone GL3) were purchased from BD Pharmingen (San Diego, CA). The appropriate BD Pharmingen isotype controls rat $IgG_{2a,\kappa}$ (clone R35-95), rat $IgG_{1,\kappa}$ (cloneR3-34) and hamster IgG, group $2,_{\lambda}$ (anti-KLH) were also purchased and used along side the specific antibodies. Biotinylated goat anti-rat Ig (multiple adsorption) was used as the secondary antibody in each experiment except those staining for γδ TCR, where anti-hamster Ig (cocktail) (clones G70-204,G94-56) was used. The lungs were removed from the thorax either as the entire pluck or as individual lobes. The tissue was then slowly infused with a solution of 20% OCT (Tissue-Tek, Inc. Torrance, CA) in 1X PBS through the trachea or at the hilus of individual lobes. The tissue was then placed in a tissue mold, completely surrounded by OCT, frozen in a bath of liquid nitrogen and stored at –70°C until used. Serial sections from each lung of 5-7 μm thick were cut in a CM 1850 cryotome (Leica Inc. Deerfield, IL), employing the Instrumedics Inc. (Hackensack, NJ) "tape transfer system', fixed in cold acetone for 10 minutes and air-dried. After first confirming the efficacy of this freezing and sectioning technique with staining protocols on the bench-top, subsequent sections were stained using an automated staining system. This produced a degree of uniformity in staining intensity that was very

hard to reproduce with manual manipulation and therefore allowed for greater accuracy of morphometric analysis. The sections were washed in APK buffer solution (Ventana Medical Systems, Tucson, AZ) for 15 -20 minutes and then incubated in a 1:20 (CD4), 1:20 (CD8), 1:50 (CD45R/B220), 1:20 (Mac-3), 1:20 (γδ TCR) and 1:20 (isotype) solution of Protein Block -goat serum (Biogenex, San Ramon, CA) and primary antibody. The sections were then placed on a Nexus automated immunostainer (Ventana medical systems, Tucson, AZ). Both the labeled avidin horse-radish peroxidase and diaminobenzine-hydrogen peroxide (DAB -H_2O_2) detection kit and the labeled avidin alkaline phosphatase and Fast Red Napthol detection kit were used through the course of these experiments. The alkaline phosphatase method produced the least amount of background staining and was used for morphometric analysis. The secondary antibody was incubated for 30 minutes at room temperature at a concentration of 1:20 in APK buffer. Sections were counterstained with Meyer's hematoxylin. Sections of spleen were also routinely examined to act as positive controls.

Criterion for Quantitative image analysis of Immunohistochemical stained lesions

To examine the percentage of lymphocyte subsets within the granulomas, multiple 10x microscopic images were captured. This magnification was deemed able to best represent the lesion as a whole. Employing Metamorph Image Analysis Software (Metamorph 4.5r5, Universal Imaging Corporation, Downington PA), cells that had stained positive were highlighted by the computer and the red, green, blue (RGB) pixel value recorded. The same pixel value was used for all captured images in this experiment. The percentage of the captured image that was occupied by positive cells was then calculated.

Isolation of cells from infected lungs for flow cytometry

At necropsy, and the pulmonary cavity was opened by reflecting the ventral two-thirds of the rib cage rostrally. Erythrocytes within the pulmonary vascular system of the lungs were cleared by perfusing through the right ventricle and pulmonary artery with 2 ml of saline containing 50 U of heparin per ml (Sigma-Aldrich, San Loius, MO). Lungs were aseptically removed and cut into small pieces in cold RPMI medium. The dissected tissue was then incubated in RPMI media 1640 with L-glutamine (Life Technologie, Rockville, MA) containing collagenase XI (0.7 mg/ml Sigma-Aldrich, San Loius, MO) and type IV bovine pancreatic DNAse (30μg/ml, Sigma-Aldrich) for 30-45 minutes at 37^0 C. The action of the enzymes was stopped by adding 10 ml of RPMI media1640 with L-glutamine, and digested lungs were further disrupted by gently pushing the tissue through a nylon screen. The single cell suspension was then washed and centrifuged at 200x *g* for 5 minutes. To lyse the remaining contaminating erythrocytes, the cell pellet was incubated for 5 minutes, at room temperature, with 5 ml of Gey's solution (NH_4Cl and $KHC0_3$). Cells were resuspended in deficient RPMI (Irvine Scientific, Santa Ana, CA) which was supplemented with 1% L-glutamine , 1% Hepes, 0.1% N_3Na and 2% FBS for flow cytometric studies.

Flow cytometry

Monoclonal antibodies specific for mouse CD3e (CD3ε chain) (clone145-2C11), CD4 (L3T4, clone H129.19), CD8 (clone 53-6.7), and NK1.1 (clone PK136) were purchased from Pharmingen (San Diego, CA) as direct conjugates to FITC, PerCP, PE or APC in a purified form. The appropriate BD Pharmingen isotype controls Armenian hamster IgG,

group 1 $_{\kappa}$, rat $IgG_{2a,\kappa}$, and rat IgM_{κ} were also purchased and used along side the specific antibodies. Cell suspensions for each individual mouse were stained with the specific monoclonal antibody against CD3, CD4, CD8 and NK1.1.

Lung cells were washed in RPMI-1640 media with L-glutamine, and stained for 30 minutes at 4^0C with the direct conjugated antibodies and then washed twice with RPMI-640 media with L-glutamine. Acquisition was performed on a FACSCalibur (Becton Dickinson, Mountain View, CA) and data was analyzed using Cell Quest (Becton Dickinson, Mountain View, CA). Cells were gated for lymphocytes by their characteristic forward and side-scatter profile and 75,000 events for this gate per sample werer counted. Due to cell aggregation and excessive clumping of lung cell suspension after 50 days post-infection, we were unable to collect data from later time points of infection.

Photomicroscopy

Photomicroscopy was performed with an Olympus AH-2 microscope linked to a Sony SKC-DK5 digital camera and Adobe Photoshop 6.0 software.

Results

Course of *M. tuberculosis* infection in the lungs of C57BL/6 mice

The progression of bacterial growth was defined in 5 stages (Figures 2.1A and 2.1B) Minimal growth of bacteria was detected in the lungs during the course of the first five days post infection (stage 1). The number of bacteria remained similar, at or just below 2 Logs (Figure 2.1A). Thereafter, bacteria grew progressively (stage 2), reaching a peak and leveling off (stage 3) at approximately 4 Logs by 30 days (Figure 2.1B). There was then a slight drop in bacterial load down to approximately 3.5 logs at 60 days post infection, followed by a long period of almost 100 days of similar bacterial load (stage 4). From day 150 post infection (stage 5) and especially towards the end of the experiment (250 to 300 days post infection) a steady increase in the bacterial number was detected (Figure 2.1B) peaking at approximately 6.0 Logs.

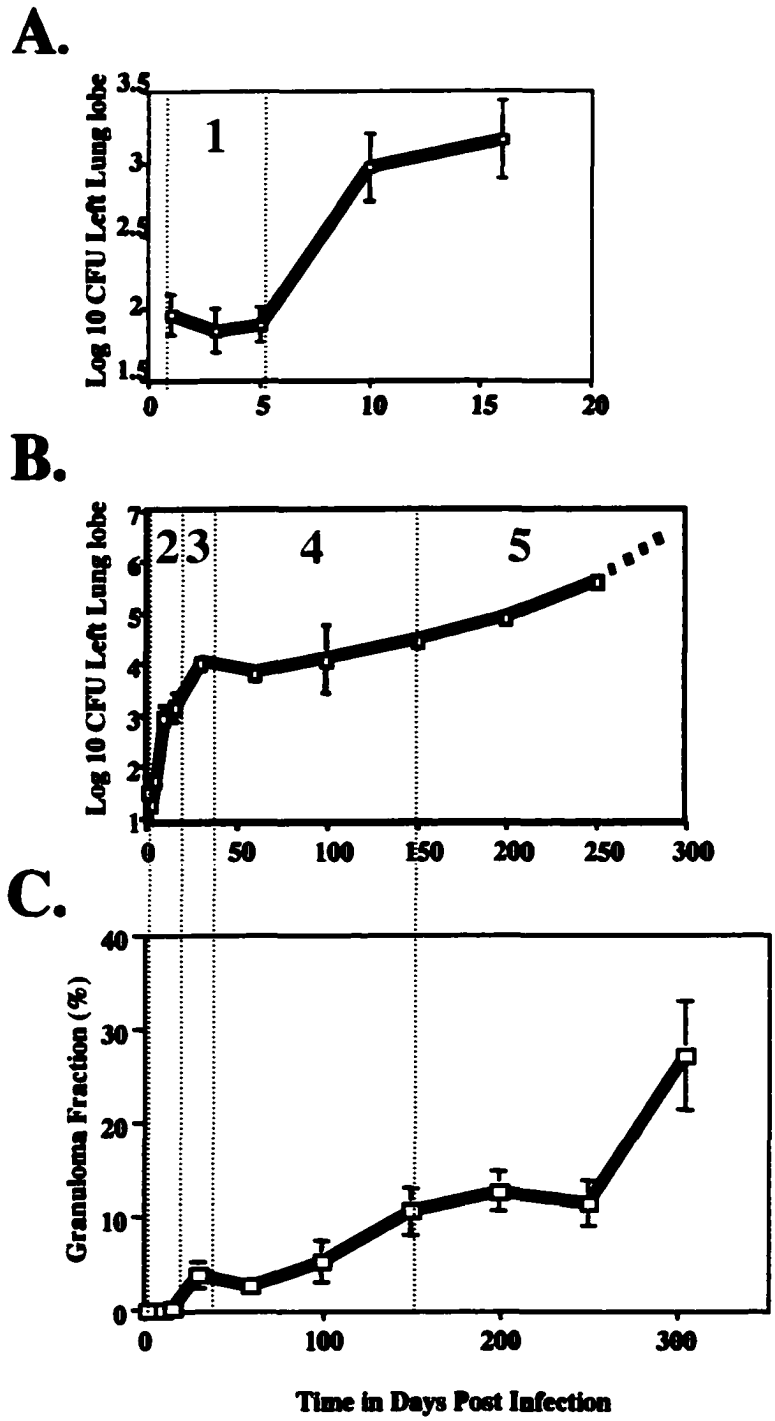

Figure 2.1. Growth curves of *M. tuberculosis* within the left lung lobe of C57BL/6 mice. (A) Growth during the first 20 days post infection. (B) Growth over the course of 250 days post infection. Data (C) is granuloma fraction over 300 days. Data A,B are expressed as the mean Log 10 numbers of colony forming units (CFU) and standard errors of the mean are indicated by the black vertical bars. Dashed vertical blue lines and red digits delineate perceived stages of infection. Four animals were sacrificed at each time point. These graphs are representative of three experiments.

Histological and Morphometric analysis

When comparing the bacterial growth curve with the histopathologic observations, the five stages were further defined. Within each stage the type of inflammatory cells detected on hematoxylin and eosin stained sections along with those detected by immunohistochemistry were noted. The mean percentage of each lymphocyte subset was recorded within multiple (minimum of 2 fields from 3 mice in two separate experiments) 10x fields of inflammation. The pathological sequelae was assessed along with the total amount of inflammation as measured by granuloma fraction.

The following Figures and tables (Figures 2.2 - 2.7 and Tables 2.1A and 2.1B) summarize these stages, followed by detailed descriptions.

Table 2.1

Summary of the histopathological and morphometric categorization of the pulmonary lesions of C57BL/6 mice infected via aerosol with *M. tuberculosis* when compared to the bacterial growth curve.

A. Inflammatory cell types present and their localization

Lesion Stage	DPI	GF%	MØ	MNGC	LØ	Plasma cells	NØ
1	0-5	0-1	Histiocyte	None	Very rare, I	None	Rare, I
2	5-25	1-3	Histiocyte epithelioid MF	None	PV and PB cuffs	None	Scattered I
3	25-35	3-10	Epithelioid and foamy, PV, PB and IA. Distinct aggregates	None	PV and PB cuffs extending into macrophage aggregates	None	Scattered MF
4	35-150	10-20	Epithelioid and Foamy, IA	None	Long PV and PB cuffs extending into macrophage aggregates	Few admixed with LØ	Prominent around necrotic foci
5	150-END	20-30	Epithelioid and Foamy. IA	Few, scattered	Scattered islands (follicles) and scattered individual cells	Prominent PV	Prominent around or adjacent to necrotic foci

Key:

AFB = Acid fast bacilli, DPI = Days post infection, GF% = Granuloma fraction, Histiocyte = Normal, resident tissue macrophage (alveolar / interstitial), I = Interstitial, IA = Intra-alveolar, LØ = Lymphocytes, MØ = Macrophages, MF = Multifocal, MNGC = Multinucleate giant cell, NØ = Neutrophils, PV = Perivascular, PB = Peribronchioloar

B. Pathological sequelae of each stage

Lesion Stage	Fibrosis	Necrosis	AFB	Airway Involvement	Pleural Involvement
1	None	None	None observed	None	None
2	None	None	None observed	None	None
3	Mild, within inflammatory foci	None	Few scattered, intracellular	None	Subpleural aggregates
4	Moderate, within inflammatory foci	MF, single cell, scattered aggregates	Scattered, intracellular, extracellular	None	Subpleural aggregates and Mild chronic pleuritis
5	Moderate to marked within inflammatory foci	MF, coalescing scattered aggregates	Scattered, intracellular, extracellular	Moderate airway epithelium erosion	Subpleural aggregates and Moderate chronic pleuritis

The data represents the results of three experiments.

Stage 1

Days 0-5 post infection. There was little histological evidence the host was aware of the presence of the pathogen. The alveoli were clear and open and the thin septae were punctuated by the normal complement of type I and II pneumocytes, endothelial cells and macrophages. Normal ciliated respiratory epithelium lined the airways, and loose collagenous connective tissue separated the airways from the adjacent blood vessels. No lymphocytes were detected by immunohistochemistry (Figure 2.2).

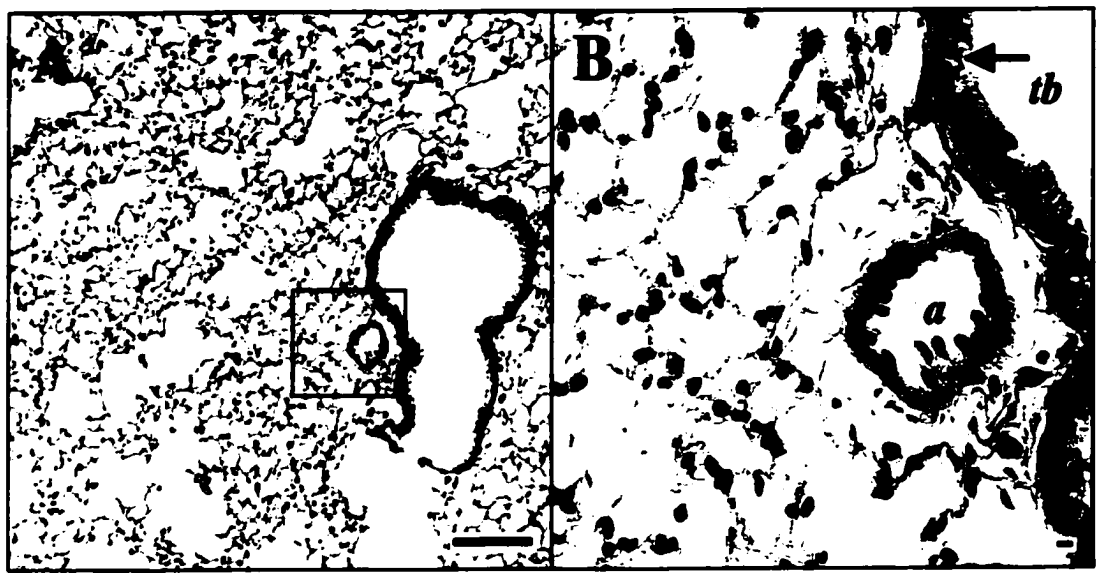

Lesion Stage	CD4	CD8	CD45R/B220	γδTCR
1	ND	ND	ND	ND

Figure 2.2. Stage 1.
A and B, representative photomicrographs of a lung from a C57BL/6 mouse, three days post low dose aerosol infection with *M. tuberculosis*. B is an high magnification of the black square in A. Clear, open terminal airways and alveoli. Thin septae are punctuated by the nuclei of type I and II pneumocytes, endothelial cells and alveolar macrophages. Normal columnar epithelium lines the terminal bronchiole (arrows). Loose collagenous connective tissue seperates airway from artery. Hematoxylin and Eosin. A, bar= 100μm, B, bar=10 μm. *tb* = Terminal bronchiole, *a* = arteriole. Table represents the results of quantitative image analysis of immunohistochemically stained sections for the indicated cell types. ND = not detected

Stage 2

Days 5 to 25 days post infection. There was a progressive locally extensive, inflammatory response expanding the interstitium surrounding airways and vasculature. Macrophages, lymphocytes and rare neutrophils along with moderate congestion and edema all served to distort the normal architecture. CD45R/B220$^+$ cells were detected by immunohistochemistry at very low levels. They were found predominantly within the alveolar septae. There was no other significant staining of lymphocytes (Figure 2.3).

Stage 3

Days 25 to 35 post infection. Distinct perivascular and peribronchial lymphoid cuffs were established. These extended to varying degrees into the surrounding parenchyma. Epithelioid macrophages were now prominent. CD4$^+$ T cells were detectable in consistently higher numbers than the CD8$^+$ T cells. CD45R/B220$^+$ cells were also prominent. Quantitative image analysis indicated that by relative numbers, CD4$^+$> CD45R/B220$^+$>CD8$^+$ within the granulomatous foci (Figure 2.4).

Stage 4

Days 35 to 150 post infection. Many of the alveoli between the prominent lymphoid cuffs were filled with a mixture of epithelioid and large foamy macrophages. In some (rare) cases, the macrophages were surrounded by an incomplete rim of lymphocytes in a manner which resembled rudimentary tubercles. The lymphoid cuffs have extended into the macrophage rich areas as distinct, tightly packed wedges. Day 150 was approximately the time when the first signs of necrosis were seen in a few individual

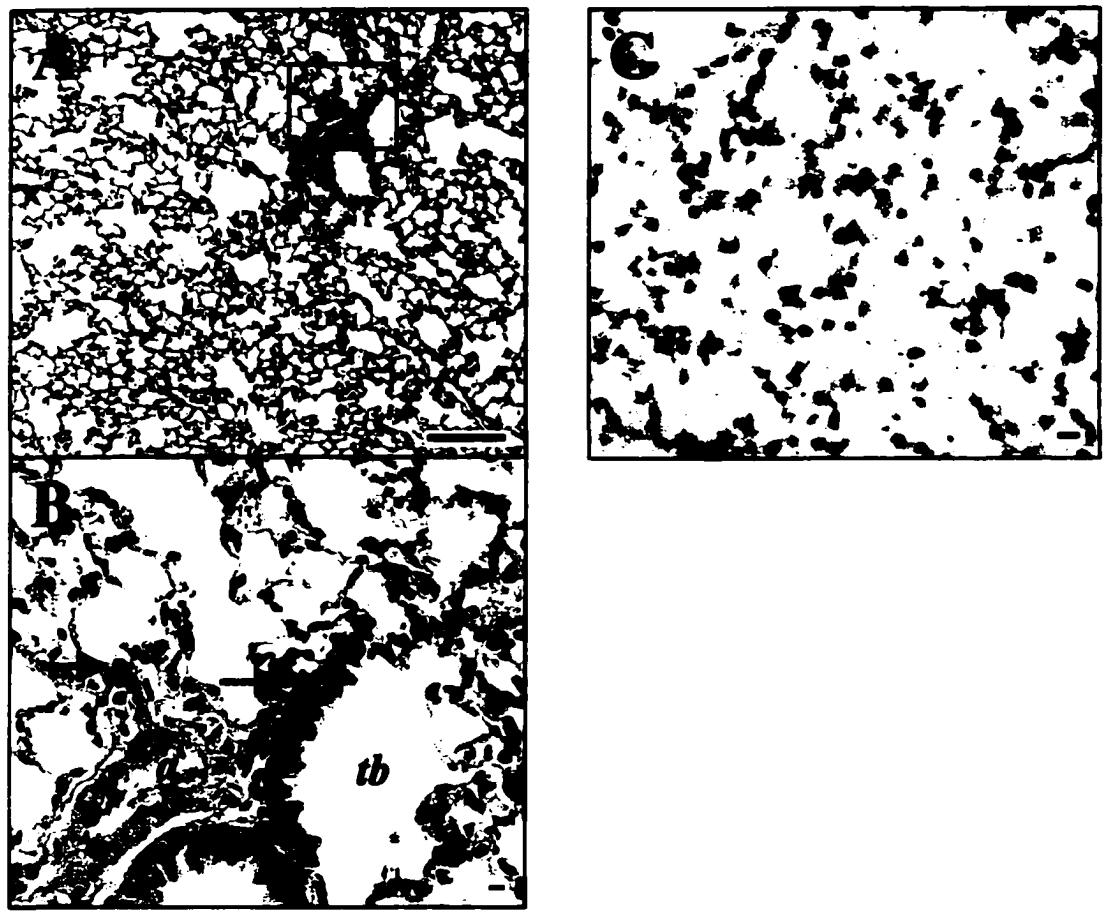

Lesion Stage	CD4	CD8	CD45R/B220	γδTCR
2	ND	ND	0.7(0.3)	ND

Figure 2.3. **Stage 2.**
A and B, representative photomicrographs of a lung from a C57BL/6 mouse, 16 days post low dose aerosol infection with *M. tuberculosis*. Alveolar septae are expanded by lymphocytes,congested blood vessels and mild edema . Alveolar macrophages are more prominent and lymphocytes can be seen in interstitium between artery and terminal bronchiole (arrows) Hematoxylin and Eosin. C, representative photomicrograph of CD45R/B220+ cells 16 days post infection. A, bar= 100μm, B, bar=10 μm. C, bar=10 μm. *tb* = Terminal bronchiole, *a* = arteriole. Table represents the results of quantitative image analysis of immunohistochemically stained sections for the indicated cell types. Figures represent mean percentage area of 10x microscopic field within inflammatory foci occupied by cells. ( ) = standard deviation. ND = not detected

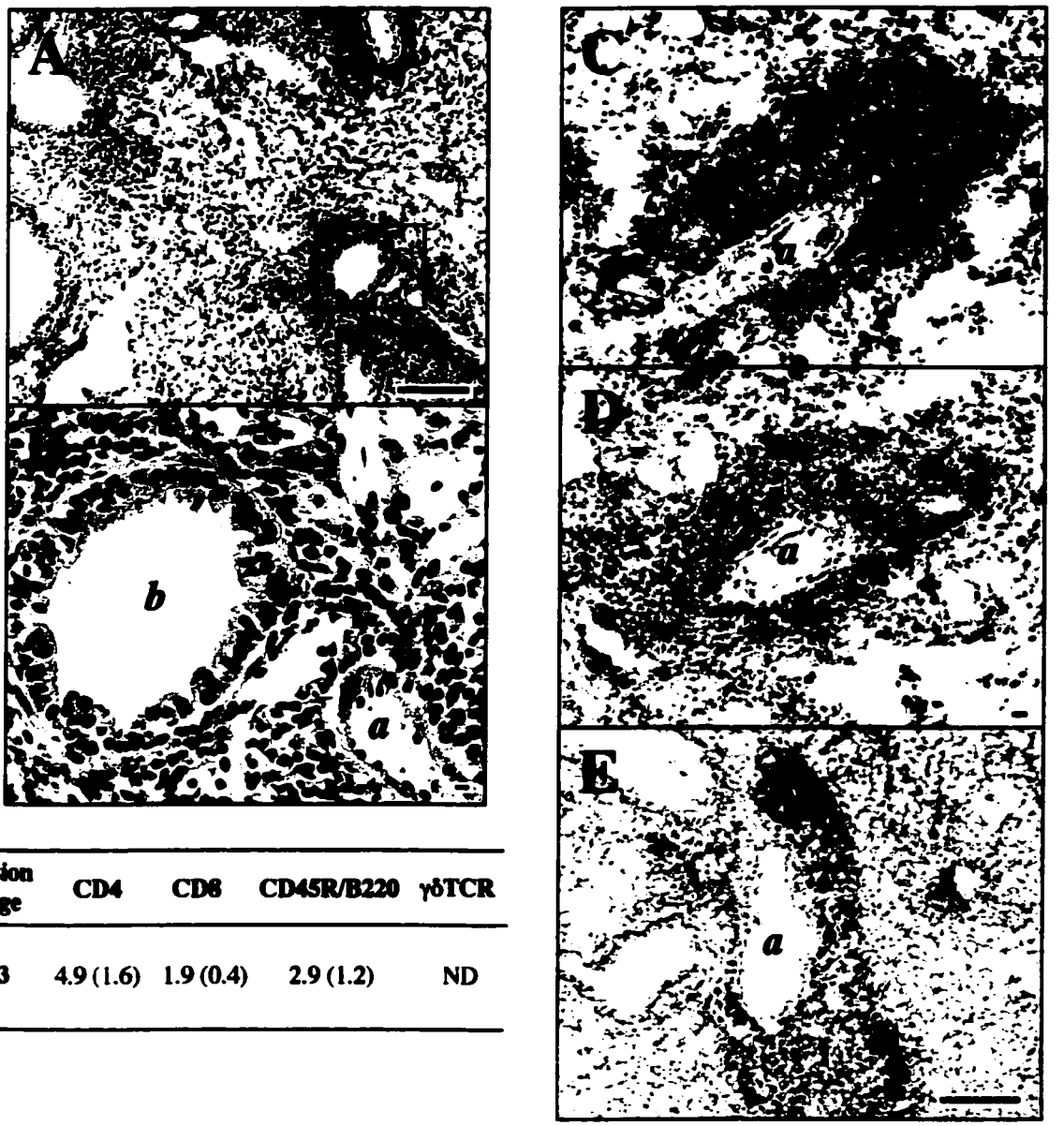

Lesion Stage	CD4	CD8	CD45R/B220	γδTCR
3	4.9 (1.6)	1.9 (0.4)	2.9 (1.2)	ND

Figure 2.4. Stage 3.
A and B, representative photomicrographs of a lung from a C57BL/6 mouse, 30 days post low dose aerosol infection with *M. tuberculosis*. B is an high magnification of the black square in A. Perivascular and peribronchial lymphoid cuffs and epithelioid macrophages are a common feature and they extend into the surrounding parenchyma and expand the alveolar septae. Hematoxylin and Eosin. C,D, E representative photomicrographs of CD4+, CD8+ and CD45R/B220+ cells at 30 days post infection. A, bar= 100μm, B, bar=10 μm. C, D bar=10 μm. E, bar = 100μm. *b*=bronchiole, *a* = arteriole. Table represents the results of quantitative image analysis of immunohistochemically stained sections for the indicated cell types. Figures represent mean percentage area of 10x microscopic field within inflammatory foci occupied by cells. ( ) = standard deviation. ND = not detected.

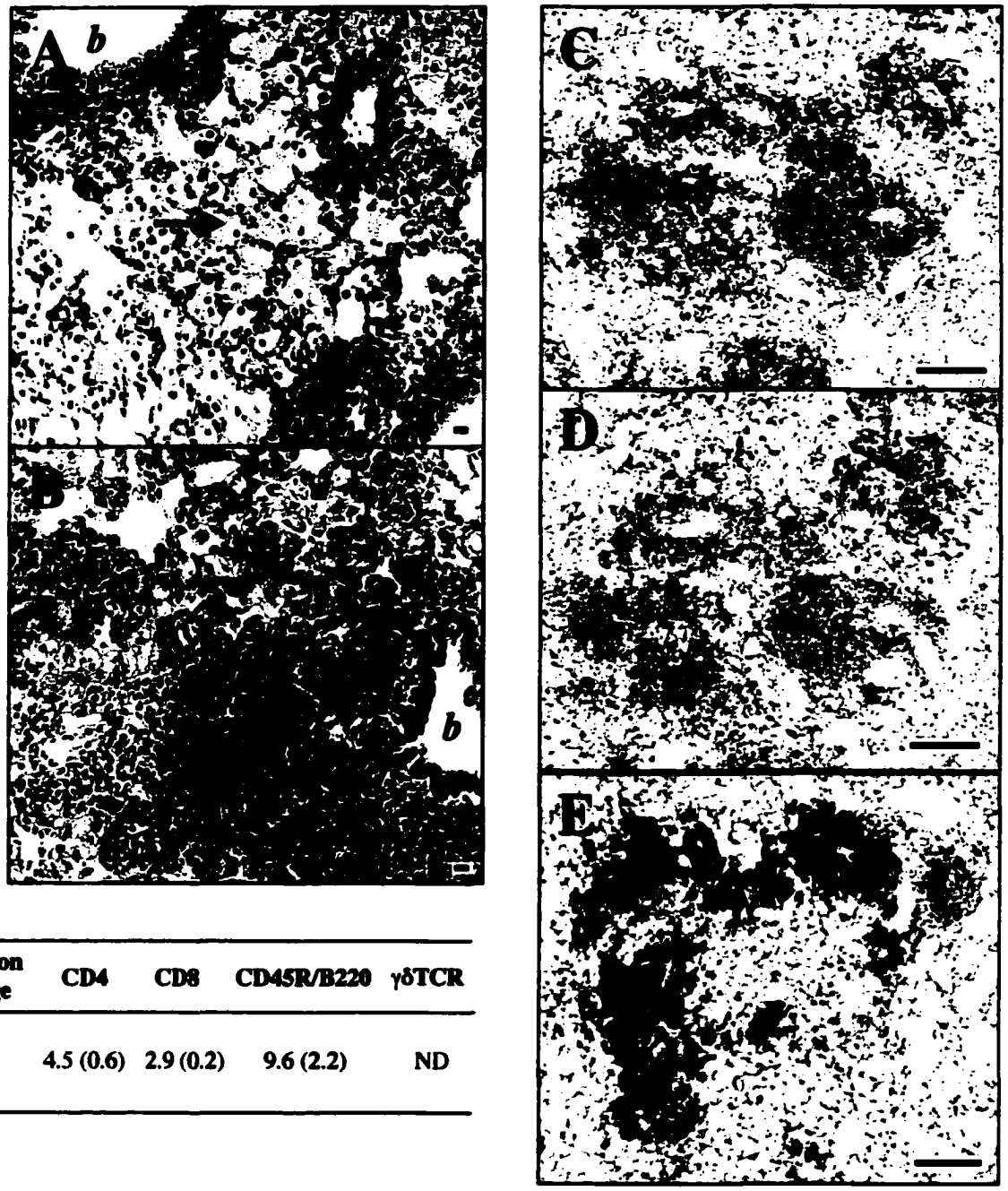

Lesion Stage	CD4	CD8	CD45R/B220	γδTCR
4	4.5 (0.6)	2.9 (0.2)	9.6 (2.2)	ND

Figure 2.5. Stage 4
A and B, representative photomicrographs of a lung from a C57BL/6 mouse, 60 and 150 days respectively post low dose aerosol infection with *M. tuberculosis*. A, perivascular and peribronchial lymphoid cuffing are prominent and the alveoli between them are filled with large foamy macrophages (arrow) and epithelioid macrophages.B, Numerous lymphocytes extend into and surround smaller number of macrophages. Hematoxylin and Eosin. C,D, E representative photomicrographs of CD4+, CD8+ and CD45R/B220+ cells 100 days post infection. A,B bar= 10μm, C, D E, bar = 100μm. *b*=bronchiole. Table represents the results of quantitative image analysis of immunohistochemically stained sections for the indicated cell types. Figures represent mean percentage area of 10x microscopic field within inflammatory foci occupied by cells. ( ) = standard deviation. ND = not detected.

cells. Similar to stage 3, $CD4^+$ cells were detectable in higher numbers than the $CD8^+$ cells. A consistent observation was that the $CD4^+$ cells were found at all levels of the lymphoid aggregates, whereas the $CD8^+$ cells were often peripheralized. $CD45R/B220^+$ cells were again prominent often in very tight aggregates. Quantitative image analysis indicated that by relative numbers, $CD4^+ > CD45R/B220^+ > CD8^+$ within the granulomatous foci (Figure 2.5).

Stage 5

From day 150 post infection to the end of the experiment. The aggregates of lymphocytes that were within the macrophage dominated areas were smaller, spherical and more compact than earlier time points. The macrophages were predominantly foamy and / or degenerating. Necrosis was now more evident, with multiple cholesterol clefts visible. By day 300 post infection, many lymphocytes were present forming thick perivascular and peribronchiolar cords. These typically extended towards the pleura where there was a flaring of the inflammatory focus. This was presumed to be associated with the subpleural lymphatic and venous plexi. Neutrophils were present both within granulomatous lesions and free within airways presumably attracted by tissue damage. Multinucleate giant cells were also occasionally seen, reflecting a disregulation in macrophage apoptosis. Plasma cells were also present, often as tight aggregates around blood vessels. (Figure 2.6) In this final stage of the disease, $CD4^+$ $CD8^+$ cells, $CD45R/B220^+$ cells and $\gamma\delta$ TCR^+ cells were detectable by immunohistochemistry. As in previous stages, the, $CD4^+$ outnumbered $CD8^+$ cells within the lymphocytic aggregates. They were both however, seen to be present at all levels of the structure. $CD45R/B220^+$

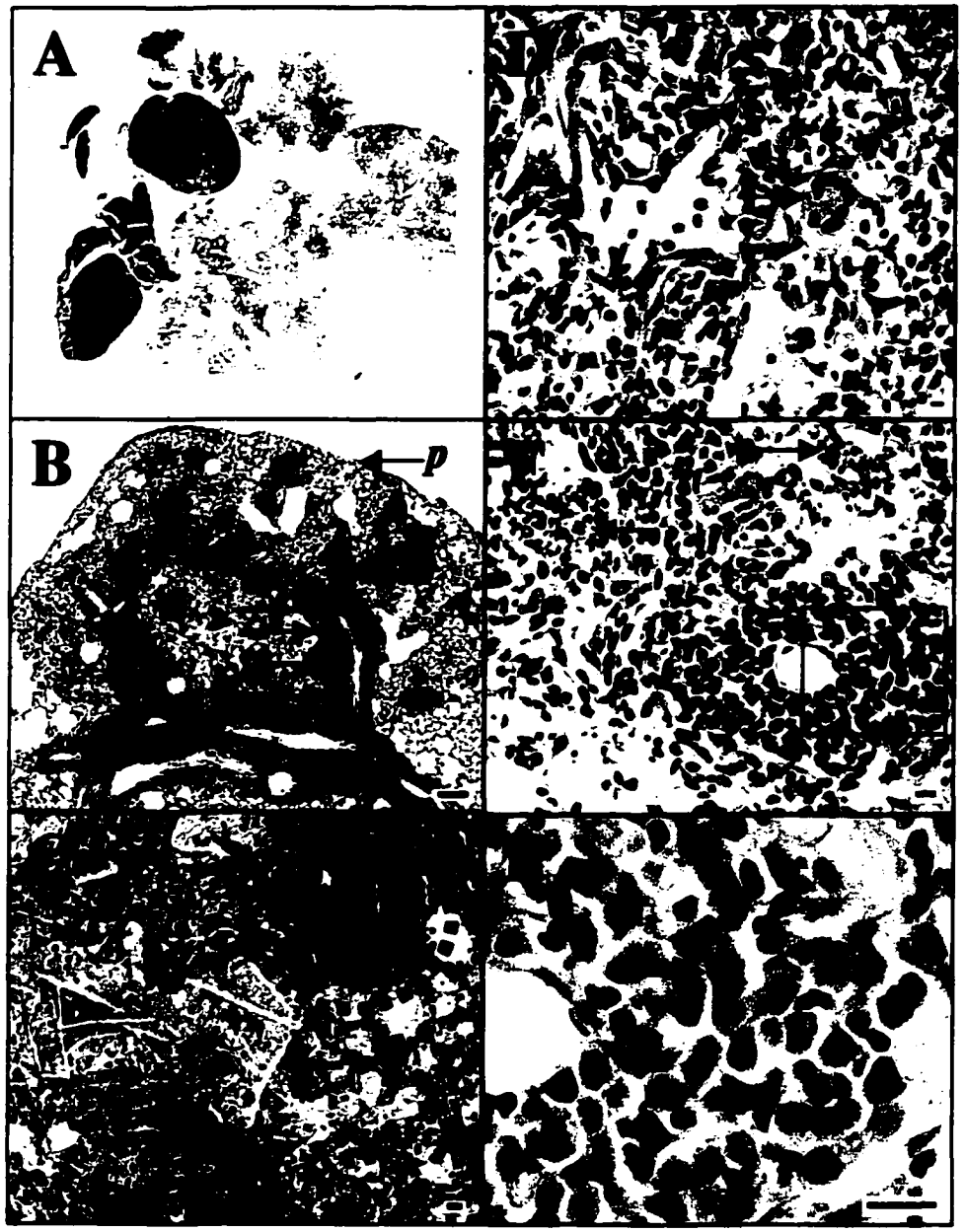

Figure 2.6. Stage 5
A-E, representative photomicrographs of a lung from a C57BL/6 mouse, 250 -300 days post low dose aerosol infection with *M. tuberculosis*.A, Pluck. (*h*)= Heart, (*Ln*)= hyperplastic lymph. B, Thick lymphocytic cords (arrows)extend along the airways and blood vessels to the pleura (*p*), bar=100μm. C,Tight lymphocytic aggregate are surrounded by foamy macrophages with multifocal necrosis. Cholesterol clefts are prominent (arrow) bar=10μm. D, Multinucleate giant cell (arrow) bar=10μm.E,pockets of neutrophils (arrows) bar=10μm. F, is high magnification of area in black boxin E.Multiple plasma cells (arrow) bar=10μm.Hematoxylin and Eosin.

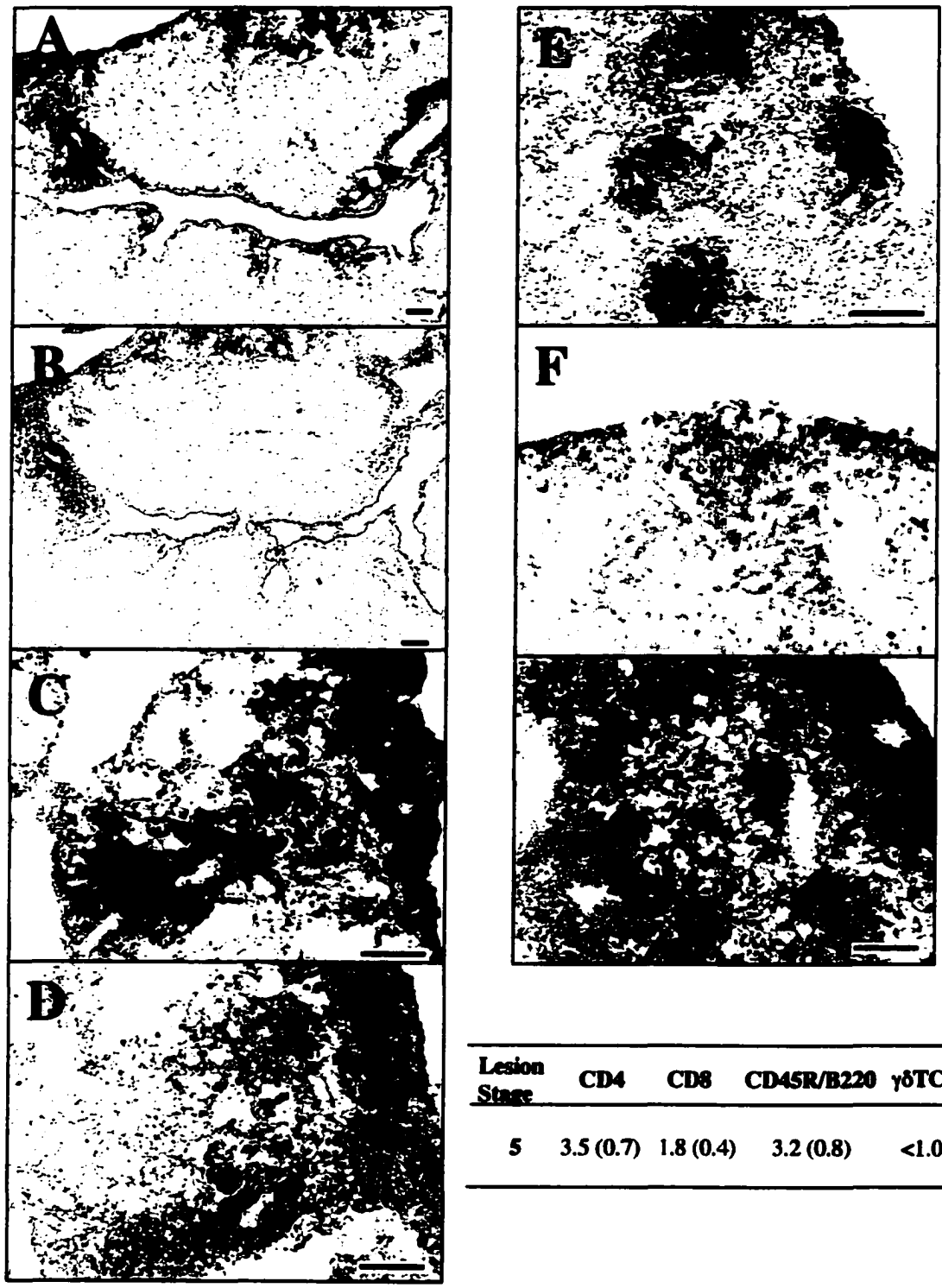

Lesion Stage	CD4	CD8	CD45R/B220	γδTCR
5	3.5 (0.7)	1.8 (0.4)	3.2 (0.8)	<1.0

Figure 2.7. Stage 5

A-G, representative photomicrographs of a lung from a C57BL/6 mouse, 250 -300 days post low dose aerosol infection with *M. tuberculosis*.A,C,CD4+ cells B,D, CD8+ cells, E, CD45R/B220+ cells , F, γδ TCR+ cells, G, Mac3+ cells. In all sections, bar= 100μm. Table represents the results of quantitative image analysis of immunohistochemically stained sections for the indicated cell types. Figures represent mean percentage area of 10x microscopic field within inflammatory foci occupied by cells. ( ) = standard deviation.

cells appeared to represent a large portion of the lymphocytes and were present in dense aggregates. γδ TCR$^+$ cells were seen most commonly within the subpleural aggregates. The prominence of the macrophages was demonstrated by the marked Mac 3 staining in these sections. (Figure 2.7)

The distribution of collagen and the detection of acid fast bacilli as detected by light microscopy was similar to that which has been previously reported (26). For both features, it was not until stage 3 that significant changes were detectable. Variably thick strands of collagen were seen to dissect through the inflammatory foci at all levels. Bacilli were present both within macrophages and free, admixed with necrotic debris (Data not shown - see chapter 3)

Anatomy of the C57BL/6 granuloma

A single Stage 4 granuloma cut at 10 x100 μm intervals depicted in Figure 2.8, demonstrates the anatomical predilection of the developing granuloma. The inflammatory focus begins (1), around a blood vessel and bronchiole and then extends peripherally to the pleura. Here it expands and flares out (7 to 10). When these images are stacked one on top of each other, and their margins delineated, it is possible to appreciate this morphology more fully (Figure 2.9). Here the flaring of the lesion at the pleural surface is obvious.

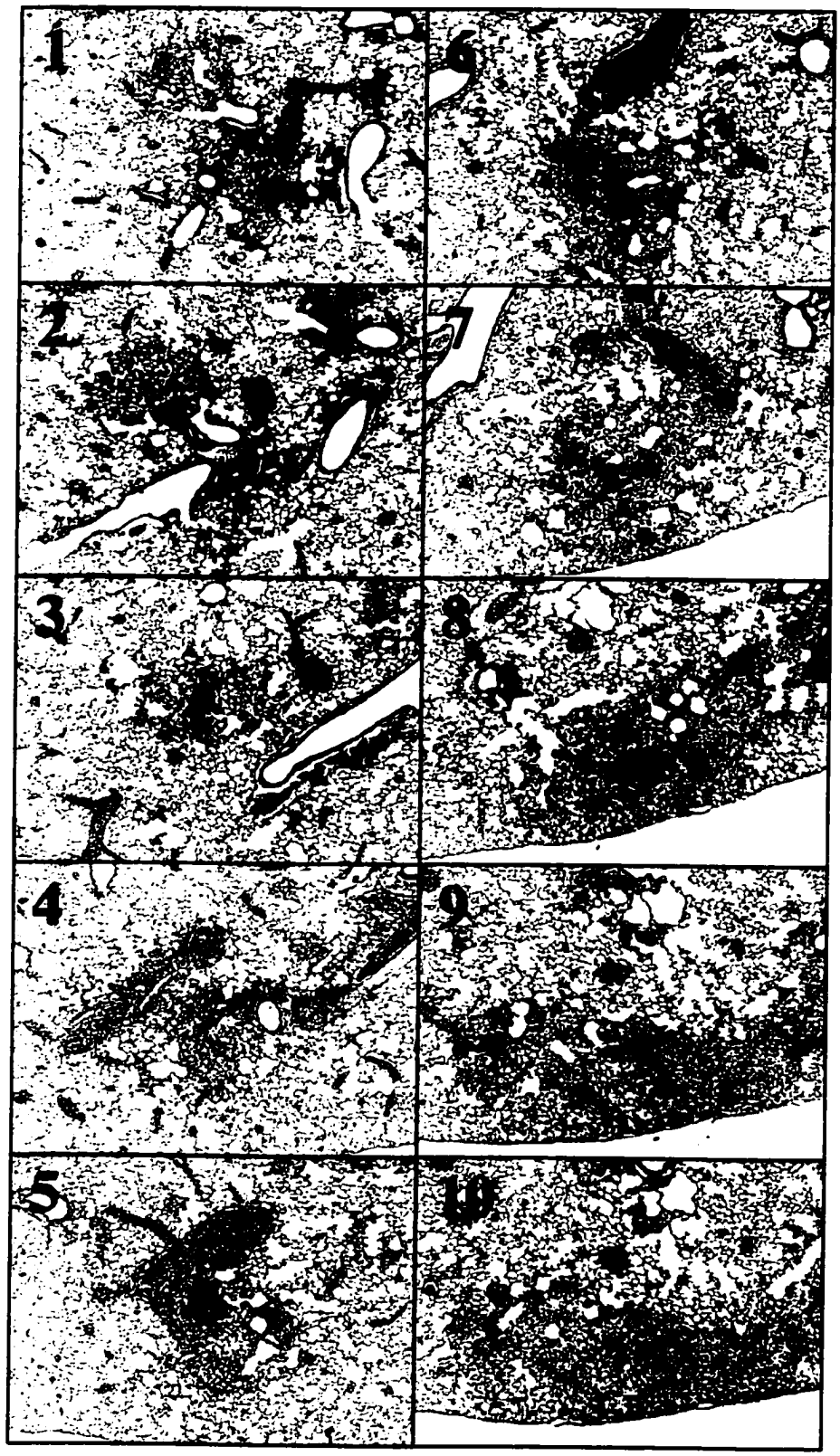

Figure 2.8
Ten serial 100 μm step sections through a pulmonary granuloma in a C57BL/6 mouse at 150 days post infection. Note association with the pleura in sections 7-10

Figure 2.9
Composite 3-D reconstruction of the ten serial 100μm step sections through the pulmonary granuloma depicted in Figure 2.8

Flow cytometric analysis

Using flow cytometry, it was possible to show that the percentage of $CD3^+$ T cells in the lungs rose during the first 30 days post infection (Figure 2.10A,B). There was a twofold increase when compared with day 1 post infection. In the same way, the percentage of $CD3^+/CD4^+$ and $CD3^+/CD8^+$ also rose during the first 30 days post infection. $CD3^+/CD4^+$ were always present in greater numbers than $CD3^+/CD8^+$ but the increases in each population paralleled each other. These showed an approximate 1.5 fold increase in both population when compared with day 1(Figure 2.10). The analysis of cells beyond the first month post infection was unrewarding, due it was thought to the difficulty in harvesting individual lymphocytes from the developing granuloma.

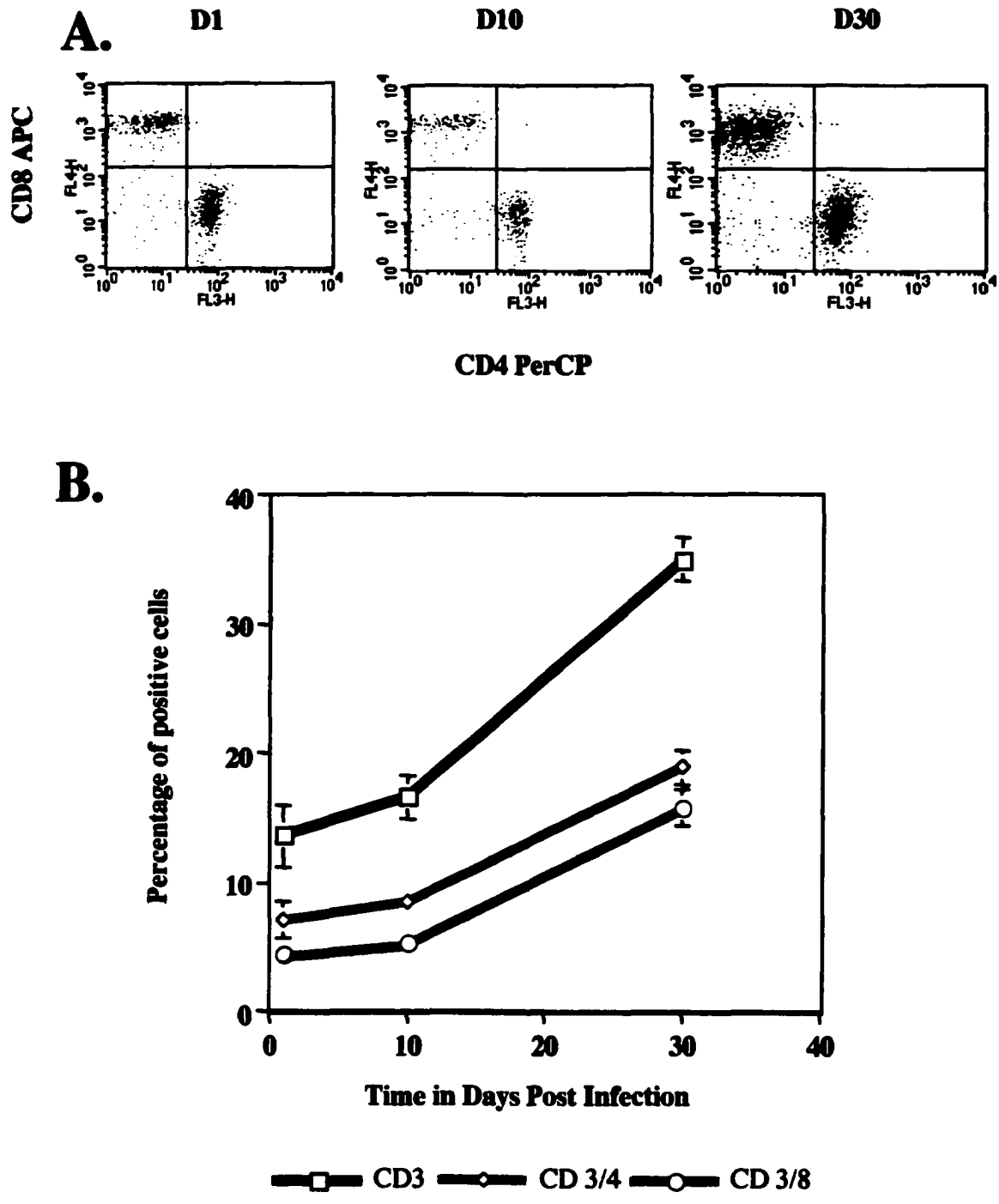

Figure 2.10

A. Representative flow cytometric dot plots of lymphocytes within the lungs at 1, 10 and 30 days post infection. CD4+ and CD8+ lymphocytes detected within the total CD3+ pool of lymphocytes B. Flow cytometric assessment of CD3+, CD3+/CD4+ and CD3+/CD8+ cells in the lungs during the first 30 days post infection. Cells were gated for lymphocytes by their characteristic forward- and side- scatter profile, and 75,000 events in the lymphocyte gate per sample were counted. Data are expressed as the mean percentage of positive cells from four individual mice. Standard errors are indicated by vertical bars. Data are representative of two independent experiments.

Discussion

The results of this study show that over the first month following aerosol exposure of *M. tuberculosis* to C57BL/6 mice there is an influx of $CD4^+$ and $CD8^+$ T cells into the lungs. However, as the granuloma continues to grow in size and become more organized the primary aggregates of T cells that are characteristic of this structure in the mouse model (27) were predominantly of the $CD4^+$ type, whereas $CD8^+$ T cells tended to be more scattered. In addition, interestingly, many of the aggregates contained a significant number of B cells.

Immunohistological examination of the lung early during the course of the infection suggested that both $CD4^+$ and $CD8^+$ T cells accumulated in a perivascular and peribronchiolar fashion as initial interstitial pneumonia began to develop into the beginnings of the granulomatous response. This suggested that both subsets were receiving inflammatory signals and possessed the correct expression of adhesion markers (such as CD11a and CD54) to allow them to cross these inflamed vessels. However, as the granuloma developed and the disease became chronic it was clearly apparent that the great majority of the T cells within the lymphocyte aggregates were $CD4^+$ T cells. It has been hypothesized elsewhere (20), that T cells in the mouse infiltrate into the epithelioid macrophage field and form these structures. It remains unknown however, whether this is because of a constant stream of such cells migrating from the regional arterioles or whether these aggregates arise from lymphocyte proliferation once they have arrived. It is also important to consider the resident bronchus associated lymphoid tissue (BALT) as a source of these cells. Breel et al. described discrete T and B-cell areas in normal

C57BL/6 BALT (5). By immunohistochemistry they showed that the majority of the T cells in BALT belonged to the L3T4$^+$ (CD4$^+$) subset.

In contrast, the pattern of distribution of the CD8$^+$ cells suggest that their migration into the granulomas is much slower and that far fewer cells are involved. Because of this much slower rate of influx the CD8$^+$ cells seemed to be more associated with the periphery of the granuloma. These kinetics of CD8$^+$ T cell accumulation are in keeping with other observations, that mice in which the CD8 gene has been disrupted control and contain a pulmonary infection in a normal manner, but the bacterial load in the lungs gradually increases as the chronic stage of the disease process ensues (30). As such, therefore, these data point to an important role for CD8$^+$ T cells in perpetuating the chronic disease state. This may take the form of immunosurveillance, designed to detect any possible dissemination of bacteria into macrophages away from the centers of the granuloma, which would be in keeping with the more peripheral distribution of this T cell subset.

Assuming this hypothesis is correct, it still remains a matter of debate as to how these cells accomplish this. Some recent studies indicate that the CD8$^+$ cells in the lungs are cytotoxic (28), but data from our laboratory suggests that perforin-deficient mice maintain a chronic disease state, and favor instead the possibility that destruction of infected cells by CD8$^+$ T cells is via an apoptotic mechanisms (30). This mechanism is attractive, because it avoids cell necrosis and local tissue damage which could otherwise be lethal.

It was also evident from these studies that the granulomas contained an appreciable number of B cells. This explains some recent observations that granulomas in chronically infected B cell gene disrupted mice are much smaller than in controls, but it casts no light as to why these cells are present in the first place (4, 31). On one hand it is possible that these cells are the source of antibodies to mycobacterial antigens, and indeed it has been suggested that these may even contribute to protection (29). On the other hand, their arrival may be purely coincidental, driven by the sustained expression of adhesion molecules in the chronically inflamed lung (22, 32) that could equally attract an influx of B cells as well as T cells.

The histological data presented here confirm and extend a classification model proposed by Rhoades (27). In this scheme, five distinct categories were defined, based on the extent of the lesions, the macrophage types, the lymphocyte organization and polymorphonuclear cell localization. The identification of a very early stage (stage 1) in the disease, where there is an apparent lag in bacterial growth, was not identified by Rhoades. It is obvious from both studies that although the bacterial load may be stationary throughout much of the chronic disease phase, there is a progressive, worsening pathology. The mouse does not produce the 'classic granuloma' as typified in the guinea pig and other mammals (15). Nevertheless, a distinct aggregate of epithelioid macrophages variably surrounded or infiltrated by lymphocytes and polymorphonuclear cells is accepted by most as the murine equivalent. There is an increasing fibrotic response over the time course of the infection. It is thought that this is what prevents the murine granuloma from degenerating in the chronic state.

As an extension of this, Cardona and his colleagues have recently proposed some modifications to this model. The Cardona model describes three forms of granuloma; primary, secondary and a combination of these two, tertiary (7). The classification is based on the arrangement of macrophages with respect to lymphocytes. A large accumulation of macrophages at the early stage of infection being a primary granuloma, a thick mantle of lymphocytes surrounding a smaller aggregate of macrophages being a secondary granuloma and the linkage of either with foamy macrophages being a tertiary lesion. This is a simpler model than the Rhoades model but does allow one to consider that granulomas may in fact operate autonomously and granulomas at different stages of development may be present within the same lung lobe. When comparing the schemes, there does seem to be some overlap and oversimplification. Cardona states that Rhoades' category three lesions are thought to be 'coincident with primary granulomas'. Whereas we feel that a category two lesion is better described as a primary granuloma. The statement that 'category 2,4 and 5 can be said to be considered tertiary granulomas' is misleading since there is a huge difference in the size and cellular make up of category 2 and 5 lesions and in our experience, foamy macrophages are still only a minor population by the end of the third week post infection.

Of particular note, is the statement that they could 'hardly identify any epithelioid cells'. Clearly, as they suggest, well delineated criteria allowing a precise definition of what an epithelioid cell is in the context of murine tuberculosis is required. We agree with Cardona that most of the foamy macrophages appear to be within the lumen of the

alveoli, and contain acid fast bacilli and so may very well act as the 'prime movers' in the dissemination of bacilli to other parts of the lung.

The evolving morphology of the granuloma may play a critical role in the pathogenesis of the disease. It is clear that granuloma structure can be markedly different between inbred strains of mice, which will be demonstrated in the next chapter. It is perhaps possible that anatomical factors, such as the development and integrity of the lymphatic tree, or microanatomical differences in the vasculature can affect granulomagenesis. The work presented here is still very preliminary with regards to addressing these issues. A detailed stereologic assessment is feasible, using design-based sampling techniques such as Cavalieri's Unbiased Estimator of Volume (2).

In summary, this study provides the first description of the spatial and temporal distribution of the two major T cell subsets within the developing lung granuloma alongside a new five stage model of histopathogenesis. These data, combined with recent data from the mouse gene knockout models, seem to indicate clear distinctions between the roles of the $CD4^+$ and $CD8^+$ T cell subsets, with the former playing an important role in the expression of acquired resistance, and the latter fulfilling a second important role in maintaining the integrity of the granuloma once a stable form of chronic disease has become established. Isolation of these lung $CD8^+$ T cells and determination of their antigen recognition may provide important information in rational vaccine design and could be used specifically to prevent reactivation disease arising from the chronic/latent state.

Acknowledgements

This work was supported by NIH grant AI-44072. The author wishes to extend special thanks to Dr Mercedes Gonzalez -Juarrero for her help and advice with this work.

References

1. **Apostolou, I., Y. Takahama, C. Belmant, T. Kawano, M. Huerre, G. Marchal, J. Cui, M. Taniguchi, H. Nakauchi, J. J. Fournie, P. Kourilsky, and G. Gachelin.** 1999. Murine natural killer T(NKT) cells [correction of natural killer cells] contribute to the granulomatous reaction caused by mycobacterial cell walls. Proc Natl Acad Sci U S A. **96:**5141-6.

2. **Bolender, R. P., D. M. Hyde, and R. T. Dehoff.** 1993. Lung morphometry: a new generation of tools and experiments for organ, tissue, cell, and molecular biology. Am J Physiol. **265:**L521-48.

3. **Boom, W. H., K. A. chervenak, M. A. Mincek, and J. J. Ellner.** 1992. Role of the mononuclear phagocyte as an antigen-presenting cell for human γδ T cells activated by live *Mycobacterium tuberculosis*. Infect Immunity. **60:**3480-3488.

4. **Bosio, C. M., D. Gardner, and K. L. Elkins.** 2000. Infection of B cell-deficient mice with CDC 1551, a clinical isolate of *Mycobacterium tuberculosis*: delay in dissemination and development of lung pathology. J Immunol. **164:**6417-25.

5. **Breel, M., M. B. van der Ende, T. Sminia, and G. Kraal.** 1988. Subpopulations of non-lymphoid cells in bronchus associated lymphoid tissue and lung of the mouse. Adv Exp Med Biol. **237:**607-13.

6. **Cardona, P. J., A. Cooper, M. Luquin, A. Ariza, F. Filipo, I. M. Orme, and V. Ausina.** 1999. The intravenous model of murine tuberculosis is less pathogenic than the aerogenic model owing to a more rapid induction of systemic immunity. Scand J Immunol. **49:**362-6.

7. **Cardona, P. J., R. Llatjos, S. Gordillo, J. Diaz, I. Ojanguren, A. Ariza, and V. Ausina.** 2000. Evolution of granulomas in lungs of mice infected aerogenically with *Mycobacterium tuberculosis*. Scand J Immunol. **52:**156-63.

8. **Caruso, A. M., N. Serbina, E. Klein, K. Triebold, B. R. Bloom, and J. L. Flynn.** 1999. Mice deficient in CD4 T cells have only transiently diminished levels of IFN-γ, yet succumb to tuberculosis. J Immunol. **162:**5407-5416.

9. **Cooper, A. M., J. E. Callahan, M. Keen, J. T. Belisle, and I. M. Orme.** 1997. Expression of memory immunity in the lung following re-exposure to *Mycobacterium tuberculosis*. Tuber Lung Dis. **78:**67-73.

10. **Cooper, A. M., D. K. Dalton, T. A. Stewart, J. P. Griffin, D. G. Russell, and I. M. Orme.** 1993. Disseminated tuberculosis in interferon gamma gene-disrupted mice. J Exp Med. **178:**2243-7.

11. **Cooper, A. M., and J. L. Flynn.** 1995. The protective immune response to *Mycobacterium tuberculosis*. Current Op Immunol. **7:**512-6.

12. **Cooper, A. M., J. Magram, J. Ferrante, and I. M. Orme.** 1997. IL-12 is crucial to the development of protective immunity in mice intravenously infected with *Mycobacterium tuberculosis*.J Exp Med. **186:**39-46.

13. **D'Souza, C. D., A. M. Cooper, A. A. Frank, R. J. Mazzaccaro, B. R. Bloom, and I. M. Orme.** 1997. An anti-inflammatory role for gamma delta T lymphocytes in acquired immunity to *Mycobacterium tuberculosis*. J Immunol. **158:**1217-21.

14. **Flynn, J. L., J. Chan, K. J. Triebold, D. K. Dalton, T. A. Stewart, and B. R. Bloom.** 1993. An essential role for interferon gamma in resistance to *Mycobacterium tuberculosis* infection. J Exp Med. **178:**2249-54.

15. **Francis, J.** 1958. Tuberculosis in Animals and Man: A study in Comparative Pathology. Cassell and co., London, England.

16. **Medina, E., and R. J. North.** 1998. Resistance ranking of some common inbred mouse strains to *Mycobacterium tuberculosis* and relationship to major histocompatibility complex haplotype and Nramp1 genotype. Immunology. **93:**270-4.

17. **North, J. N.** 1995. *Mycobacterium tuberculosis* is strikingly more virulent for mice when given via the respiratory than the intravenous route. J Inf Dis. **172:**1550-1553.

18. **Orme, I., P. Andersen, and W. Boom.** 1993. T cell response to *Mycobacterium tuberculosis*. [Review]. J Inf Dis. **167:**1481-97.

19. **Orme, I., and F. Collins.** 1983. Protection against *Mycobacterium tuberculosis* infection by adoptive immunotherapy. Requirement for T cell-deficient recipients. J Exp Med. **158:**74-83.

20. **Orme, I. M.** 1998. The immunopathogenesis of tuberculosis: a new working hypothesis. Trends Microbiol. **6:**94-7.

21. **Orme, I. M.** 1987. The kinetics of emergence and loss of mediator T lymphocytes acquired in response to infection with *Mycobacterium tuberculosis*. J Immunol. **138:**293-8.

22. **Orme, I. M., and A. M. Cooper.** 1999. Cytokine/chemokine cascades in immunity to tuberculosis. Immunol Today. **20:**307-12. 00001438 00001438.

23. **Orme, I. M., A. D. Roberts, J. P. Griffin, and J. S. Abrams.** 1993. Cytokine secretion by CD4 T lymphocytes acquired in response to *Mycobacterium tuberculosis* infection. J Immunol. **151:**518-25.

24. **Orrell, J. M., S. J. Brett, J. Ivanyi, G. Coghill, A. Grant, and J. S. Beck.** 1991. Measurement of the tissue distribution of immunoperoxidase staining with polyclonal anti-BCG serum in lung granulomata of mice infected with *Mycobacterium tuberculosis*. J Pathol. **164:**41-5.

25. **Orrell, J. M., S. J. Brett, J. Ivanyi, G. Coghill, A. Grant, and J. S. Beck.** 1992. Morphometric analysis of *Mycobacterium tuberculosis* infection in mice suggests a genetic influence on the generation of the granulomatous inflammatory response. J Pathol. **166:**77-82.

26. **Rhoades, E. R., A. M. Cooper, and I. M. Orme.** 1995. Chemokine response in mice infected with *Mycobacterium tuberculosis*. Infect Immun. **63:**3871-7.

27. **Rhoades, E. R., A. A. Frank, and I. M. Orme.** 1997. Progression of chronic pulmonary tuberculosis in mice aerogenically infected with virulent *Mycobacterium tuberculosis*. Tuber Lung Dis. **78:**57-66.

28. **Serbina, N. V., C. C. Liu, C. A. Scanga, and J. L. Flynn.** 2000. CD8+ CTL from lungs of *Mycobacterium tuberculosis*-infected mice express perforin in vivo and lyse infected macrophages. J Immunol. **165:**353-63.

29. **Teitelbaum, R., A. Glatman-Freedman, B. Chen, J. B. Robbins, E. Unanue, A. Casadevall, and B. R. Bloom.** 1998. A mAb recognizing a surface antigen of *Mycobacterium tuberculosis* enhances host survival. Proc Natl Acad Sci U S A. **95:**15688-93.

30. **Turner, J., C. D. D'Souza, J. E. Pearl, P. Marietta, M. Noel, A. A. Frank, R. Appelberg, I. M. Orme, and A. M. Cooper.** 2001. CD8- and CD95/95L-dependent mechanisms of resistance in mice with chronic pulmonary tuberculosis. Am J Respir Cell Mol Biol. **24:**203-9.

31. **Turner, J., A. A. Frank, J. V. Brooks, M. Gonzalez-Juarrero, and I. M. Orme.** 2001. The progression of chronic tuberculosis in the mouse does not require the participation of B lymphocytes or interleukin-4. Exp Gerontol. **36:**537-45.

32. **Turner, J., M. Gonzalez-Juarrero, B. M. Saunders, J. V. Brooks, P. Marietta, D. L. Ellis, A. A. Frank, A. M. Cooper, and I. M. Orme.** 2001. Immunological basis for reactivation of tuberculosis in mice. Infect Immun. **69:**3264-70.

33. **Zumla, A. Geraint James, D.** 1999. The Granulomatous Disorders, First ed. Cambridge University Press, cambridge.

Chapter Three

Immunopathology of Pulmonary Tuberculosis in Mice Unable to Control the Growth of *Mycobacterium tuberculosis* in the Lung

Abstract

In this study we compared a spectrum of pulmonary immunopathologic features of granulomagenesis in three inbred mouse strains, C57BL/6, IFN- γ gene-disrupted (GKO) and SWR, after a low dose aerosol infection with *Mycobacterium tuberculosis*. C57BL/6 mice were used as a model for the arrest and reactivate scenario in man and GKO mice were used as a model for the rapid, progressive disease. SWR mice have not previously been investigated in tuberculosis studies but appeared to present as a strain that fell in between these two paradigms, as far as ability to control bacterial growth in the lungs, and cumulative survival. It was hoped that these mice might shed new light on pathogenesis that could be applicable to human studies. The study focused on characterizing the lung pathology, lymphocyte subsets, their spatial and temporal arrangements, and their activation and proliferation status during infection. As expected, C576BL/6 and GKO mice developed distinctly different lung pathology concurrent with either an arrest of bacterial proliferation or progressive, uncontrolled growth respectively. In the chronic stages of disease, pathology was characterized in C57BL/6 by multifocal granulomatous inflammation, typified by mixed aggregates of lymphocytes and epithelioid macrophages and random necrosis and apoptosis. In GKO mice, there was

severe, extensive necrotizing granulomatous pneumonia with abundant necrosis, apoptosis and peripheralized lymphocytes. We have shown that in SWR mice in contrast, bacterial growth was continuous but not as rapid as that in GKO mice. Pathology was characterized in the chronic stages by a diffuse granulomatous inflammation with sheets of large epithelioid and foamy macrophages, multifocal necrosis, a moderate amount of apoptosis, scattered neutrophil accumulation, and relatively fewer lymphocytes compared to C57BL/6. Some of these SWR macrophages contained ultrastructural intracytoplasmic crystalloid inclusions, thought to represent the degradative residue of phagocytized neutrophils and/or eosinophils. Key lymphocyte differences between C57BL/6 and SWR included a low percentage of $CD4^+$ lymphocytes that produced intracellular IFN-γ, a lower percentage of proliferating $CD4^+$ cells and slower accumulation of memory cells in SWR mice. Deficiencies in these parameters appear to affect the ability to contain the infection, leading to a progressive, fatal disease.

Introduction

In human tuberculosis, three basic paradigms of bacterial growth and disease progression are observed. The bacteria may all be killed and the human is cured, the bacteria are contained (arrested) at a low level, and 'reactivate' at a later time point, or, there is progressive growth and associated pneumonia. Resistance against development of tuberculosis in humans is known to be affected by several host factors including previous exposure to mycobacteria, age, family, history of tuberculosis ethnicity, malnutrition and concurrent disease (2-5, 14, 34). These variables influence both the ability to contain the

primary infection and severity of the progressive disease. How these factors are interrelated however remains to be fully elucidated.

The panoply of potential 'resistance factors' is daunting, however, one rational approach to searching for mechanisms involved in tuberculosis control is the comparative analysis of mouse strains that clearly differ in a maximum number of commonly used parameters of susceptibility. These include the number of colony forming units recovered from internal organs, mean survival times, and lung pathology.

To this end, the purpose of the study presented here was to characterize key differences in the developing pulmonary immunopathology between three inbred mouse strains C57BL/6, IFN- γ gene-disrupted (GKO) mice and SWR mice, that have been shown to differ in their resistance to aerosol infection. C57BL/6 mice are one of the most common strains of laboratory mice, characterized as a general purpose research tool, with no specific immunological defects. The pathological response to tuberculosis has been described in these mice by various groups (7, 28) and are generally considered a 'resistant' strain (19). This term refers to its ability to control bacterial growth and resist reactivation disease for a relatively long period of time. GKO mice have been used in immunological and inflammatory research for almost ten years, with their hypersusceptibility (inability to control bacterial growth) to tuberculosis known for a similar length of time (9, 13). SWR mice are utilized in a variety of research fields including carcinogenesis, diabetes, and experimental allergic encephalomyelitis (20). No studies to date report on their response to tuberculosis. Our preliminary studies however,

indicated that it might present as a novel phenotype with regards to tuberculosis pathogenesis.

After low dose aerosol infection of *M.tuberculosis*, the C57BL/6 mice expressed the expected features of mice that fit into the human 'arrest and reactivate' model and the GKO mice the 'progressive' model. In C57BL/6 mice this was demonstrated by a long survival time, an ability to stabilize pulmonary bacterial growth, and a multifocal granulomatous inflammation characterized by aggregates of lymphocytes admixed with epithelioid macrophages. In the GKO mice there was a short survival time, no ability to control bacterial growth and a severe extensive necrotizing, granulocytic, granulomatous pneumonia. In contrast the SWR mice expressed features in-between these with regards to bacterial growth, survival time and pathology. Lesions were exemplified by a diffuse granulomatous pneumonia dominated by large epithelioid and foamy macrophages, multifocal necrosis and neutrophil accumulation and scant aggregates of lymphocytes. The SWR mice had crystalloid inclusions within macrophages, seen rarely in the GKO mice and never in the C57BL6 mice. In addition, lymphocytes within the lungs of SWR mice had significantly different phenotypes when compared to C57BL/6 mice. In particular, there was a consistently lower percentage of $CD4^+$ IFN-γ producing lymphocytes, a lower percentage of proliferating $CD4^+$ cells, and a lower percentage of $CD4^+$ and $CD8^+$ lymphocytes with memory markers in SWR mice compared to those in the C57BL/6 mice. Taken together, these features point to a new immunopathological model, that might assist in the diagnosis of human disease.

Materials and Methods

Mice

Specific-pathogen-free, female C57BL/6, C57BL/6-Ifngtm1Ts (GKO) and SWR mice of 6-8 weeks of age were purchased from the Jackson Laboratories (Bar Harbor, ME, USA). Infected and uninfected control mice were maintained in a biosafety level-3 facility at Colorado State University. All animals had free access to water and standard mouse chow. The specific-pathogen-free nature of the mouse colonies was demonstrated by testing sentinel animals. These were shown to be negative for 12 known mouse pathogens. In each experiment, 4 or 5 animals were used at each time point, with at least one uninfected control mouse.

Bacteria and infection

M. tuberculosis strain Erdman (TMCC #107) was grown from low passage seed lots in Proskauer-Beck liquid media containing 0.02% Tween 80 to mid-log phase, then aliquoted and frozen at -70^{0}C until use. Mice were infected via the aerosol route with a low dose of bacteria. Briefly, the nebulizer compartment of a Middlebrook airborne infection apparatus (Glas-col, Terre Haute, IN) was filled with 5 ml of H_2O containing a suspension of bacteria resulting in delivery of approximately 100 bacteria per lung during a 30 minutes exposure.

Enumeration of bacteria

At the times indicated, mice were euthanized by carbon-dioxide asphyxiation. Lungs were aseptically removed from the thoracic cavity and the number of viable bacteria

present was assessed by plating serial dilutions of left lung lobe homogenates onto Middlebrook 7H11 nutrient agar. After three weeks incubation at 37^{0}C in humidified air, the number of bacterial colonies for each dilution were counted with a 4x magnification dissecting microscope. The data are representative of one to three experiments and are expressed as the log10 value of the mean number of colony forming units counted, with standard error of the mean indicated by vertical bars.

Gross lesion assessment

At each time point, an appraisal of gross lesions within the lung and thorax was made. All animals that died unexpectedly were necropsied and cumulative survival curves were generated.

Histology

The lungs were removed from the thoracic cavity either as the entire pluck or as individual lobes. The right cranial lung lobe, or all lung lobes, from each mouse was slowly infused with and then submerged in 10% neutral buffered formalin for a minimum of 72 hours. Tissues were prepared routinely and sectioned for light microscopy with lobe orientation designed to allow for the maximum surface area of each lobe to be seen. Consecutive sections were stained with hematoxylin and eosin, the Ziehl-Neelsen method for the detection of acid-fast bacilli, and Masson's Trichrome for detection of type IV collagen. All tissue identification was masked and the order was randomized to preclude experimental group bias. Sections were examined at least three times to verify the reproducibility of the observations.

Criterion for assessment of pulmonary lesions

An assessment of all of the parenchymal and non-parenchymal tissue elements was performed in all sections, a minimum of three times. This included trachea, bronchi, bronchioles, alveoli, pleura and vasculature. In each case the presence and distribution of inflammatory cell types was noted. This included macrophages, mononuclear cells (lymphocytes and plasma cells), multinucleated giant cells and neutrophils. The presence and distribution of acid fast bacilli, type IV collagen and necrosis was also noted. All tissue identification was masked and the order was randomized to preclude experimental group bias. A correlation to the C57BL/6 1 to 5 grading scheme previously described was made in an attempt to further define the histopathological differences between these strains of mice.

Detection of apoptosis

The ApopTag plus peroxidase *In situ* Apoptosis Detection kit S7101 (Intergen, Purchase NY) was used to detect apoptotic cells in paraffin-embedded tissue. This kit employs the terminal transferase-mediated dUTP nick-end labeling (TUNEL) method (32) to distinguish fragmented DNA present in apoptotic bodies. Two or three 5-micron sections of the same tissue used for histological analysis were analyzed per time point.

Electron Microscopy

At each time point, the right accessory lung lobe was aseptically removed, diced into pieces no larger than 2mm in diameter and placed in a 4% formaldehyde-1.25% gluteraldehyde solution for a minimum of 72 hours. The tissue was the processed for

routine electronmicroscopic examination. Using a JEOL JEM-1200EX electron microscope with an accelerating voltage of 80KV multiple sections of lung from both strains were examined. Since *M. tuberculosis* infects pulmonary macrophages, particular attention was paid to these cells.

Immunohistochemistry

Purified rat anti-mouse monoclonal antibodies specific for mouse CD4 (L3T4 clone H129.19), CD8 (Ly-2 clone 53-6.7) and CD45R/B220 (clone RA3-6B2) were purchased from BD Pharmingen (San Diego, CA). The appropriate BD Pharmingen isotype controls rat $IgG_{2a,\kappa}$ (clone R35-95), and rat $IgG_{1,\kappa}$ (cloneR3-34) were also purchased and used along side the specific antibodies. Biotinylated goat anti-rat Ig (multiple adsorption) was used as the secondary antibody in each experiment. The lungs were removed from the thorax either as the entire pluck or as individual lobes. The tissue was then slowly infused with a solution of 20% OCT (Tissue-Tek, Inc. Torrance, CA) in 1X PBS through the trachea or at the hilus of individual lobes. The tissue was then placed in a tissue mold, completely surrounded by OCT, frozen in a bath of liquid nitrogen and stored at –70° C until used. Serial sections from each lung of 5-7μm thick were cut in a CM 1850 cryotome (Leica Inc. Deerfield, IL), employing the Instrumedics Inc.(Hackensack NJ) 'tape transfer system', fixed in cold acetone for 10 minutes and air-dried. After first confirming the efficacy of this freezing and sectioning technique with staining protocols on the bench-top, subsequent sections were stained using an automated staining system. This produced a degree of uniformity in staining intensity that was very hard to reproduce with manual manipulation and so allowed for greater accuracy of morphometric analysis.

The sections were washed in APK buffer solution (Ventana Medical Systems, Tucson, AZ) for 15 -20 minutes and then incubated in a 1:20 (CD4), 1:20 (CD8),1:50 (CD45R/B220), and 1:20 (isotype) solution of Protein Block -goat serum (Biogenex, San Ramon, CA) and primary antibody. The sections were then placed on a Nexus automated immunostainer (Ventana medical systems, Tucson, AZ). Both the labeled avidin horse-radish peroxidase and DAB -H_2O_2 detection kit and the labeled avidin alkaline phosphatase and Fast red Napthol detection kit were employed through the course of these experiments. The secondary antibody was incubated for 30 minutes at room temperature at a concentration of 1:20 in APK buffer. Sections were counterstained with Meyer's hematoxylin. Sections of spleen were also routinely examined to act as positive controls.

FACS analyses of cell surface markers

Lung lymphocytes from C57BL/6 and SWR mice were analyzed at day 30 and day 60 post infection by flow cytometry. A single cell suspension was prepared from lungs as described previously (15). Cells were stained for cell surface markers using rat anti-mouse monoclonal antibodies specific for mouse CD4 (L3T4 clone GK1.5,), CD8 (Ly-2 clone 53-6.7), CD25 (clone PC61), CD44 (clone IM7), CD45RB (clone 16A), CD62l(L-selectin clone MEL-14), CD69 (cloneH1.2F3), CD122 (IL-2 receptor β chain clone 5H4), γδ TCR (clone GL3), OX40L (clone RM 134L), Pan-NK cells (clone DX5) and NK1.1 (clone PK 136). Appropriate isotype staining was also performed. All staining procedures were performed in RPMI media 1640 without glutamine (Life Technologie, Rockville, MA) with 0.1% Azide. All Abs were used at 0.2μg/10^6 cells and obtained from

BD Pharmingen (San Diego, CA) as direct conjugates to FITC, PerCP, PE or APC. Acquisition was performed on a FACSCalibur instrument (BD immunocytometry Systems, San Jose, CA), and data was analyzed using CellQuest software (BD immunocytometry Systems, San Jose, CA). Cells were gated for lymphocytes by their characteristic forward and side-scatter profile, and 50,000 events in the lymphocyte gate per sample were counted. Markers are represented as a percentage of the cell population being analyzed. It must be noted that representation of this, and all flow cytometric data in this experiment as percentages does not allow for an assessment of total cell numbers in each mouse. Cell number data is thus also presented to facilitate a more complete analysis of the immunopathology.

Assessment of T cell proliferation by Brdu incorporation

Mice infected with *M. tuberculosis* for 30 days and 60 days were administered a solution of 5'-bromodeoxyuridine (BrdU) (catalog no. B5002; Sigma-Aldrich) at 0.8mg/ml in sterile water for three days (72 hours) prior to harvest of lungs. Single cell suspensions of lung tissue were stained with FITC-anti-BrdU Ab or FITC-IgG isotype Ab according to the manufacturer's instructions (BD Pharmingen Brdu kit catalog no.2354KK). Briefly, cells were harvested, resuspended at $5x10^6$ / ml in D-PBS + 0.1% Azide and stained for CD4 -FITC and CD8 - PE cell surface Ags. The cells were fixed and permeabilized at 4°C for 20 minutes according to the manufacturers instructions (using kit reagents, no ethanol), incubated with DNAse for 60 minutes at 37°C, and labeled with anti Brdu. Analysis was performed by gating total lymphocytes by forward and side scatter.

Assessment of intracellular IFN-γ production

Single cell suspensions of lungs at 30 and 60 days after aerosol infection were prepared and stained for intracellular IFN-γ. Briefly, cells were either stimulated with anti-CD3 (clone 145-2C11, 0.1 μg/ml) and anti-CD28 (clone 37.51, 1 μg/ml) Abs (BDPharmingen) or left unstimulated for 5–6 h in the presence of 3 μM monensin (Sigma-Aldrich, St. Louis, MO). At the end of the stimulation period, cells were stained for CD4 and CD8, fixed, permeabilized, and stained for intracellular IFN-γ. Cells were resuspended at $5x10^6$ / ml in complete D-RPMI with 10% FBS. Analysis was performed by gating total lymphocytes by forward and side scatter.

Photomicroscopy and morphometry

Photomicroscopy was performed with an Olympus AH-2 microscope linked to a Sony SKC-DK5 digital camera and Adobe Photoshop 6.0 software. In an attempt to further classify the pulmonary lesions, the granuloma fraction was calculated from each of the hematoxylin and eosin stained histological slides. In brief, using Metamorph Image Analysis Software (Metamorph 4.5r5, Universal Imaging Corporation, Downington PA), images of individual lobes or all lobes were acquired. These were calibrated, measured and the perceived inflammatory area was defined and expressed as a percentage of the total lung area. This percentage of affected tissue was termed the granuloma fraction (25, 26)

Statistical analysis

Statistical analysis was performed with the Sigma Stat 2 software program. The one-way analysis of variance (ANOVA) and Student t-test were used to analyze bacterial growth curve data. The Mann-Whitney Rank Sum test was used for the analysis of granuloma fraction and Kaplan-Meier analysis was employed for cumulative survival. Statistical significance was taken as $P=<0.05$.

Results

Course of *M. tuberculosis* infection in the lungs of C57BL/6, GKO and SWR mice as measured by bacterial load, granuloma fraction and cumulative survival.

Over the course of the first 10 days post infection the bacterial load in all three strains increased at a similar rate. Thereafter however, the bacterial load in the GKO mice increased rapidly from 2.0 logs to 7.0 logs at which time the mice died. There was no containment of growth. Concomitant with the bacterial growth was a rapid increase in granuloma fraction up to 60%, and low cumulative survival over time (Figure 3.1B,C). All these features were consistent with the lethal, progressive disease previously described in this strain of mice (9,13). A significantly higher load of bacteria was present in the lungs of GKO mice compared to SWR and C57BL/6 mice from as early as 15 days. Bacteria grew progressively in the lungs of SWR mice but there was evidence that growth slowed down at approximately 30 days post infection. It was significantly higher than in C57BL/6 however, at all subsequent time points, peaking at approximately 6.5logs (Figure 3.1A). Granuloma fraction rose along with increasing bacterial load in the SWR mice reaching a peak of almost 70%, and cumulative survival was longer than the

GKO mice but less than the C57BL/6 mice over time (Figure 3.1B,C). The C57BL/6 mice exhibited bacterial growth, pathology and survival characteristics consistent with arrest and reactivation as previously described in chapter 2. Bacterial growth was relatively stable until late in infection, when it started to increase. Granuloma fraction increased slowly throughout the disease and cumulative survival was relatively high throughout the disease (Figure 3.1B,C). The survival curves were generated using the Kaplan-Meier method, and the increased mortality of GKO and SWR mice compared to C57BL/6 mice and to each other was statistically significant ($p<0.05$ by the log rank test). It is important to note that survival data was generated from a low number of animals (n=11) and the combined results of two experiments.

Gross lesions

Figure 3.2 highlights the comparative differences in the gross lesions in chronic stages of disease. In each strain the granulomas had a multifocal, distribution. In the GKO mice, by 69 days post infection, the lungs were larger, than the C57BL/6 mice, probably due to the massive cellular influx, and they had very prominent, necrotic granulomas (Figure 3.2 A). Pleuritis was also a consistent feature in the GKO mice with fibrinous and fibrous adhesions between visceral and parietal surfaces commonly seen. No pleuritis was detected in the C57BL/6 mice. The SWR mice had granulomas that had a more diffuse margin than the C57BL/6 mice (Figure 3.2 B). SWR lungs exhibited a moderate increase in size with moderate pleuritis at the end stage of disease.

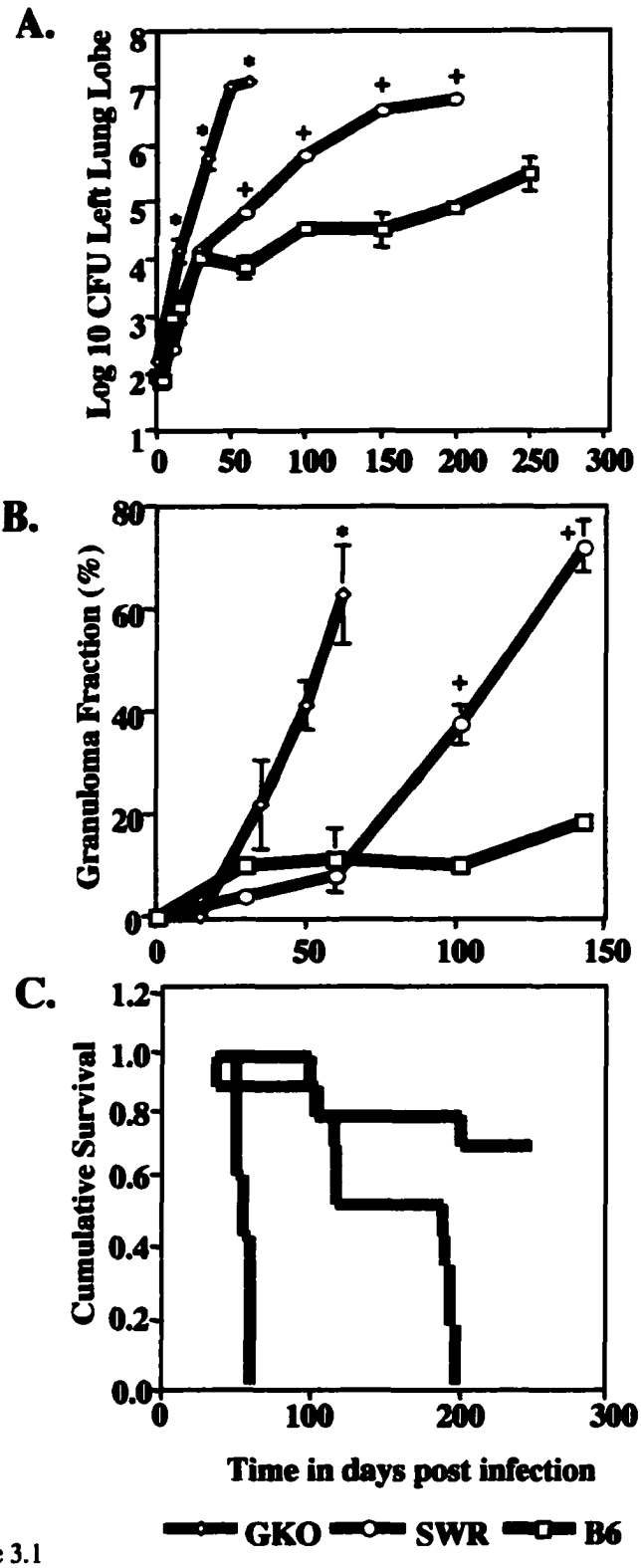

Figure 3.1
A, Representative growth curves of *M. tuberculosis* and B, granuloma fraction in the lungs of interferon gamma knockout (GKO), SWR and C57BL/6 (B6) mice after low dose aerosol infection. C, cumulative survival curves. * statistically significant differences between all three strains, + statistically significant differences between SWR and B6 only. All survival curves are significantly different by the Kaplan-Meier method Data is representative of one to three experiments.

A.

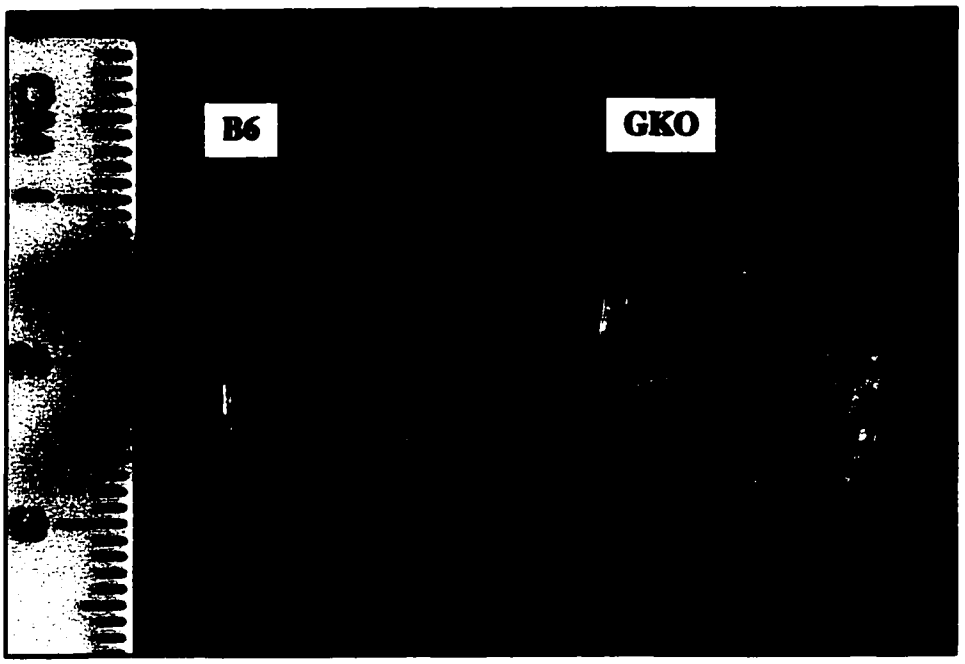

B.

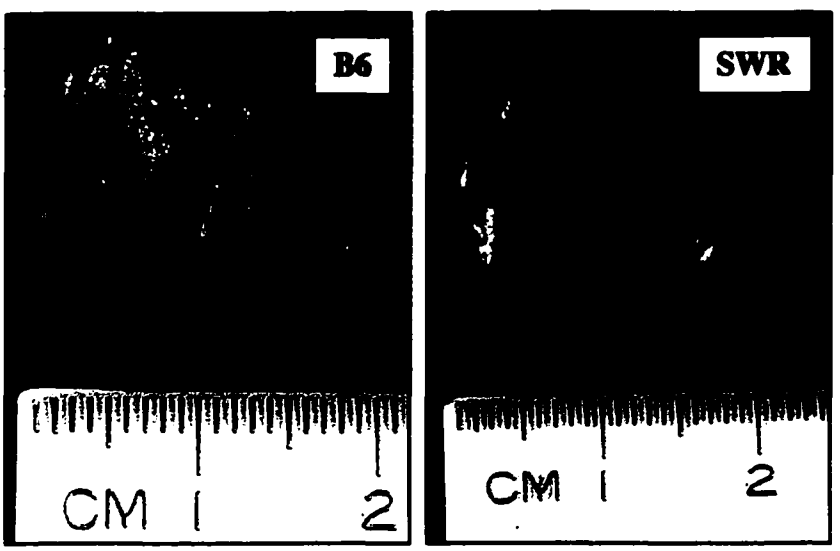

Figure 3.2
Representative photographs of plucks from C57BL/6 (B6), interferon gamma knockout (GKO) and SWR mice after aerosol infection with *M.tuberculosis*. In each image a typical granuloma is highlighted by a black circle. A. 69 days post infection. B. 143 days post infection. Data is representative of one to three experiments.

Histopathological assessment

The following tables and figures depict comparative assessments made between the three mouse strains. Hematoxylin and eosin stained sections from C57BL/6 mice have previously been described previously and so only SWR and GKO lesions are presented.

Table 3.1

Summary of the histopathological and morphometric categorization of the pulmonary lesions of **SWR mice** compared to C57BL/6 mice infected via aerosol with *M. tuberculosis.*

A. Inflammatory cell types present and their localization

C57BL/6 Lesion Stage	DPI	MØ	MNGC	LØ	Plasma Cell	NØ	EØ
1	0-5	ND	ND	ND	ND	ND	ND
2	5-25	Histiocyte Epithelioid MF, I	None	MF, I	None	MF I	None
3	25-35	Epithelioid, Foamy MF, I, IA	None	PV, PB	None	MF.I	MF
4	35-150	Foamy, MF, IA, Diffuse	Scattered	PV, PB	PV,PB	MF	MF
5	>150	Foamy, MF, IA, Diffuse	Scattered, anisokaryosis	PV, PB	PV,PB	MF	MF

Figure 3.3 further highlights the key components of granulomagenesis seen in these mice

Key:
DPI = Days post infection, I = Interstitial, IA = Intra-alveolar, PV = Perivascular, PB = Peribronchioloar, MF = Multifocal, LØ = Lymphocytes, MØ = Macrophages, MF = Multifocal, MNGC = Multinucleate giant cell, NØ = Neutrophils , EØ = Eosinophil, Histiocyte = Normal, resident tissue macrophage (alveolar / interstitial). ND = not done, NS=not seen, GF = granuloma fraction.

Note: Eosinophils were generally few to rare, and not as abundant as neutrophils. A comparison is made with the 5 stage C57BL/6 model to illustrate the different pathology in the SWR mice at the corresponding time points.

B. Sequelae of each stage

C57BL/6 Lesion Stage	Fibrosis	Necrosis	AFB	Airway Involvement	Pleural Involvement	GF%
1	ND	ND	ND	ND	ND	ND
2	None	None	None observed	None	None	0-1
3	None	None	Few, intracellular	None	Subpleural aggregates	1-5
4	diffuse	MF	Multiple	Necrotic cellular debris in airways	Subpleural aggregates. Chronic pleuritis	5-70
5	diffuse	MF	Multiple	Necrotic cellular debris in airways	Subpleural aggregates. Chronic pleuritis	>70

The data represents the results of three experiments.

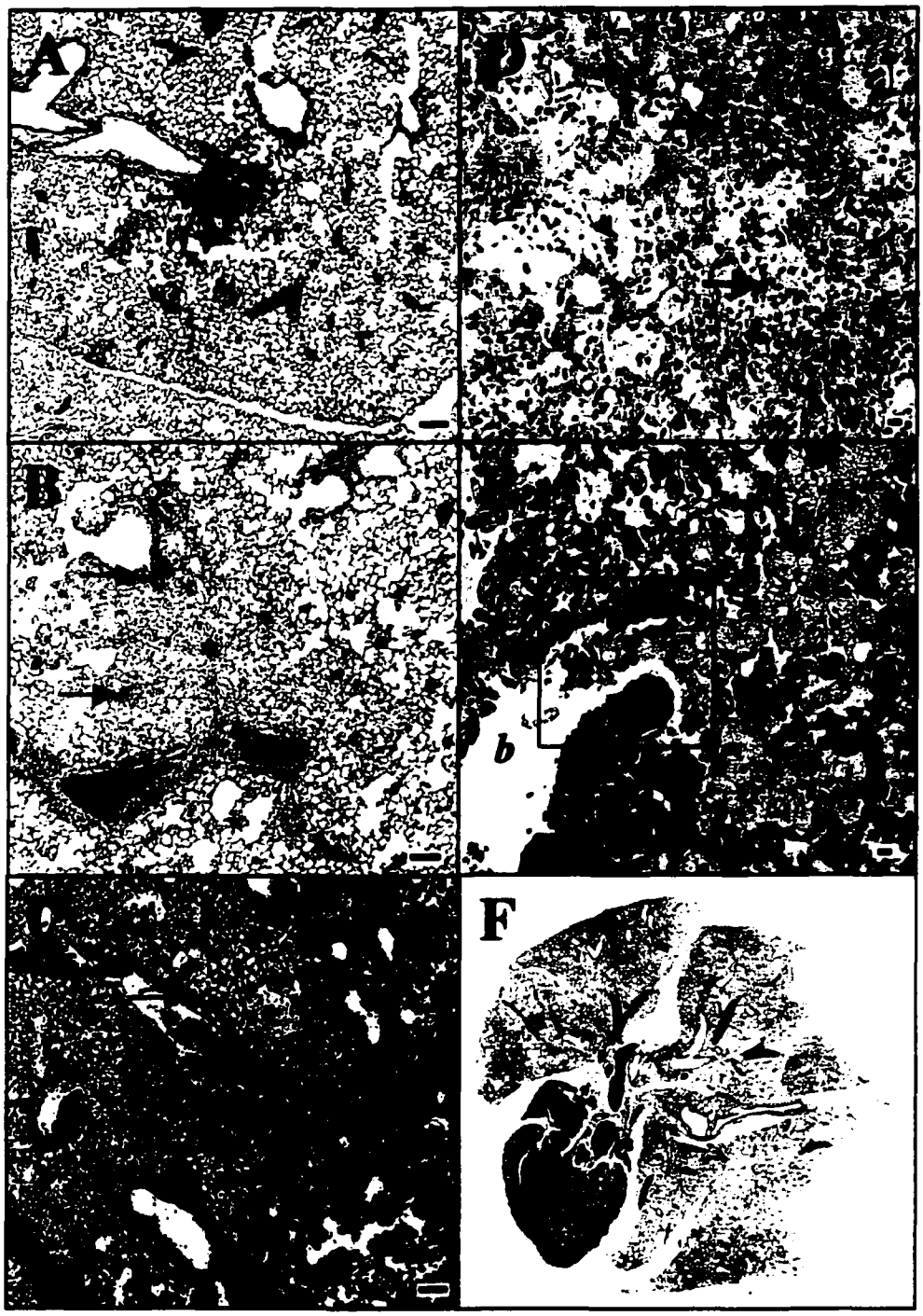

Figure 3.3

Representative photomicrographs of lung from SWR mice after low dose aerosol infection with *M. tuberculosis*. A. 30 days post infection, perivascular lymphocytes (arrow) bar=100μm. B. 60 days post infection, perivascular lymphocytes (arrows) with macrophages *, bar=100μm. C. 200 days post infection, perivascular lymphocytes (arrows) with extensive macrophages *, bar=100μm. D 200 days post infection. neutrophils (arrows), cholesterol cleft (arrow head), bar=10μm E. 200 days post infection.Multiple foamy macrophages * filling lumen of bronchiole *(b)*. F. Pluck, 1x magnification. *h* = heart. Note extensive consolidation of all lobes. Hematoxylin and eosin. Data is representative of one to three experiments.

Table 3.2

Summary of the histopathological and morphometric categorization of the pulmonary lesions of **GKO mice** compared to C57BL/6 mice infected via aerosol with *M. tuberculosis.*

A. Inflammatory cell types present and their localization

C57BL/6 Lesion Stage	DPI	MØ	MNGC	LØ	Plasma Cell	NØ	EØ
1	1	Histiocyte, Epithelioid. IA	None	PV, PB	None	None	PV, PB
2	15	Histiocyte, Epithelioid. IA	None	PV, PB	None	None	PV, PB, IA
3	35	Epithelioid Foamy Acidophilic. IA	MF	PV, PB. IA	None	MF	PV, PB, IA
4	50-62	Foamy, Acidophilic. IA	Multiple, MF	MF	Few	Extensive	MF

Figure 3.4 further highlights the key components of granulomagenesis seen in these mice.

Note: Acidophilic macrophages are depicted in Figure 3.4F.

Key:
DPI = Days post infection, I = Interstitial, IA = Intra-alveolar, PV = Perivascular, PB = Peribronchioloar, MF = Multifocal, LØ = Lymphocytes, MØ = Macrophages, MF = Multifocal, MNGC = Multinucleate giant cell, NØ = Neutrophils , EØ = Eosinophil, Histiocyte = Normal, resident tissue macrophage (alveolar / interstitial). ND = not done, NS=not seen, GF = granuloma fraction.

Note: A comparison is made with the 5 stage C57BL/6 model to illustrate the different pathology in the SWR mice at the corresponding time points.

B. Sequelae of each stage

C57BL/6 Lesion Stage	Fibrosis	Necrosis	AFB	Airway Involvement	Pleural Involvement	GF%
1	None	None	None observed	None	None	0-0.5
2	None	None	None observed	None	None	0.5-1
3	Extensive	MF	Multiple Intra and extracellular	Occasional cellular debris	Subpleural aggregates Chronic pleuritis	20
4	Circumferential	Extensive, MF	Multiple Intra and extracellular	Necrotic, suppurative debris with fibrin	Chronic, suppurative	60

The data represents the results of one experiment.

Figure 3.5 highlights the key differences in the appearance of bacilli and collagen deposition in chronic lesions in these in these mice.

Apoptosis

The general trend was one of increasing abundance of cells staining positive for apoptosis within the lesions of C57BL/6 to SWR to GKO (Figure 3.6). Quantification of this phenomenon proved very difficult due to the inconsistency of staining and variable lesion morphology. Of particular note, however, was the abundance of positive cells around the margins of the GKO granulomas (Figure 3.6 E,F)

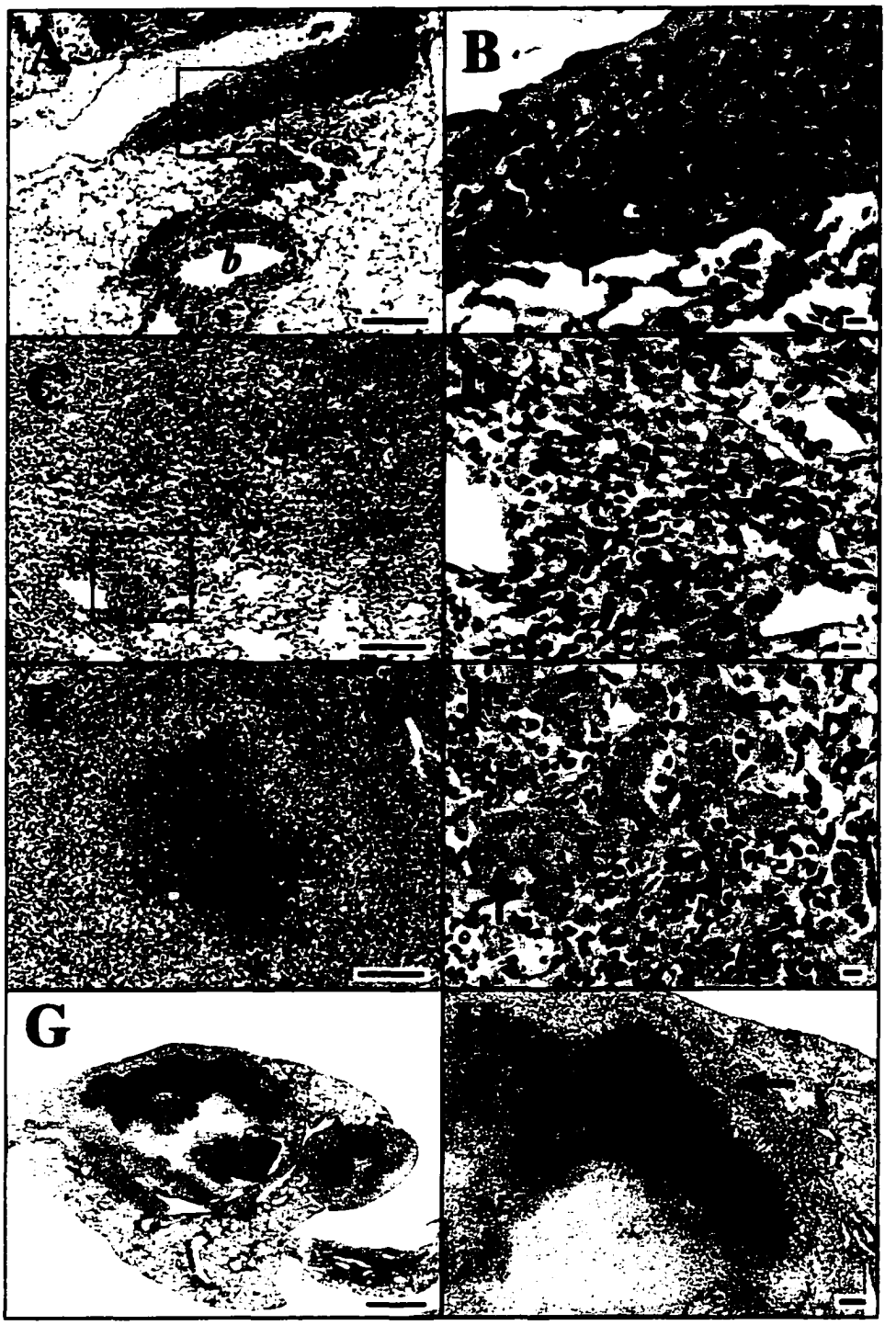

Figure 3.4

Representative photomicrographs of lung from interferon gamma knockout mice after low dose aerosol infection with *M. tuberculosis*. A,B 15 days post infection. A. Thick perivascular and peribronchiolar lymphocyte and eosinophil aggregates. *b*=bronchiole bar=100μm. B High magnification of area within black box in A, eosinophils (arrows) bar=10μm. C ,D 35 days post infection. C Extensive consolidation, bar=100μm. D neutrophils (arrows) bar=10μm E,F 50 days post infection. E * (necrosis) bar=100μm. F acidophilic macrophages (arrows) eosinophils (arrow head) bar=10μm G,H 62 days post infection. G * (granuloma) bar=1mm.H High magnification of margin of granuloma in G. Thick capsule (arrow). bar=100μm. Hematoxylin and eosin.

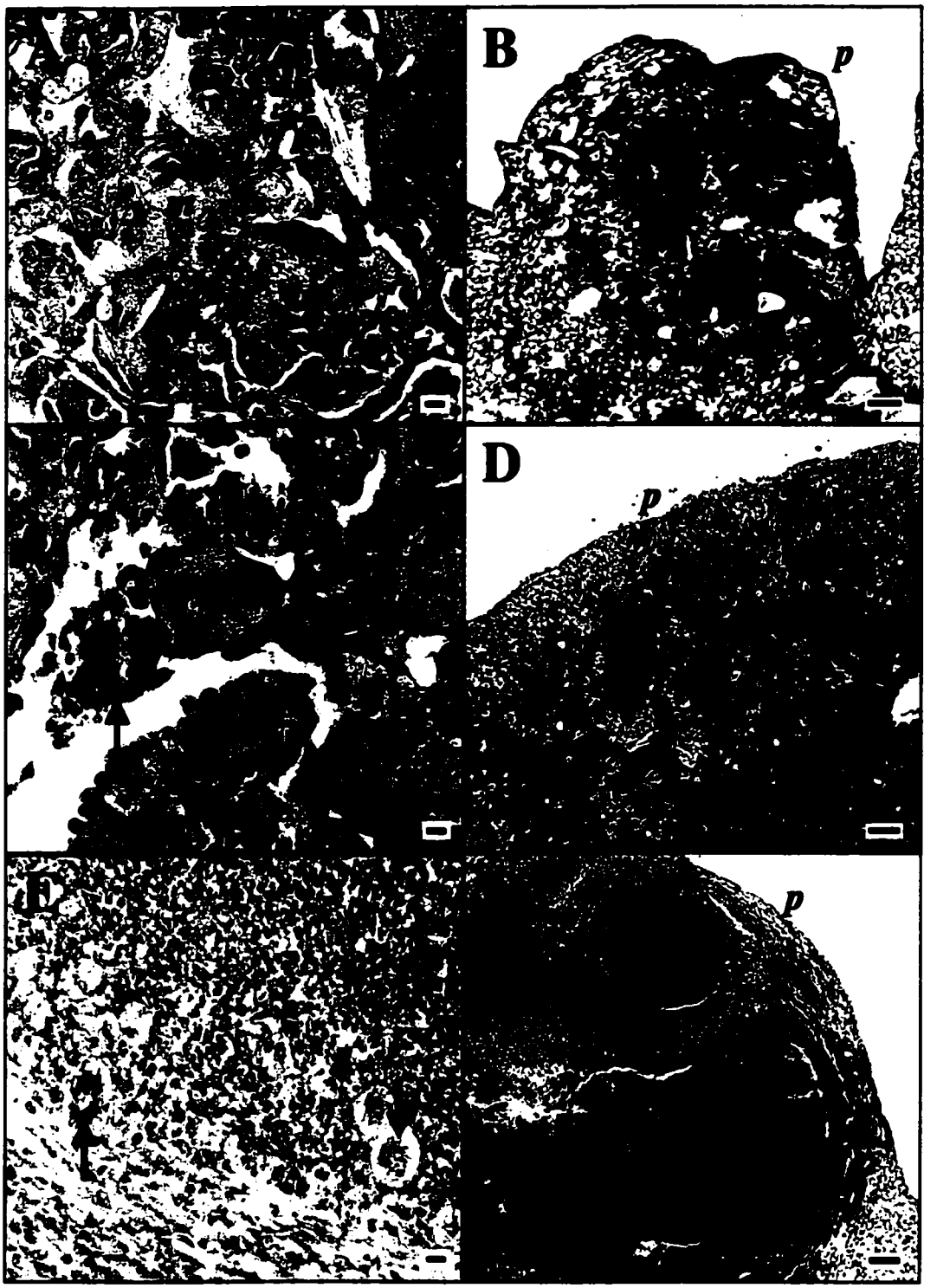

Figure 3.5

Representative photomicrographs of lung stained for acid fast bacilli - red (Ziehl Neelson method) (A,C,E bar=10μm) and type IV collagen - blue (Masson's Trichrome) (B,D,F bar = 100μm) following low dose aerosol infection with *M. tuberculosis*. C57BL/6 mice (A,B), 250 days post infection, SWR mice (C,D) 150 days post infection and gamma interferon knockout mice (E,F), 65 days post infection. Arrows = acid-fast bacilli, *m* =macrophage, *p*=pleura and * = thick collagenous capsule. Data is representative of one to three experiments.

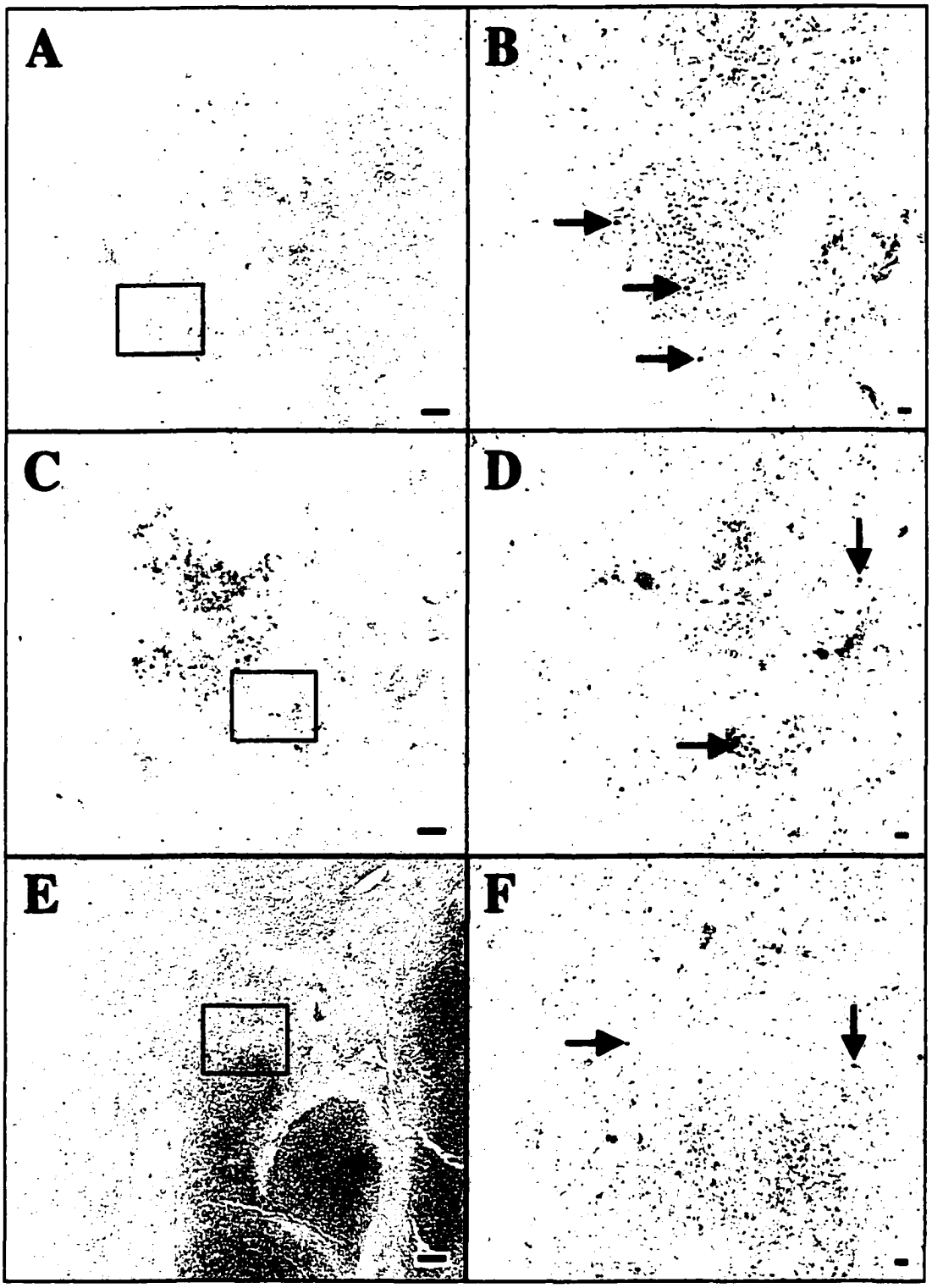

Figure 3.6

Representative photomicrographs of lung following low dose aerosol infection with *M. tuberculosis* stained for apoptosis (brown), using TUNEL. C57BL/6 mice (A,B), 150 days post infection, SWR mice (C,D) 150 days post infection and gamma interferon knockout mice (E,F), 65 days post infection. The black boxes in the images on the left(A,C,E bar=100μm) are shown at higher magnification in the images on the right (B,D,F bar = 10μm). Arrows = individual apoptotic cells. Data is representative of one to three experiments.

Ultrastructural changes

Many of the macrophages in the SWR mice had ultrastructural inclusions that were characterized as crystalloid, acicular and electron dense as shown in Figure 3.7. Such inclusions were occasionally seen in GKO mice, but never in C57BL/6 mice. It is thought that the inclusions may represent phagocytosed eosinophil and or neutrophil granules. These inclusions and the intense eosinophilic nature of the macrophage cytoplasm in the GKO lesions are very similar to those described in the idiopathic condition, acidophilic macrophage pneumonia (21). An association between the light and electronmicroscopic findings and granulomagenesis is yet to be established.

Immunohistochemical assessment

Figures 3.8 and 3.9 depict the accumulation of $CD4^+$, $CD8^+$ and $CD45R/B220^+$ cells in the typical inflammatory foci of SWR and GKO mice at 60 to 70 days respectively. In each case, there were more CD4+ than CD8+ cells. In the SWR lesion, the cells are mainly perivascular and peribronchiolar, strongly suggestive of BALT. $CD45R/B220^+$ are present in greater numbers than $CD8^+$ cells. These findings are similar to those in the C57BL/6 mice previously described. In the GKO mice, the cells were arranged around granulomas. CD4+ cells were present in greater number than CD8+ cells. $CD45R/B220^+$ cells were arranged in individual tight aggregates around the margin of the granulomas.

Figure 3.7
Representative transmission electron micrographs of alveolar macrophage from SWR/J mice at 99 days post low dose aerosol infection with *M. tuberculosis*. A, multiple acicular, crystalline, osmiophilic intracytoplasmic inclusions (arrow), magnification = x2500. B, individual and grouped, membrane bound inclusions (arrows),magnification = x15,000. C, note central rectilinear lattice to each inclusion (arrow), magnification = x40,000.

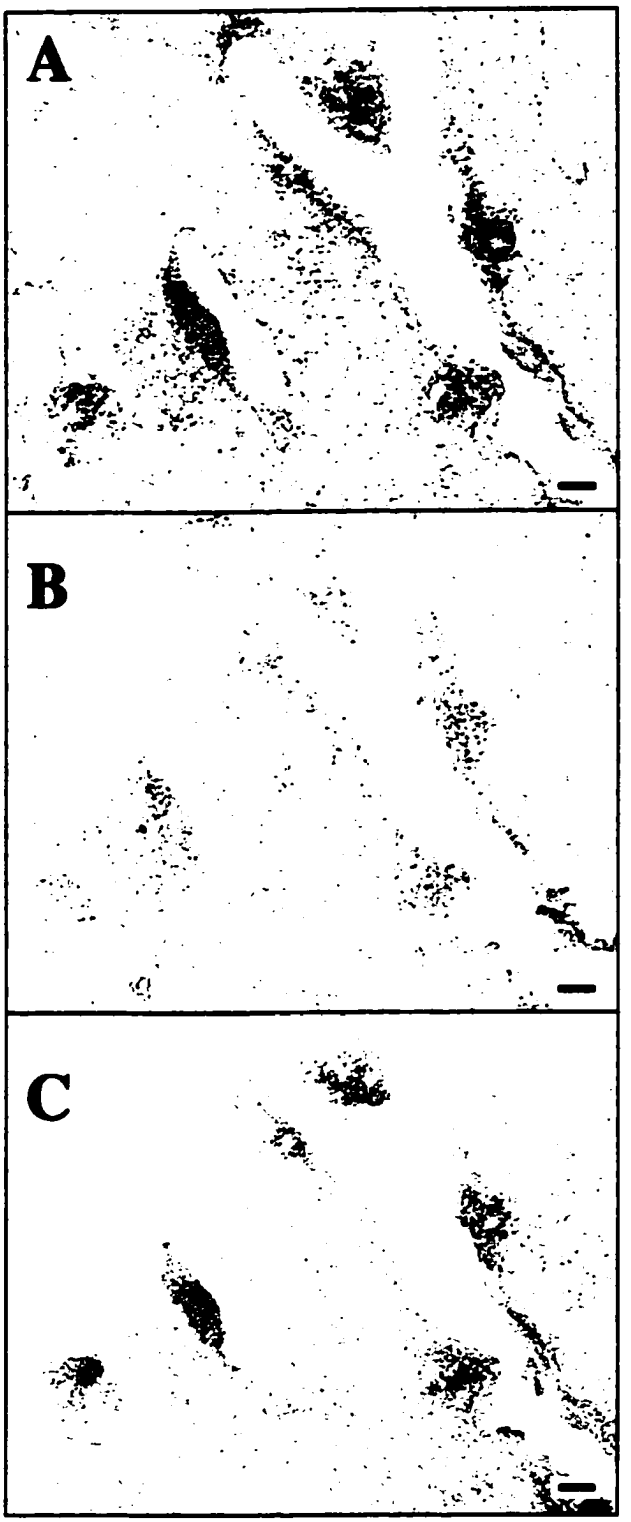

Figure 3.8
Representative photomicrographs of immunohistochemically stained frozen lung. A. CD4, B. CD8 and C. CD45R/B220 positive cells (red)within the perivascular and peribronchiolar lymphocyte aggregates of SWR mice 60 days post low dose aerosol infection with *M. tuberculosis*. Bar=100μm.

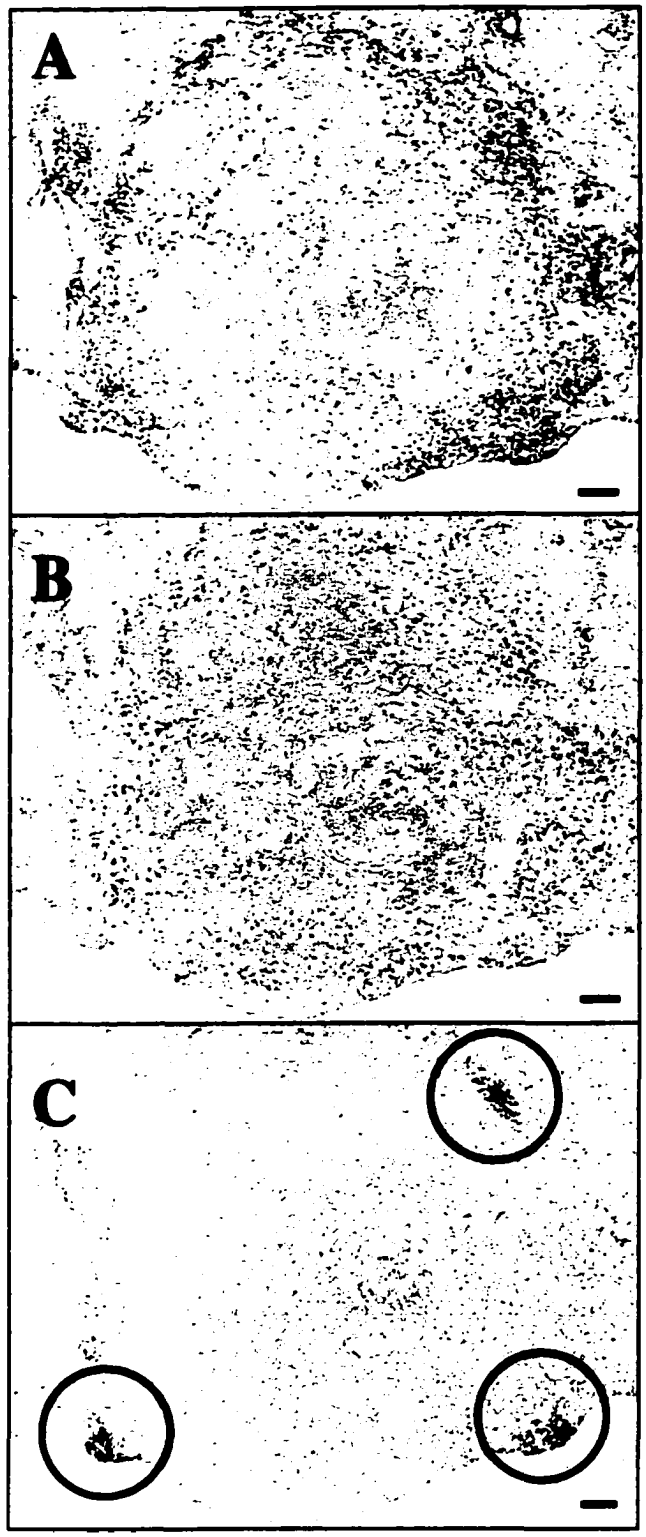

Figure 3.9
Representative photomicrographs of immunohistochemically stained frozen lung. A. CD4, B. CD8 and C. CD45R/B220 positive cells (red)(see black circles within a granuloma of gamma interferon knockout mice 69 days post low dose aerosol infection with *M. tuberculosis*. Bar=100μm.

Flow cytometric analysis

Table 3.3 depicts the mean percentages of the different $CD4^+$ and $CD8^+$ T cells from the lungs of C57BL/6 and SWR mice at 30 and 60 days post infection. The percentage $CD4^+$ and $CD8^+$ lymphocytes was similar in both mouse strains at day 30, as was the CD4 count at day 60. The CD8 count however, was approximately twice as high in the SWR mice as the C57BL/6 mice at day 60. The CD4 to CD8 ratio was approximately 2:1 in all cases apart from the SWR mice at day 60 where it was approximately 1:1. The percentage of lymphocytes in the C57BL/6 $CD4^+$ memory pool was approximately 2.5 times that of the SWR pool at day 30, but similar at day 60. Figure 3.10 depicts a representative dot-plot of the $CD4^+$ lymphocyte memory pool ($CD44^{hi}$/CD45RB $^{lo\text{-}med}$) at day 30 illustrating this difference between the two mouse strains. The percentage of lymphocytes in the C57BL/6 CD8+ memory pool was approximately 1.5 times that of the SWR pool at day 30, but similar at day 60. The percentage of cells in the $CD4^+$ activation pool was similar in both strains at both time points. The percentage of lymphocytes in the C57BL/6 $CD8^+$ activation pool was approximately 1.5 times that of the SWR pool at both time points. Table 3.4 depicts the total number of lymphocytes and the number of $CD4^+$ and $CD8^+$ subsets that could be found in the lungs of the SWR and C57BL/6 mice at 30 and 60 days post infection. At 30 days after infection, the numbers were similar, however, of note is the large increase in all cell types in the SWR mice compared to the C57BL/6 mice by 60 days post infection.

Table 3.3

Flow cytometric analysis of pulmonary lymphocytes from C57BL/6 and SWR mice after a low dose aerosol infection with *M. tuberculosis*

	Day 30		Day 60	
	CD4	CD8	CD4	CD8
C57BL/6				
Percentage lymphocytes	31% (2)	18% (3)	29% (3)	13% (2)
Memory ♦	76% (1)	51% (5)	66% (6)	32% (7)
Activation ♦ ♦	40% (5)	20% (1)	47% (8)	35% (3)
SWR				
Percentage lymphocytes	33% (8)	13% (1) *	32% (7)	31% (2) *
Memory	33% (9)*	36% (4) *	59% (6)	35% (5)
Activation	45% (9)	13% (2) *	43% (5)	32% (17)

( ) represents standard deviation
* Statistical difference between corresponding value in C57BL/6, by Student's t-test, $P<0.05$
♦ Memory is defined as Cd44hi/CD45RB lo-med (CD45/CD45RB)
♦ ♦ Activation assessed by CD69 bright staining
Also not shown CD25, CD122, OX40L no differences between groups, time points

Table 3.4

Representative total number of $CD4^+$ and $CD8^+$ lymphocytes derived from the entire lung of C57BL/6 and SWR mice at 30 and 60 days post aerosol infection with *M. tuberculosis*

	Day 30		Day 60	
C57BL/6	**CD4**	**CD8**	**CD4**	**CD8**
Total lymphocytes	4,750,750 (907,544)	2,758,500 (526,961)	6,169,750 (461,026)	2,765,750 (206,667)
♦Memory	3,610,570	1,406,835	4,072,035	885,040
♦♦Activation	1,900,300	551,700	2,899,782	968,012
SWR	**CD4**	**CD8**	**CD4**	**CD8**
Total lymphocytes	6,146,250 (666,754)	2,421,250 (262,660)	12,264,000 (1,326.256)	11,880,750 (1,284,810)
Memory	2,028,263	871,650	7,235,760	4,158,263
Activation	2,765,813	314,763	5,273,520	3,801,840

Total lymphocyte numbers were derived from standard lung homogenization and Coulter Counter protocol (15). n=4, ( ) represents standard deviation.
♦Memory is defined as CD44hi/CD45RB lo-med
♦♦Activation assessed by CD69 bright staining
Memory and activation values were derived from percentage of total lymphocytes using values presented in table 3.3

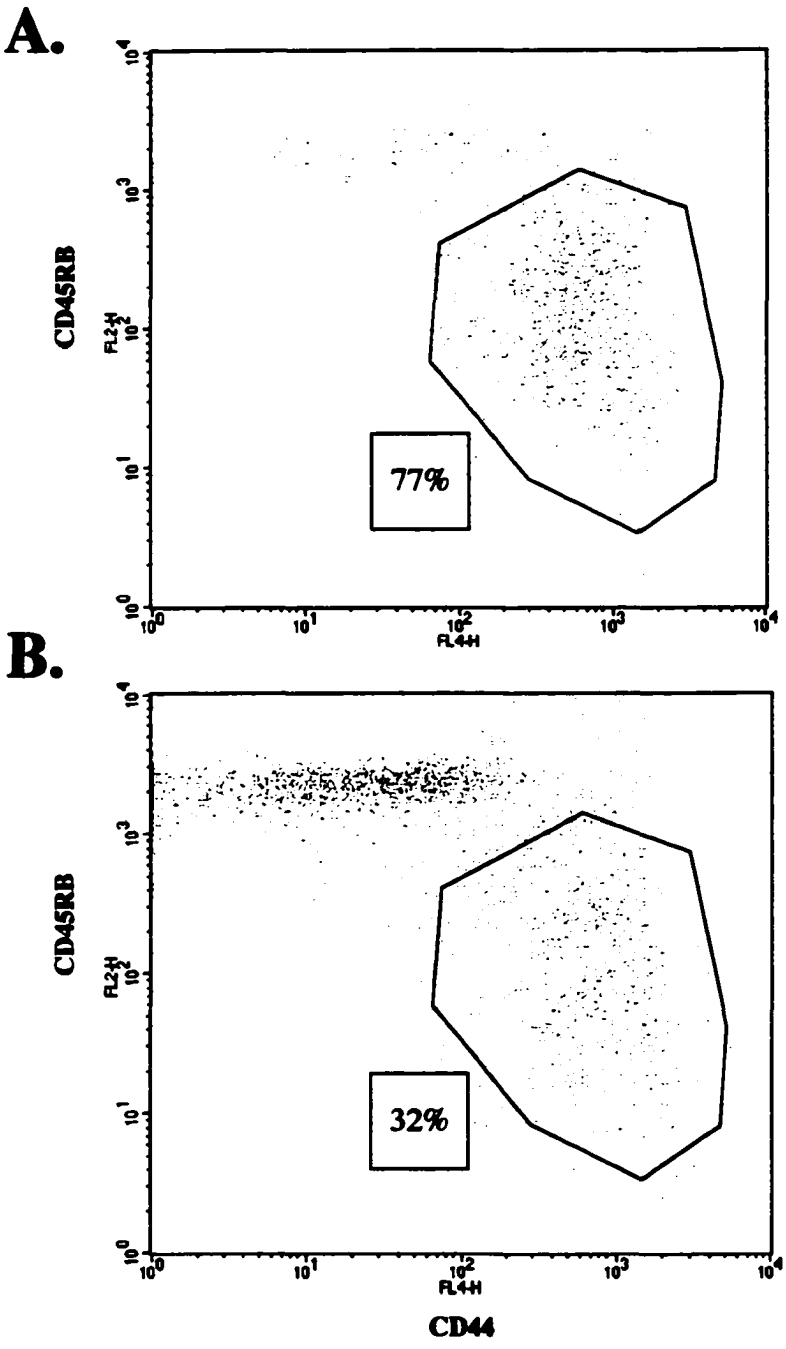

Figure 3.10
Representative flow-cytometric dot plots of CD4+ lung lymphocytes from C57BL/6 mice (A) and SWR mice (B) staining positive for the memory phenotype CD44hi/CD45RBlo-med at 30 days post aerosol infection with *M.tuberculosis*

Bromodeoxyuridine proliferation assay

Figures 3.11 and 3.12 depict the results of the Brdu assay. The percentage of Brdu positive $CD4^+$ and $CD8^+$ lymphocytes in the SWR mice was similar at both time points. The percentage of Brdu positive $CD4^+$ lymphocytes in the C57BL/6 mice however, was approximately 2.5 times that of the SWR mice at day 30 and approximately 1.5 times that of the SWR mice at day 60. The percentage of Brdu positive $CD4^+$ lymphocytes in the C57BL/6 dropped between day 30 and day 60. The percentage of Brdu positive $CD8^+$ lymphocytes in the C57BL/6 at days 30 and 60 was similar to the SWR mice (Figure 3.12).

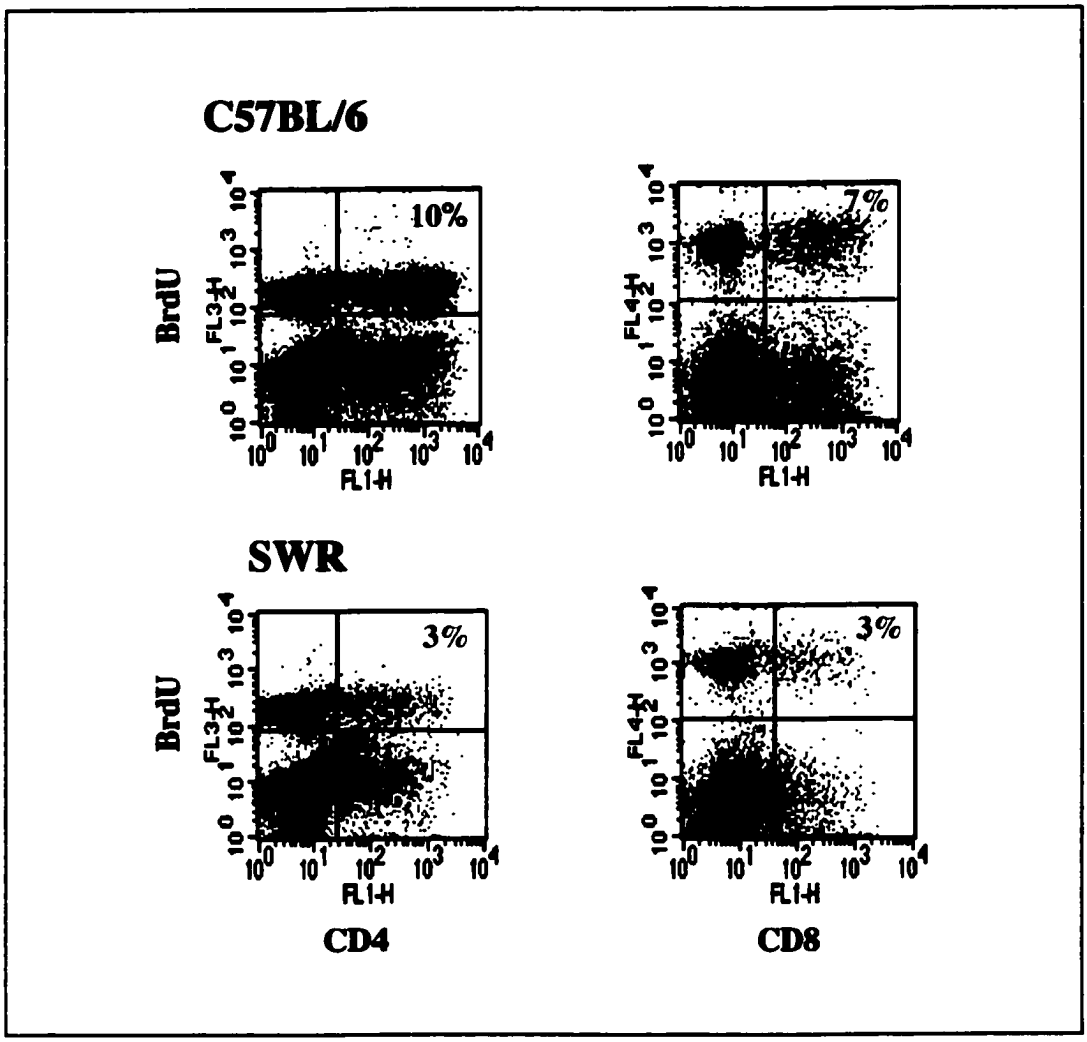

Figure 3.11
Representative flow-cytometric dot-plots of Brdu incorporation within CD4+ and CD8+ lung lymphocytes in C57BL/6 and SWR mice, 30 days post low dose aerosol infection with *M. tuberculosis*.

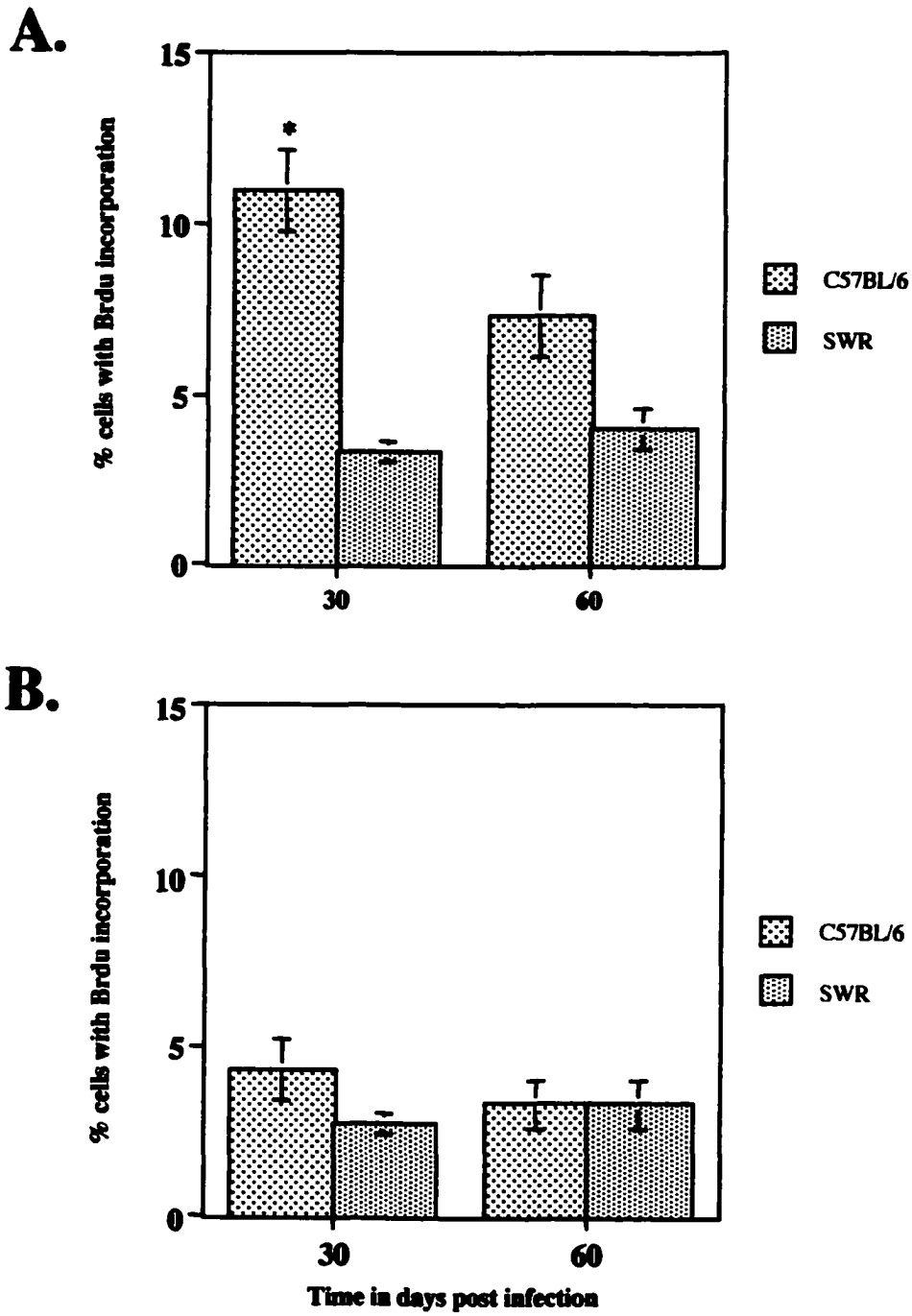

Figure 3. 12
Assessment of lung lymphocyte proliferation in C57BL/6 and SWR mice using Brdu incorporation (A. CD4+ B. CD8+) following low dose aerosol with *M. tuberculosis*. Data are expressed as mean values (n=3)with standard error indicated with vertical bars. * significant difference between values, using Student's t-test, where $P< 0.05$.

Intracellular IFN-γ production assay

Figures 3.13 depicts the results of the intracellular IFN-γ production assay. The percentage of CD4+ lymphocytes producing intracellular IFN-γ in the C57BL/6 mice was approximately 3 times that of the SWR mice at both time points. The percentage of CD8+ lymphocytes producing intracellular IFN-γ in the C57BL/6 mice however, was similar to that of the SWR mice at day 30 but approximately 1.5 times that of the SWR mice at day 60. The percentage of CD4+ lymphocytes producing intracellular IFN-γ remained similar in both strains at both time points yet the percentage of CD8+ lymphocytes producing intracellular IFN-γ increased approximately 1.5 time in the C57BL/6 mice between the two time points. The percentage of CD8+ lymphocytes producing intracellular IFN-γ remained similar in the SWR mice between the two time points. In C57BL/6 there was a greater percentage of CD4+ lymphocytes producing IFN-γ than CD8+ lymphocytes at both time points. This level however was similar for both subsets at both time points in the SWR mice (Figure 3.13).

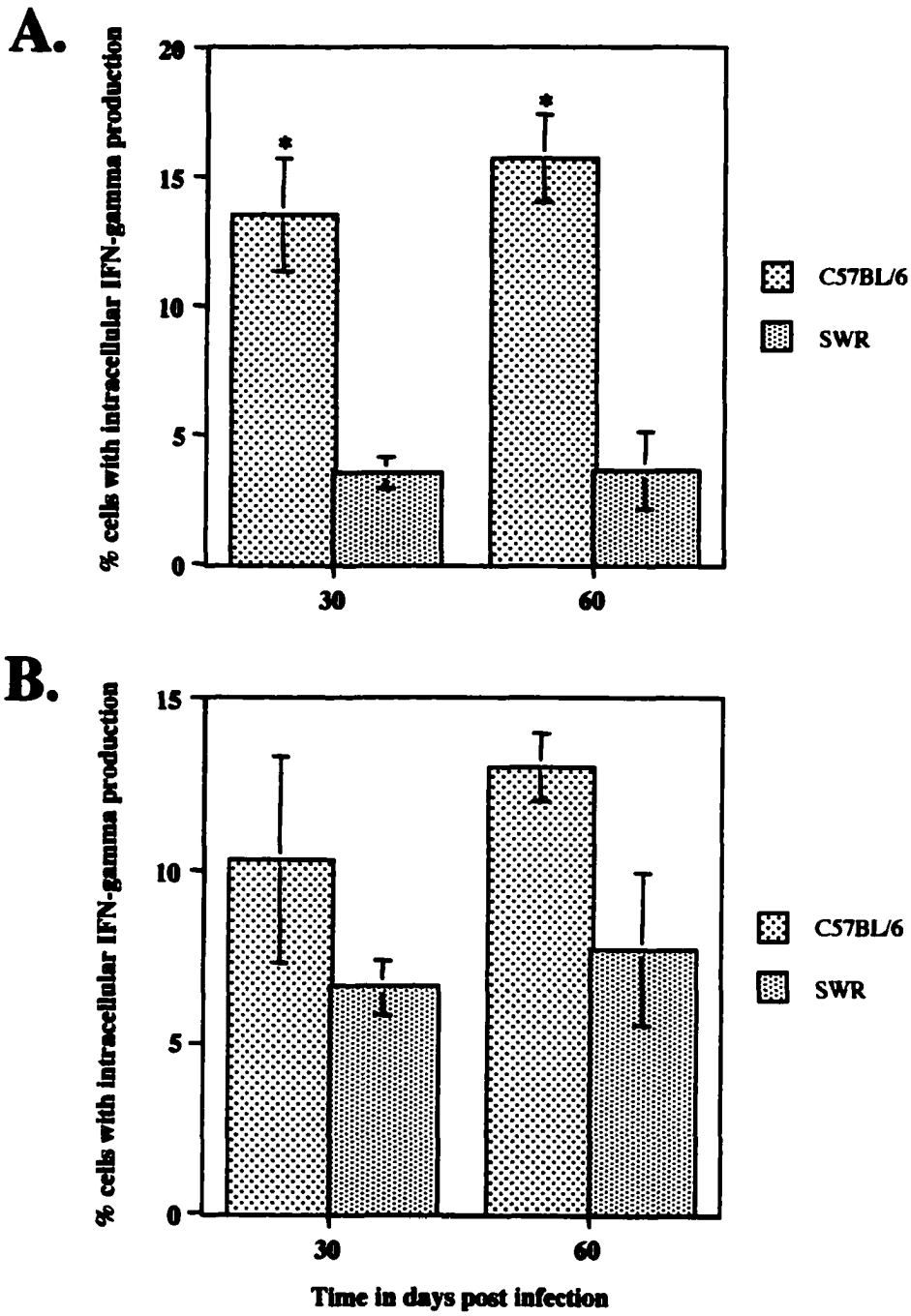

Figure 3.13
Intracellular IFN- gamma production in lung lymphocytes of C57BL/6 and SWR mice (A. CD4+ B. CD8+) following lowdose aerosol infection with *M. tuberculosis*. Data are expressed as mean values (n=3) with standard error indicated with vertical bars. * significant difference between values, using Student's t-test, where $P< 0.05$.

Discussion

The differences in the ability of C57BL/6, GKO and SWR mice to control the progression of pulmonary tuberculosis was marked by multiple factors. The most important however, with regards to application to the human setting are likely to be related to lymphocyte phenotypes, cytokine profiles and granuloma morphology.

The previously unstudied SWR mice exhibited a hypersusceptible phenotype. The most compelling reasons for this was the low percentage of $CD4^+$ T cells that were proliferating and producing IFN-γ, along with the low percentages of memory and activated cells. Histologically these mice had an abundance of macrophages with a scarcity of lymphocytes in their lesions compared to the C57BL/6 mice. It is reasonable therefore to speculate that in SWR mice, the reduced lymphocyte population and IFN-γ leads to reduced macrophage activation and so increased bacterial load which then serves to precipitate increased pathology.

Proliferation as measured by Brdu incorporation is a measure of DNA synthesis (11). The initial encounter with specific antigen in the presence of the required co-stimulatory signal triggers the entry of a T cell into the G1 phase of the cell cycle and, at the same time, induces the synthesis of the T cell growth factor IL-2, along with the α chain of the IL-2 receptor (16). A low level of Brdu incorporation in the $CD4^+$ lymphocytes of the SWR mice suggests that there may be defects at the point of antigen interaction, IL-2 production or within the IL-2 receptor.

A low memory response of both T cell subtypes at day 30 post infection in the SWR mice, the critical stage 3 in the C57BL/6 mice when bacterial load is stabilized, suggests that there has been less recognition of antigen by lymphocytes, or that transition to memory is impaired in SWR mice. This would lead to less clonal expansion, and so a reduced number of cells to be recalled and respond at a more rapid, effective rate, typical of memory cells. The way memory is actually measured on lymphocytes however, is still controversial. Classically, significant changes in three cell-surface proteins - L selectin, CD44, and CD45RB are indicative of a T cell memory phenotype: L-selectin is lost, whereas CD44 levels increase on all memory T cells after priming, and the isoform of CD45RB changes because of alternative splicing of exons that encode the extracellular domain of CD45 (CD45RA =naïve, CD45RO=memory or effector CD4 T cells) (16). In this experiment $CD44^{hi}/CD45RB^{lo\text{-}med+}$ cells were designated memory cells, however, a recent paper by Andersen suggests that $CD44^{lo}/CD45RB^{hi}$ are more indicative of this phenotype (1). Andersen also suggests that some $CD45^{lo}$ cells revert to the $CD45^{hi}$ phenotype. Serbina has also recently proposed the $CD69^{lo}$, $CD25^{lo}$, $CD44^{hi}$ $CD4^{+}$ and $CD8^{+}$ phenotypes as being important in memory and recall immunity (30).

Assessment of lymphocyte activation is also an area of debate. The mechanism that controls T-cell activation in tuberculosis is not yet known. Recent data by Pearl et al. indicates that lymphocytes in GKO mice have higher activation levels than wild type mice (27). In this study, splenocytes from intravenously infected mice from early in infection were analyzed for the expression of CD44 and CD62L. After 15 days there was a greater number of activated cells in the GKO mice spleens than in the, wild-type

spleens. In a further confounding study, Lyadova et al. demonstrated a marked accumulation of activated $CD4^+$ and $CD8^+$ cells, characterized by the expression of $CD44^{hi}/CD45RB^{lo}$ cells in the lungs of infected susceptible I/St and resistant A/Sn inbred mice (18).

Although the level of $CD4^+$ and $CD8^+$ activation was similar in SWR and C57BL/6 mice, (apart from $CD8^+$ cells at day 30), the level of intracellular IFN-γ production was lower in SWR mice. As they are proliferating at a low level, is it actually correct to think of them as activated? It is perhaps better to infer that there is more than a mere intrinsic lack of IFN-γ production in these mice. It is more likely that a deficiency in (i) antigen presentation, or (ii) co-stimulatory activity of antigen presenting cells or (iii) common signal transduction machinery such as NFκB is involved, which may affect multiple, but not all pathways, hence increased expression of CD69, CD25 activation but no IFN-γ production or cell cycling. The fact that there is no significant difference in bacterial load at day 30 post infection between SWR and C57BL/6 mice but there are immunological disparities, points to underlying defects that lead to the increased pathology and more rapid disease progression.

The total number of $CD4^+$ and $CD8^+$ lymphocytes within the infected lungs of these two strains of mice is a very important consideration with regard to pathogenesis. They were similar at 30 days after infection, however, by day 60 there was approximately two times as many $CD4^+$ lymphocytes in the SWR mice compared to the C57BL/6 mice, and four times as many $CD8^+$ lymphocytes. Consistent with the increase in total numbers in the SWR mice over the C57BL/6 mice, there was a concomitant increase in the number of

cells staining positive for the memory and activation phenotypes. In light of the flow cytometric data presented as percentages of 50,000 gated lymphocytes, this data suggests that although there may be more lymphocytes in the infected SWR lung, the relative proportion of the different subsets is not effective in controlling the infection. Viewed in another way, it is important to appreciate that although there are far more lymphocytes in the SWR lung than the C57BL/6 lung at 60 days after infection, many of which express activation markers and are producing IFN-γ, the progressive increase in bacterial burden and pathology is not curtailed. This points to possible defects in macrophage activation by the lymphocytes or intrinsic macrophage anomalies that adversely affect their ability to kill *M. tuberculosis*. The high macrophage to lymphocyte ratio in the SWR lesions may underlie or be a reflection of each of these phenomena, both of which would ultimately lead to an increase in the bacterial load in the lung. It is important also to note that the ratio of, and the total number of $CD4^+$ to $CD8^+$ lymphocytes in the SWR mice at 60 days after infection was similar, however, in the C57BL/6 mice there was an approximately two times as many $CD4^+$ lymphocytes as $CD8^+$ lymphocytes (which was seen in both strains at 30 days after infection). As was shown in the C57BL/6 mice (15), a lesion with more $CD4^+$ lymphocytes than $CD8^+$ lymphocytes is consistent with one that can contain the bacterial load. In the SWR lesion, hyperactivation may be driving an excess of $CD4^+$ apoptosis to result in this skewed ratio of lymphocytes. The presence of more cells staining for apoptosis in the SWR mice than the C57BL/6 mice in these studies may be indicative of this. Alternatively, an excess of $CD8^+$ T cells may be driving an immunosuppressive phenomenon, perhaps by the excess production of cytokines such as IL-4, or IL-10, or they may be acting in a potent cytolytic fashion.

The morphological abnormalities of the macrophages of the SWR mice may certainly play a large role in the ability of these mice to contain infection. The pathogenesis of the cytoplasmic inclusions in particular, remains to be elucidated. Their similarity to the lesion seen in acidophilic macrophage pneumonia strongly suggests that they may represent the accumulation of, and abnormal metabolism of cytoplasmic granules form either neutrophils and/or eosinophils (21). This in turn points to perhaps another inherent defect in these macrophages that might hinder normal control of mycobacterial growth.

The development of pneumonia in other susceptible mouse strains has been characterized by lesions consisting predominantly of macrophages and fewer lymphocyte aggregates (33). Turner showed in CBA/J and DBA/2 mice, that as the infection progressed and the bacterial load increased, the lesions became degenerative, with evidence of macrophage breakdown and an influx of neutrophils. A similar pattern was seen with the SWR mice. Turner, also showed that the CBA/J and DBA/2 mice was less able to upregulate the adhesion molecules CD11a and CD54 on circulating lymphocytes. In the chronic lung lesions of SWR mice we saw a paucity of lymphocytes, suggesting that recruitment of these cells may be impaired, and this may also play a role in pathogenesis.

The high number of granulocytes (both neutrophils and eosinophils), in GKO mice and to a lesser degree SWR mice may be due to the absence or low levels of IFN-γ. The underlying mechanism is again, poorly understood. Blockade of eosinophil proliferation and recruitment in to the lung by treatment with anti-interleukin-5 monoclonal antibody only marginally reduced mycobacterial growth within the lungs of BCG infected GKO

mice (17). Therefore they probably don't contribute to pathogenesis. It is possible that too many lymphocytes may physically hinder lymphocytes from forming a protective granuloma.

Many potential mediators of apoptosis, including IFN-γ have been described (10). One particularly important factor as far macrophages are concerned is nitric oxide (NO) (8). The presence of caseous necrosis in NOS2 knockout mice after *M.tuberculosis* infection adds further weight to the argument (12). The relatively high levels of apoptosis seen in the GKO mice suggests that it might be an important factor in pathogenesis in this setting, perhaps driven by a low level of NO in macropahges due to low activation. It interesting to speculate that macrophage NO levels in the SWR mice are also low.

The genetic differences in these mice may certainly play a large role in the pathogenesis. Categorization of mouse strains as susceptible or resistant in a *M. tuberculosis* H37Rv intravenous or intraperitoneal challenge model revealed different patterns of *H-2* complex control. Brett et al. showed that mice with the $H\text{-}2^k$ haplotype were more susceptible to lung infection (6). Other studies have shown that $H\text{-}2^b$ mice have a higher mortality after infection with *M. tuberculosis*. The $H\text{-}2^b$ haplotype has been linked to elevated immune responses to several mycobacterial antigens (22). Mice of the $H\text{-}2^b$ haplotype carrying gene deletions in both $H\text{-}2^k$ and $H\text{-}2^d$ have shown increased susceptibility to *M. tuberculosis* infection compared with immunocompetent animals. Equivocal evidence suggests that the innate *Bcg* gene influences the early clearance of bacteria (31), and that the *IgH / Nramp-1* genes affect the extent of bacillus Calmette-Guerin (BCG) adjuvant-induced granulomatous reaction (29). In a study by North et al., however, *Nramp* was

shown not to be important in antimycobacterial resistance (24). The restricted impact of any individual gene is illustrated by the fact that the *Bcg* gene influences bacterial load following intravenous but not aerosol infection (22). C57BL/6 and GKO are of the H-2^b haplotype and therefore suggests that H-2^b is not associated with an ability to resist bacterial growth. SWR are of the H-2^q haplotype and to date, no studies have described tuberculosis susceptibility traits attributable to it.

There are other potential explanations for the differences in pathogenesis in these mice. Nabors for example demonstrated a site-specific immunity to *Leishmania major* in SWR mice, whereby the site of infection (footpad vs dorsum) influenced susceptibility and expression of the antileishmanial immune response (23). It is possible that such factors may be playing a similar role in pulmonary tuberculosis.

In conclusion, these studies have identified SWR as a new mouse model of hypersusceptibilty to tuberculosis. It is not possible at this stage to know the significance of all of the observed anomalies, however, it is hoped that application of this knowledge will prove useful in the human setting.

Acknowledgements

This work was supported by NIH grant AI-44072. The author wishes to extend special thanks to Drs Joanne Turner and Robert Keefe for their help and advice with this work.

References

1. **Andersen, P., and B. Smedegaard.** 2000. CD4(+) T-cell subsets that mediate immunological memory to *Mycobacterium tuberculosis* infection in mice. Infect Immun. **68:**621-9.

2. **Bellamy, R.** 2000. Identifying genetic susceptibility factors for tuberculosis in Africans: a combined approach using a candidate gene study and a genome- wide screen. Clin Sci (Lond). **98:**245-50.

3. **Bellamy, R., N. Beyers, K. P. McAdam, C. Ruwende, R. Gie, P. Samaai, D. Bester, M. Meyer, T. Corrah, M. Collin, D. R. Camidge, D. Wilkinson, E. Hoal-Van Helden, H. C. Whittle, W. Amos, P. van Helden, and A. V. Hill.** 2000. Genetic susceptibility to tuberculosis in Africans: a genome-wide scan. Proc Natl Acad Sci U S A. **97:**8005-9.

4. **Bellamy, R., and A. V. Hill.** 1998. Genetic susceptibility to mycobacteria and other infectious pathogens in humans. Curr Opin Immunol. **10:**483-7.

5. **Bellamy, R., C. Ruwende, T. Corrah, K. P. McAdam, H. C. Whittle, and A. V. Hill.** 1998. Variations in the NRAMP1 gene and susceptibility to tuberculosis in West Africans. N Engl J Med. **338:**640-4.

6. **Brett, S., J. M. Orrell, J. Swanson Beck, and J. Ivanyi.** 1992. Influence of H-2 genes on growth of *Mycobacterium tuberculosis* in the lungs of chronically infected mice. Immunology. **76:**129-32.

7. **Cardona, P. J., R. Llatjos, S. Gordillo, J. Diaz, I. Ojanguren, A. Ariza, and V. Ausina.** 2000. Evolution of granulomas in lungs of mice infected aerogenically with *Mycobacterium tuberculosis*. Scand J Immunol. **52:**156-63.

8. **Chan, E. D., J. Chan, and N. W. Schluger.** 2001. What is the role of nitric oxide in murine and human host defense against tuberculosis? Current knowledge. Am J Respir Cell Mol Biol. **25:**606-12.

9. **Cooper, A. M., D. K. Dalton, T. A. Stewart, J. P. Griffin, D. G. Russell, and I. M. Orme.** 1993. Disseminated tuberculosis in interferon gamma gene-disrupted mice. J Exp Med. **178:**2243-7.

10. **Dalton, D. K., L. Haynes, C. Q. Chu, S. L. Swain, and S. Wittmer.** 2000. Interferon gamma eliminates responding CD4 T cells during mycobacterial infection by inducing apoptosis of activated CD4 T cells. J Exp Med. **192:**117-22.

11. **Dolbeare, F.** 1995. Bromodeoxyuridine: a diagnostic tool in biology and medicine, Part I: Historical perspectives, histochemical methods and cell kinetics. Histochem J. **27:**339-69.

12. **Ehlers, S., S. Kutsch, J. Benini, A. Cooper, C. Hahn, J. Gerdes, I. Orme, C. Martin, and E. T. Rietschel.** 1999. NOS2-derived nitric oxide regulates the size, quantity and quality of granuloma formation in *Mycobacterium avium*-infected mice without affecting bacterial loads. Immunology. **98:**313-23.

13. **Flynn, J. L., J. Chan, K. J. Triebold, D. K. Dalton, T. A. Stewart, and B. R. Bloom.** 1993. An essential role for interferon gamma in resistance to *Mycobacterium tuberculosis* infection. Journal of Experimental Medicine. **178:**2249-54.

14. **Goldfeld, A. E., J. C. Delgado, S. Thim, M. V. Bozon, A. M. Uglialoro, D. Turbay, C. Cohen, and E. J. Yunis.** 1998. Association of an HLA-DQ allele with clinical tuberculosis. Jama. **279:**226-8.

15. **Gonzalez-Juarrero, M., O. C. Turner, J. Turner, P. Marietta, J. V. Brooks, and I. M. Orme.** 2001. Temporal and spatial arrangement of lymphocytes within lung granulomas induced by aerosol infection with *Mycobacterium tuberculosis*. Infect Immun. **69:**1722-8.

16. **Janeway, C. A., Travers, P., Walport, M and Capra, J.D.** 1999. Immunobiology. The Immune System in Health and Disease, Fourth ed. Current Biology Publications, London, UK.

17. **Kirman, J., Z. Zakaria, K. McCoy, B. Delahunt, and G. Le Gros.** 2000. Role of eosinophils in the pathogenesis of *Mycobacterium bovis BCG* infection in gamma interferon receptor-deficient mice. Infect Immun. **68:**2976-8.

18. **Lyadova, I. V., E. B. Eruslanov, S. V. Khaidukov, V. V. Yeremeev, K. B. Majorov, A. V. Pichugin, B. V. Nikonenko, T. K. Kondratieva, and A. S. Apt.** 2000. Comparative analysis of T lymphocytes recovered from the lungs of mice genetically susceptible, resistant, and hyperresistant to *Mycobacterium tuberculosis*-triggered disease. J Immunol. **165:**5921-31.

19. **Medina, E., and R. J. North.** 1998. Resistance ranking of some common inbred mouse strains to *Mycobacterium tuberculosis* and relationship to major histocompatibility complex haplotype and Nramp1 genotype. Immunology. **93:**270-4.

20. **Mice, Jax.** June 2001-May 2003 Catalog. JAX MICE. The Jackson Laboratory.

21. **Murray, A. B., and A. Luz.** 1990. Acidophilic macrophage pneumonia in laboratory mice. Vet Pathol. **27:**274-81.

22. **Musa, S. A., Y. Kim, R. Hashim, G.-Z. Wang, C. Dimmer, and D. W. Smith.** 1987. Response of inbred mice to aerosol challenge with *Mycobacterium tuberculosis.* Infect Immun. **55:**1862-1866.

23. **Nabors, G. S., and J. P. Farrell.** 1994. Site-specific immunity to *Leishmania major* in SWR mice: the site of infection influences susceptibility and expression of the antileishmanial immune response. Infect Immun. **62:**3655-62.

24. **North, R. J., and E. Medina.** Significance of the antimicrobial resistance gene, *Nramp1*, in resistance to virulent *Mycobacterium tuberculosis* infection. 67th Forum in Immunology. 1996.

25. **Orrell, J. M., S. J. Brett, J. Ivanyi, G. Coghill, A. Grant, and J. S. Beck.** 1991. Measurement of the tissue distribution of immunoperoxidase staining with polyclonal anti-BCG serum in lung granulomata of mice infected with *Mycobacterium tuberculosis.* J Pathol. **164:**41-5.

26. **Orrell, J. M., S. J. Brett, J. Ivanyi, G. Coghill, A. Grant, and J. S. Beck.** 1992. Morphometric analysis of *Mycobacterium tuberculosis* infection in mice suggests a genetic influence on the generation of the granulomatous inflammatory response. J Pathol. **166:**77-82.

27. **Pearl, J. E., B. Saunders, S. Ehlers, I. M. Orme, and A. M. Cooper.** 2001. Inflammation and lymphocyte activation during mycobacterial infection in the interferon-gamma-deficient mouse. Cell Immunol. **211:**43-50.

28. **Rhoades, E. R., A. A. Frank, and I. M. Orme.** 1997. Progression of chronic pulmonary tuberculosis in mice aerogenically infected with virulent *Mycobacterium tuberculosis.* Tuber Lung Dis. **78:**57-66.

29. **Schrier, D. J., J. L. Sternick, E. M. Allen, and V. L. Moore.** 1982. Immunogenetics of BCG-induced anergy in mice: control by genes linked to the Igh complex. J Immunol. **128:**1466-9.

30. **Serbina, N. V., and J. L. Flynn.** 2001. CD8(+) T cells participate in the memory immune response to *Mycobacterium tuberculosis.* Infect Immun. **69:**4320-8.

31. **Skamene, E.** 1986. Genetic control of resistance to mycobacterial infection. Curr Top Microbiol Immunol. **124:**49-66.

32. **Stadelmann, C., and H. Lassmann.** 2000. Detection of apoptosis in tissue sections. Cell Tissue Res. **301:**19-31.

33. **Turner, J., M. Gonzalez-Juarrero, B. M. Saunders, J. V. Brooks, P. Marietta, D. L. Ellis, A. A. Frank, A. M. Cooper, and I. M. Orme.** 2001. Immunological basis for reactivation of tuberculosis in mice. Infect Immun. **69:**3264-70.

34. **Zumla, A. and Geraint James, D.** 1999. The Granulomatous Disorders, First ed. Cambridge University Press, cambridge.

Chapter Four

Immunopathogenesis of Pulmonary Granulomas in the Guinea Pig Following Infection with *Mycobacterium tuberculosis*

Abstract

Pulmonary tuberculosis in the guinea pig has several similarities to the pathology of the disease in humans and is accordingly widely used as an animal model to test new tuberculosis vaccines. The primary site of the expression of acquired immunity against mycobacteria and the hallmark of pulmonary tuberculosis is the lung granuloma. Although the morphology of the tuberculosis granuloma is well described from a pathology perspective, there is virtually no information regarding the nature of the T cell subset influx in this mammal. In this present study the course of pulmonary tuberculosis was followed in guinea pigs that had either not been vaccinated or were vaccinated with *M.bovis BCG* six weeks prior to aerosol infection with *M.tuberculosis*. In both groups four stages of the disease process were described, from the early cellular response through to the eventual degeneration of the lesions. It was found that through all four stages there was a similar number and arrangement of $CD4^+$ and $CD8^+$ T cells in the granulomas. B cells were only occasionally seen. There were only a small number of apoptotic lymphocytes and these were either distributed evenly throughout the granuloma, or concentrated around and within the lesion core. Acid fast bacilli were visible both within macrophages and free within the airway debris as the degeneration

process proceeded. This latter event was associated with the presence of destructive sequellae such as fibrin deposition, fibrosis, necrosis, mineralization, airway epithelium erosion and filling of airways with cellular debris. A key finding of the study was the observation that the development of the necrotic core was an early event and almost certainly preceded any emergence of the acquired immune response. This suggested that the necrotic process was resulting in irreversible tissue damage that the subsequent acquired response was unable to reverse or prevent. As such this finding is very different to the current dogma that holds that excessive activity of T cells mediating delayed type hypersensitivity and cellular cytolysis is the root cause of the necrosis. In the vaccinated Guinea Pigs, the bacterial load was consistently 0.5 to 1.0 Log 10 lower than that in the non-vaccinated group, but there was a similar spectrum of histopathological events. The speed of disease progression however, was slightly slower. The number of $CD4^+$ T cells in the granulomas was similar to the $CD8^+$ T cell subset. Further studies are required to resolve the differences afforded by vaccination.

Introduction

There are now several different animal models available with which to test new vaccines, ranging (in size and expense) from the mouse to primate models. It is widely accepted, however, that perhaps the best model is the guinea pig (*Cavia porcellus*), given the similarities to humans infected with tuberculosis in terms of the formation of the lung granuloma and its subsequent necrosis and mineralization (15, 21, 32)

The formation of the lung granuloma is the classical hallmark of pulmonary tuberculosis. Morphology of the granuloma is characterized by a caseous necrotic core that is

surrounded by a layer of epithelioid macrophages, which in turn is surrounded by concentric layers of lymphocytes and fibrosis (5). Multinucleated giant cells and occasional plasma cells are also seen. The influx of leukocytes and fibroblasts forming these structures is an attempt to segregate the infection, to prevent bacterial dissemination to the remainder of the lung and to other organs, and to focus the immune response directly at the site of implantation. Its development involves an elaborate production and interaction of chemokines and cytokines by effector cells as well as local tissue cells. In addition, the upregulation of receptors both for these molecules as well as adhesion and integrin molecules on responder cells facilitates the proper coordination of the recruitment, migration and retention of cells into the granuloma (34).

Because of the significant ways in which it resembles both the normal human physiology and the pathophysiology of pulmonary tuberculosis, the guinea pig is one of the more extensively studied animal models of tuberculosis (35). Following exposure to a small number of bacilli delivered via aerosol, the infection in the guinea pig lung grows progressively for about 30 days (36) before being contained by the host response (26). In similarity to other animal models, however, this expression of host immunity is not completely effective and as a result, many bacilli survive giving rise to a chronic state of disease.

Although it has long been realized that the protective process in the guinea pig lung involves the formation of granulomas, there is surprisingly little further description of this event. For example, previous descriptions have characterized 'primary' and

'secondary' lesions with reference to only the size and amount of necrosis in the lesions (37). The guinea pig is well known as a susceptible animal model, containing bacterial growth in its lungs for only a relatively short time and develops granulomas with prominent central caseation and extensive connective tissue deposition. knowledge of the arrangement of these elements over time however, remains obscure. In addition, the influx of T cell subsets, only recently described in the mouse model (13) have yet to have been documented in the guinea pig.

Given the importance of the model to current vaccine development work, the purpose of this study was to chronicle the temporal and spatial arrangement of the cell influx, as well as other aspects of the overall process, and to attempt to relate this data to the known pathological process. By comparing *M. bovis BCG* vaccinated animals with non-vaccinated animals, we hoped to detect a possible immunohistopathological vaccine affect. Four distinct histopathological stages were observed, within each the number and arrangement of $CD4^+$ and $CD8^+$ T cells was similar. The development of a necrotic core was seen to be a very early event, perhaps even before the development of acquired immunity. This suggested a new paradigm for tissue destruction in these lesions, one driven by innate mechanisms and not excessive T cell activity. It was not possible to resolve a significant immunohistopathological difference between the two groups of animals.

Materials and Methods

Guinea pigs

Female Hartley guinea pigs were obtained from Charles River Laboratories (Willmington, MA). They were housed under biosafety level 3 conditions at Colorado State University, and fed standard guinea pig chow and water ad libitum. After infection animals were assessed using a Karnofsky scale for pain and distress.

Bacteria and infection

M.tuberculosis Erdman (TMCC #107) was previously grown from low-passage seed lots in Proskauer-Beck liquid media containing 0.05% Tween 80 to early mid-log phase. Cultures were aliquoted into 1-ml tubes and frozen at -70°C until used. Thawed aliquots were diluted in double-distilled sterile water to the desired inoculum concentrations. Guinea pigs were infected via the aerosol route with a low dose of bacteria. Briefly, the nebulizer compartment of a Middlebrook airborne infection apparatus (Glas-Col, Terre Haute, Ind.) was filled with 5 ml of distilled water containing a suspension of bacteria known to deliver approximately 20-50 bacteria into the lungs.

Vaccination

Six weeks prior to *M.tuberculosis* infection, half of the animals were randomly chosen to receive a single, ventral abdominal intradermal injection of $1x10^5$ viable *M.bovis BCG* Japan bacilli suspended in 0.5 ml of sterile 1x phosphate buffered saline (PBS). The remaining half of the animals were injected in the same manner with 0.5ml of 1x PBS only.

Enumeration of bacteria

Guinea pigs were sacrificed at multiple time points between 10 and 100 days after aerosol infection. The number of viable bacteria in the lungs was monitored over time by plating serial 10 fold dilutions of right cranial lung lobe homogenates onto nutrient Middlebrook 7H11 agar. The bacterial colony formations were counted after 21 days incubation at 37°C and 5% CO_2. The data was expressed as the log10 value of the mean number of bacteria recovered.

Histology

At necropsy, the right middle lung lobe was first slowly infused through the major vessels at the hilus with 10% neutral buffered formalin. The lobe was then submerged in formalin. After a minimum of 72 hours, the tissue was prepared and sectioned for light microscopy with lobe orientation designed to allow for maximum surface area to be seen. Consecutive sections were stained with hematoxylin and eosin, and with Ziehl-Neelsen stain for the detection of acid-fast bacilli. Sections were also stained with the Masson's trichrome method for the detection of collagen and with the Fraser-Lendrum method for the detection of fibrin. All tissue identification was masked and the order was randomized to preclude experimental group bias. Sections were examined at least three times to verify the reproducibility of the observations.

Immunohistochemistry

Mouse anti-guinea pig monoclonal antibodies specific for guinea pig CD4 (clone CT7), a CD8 (clone CT6), and Pan B (MsGp9) were purchased from Serotec (Oxford, England). In each case, the Serotec mouse IgG1 negative control (clone W3/25) was used as the isotype control. $F(ab')_2$ rabbit anti mouse Ig:Biotin, also from Serotec was used as the

secondary antibody. At necropsy, the left cranial lung lobe was first slowly infused with a 20% OCT (Tissue-Tek, Inc. Torrance, CA) 1x PBS solution through the major vessels at the hilus. They were then placed in a tissue mold, completely surrounded by OCT, frozen in a bath of liquid nitrogen and stored at –70° C until used. Serial sections from each lung of 5μm thick were cut in a CM 1850 cryotome (Leica, Deerfield, IL), employing the Instrumedics Inc. (Hackensack, NJ) 'Tape Transfer System', fixed in cold acetone for 5-10 minutes and then air-dried. Next, the sections were washed in APK buffer solution (Vetana Medical Systems, Tucson, AZ) for 15 -20 minutes and then incubated in a 1:50 (CD4), (Pan B) or 1:100 (CD8) solution of Protein Block -goat serum (Biogenex, San Ramon, CA) and primary antibody. The sections were then placed on a Nexus automated immunostainer (Ventana medical systems, Tucson, AZ). The labeled avidin-alkaline phosphatase and Fast red / Napthol detection kit was employed. The secondary antibody was incubated for 30 minutes at room temperature. Sections were counterstained with Meyer's hematoxylin. Sections of spleen were also examined in each experiment to act as positive controls.

Detection of apoptosis.

The ApopTag plus peroxidase *In situ* Apoptosis Detection kit S7101 (Intergen, Purchase NY) was used to detect apoptotic cells in paraffin-embedded tissue. This kit employs the terminal transferase-mediated dUTP nick-end labeling (TUNEL) method (38) to distinguish fragmented DNA present in apoptotic bodies. Two or three 5-micron sections of the same tissue used for histological analysis were analyzed per time point.

Photomicroscopy and Morphometry

Photomicroscopy was performed with an Olympus AH-2 microscope linked to a Sony SKC-DK5 digital camera and Adobe Photoshop 6.0 software. In an attempt to further classify the pulmonary lesions, the granuloma fraction was calculated from each of the hematoxylin and eosin stained histological slides. In brief, using Metamorph software (Metamorph 4.5r5, Universal Imaging Corporation), images of individual lobes or all lobes were acquired. Theses were calibrated, measured and the perceived inflammatory area was defined and expressed as a percentage of the total lung area. This percentage of affected tissue was termed the granuloma fraction (28).

To explore the shape of the granuloma, SURFdriver 3.5 software was employed (Kailua, HI). Ten 100μm step-sections of granulomas were cut from the paraffin blocks and stained with hematoxylin and eosin. A representative granuloma was selected and imaged from each of the step-sections. All images were captured from the same position and at the same magnification. The series of images were then imported in to the SURFdriver program and stacked, and joined together to present a 3-D reconstruction. Only granulomas from chronic disease were examined in this fashion.

Statistical Analysis

All statistical analysis was performed using Sigma Stat.Version 2, statistical software. The Mann-Whitney Rank Sum Test was used to analyze bacterial growth curve data. Statistical significance was taken as $P=<0.05$.

Results

Course of *M. tuberculosis* infection in the lungs of guinea pigs.

The course of the infection after aerosol exposure is shown in Figure 4.1. As anticipated, the infection grew progressively for the first three weeks until stabilizing into an apparent chronic state of disease. In the later stages of the experiment there was evidence of an increase in the bacterial load, consistent with the worsening pathology described below. At this time, the experiment was terminated due to the surviving animals showing Karnovsky scores in excess of 8, indicative of severe distress. In the BCG vaccinated animals, there was consistently 0.5 to 1 Log 10 less bacilli detected at each time point. The difference in the median values between the two groups however, was not great enough to exclude the possibility that the difference was due to random sampling variability and hence was not statistically significant. The small group size was likely the main confounding factor.

Distinct cell populations are seen in guinea pig lung granulomas after aerosol infection with *M. tuberculosis*

The lesions that formed in response to the *M. tuberculosis* infection in the non vaccinated animals over time could generally be resolved into four histological stages that are summarized in Table 4.1, and examples of each stage are shown in Figure 4.2. In several experiments it was found that this progression was evident and reproducible. Detailed descriptions of the four stages are listed below.

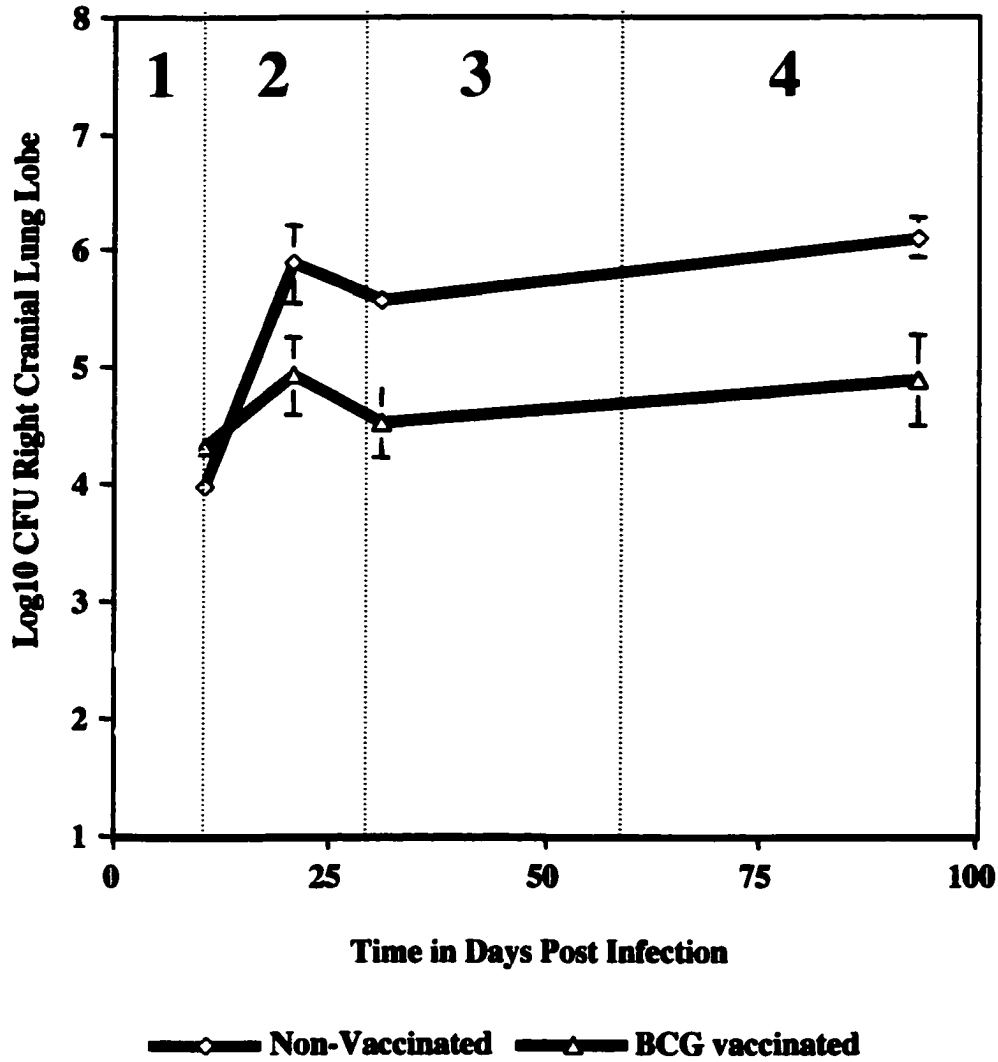

Figure 4.1
Growth curves of *M. tuberculosis* within the right cranial lung lobe of Hartley Guinea pigs that either did or did not receive *M. bovis BCG* vaccine six weeks prior to challenge. Data are expressed as the mean Log 10 numbers of colony forming units (CFU) and standard errors of the mean are indicated by the black vertical bars. Vertical bashed blue bars and red digits delineate perceived stages of infection. Two or three animals were sacrificed at each time point. The graph is representative of two experiments. No statistically significant difference was noted between the groups

Table 4.1

Four stage categorization of the pulmonary lesions in *M. tuberculosis* infected guinea pigs.

Lesion Stage (DPI)	Extent of Lesions (GF%)	Macrophage types	Lymphocyte organization	Neutrophil localization	Stage sequelae
1 (10)	Single 0-1	Histiocytes, epithelioid	Few, scattered	Prominent, scattered	Alveolitis
2 (20)	Multifocal 10-20	Histiocytes, epithelioid	Few, scattered with small aggregates at margin	Prominent, scattered,around and in the core	Karyorrhectic debris, fibrin deposition in the core and surrounding mantle. Fibroplasia Granulomatous lymphadenitis
3 (30)	Multifocal 20-40	Epithelioid, foamy	Scattered plus a prominent halo surrounding macrophages	Prominent, scattered around and in the core	'Classical' granuloma. Necrosis and fibroplasia. Granulomatous lymphadenitis
4 (60)	Coalescing >40	Epithelioid, foamy	Scattered aggregates or individual cells	Prominent, scattered throughout macrophage focus, around and in the core and amid airway debris	Necrosis, mineralization, marked fibroplasia. Multinucleated giant cells. Airway epithelium erosion and purulent airway exudate. Granulomatous lymphadenitis

Hematoxylin and eosin stained lung sections were examined by standard light microscopy, and several parameters of the lesions were characterized. The parameters included morphometric assessment of the extent of the pulmonary involvement (GF = Granuloma fraction), the predominant macrophage types present as well as the overall arrangement of lymphocytes and neutrophils in the lesions. Several sequelae of each stage were also noted. (DPI) = Days post infection when this lesion was first seen.

Figure 4.2.
Representative photomicrographs of the four stages of pulmonary granuloma development. (A) Stage 1 granuloma (day 10). Single discrete spherical focus of macrophages admixed with neutrophils and small numbers of lymphocytes adjacent to a large blood vessel and airway; *a*=artery, *b*=bronchiole, *ca*=cartilage, bar=100μm. (B) Stage 1 granuloma; area delineated by black rectangle in A. Note the abundance of neutrophils (arrows) intermixed with epithelioid macrophages and the lack of normal alveolar structure. bar=10μm. (C) Stage 2 granuloma (day 20). Single discrete spherical focus of macrophages with an eosinophilic, necrotic core (*c*) abutting a bronchiole (*b*). bar=100μm. (D) Stage 2 granuloma; area delineated by black rectangle in C. Note the abundance of neutrophils (arrows) intermixed with epithelioid macrophages and lymphocytes. Karyorrhectic debris is present in and around the core (*c*) and there are multiple small scattered islands of fibrin (*). bar=10μm. (E) Stage 3 granuloma (day 30). A discrete spherical lesion with a distinct necrotic core (*c*) is surrounded by a layer of epithelioid and foamy macrophages. This is in turn surrounded by a prominent darkly staining layer of lymphocytes (*) which are admixed with further macrophages at the extreme margins of the lesion. A bronchiole (*b*) is present at one margin. bar=100μm. (F) Stage 3 granuloma; area delineated by black rectangle in E. Note the karyorrhectic debris in and around the core area to the right (*c*), the dense sheet of epithelioid and foamy macrophages infiltrated by neutrophils surrounding it, and |on the left side| a region rich in lymphocytes in between which there is considerable collagen deposition (arrow) beyond this. bar=10μm. (G) Stage 4 granuloma (day 90). The core (*c*) has become mineralized and fractured. Epithelioid and foamy macrophages admixed with lymphocytes surround it enveloped in an elaborate network of fibrosis (*f*). A medium sized artery (*a*) and bronchiole (*b*) are present at the margins. bar=100μm (H) Stage 4 granuloma; area of lesion showing longitudinal section of a bronchiole (*b*) which is blocked with neutrophilic and necrotic debris (arrows) filling the lumen. Dense sheets of macrophages with scattered lymphocytes and interweaving fibrosis (*f*) surround the airway. bar =100μm. All sections are stained with hematoxylin and eosin.

Stage 1

Within 7-10 days after infection, small (up to approximately 500μm in diameter), discrete, spherical lesions composed of tight accumulations of epithelioid macrophages admixed with neutrophils. (Figure 4.2 A/B). As can be seen, the guinea pig neutrophil has eosinophilic cytoplasmic granules and is sometimes referred to as a pseudoeosinophil (15). Similar numbers of lymphocytes were also present. The lesions were most commonly seen in the parenchyma, close to major airways and blood vessels, effacing and expanding alveolar septae.

Stage 2

In this stage (Figure 4.2C/D) at around day 20, scattered discrete spherical lesions with a similar distribution to the earlier stage 1 were seen. The diameter of each lesion was substantially increased [up to approximately 1mm]. While epithelioid macrophages formed the bulk of these foci, neutrophils and lymphocytes were also seen scattered throughout the lesion with the exception of the central core. Occasionally, a thin band of lymphocytes was visible at the margin of the granuloma. The core of these lesions was characterized by a small but distinct accumulation of karyorrhectic debris admixed with a fibrillar eosinophilic material. Similar eosinophilic deposits were present randomly within the tight aggregate of cells surrounding the core.

Stage 3

By day 30 the lesion was taking the form of the "classical granuloma" with a diameter of up to 2mm (Figure 4.2E/F). There was a prominent central necrotic eosinophilic core,

which was packed with karyorrhectic debris. The core was surrounded by epithelioid macrophages and neutrophils, and lymphocytes were also present. Beyond this, the lesion contained a prominent collar of lymphocytes.

Stage 4

These lesions (Figure 4.2G/H) represented the end stage spectrum of granuloma evolution (example shown is day 90). There was extensive coalescence of multiple granulomas into a dense sheet of inflammation often effacing more than half of the lung sections. The necrotic cores were typically mineralized and surrounded by epithelioid macrophages. An elaborate fibrous web that had enveloped large foamy macrophages marked the previous outer margin of the granulomas. Neutrophils and lymphocytes were randomly spread at all levels of the inflammation. A few multinucleated giant cells were scattered throughout the lesions. Acid -fast bacilli were often detected both within the macrophages effacing the lung parenchyma and free within the suppurative airway debris (Figure 4.3).

A similar spectrum of lesions was seen in the BCG vaccinated animals (data not shown). However, the progression through the various stages was slower in these animals. Calculation of the granuloma fraction indicated that the size of the entire inflammatory was slightly less in vaccinated animals (Figure 4.4). This difference however, was not statistically significant.

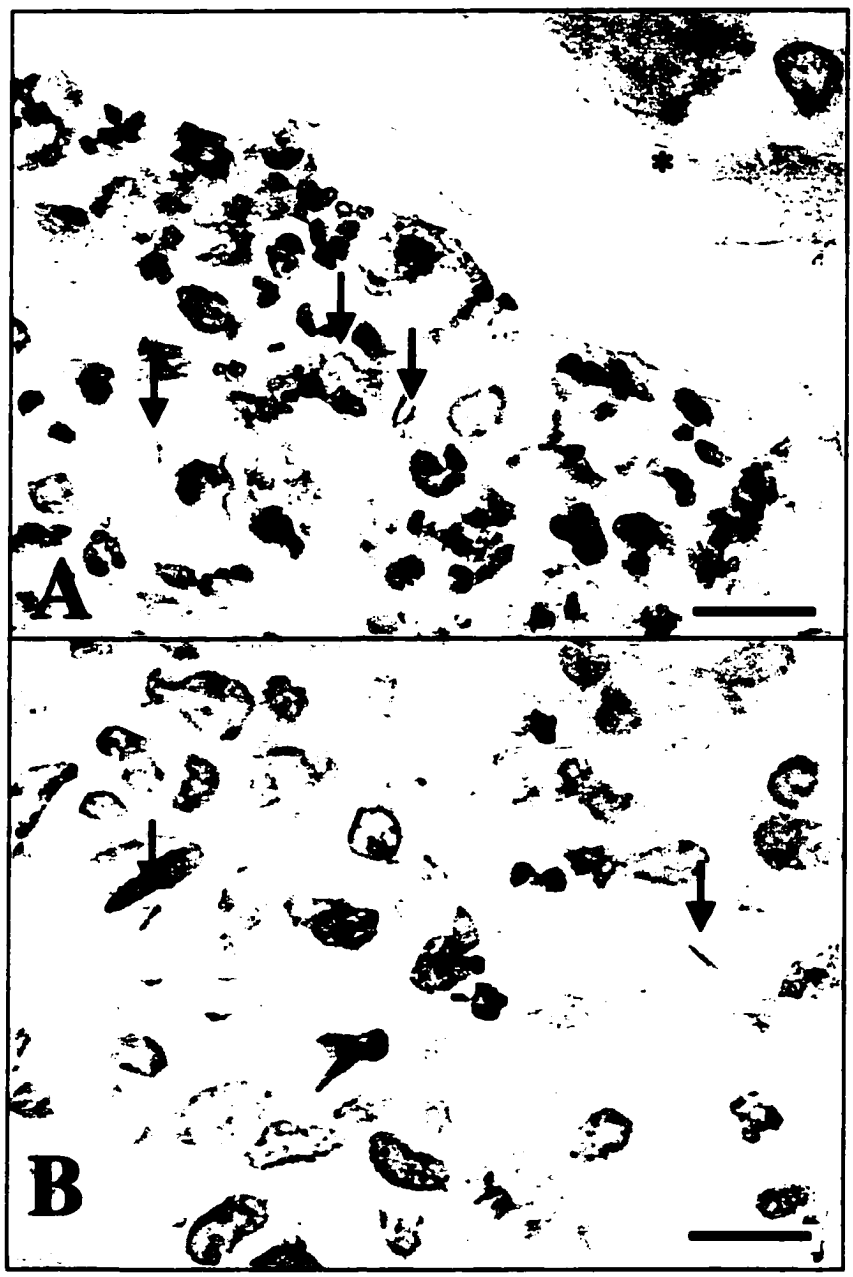

Figure 4.3
Representative photomicrographs of the distribution of acid-fast bacilli within the fourth stage of pulmonary lesions. (A) Extracellular acid fast bacilli (arrows) admixed with suppurative debris within the lumen of a bronchiole. Note cilia on adjacent epithelial surface (*). bar = 10μm. (B) Cytoplasmic acid fast bacilli (arrows) within macrophages that have effaced normal parenchyma. bar = 10μm. Sections stained by Ziehl-Neelson method.

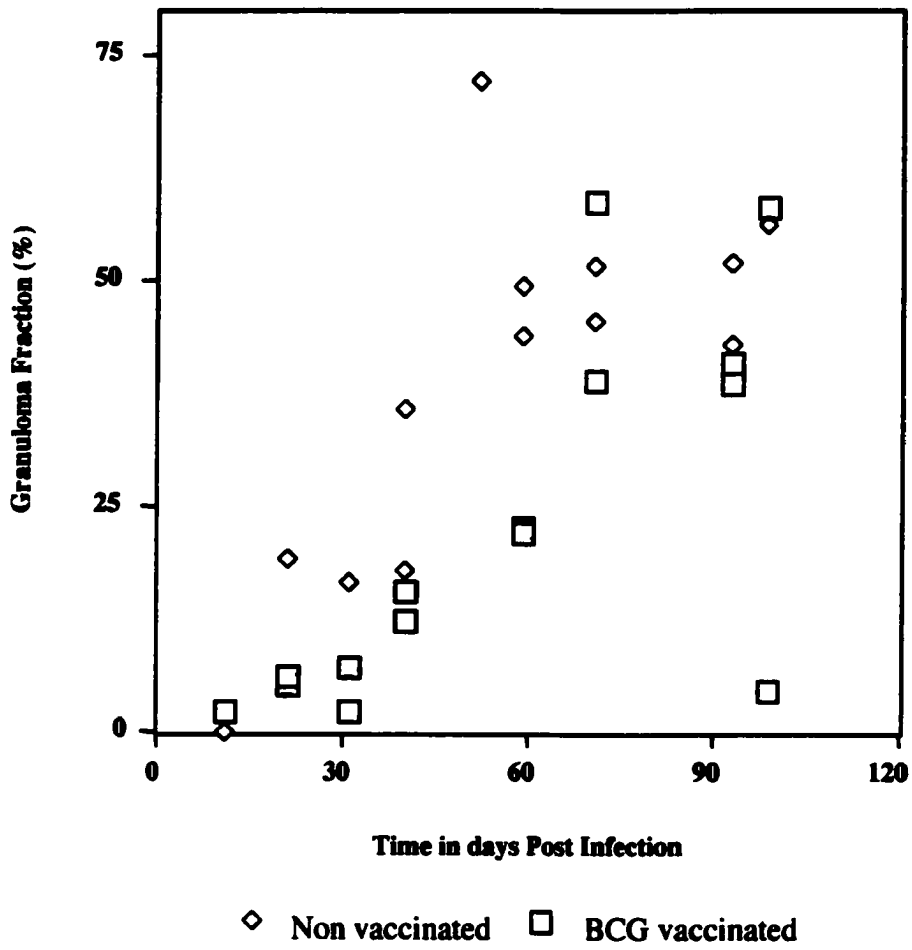

Figure 4.4
Scatter plot depicting the granuloma fraction of the right middle lung lobe from all guinea pigs in one of two experiments. Histological sections were measured using Metamorph Imaging Software. No statistically significant difference was noted between the two groups.

Anatomy of the Guinea Pig Granuloma

A single Stage 3 granuloma cut at ten 100 μm intervals depicted in Figure 4.5 demonstrates the anatomical predilection of the developing granuloma. The inflammatory focus begins (1), within the parenchyma around blood vessels and bronchioles. It then expands and then returns to a similar size (10). When these images are stacked one on top of each other by computer software, and the approximate outer margin of each slice is overlaid, it is possible to appreciate this morphology more fully. In this case appearing as an elliptical entity (Figure 4.6). This analysis does not address the point of origin of the inflammation.

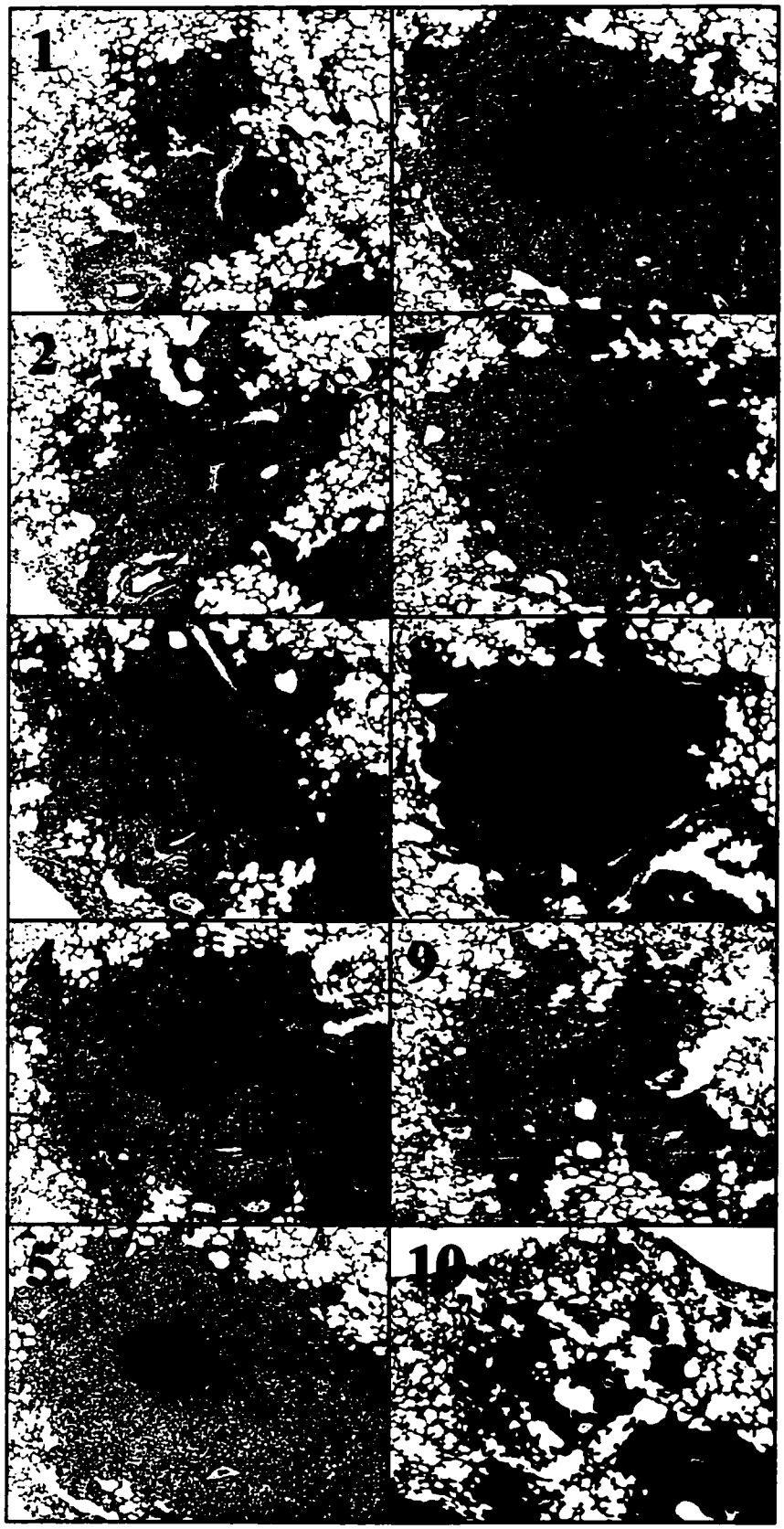

Figure 4.5
Ten serial 100μm step sections through a pulmonary granuloma in a Hartley Guinea Pig at 30 days post infection.

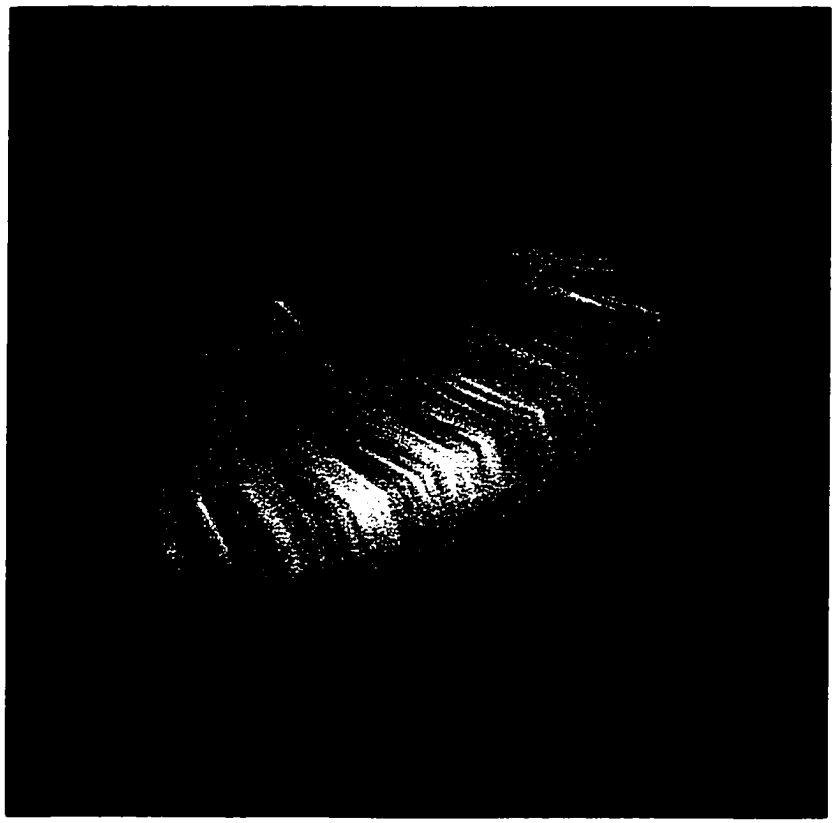

Figure 4.6
Composite 3-D reconstruction of the ten serial 100μm step sections through the pulmonary granuloma depicted in Figure 4.5

Localization of lymphocyte subsets by immunohistochemistry.

The distribution of $CD4^+$ and $CD8^+$ T cells in the developing lesions is shown in Figure 4.7. The distribution of cells positive for the Pan B marker is shown in figure 4.8. On day 10 small numbers of lymphocytes were evident. There were apparently similar numbers of $CD4^+$ and $CD8^+$, and there was no evidence of cellular aggregation. This pattern was similar on days 20 and 30, as the lesions considerably increased in size. As the lesions degenerated and mineralized, lymphocytes could still be detected, but were relatively fewer in number. The lesions looked similar in the BCG vaccinated animals. On occasion, there appeared to be less $CD8^+$T cells than $CD4^+$T cells in the same granuloma however, this was not a consistent finding (data not shown). The positive staining of cells for the Pan B marker was often difficult to interpret due to a very weak signal. Figure 4.8A indicates that the staining within splenic follicles was strongly specific for B cells. When positive cells were seen in the lung, then were often arranged in cords or groups (Figure 4.8B,C). They were only detected at and beyond stage 3. An accurate appreciation of the accumulation of B cells over time was not achieved.

Characterization of the fibrotic response.

The development of lesion fibrosis was followed using specific staining methods (Figure 4.9). No early response was seen until day 20, when small discrete regions peripheral to the core and extending towards the outer margin of the granuloma stained positive for fibrin (Figure 4.9D), indicating vascular damage. Collagen was also detected (Figure 4.9C), forming irregular cords around cells adjacent to the core lesions. By day 30, the prominent lymphocyte collar now present was interlaced by bands of collagen of variable

thickness (Figure 4.8E), whereas fibrin deposits were spread throughout the granulomas, as well as prominently focused around the core (Figure4.9F).

By day 90 the structure was dominated by thick bands of collagen deposition, forming a thick web appearing to trap large numbers of foamy macrophages in addition to completely surrounding the mineralized core lesion (Figure 4.9G). In contrast, fibrin deposition was absent at this stage (Figure 4.9H). The development of fibrosis within the lesions of BCG vaccinated animals was similar to that of the non-vaccinated animals, however, similar to the development of the overall lesion morphology, the progression was slower.

Distribution of apoptotic cells.

It has been suggested that apoptosis of infected cells may be a major defense mechanism against *M.tuberculosis*. As shown in Figure 4.10 very few apoptotic cells could be detected at all four stages of the disease process. On days 10 through 30 some could be seen close to the developing core lesion, but later during the course of the infection only a few cells stained positive for apoptosis and appeared to be randomly distributed. The staining distribution of apoptotic cells was similar in the vaccinated compared to the non-vaccinated animals (data not shown).

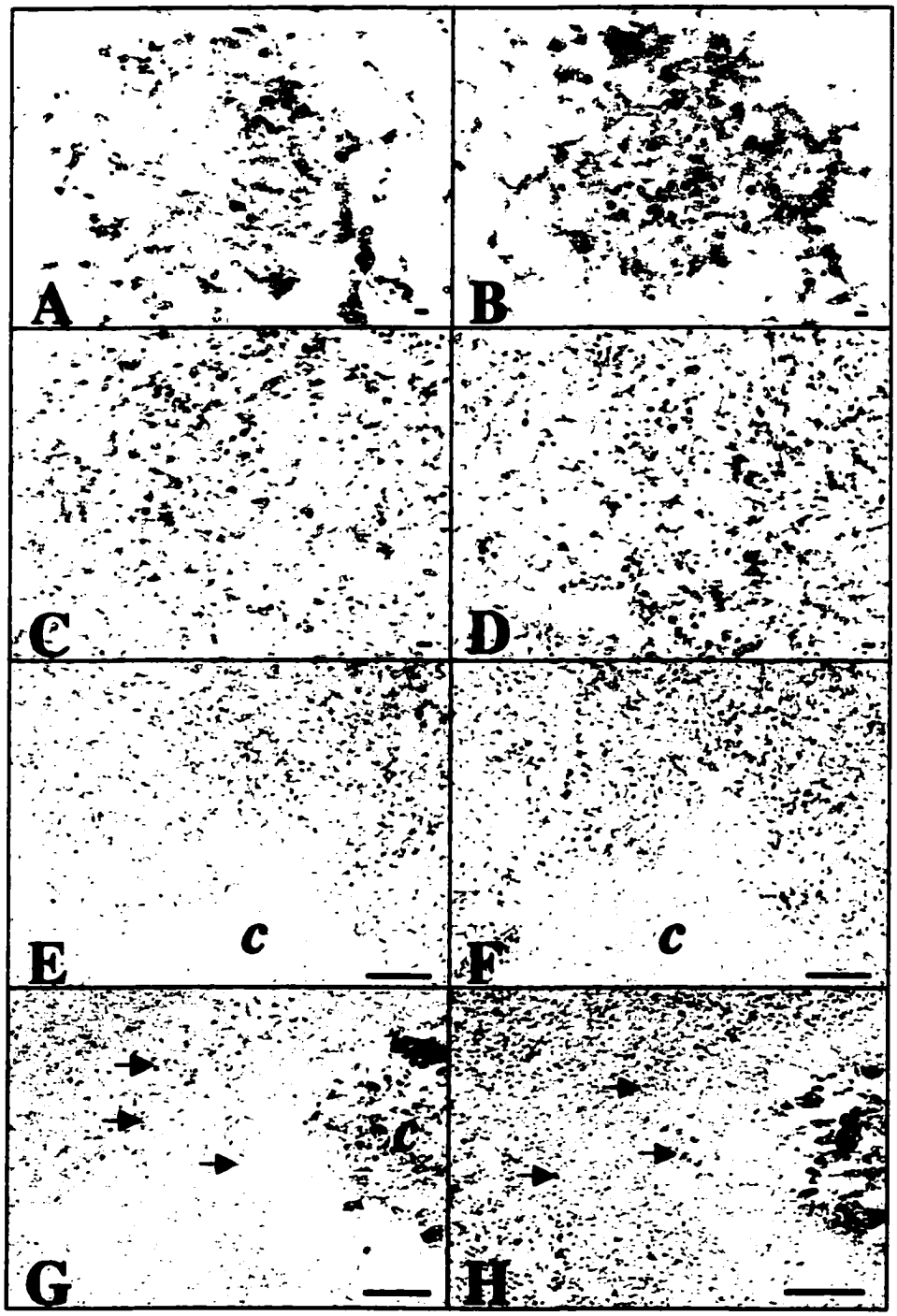

Figure 4.7

Representative photomicrographs showing immunohistochemical staining for CD4+ [left column] and CD8+ [right column] T cells within the four stages of pulmonary granuloma formation for stages 1 [A/B], stage 2 [C/D],stage 3 [E/F] and stage 4 [G/H]. For the top six panels the size bar =10μm. *c* represents the necrotic core. Arrows indicate individual positive cells. Labeled avidin-alkaline phosphatase with Napthol Red method was used in all sections and counter-stained with hematoxylin. CD4+ T cells were stained with Serotec clone CT7 and CD8+ T cells were stained with Serotec clone CT6.Biotin labeled $F(ab')_2$ rabbit anti mouse Ig was used as the secondary antibody.

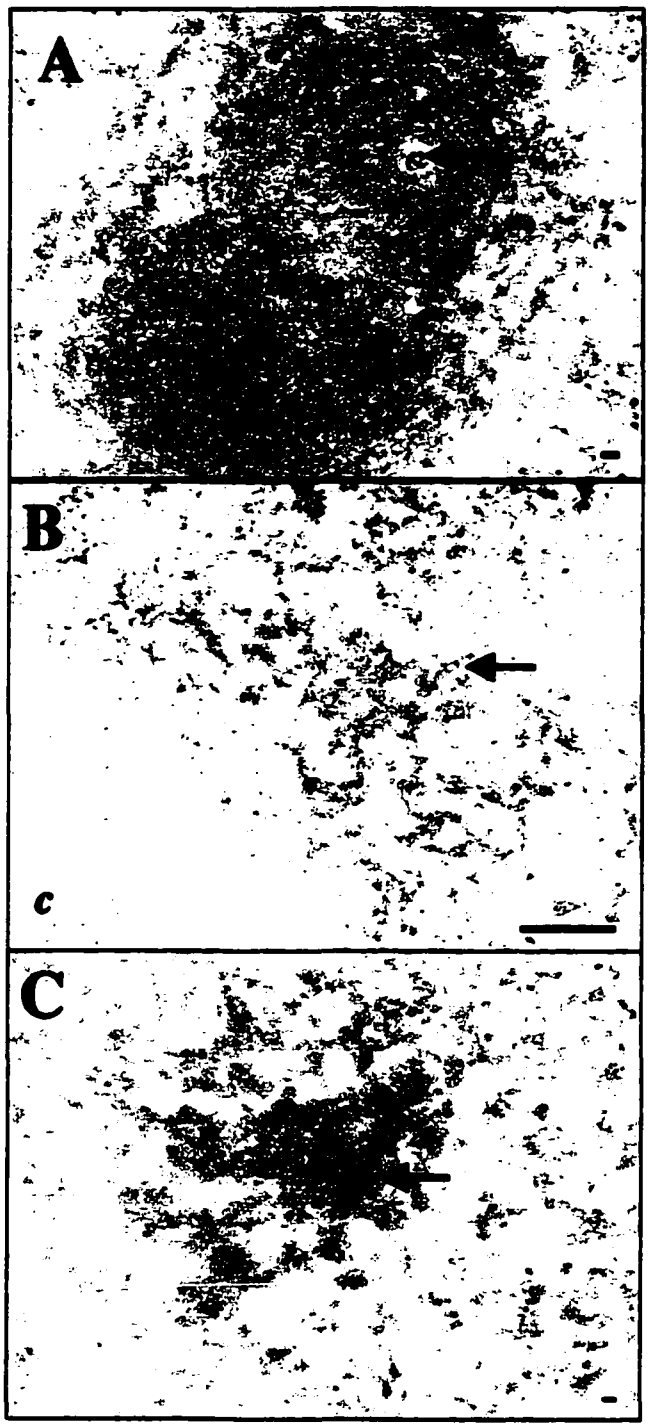

Figure 4.8
Representative photomicrographs of frozen guinea pig spleen (A) and lung (B,C) immunohistochemically stained for the Pan B cell marker MSGp9. A. Lymphoid follicle. Arrow = central arteriole, * = B cell corona, bar=10 μm. B. Stage 3 granuloma, *c*=necrotic core. Interlacing bands of positive cells (arrow) are present within the mantle of cells surrounding the core, bar=100μm. C. Stage 4 granuloma. Small dense aggregate of positive cells (arrow) within a large sheet of macrophages, bar=10 μm.

Figure 4.9
Representative photomicrographs of collagen and fibrin deposition through the four stages of pulmonary granuloma formation. The left column shows collagen staining and the right hand column shows fibrin staining. (A, B) Stage 1 granuloma; no positive staining. bar=100μm. (C, D) Stage 2 granuloma. Note blue collagen cords (C: area outlined by black box and arrow within inset) irregularly extending between cells adjacent to the core. Note also multiple aggregates of red fibrin associated with the core and the surrounding tissue (D: bright red foci outlined by black box). Note meshwork arrangement of red stained material in D high magnification inset. C bar= 100μm, C inset bar =10μm, D bar= 100μm, D inset= 10μm. (E-F) Stage 3 granuloma. Note cords of blue collagen interwoven with bands of lymphocytes (E: Area outlined by black box and arrow within inset). Also note the multiple aggregates of fibrin associated with the core and the surrounding tissue (F: bright red foci outlined by black box). E bar= 100μm, E inset bar =10μm, F bar= 10μm. (G-H) Stage 4 granuloma. Note thick web of blue collagen punctuated by macrophages surrounding the core (G: area outlined by black box and within inset). Note no significant fibrin associated with the core and the surrounding tissue. Light green tissue corresponds to collagen. G bar= 100μm, G inset bar =10μm, H bar= 100μm. *c* = core. Collagen staining by Masson's Trichrome, fibrin staining by Fraser-Lendrum fibrin method.

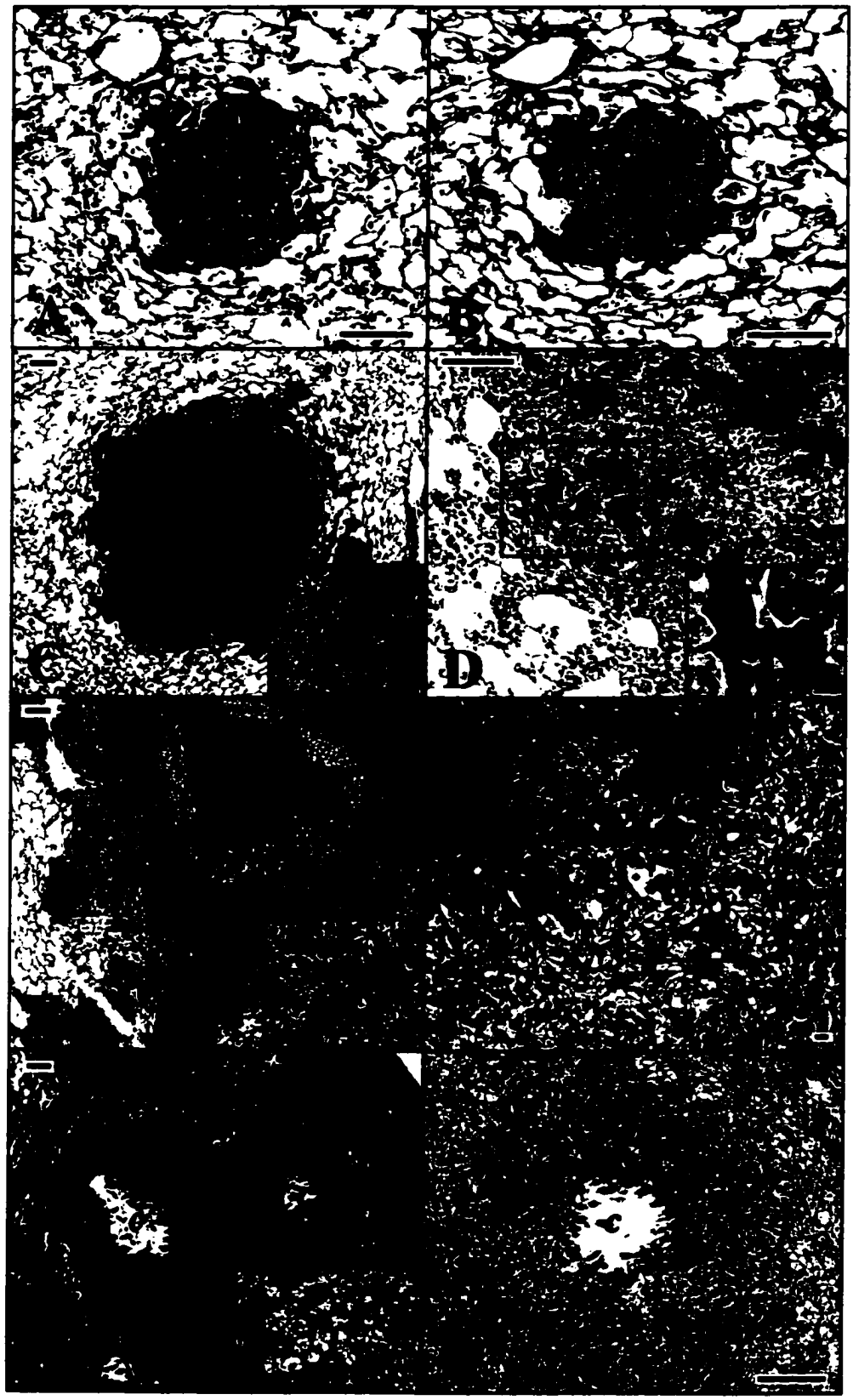

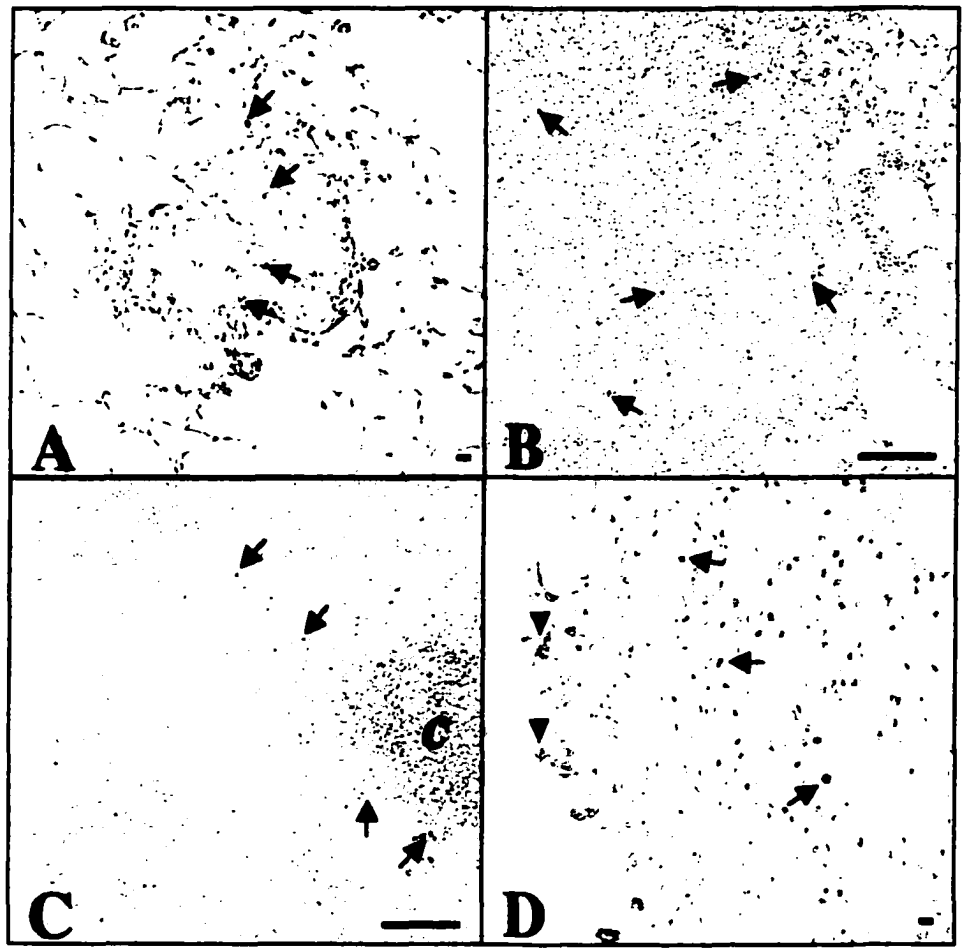

Figure 4.10
Representative photomicrographs of the distribution of apoptotic cells within the four stages of pulmonary granuloma formation. (A) Stage 1 granuloma. A few scattered single apoptotic cells are indicated by the arrows. bar= 10μm. (B) Stage 2 granuloma. bar= 100μm. (C) Stage 3 granuloma. At this time point most apoptotic cells tended to be adjacent to the core (c). bar= 100μm. (D) Stage 4 granuloma. Note the similar distribution to (C). The arrow heads point to mineral debris at the margin of the core. bar= 10μm. All sections stained with the Apo-Tag TUNEL method, using diamonbenzidine as the chromogen and Methyl Green as the counter-stain.

Discussion

The guinea pig is widely considered the consummate animal model of human tuberculosis given the similarities in the pathological response to pulmonary infection, and as a result, is an important tool in the search for new vaccines. The results shown here are the first attempt to provide a comprehensive description of the stages of the disease in concert with immunohistochemical analysis documenting the influx of CD4 and CD8 T cells into the developing lesions. The results of the study raise a variety of issues that challenge current dogma.

The results show that there is a very rapid response to low dose aerosol infection, with small discrete granulomatous structures already evident just ten days post exposure. The predominant cell population forming these structures consisted of macrophages, but another obvious population consisted of the eosinophilic granule laden neutrophils characteristic of the guinea pig. Small numbers of lymphocytes were also present, with equal numbers of $CD4^+$ and $CD8^+$ cells distributed evenly across the lesion.

Between day 10 and 20 the structure became much larger, and a central necrotic core was now obvious. Macrophages still predominated, but there appeared to be an increasing number of lymphocytes. Pockets of neutrophils were still evident, and there appeared to be multiple small areas of fibrin deposition suggesting vascular damage or leakage. By day 30, at a time that the bacterial load had been initially contained within the lungs, the lesion was now very large with a prominent necrotic core, and with large numbers of activated foamy epithelioid macrophages surrounded by an outer zone packed with

lymphocytes. This consisted of an apparently equal mixture of $CD4^+$ and $CD8^+$ T cells surrounded on the outer edge by considerable collagen deposition. Cells staining positive for the Pan B cell marker were found as cords and/or aggregates only in the later stages of the disease. No specific role for these cells has been suggested to date.

These dynamic changes to the appearance of the granuloma seem to stabilize for much of the chronic stage of the disease between days 30 and 90. Granulomas in various stages could be found during this time, reflecting the asynchronous, episodic spread of bacilli around the lung. During this time the necrotic core gradually mineralized and the overall structure became surrounded by fibrosis. It is usually considered that the fibrosis contains the bacilli, but despite the elaborate ring of collagen, bacilli were still to be found in the airways. Due to the size of the structure there was damage to surrounding airways, and as a result erosion and ulceration of respiratory epithelium and blockage of these vessels with inflammatory cell debris was commonplace. As early as stage 2, a granulomatous pulmonary lymphadenitis was present.

The current dogma to explain the pathologic process in the guinea pig and rabbit is based on the historic studies of Lurie, and more recently by Dannenberg (7-11,19, 20). In that model it is held that the initial presence of the bacilli causes no detectable tissue damage at first. Then, as cell mediated immunity is triggered 'excessive DTH' mediating the cellular influx and inflammation, in concert with cytolytic T cell activity, leads to the necrotic degeneration of the center of the lesion. It was further proposed that the

development of this caseous necrosis initially limits the growth of extracellular bacteria, until [in the rabbit] the lesion liquefies and the animal dies.

We propose a new hypothesis, which differs considerably from the Lurie/Dannenberg model. It is apparent to us that there is a very rapid response to the infection despite the very low dose, and hence it is highly probable that this response is innate in nature. Given the preponderance of macrophages, which are already present in significant numbers in the lesion by day ten, this may involve CD1 or Toll receptor mediated mechanisms (3, 4, 22, 23, 30, 41). In addition, however, there are also obvious and prominent pockets of neutrophils. These may represent a double-edged sword, in that they may be contributing to early protection, as has been suggested (1, 29), but their accumulation in response to local tissue damage and their own subsequent degranulation [perhaps merely due to their short lifespan] may also contribute to the local pathologic process. Given the presence of neutrophils throughout the early response, the data suggests that these cells are continuously accumulating in the lesions over this period of time.

It is possible that this activity, which happens very early during the course of the infection, may be the trigger to the initial development of the characteristic central necrotic core. This structure is already obvious by the day 20 point, which seems to indicate that it has begun development long before the emergence of the acquired response. This latter response seems to peak about ten days later, and is associated with a large number of lymphocytes (again a mixture of $CD4^+$ and $CD8^+$ cells) entering the lesion and forming a layer of cells peripheral to the central core. Morecver, in this region

there are multiple scattered areas of fibrin deposition which are suggestive of increased vascular permeability, which in turn would create local hypoxic conditions and cause the lesion to further increase in size. In contrast there was no evidence for the hypothesis that the central core was promoted by cytolytic T cells, since there were no aggregates of either $CD4^+$ or $CD8^+$ cells adjacent to the lesion. Accordingly, our new hypothesis suggests that these very early mechanisms resulted in a process of irreversible damage that the subsequent emergence of the acquired response was too slow to prevent.

In a sense, the period of chronic disease seen between about day 30 and 90 might also be controlled in part by innate mechanisms. There is no evidence that the process of mineralization has an immune basis, and the substantial fibrotic response could also be regarded as a primitive event designed to wall off the lesion. Unfortunately, however, this process of consolidation is itself damaging, allowing erosion of cellular debris [including extracellular bacteria] into surrounding airways.

These guinea pigs succumb to the disease about 100-140 days after exposure. We propose that this event underlies at least two mechanisms. First, the size of the lesion consolidates the lung lobe and interferes with efficient gas exchange. Second, the dissemination of the infection via the airways results in fresh ingestion by macrophages/monocytes and the subsequent triggering of IFN-γ by memory T cells. As a result, activated macrophages secrete large quantities of TNF, leading to the weight loss invariably seen for a week or so prior to death of the animal.

Both BCG and several new candidate vaccines are highly protective in the guinea pig model, which seems to suggest that this animal is capable of generating a potent memory T cell response (2, 16). This in turn explains the very rapid lymphocytic response seen in vaccinated animals, which would be needed to prevent the development of the central necrotic core. As has been suggested elsewhere (27), this appears to be an important parameter of effective vaccination in this animal model. In this study however, it was difficult to resolve any significant difference in histopathology, other than speed of progression of pathology, between BCG vaccinated and non-vaccinated animals. This may be a reflection of vaccine dose, strain or the dose of *M.tuberculosis*. Too little vaccine or too much vaccine may result in a spurious result. Other studies have further demonstrated the remarkable ability of BCG to slow disease progression, however, much still needs to be done to explain this, both immunologically and pathologically.

Another important finding here was the observation that very few lymphocytes stained positive for apoptosis, suggesting that this mechanism does not play any significant role in the disease process. This finding is rather contrary to the bulk of the literature (6, 12, 14, 17, 18, 24, 25, 33, 42) that holds that apoptosis of both T cells and infected macrophages is an important defense mechanism, although we note that most of these observations were made in vitro.

Finally, although the mouse and guinea pig are considered quite different models of tuberculosis, there are also some similarities. If one regards the course of the disease in the guinea pig as having a stage of chronic disease followed by subsequent reactivation,

then the fact that the latter stage is predisposed by much earlier events has certain similarities to various inbred mouse strains that are also prone to this event (39) Moreover, both animal models show evidence of a very efficient fibrotic response leading to deposition of collagen to provide some degree of integrity to the granuloma (26, 31)

Where there appear to be some interesting differences are in terms of the lymphocyte response. We have previously pointed to differences in terms of the propensity of mouse lymphocytes to accumulate towards the center of the granuloma (13, 26) and it may be that the reason that lymphocytes in the guinea pig occupy a more peripheral position may simply be because of the presence of the central necrosis. In the mouse we have described clear distinctions between the CD4 and CD8 responses, with $CD4^+$ cells forming large aggregations dominating the granulomas, with $CD8^+$ cells more sparse and distributed more towards the periphery of the lymphocyte aggregates (13) This data, when viewed with the data on CD8 gene knockout mice (39) is consistent with an immunosurveillance role for the $CD8^+$ T cell population.

In the guinea pig, the distribution of the two T cell subsets seems to be very different. Although large numbers of lymphocytes entered the lesions by day 30, they remained an even randomized mixture of both $CD4^+$ and $CD8^+$ cells, with no evidence of any cellular aggregation. In addition, they did not appear to collectively represent the entire population of lymphocytes, suggesting that the additional cells might be the poorly stained B cells and other cells, as previously seen in the mouse model (13, 40). Whether

this implies that $CD8^+$ cells play a more prominent role in the early protective response in the guinea pig as compared to the mouse is impossible to say at this point.

Acknowledgements

This work was sponsored by the US Public Health service grants AI-44072 and AI-45707 from the NIAID, NIH. We thank Drs Andrea Cooper, Tony Frank, and Christopher Dascher for their helpful advice towards this project, and Dr David McMurray for his continued encouragement

References

1. **Appelberg, R., and A. M. Sarmento.** 1990. The role of macrophage activation and of bcg-encoded macrophage function(s) in the control of *Mycobacterium avium* infection in mice. Clinical and Experimental Immunology. **80:**324-327.

2. **Baldwin, S., D. D'Souza, A. Roberts, B. Kelly, A. Frank, M. Lui, J. Ulmer, K. Huygen, D. McMurray, and I. Orme.** 1998. Evaluation of new vaccines in mouse and guinea pig models of tuberculosis. Infect Immun. 66(6):2951-9.

3. **Bendelac, A., M. N. Rivera, S. H. Park, and J. H. Roark.** 1997. Mouse CD1-specific autoreactive T cells. Development, specificity and function. Annual Review of Immunology. **15:**535-550.

4. **Brightbill, H. D., D. H. Libraty, S. R. Krutzik, R. B. Yang, J. T. Belisle, J. R. Bleharski, M. Maitland, M. V. Norgard, S. E. Plevy, S. T. Smale, P. J. Brennan, B. R. Bloom, P. J. Godowski, and R. L. Modlin.** 1999. Host defense mechanisms triggered by microbial lipoproteins through toll-like receptors. Science. **285:**732-6.

5. **Cotran, R. S., Kumar, V and Collins T.** 1999. Robbins Pathologic Basis of Disease, Sixth ed. W.B Saunders Co, Philadelphia.

6. **Dalton, D. K., L. Haynes, C. Q. Chu, S. L. Swain, and S. Wittmer.** 2000. Interferon gamma eliminates responding CD4 T cells during mycobacterial infection by inducing apoptosis of activated CD4 T cells. J Exp Med. **192:**117-22.

7. **Dannenberg, A. M., Jr.** 1990. Controlling tuberculosis: the pathologist's point of view. Res Microbiol. **141:**192-6; discussion 262-3.

8. **Dannenberg, A. M., Jr.** 1991. Delayed-type hypersensitivity and cell-mediated immunity in the pathogenesis of tuberculosis. Immunol Today. **12:**228-33.

9. **Dannenberg, A. M., Jr.** 1989. Immune mechanisms in the pathogenesis of pulmonary tuberculosis. Rev Infect Dis. **11 Suppl 2:**S369-78.

10. **Dannenberg, A. M., Jr.** 1993. Immunopathogenesis of pulmonary tuberculosis. Hosp Pract (Off Ed). **28:**51-8.

11. **Dannenberg, A. M.** 1994. Rabbit model of tuberculosis. Coordinating ed., B. R. Bloom. ASM Press, Washington D.C.

12. **Fratazzi, C., R. D. Arbeit, C. Carini, M. K. Balcewicz-Sablinska, J. Keane, H. Kornfeld, and H. G. Remold.** 1999. Macrophage apoptosis in mycobacterial infections. J Leukoc Biol. **66:**763-4.

13. **Gonzalez-Juarrero, M., O. C. Turner, J. Turner, P. Marietta, J. V. Brooks, and I. M. Orme.** 2001. Temporal and spatial arrangement of lymphocytes within lung granulomas induced by aerosol infection with *Mycobacterium tuberculosis*. Infect Immun. **69:**1722-8.

14. **Hirsch, C. S., Z. Toossi, J. L. Johnson, H. Luzze, L. Ntambi, P. Peters, M. McHugh, A. Okwera, M. Joloba, P. Mugyenyi, R. D. Mugerwa, P. Terebuh, and J. J. Ellner.** 2001. Augmentation of apoptosis and interferon-gamma production at sites of active *Mycobacterium tuberculosis* infection in human tuberculosis. J Infect Dis. **183:**779-88.

15. **Hopewell, P. C.** 1994. Overview of Clinical Tuberculosis: Tuberculosis: Pathogenesis, protection, and control., 1st ed. Coordinating ed., B. R. Bloom. ASM, Washington, D. C.

16. **Horwitz, M. A., B.-W. E. Lee, B. J. Dillon, and G. Harth.** 1995. Protective immunity against tuberculosis induced by vaccination with major extracellular proteins of *Mycobacterium tuberculosis*. Proceedings of the National Academy of Sciences, USA. **92:**1530-1534.

17. **Keane, J., M. K. Balcewicz-Sablinska, H. G. Remold, G. L. Chupp, B. B. Meek, M. J. Fenton, and H. Kornfeld.** 1997. Infection by *Mycobacterium tuberculosis* promotes human alveolar macrophage apoptosis. Infect Immun. **65:**298-304.

18. **Klingler, K., K. M. Tchou-Wong, O. Brandli, C. Aston, R. Kim, C. Chi, and W. N. Rom.** 1997. Effects of mycobacteria on regulation of apoptosis in mononuclear phagocytes. Infect Immun. **65:**5272-8.

19. **Lurie, M. B.** 1964. Resistance to tuberculosis: Experimental studies in native and acquired defensive mechanisms. Harvard University Press, Cambridge, MA.

20. **Lurie, M. B. a. D., A.** 1965. Macrophage function in infectious disease with inbred rabbits. Bacteriol. Rev. **29:**466-476.

21. **McMurray, D. N., F. M. Collins, A. M. Dannenberg, Jr., and D. W. Smith.** 1996. Pathogenesis of experimental tuberculosis in animal models. Curr Top Microbiol Immunol. **215:**157-79.

22. **Means, T. K., S. Wang, E. Lien, A. Yoshimura, D. T. Golenbock, and M. J. Fenton.** 1999. Human toll-like receptors mediate cellular activation by *Mycobacterium tuberculosis*. J Immunol. **163:**3920-7.

23. **Modlin, R. L., H. D. Brightbill, and P. J. Godowski.** 1999. The toll of innate immunity on microbial pathogens. N Engl J Med. **340:**1834-5.

24. **Molloy, A., P. Laochumroonvorapong, and G. Kaplan.** 1994. Apoptosis, but not necrosis, of infected monocytes is coupled with killing of intracellular Bacillus Calmette-Guerin. J Exp Med. **180:**1499-1509.

25. **Oddo, M., T. Renno, A. Attinger, T. Bakker, H. R. MacDonald, and P. R. A. Meylan.** 1998. Fas ligand-induced apoptosis of infected human macrophages reduces the viability of intracellular *Mycobacterium tuberculosis*. Journal of Immunology. **160:**5448-5454.

26. **Orme, I. M.** 1998. The immunopathogenesis of tuberculosis: a new working hypothesis. Trends Microbiol. **6:**94-7.

27. **Orme, I. M.** 1999. Vaccination against tuberculosis: recent progress. Adv Vet Med. **41:**135-43.

28. **Orrell, J. M., S. J. Brett, J. Ivanyi, G. Coghill, A. Grant, and J. S. Beck.** 1992. Morphometric analysis of *Mycobacterium tuberculosis* infection in mice suggests a genetic influence on the generation of the granulomatous inflammatory response. J Pathol. **166:**77-82.

29. **Pedrosa, J., B. M. Saunders, R. Appelberg, I. M. Orme, M. T. Silva, and A. M. Cooper.** 2000. Neutrophils play a protective, non-phagocytic, role in systemic *Mycobacterium tuberculosis* infection of mice. Infection and Immunity. **68:**in press.

30. **Porcelli, S. A., and R. L. Modlin.** 1999. The CD1 system: antigen-presenting molecules for T cell recognition of lipids and glycolipids. Annu Rev Immunol. **17:**297-329.

31. **Rhoades, E. R., A. A. Frank, and I. M. Orme.** 1997. Progression of chronic pulmonary tuberculosis in mice aerogenically infected with virulent *Mycobacterium tuberculosis*. Tuber Lung Dis. **78:**57-66.

32. **Ridley, D. S., and M. J. Ridley.** 1987. Rationale for the histological spectrum of tuberculosis. A basis for classification. Pathology. **19:**186-92.

33. **Rojas, M., M. Olivier, P. Gros, L. F. Barrera, and L. F. Garcia.** 1999. TNF-alpha and IL-10 modulate the induction of apoptosis by virulent *Mycobacterium tuberculosis* in murine macrophages. J Immunol. **162:**6122-31.

34. **Saunders, B. M., and A. M. Cooper.** 2000. Restraining mycobacteria: role of granulomas in mycobacterial infections. Immunol Cell Biol. **78:**334-41.

35. **Smith, D. W., and G. E. Harding.** 1977. Animal model of human disease. Pulmonary tuberculosis. Animal model: Experimental airborne tuberculosis in the guinea pig. Am J Pathol. **89:**273-6.

36. **Smith, D. W., D. N. McMurray, E. H. Wiegeshaus, A. A. Grover, and G. E. Harding.** 1970. Host-parasite relationships in experimental airborne tuberculosis. IV. Early events in the course of infection in vaccinated and nonvaccinated guinea pigs. Am Rev Respir Dis. **102:**937-49.

37. **Smith, D. W., and E. H. Wiegeshaus.** 1989. What animal models can teach us about the pathogenesis of tuberculosis in humans. Rev Infect Dis. **11 Suppl 2:**S385-93.

38. **Stadelmann, C., and H. Lassmann.** 2000. Detection of apoptosis in tissue sections. Cell Tissue Res. **301:**19-31.

39. **Turner, J., C. D. D'Souza, J. E. Pearl, P. Marietta, M. Noel, A. A. Frank, R. Appelberg, I. M. Orme, and A. M. Cooper.** 2001. CD8- and CD95/95L-dependent mechanisms of resistance in mice with chronic pulmonary tuberculosis. Am J Respir Cell Mol Biol. **24:**203-9.

40. **Turner, J., A. A. Frank, J. V. Brooks, M. Gonzalez-Juarrero, and I. M. Orme.** 2001. The progression of chronic tuberculosis in the mouse does not require the participation of B lymphocytes or interleukin-4. Exp Gerontol. **36:**537-45.

41. **Underhill, D. M., A. Ozinsky, K. D. Smith, and A. Aderem.** 1999. Toll-like receptor-2 mediates mycobacteria-induced proinflammatory signaling in macrophages. Proc Natl Acad Sci U S A. **96:**14459-63.

42. **Watson, V. E., L. L. Hill, L. B. Owen-Schaub, D. W. Davis, D. J. McConkey, C. Jagannath, R. L. Hunter, Jr., and J. K. Actor.** 2000. Apoptosis in *Mycobacterium tuberculosis* infection in mice exhibiting varied immunopathology. J Pathol. **190:**211-20.

Chapter Five

Comparative Immunomorphology of Pulmonary Tuberculosis

Abstract

In a variety of countries around the world, native wild animals act as reservoirs of tuberculosis and threaten domestic cattle, and hence human populations. How pulmonary granulomas in these various species compare to one another is poorly understood, and whether immunomorphology is perhaps indicative of epidemiology or clinical pattern even less so. A comparative histolopathological appraisal of lung tissue from adult European badgers (*Meles meles*), New Zealand brushtail possums (*Trichosurus vulpecula*), and Holstein dairy cows (*Bos taurus*) with experimental or natural primary *M.bovis* infection was performed. Only chronic lesions were examined. Significant differences between these species and the C57BL/6 mouse and guinea pig laboratory models of *M. tuberculosis* infection were detected and then further compared to reported human data. Special attention was paid to the intragranuloma lymphocyte arrangement and the overall morphology of the granulomas. The badger lesions had a unique bronchitis, but also some similarities to C57BL/6 mice. The possum and cattle granulomas had abundant necrosis, variable fibrous capsule development and lymphocytes that were found at various sites and in various arrangements. In addition, cattle lesions had an abundance of multinucleate giant cells. Possum and cattle granulomas resembled the guinea pig lesions, which in turn had similarities to human

lesions. In light of these findings, we speculate on the possible threat to cattle posed by badgers, and possums, and the applicability of animal models to human studies.

Introduction

The epidemic of human immunodeficiency virus infection in developing countries, together with the widespread incidence of *M.bovis* infection in domestic and wild animals and conditions that favor zoonotic transmission, provides opportunity for zoonotic tuberculosis to become a serious public health problem (3, 7). Programs to eradicate bovine tuberculosis based on a "test and slaughter" approach eliminate animals identified as being infected with *M. bovis*. These programs however, have been only partially effective in countries such as New Zealand, the United Kingdom and Ireland, which have a wildlife reservoir of infected animals. Furthermore, this approach to the control of bovine tuberculosis is economically and socially unacceptable in many African countries. Therefore, in both developed and developing countries, an improved understanding of immunopathogenesis is required. This will hopefully lead to the development of more efficient vaccines and reduce the toll of tuberculosis.

The primary reservoir for *M.bovis* in New Zealand is *Trichosurus vulpecula,* the brushtail possum. While the prevalence of *M.bovis* in New Zealand cattle is less than 1%, with nearly 3% of the herds on movement restriction, the prevalence of *M.bovis* in the possums is estimated to be 1-5% (1). This means that there are between 700,000 and 3.5 million infected possums in New Zealand. Furthermore, these animals excrete and harbor large numbers of bacteria (1). The control of possum populations by poison has dramatically reduced the prevalence of *M.bovis* in cattle (2).

The major barrier to the eradication of *M.bovis* from England and Ireland is thought to be the existence of *M.bovis* in badgers. The control of this reservoir is much more complicated than with the possums of New Zealand because the badger is a protected species. Recently the British government sponsored a large bovine tuberculosis experiment in badgers, designed to definitively demonstrate that badgers are capable of transmitting *M.bovis* to cattle (6).

Not nearly as much is known regarding the immune response to *M.bovis* in possums, badgers and cattle as is known about the human and murine responses to *M.tuberculosis.* The similarities of most mammalian immune systems and the similarities between *M.bovis* and *M.tuberculosis* have led to the erroneous assumption by some that many responses in one host to one organism are similar in another host to another organism.

The comprehensive comparative studies by Francis (4) and Karlson (5), however, attest to the varied nature of the tuberculous granuloma. In particular, they highlight the considerable variation in cellular composition of the lesions. In light of the growing data on granulomagenesis in laboratory animals, however, it is now possible to hypothesize that differences in granuloma morphology can be useful in developing new prognostic indicators of disease progression. Greater appreciation of natural infections may facilitate the development of better control strategies including the use of chemotherapeutic agents and vaccines.

To this end, lung tissue from adult European badgers (*Meles meles*), New Zealand brushtail possums (*Trichosurus vulpecula*), and Holstein dairy cows (*Bos taurus*) that had had a primary *M.bovis* infection via either experimental or natural means were examined histopathologically. Significant differences between these species and the mouse and guinea pig laboratory models of *M. tuberculosis* infection were recorded and then further compared to reported human data. Special attention was paid to the intragranuloma lymphocyte arrangement and the overall morphology of the granulomas.

Specific species differences were found. The badger consistently had a florid granulomatous bronchitis, in addition to parenchymal granulomas that had lymphocyte arrangement and lack of central necrosis similar to C57BL/6 mice. The possum had multifocal granuloma necrosis. The possum and cattle granulomas were characterized by central necrosis, a variably thick fibrous capsule and lymphocytes that were present either as thick sheets at the pericapsular margin or individually, randomly spread throughout. In addition cattle lesions had an abundance of multinucleate giant cells. The possum and cattle granulomas resembled the guinea pig lesions, which in turn had similarities to human lesions. The guinea pig is classically seen as a species that is 'sensitive' to tuberculosis. By extrapolation, perhaps the possum and cattle represent similar scenarios and succumb to infection relatively quickly. The badger in turn may represent an animal that would be classified by some as 'resistant' and harbor the disease for a longer period of time before being seen as a threat to cattle. However, the striking bronchitis is a confounding feature. These animals represent variably useful pathological correlates to man. Further work to see how these granulomas are modified in the vaccinated animals should be explored.

Materials and Methods

Collection of lung tissue

Representative photographs of the chronic lesions were collected from each species that was to be examined histopathologically. Samples of diseased lung were collected at necropsy from a total of eleven wild adult male and female European Badgers (*Meles meles*), six experimental adult male and female New Zealand brushtail possums (*Trichosurus vulpecula*) and eleven experimental adult female Friesian-cross cows (*Bos taurus*). The badgers had been snared under licence. All were part of the East Offaly Badger Project in county Offaly, Ireland (1999 - 2000). The possums and cows were housed at the Wallaceville Animal Research Center, Ward Street, Upper Hutt, New Zealand. As part of a *M.bovis* vaccine trial, each possum had been infected via the aerosol route with 20-100 colony forming units of *M.bovis* strain WAg 201 (that was originally isolated form a wild tuberculous possum in New Zealand) and were euthanized 55-57 days later. The cows had been purchased at approximately 6 months old, and were obtained from tuberculosis-free accredited herds from an area of New Zealand where both farmed and feral animals were free of tuberculosis. All the cows were part of a *M.bovis* vaccine trial (10). Prior to the experiment, the cattle tested negative for reactivity to bovine PPD in the whole-blood IFN- assay (9). The cattle were grazed on pasture in an isolation unit. They had been challenged intratracheally with $5x10^3$ *M.bovis* strain WAg 201 and euthanized 17 weeks later. For each species, the lesions that were selected for histopathological examination represented those typical of tuberculosis. Images of human lesions were kindly donated by Dr. Lee from the Asan Medical Center, Soeul South Korea.

Results

Gross lesions

Figure 5.1 compares the macroscopic lesions of chronic tuberculosis in the six species. In each, the granulomas were typically spherical, pale-tan and with a multifocal / miliary distribution. In the mouse (A), granulomas had a maximum diameter of approximately 2mm with no obvious caseation. Guinea pig (B) granulomas reached approximately 5mm in diameter and often had a white (mineralized) necrotic core. The badger granulomas (C) were relatively small reaching a maximum of approximately 1cm and with limited necrosis. The possum (D), had lesions of a similar size to the badger but with necrosis. Cattle granulomas (E) were often composed of multiple small caseous granulomata within a larger focus. The human lesion depicted in (F) is of a single granuloma with a caseous core. The brown and black mottling to the parenchyma is suggestive of extreme carbon deposition from a history of smoking.

Comparative granuloma histology

Tables 5.1 to 5.3 and figures 5.2 and 5.3 characterize the principal histologic features in the granulomas of the various species. The lesions were scored on a + to +++ scale as an indicator of perceived prevalence - indicates an absence of that feature. For each lesion, an examination was performed at least three times in a randomized, blinded fashion. All tissues examined were found to contain acid fast bacilli, but no assessment of bacillary load was attempted. At the bottom of each table is a list of additional important morphological features. Table 5.4 attempts to highlight the important histomorphological differences between these species.

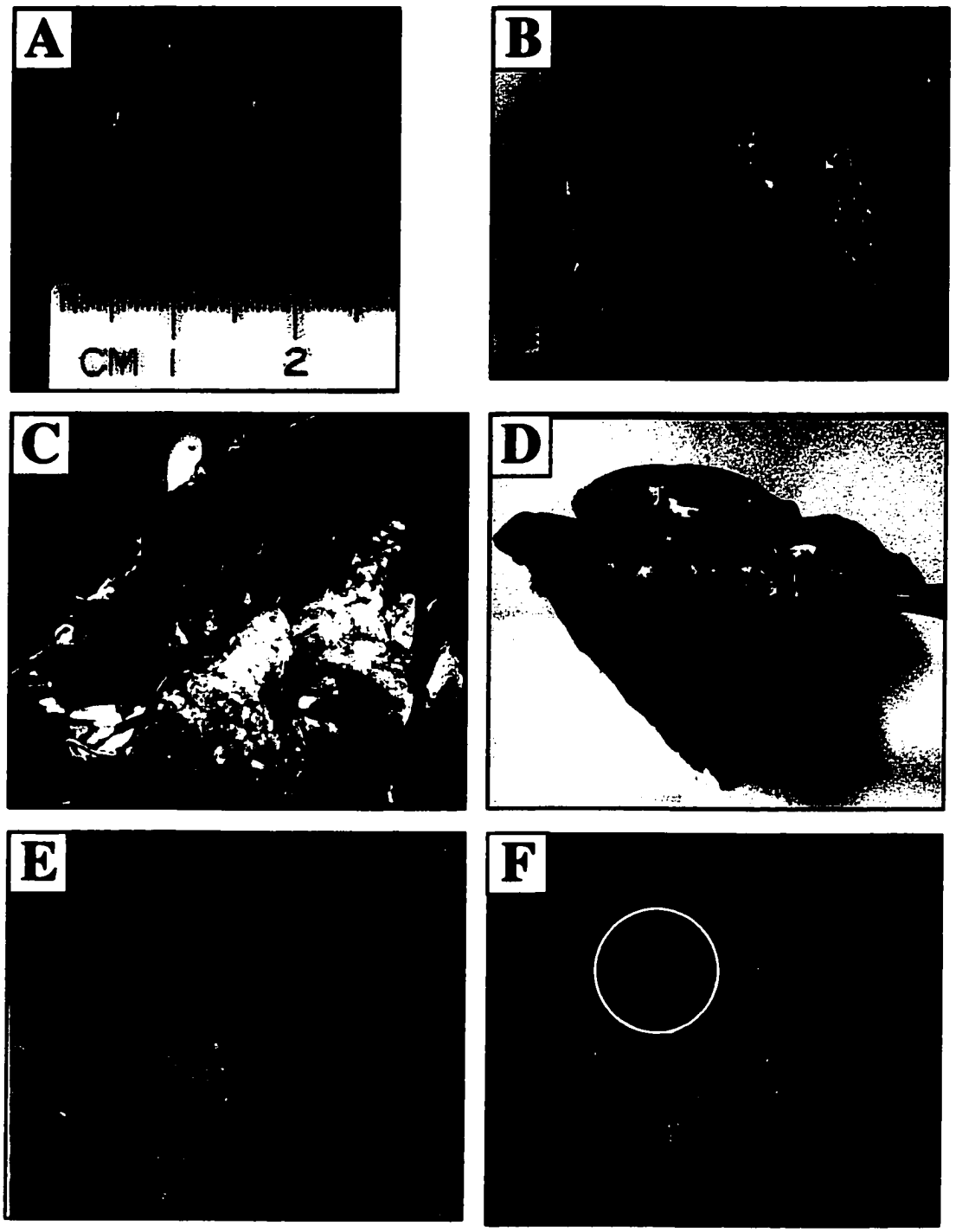

Figure 5.1.
Representative photographs of gross lesions of pulmonary tuberculosis.
A. C57BL/6 Mouse: *Mus musculus*, B. Hartley guinea pig: *Cavia porcellus* C. European badger: *Meles meles*. D.Brushtail possum: *Trichosurus vulpecula* E. Holstein cow: *Bos taurus*.
F. Human: *Homo sapiens*.Granulomas are Indicated by arrows or black / white circles.

Table 5.1

Histopathological comparison of granulomas in adult cattle experimentally infected with *M.bovis* (Tissue from *M.bovis* vaccine trial, Wallaceville, New Zealand)

Animal #	Necrosis	Mineralization	Giant cells	Neutrophils	Lymphocytes
2	+++	++	+	++	++
6	+++	++	+	++	++
8	+++	++	++	++	++
9	+++	+++	++	+	++
10	+++	+++	++	++	+++
12	+++	++	+++	+	+++
41	+++	++	+	++	++
43	++	++	+++	+	+++
62	+++	++	+	++	++
72	+++	++	+	+	++
85	+	+	++	+	+++

Other Morphological features of each granuloma

- Multilobular, coalescing, expansile, targetoid (Figure 5.2 E)
- Thick fibrous capsules
- Neutrophils at interface of necrosis and lymphocytes
- Marginated lymphocytes - beneath capsule - scattered as individual cells or as thick sheets
- Lymphocytes and giant cells often mixed in thick sheets (Figure 5.3 E)

Table 5.2

Histopathological comparison of granulomas in adult European badgers naturally infected with *M.bovis* (Tissue from East Offaly Badger Project. Co Offaly, Ireland)

Animal #	M/F	Mass (kg)	Necrosis	Mineral	GC	Neutrophils	Lymphocytes
92	F	7.3	+	+	_	+++	++
101	F	101	+	_	_	+	+
109	F	10.0	++	_	_	+	+++
122	M	11.0	+	_	_	+	++
146	M	10.4	+	_	_	++	++
224	F	9.3	+	_	_	++	++
227	F	10.0	++	_	_	+	++
258	F	8.1	+	_	_	+	+
279	F	8.0	+	_	_	+	++
356	M	8.5	+	_	+	+	++
436	M	8.0	+	_	_	++	++

M/F = male / female, GC = giant cells

Other Morphological features of each granuloma

- Severe granulomatous bronchitis, with granulomatous inflammation expanding the submucosa and necrotic cellular and suppurative debris variably filling airway lumens (Figure 5.2C).
- Lymphocytes are arranged around margins and dissecting through granulomas with limited perivascular and peribronchiolar involvement (Figure 5.3C).
- Neutrophils have a central predilection
- Occasional thrombosis
- Variable edema , hemorrhage
- Thin fibrous capsules, fibroplasia within granulomata
- Variable hemosiderin deposition and accumulation of hemosiderin laden macrophages
- Multilobular granulomas

Table 5.3

Histopathological comparison of granulomas in adult brushtail possums experimentally infected with *M.bovis* (Tissue from *M.bovis* vaccine trial, Wallaceville, New Zealand)

Animal #	Necrosis	Mineral	GC	Neutrophils	Lymphocytes
1	+++	–	–	++	+++
5	+++	–	–	++	+++
13	+++	–	–	++	++
17	+++	–	–	+++	++
20	++	–	–	+	++
21	+++	–	–	+	+

GC = giant cells

Other Morphological features of each granuloma

- Expansile granuloma with thin fibrous capsule (Figure 5.2 D)
- Lymphocytes spread throughout lesion. Some (minimal) perivasular and peribronchiolar distribution, within and away from the granuloma (Figure 5.3 D)

Table 5.4
Summary of comparative histopathological examination of chronic tuberculous lesions

Species Animal / Mycobacteria	Significant species specific differences in chronic granulomas
C57BL/6 Mice *M. tuberculosis*	Subpleural wedges. Multifocal lymphocyte aggregates. Patchy necrosis.
Hartley Guinea Pig *M. tuberculosis*	Coalescing targetoid lesions with rim of lymphocytes and fibroplasia and central necrosis,
Badger *M.bovis*	Granulomatous bronchitis with parenchymal granulomas characterized by multifocal lymphocyte aggregates and patchy necrosis
Possum *M.bovis*	Pleural and parenchymal lesions with variably thick fibrous capsule. Scattered lymphocytes, multifocal necrosis
Cattle *M.bovis*	Pleural and parenchymal lesions variably thick fibrous capsule, multiple giant cells. Scattered and subcapsular lymphocytes. Central necrosis with mineralization.
Human *M. tuberculosis*	Subpleural and parenchymal lesions. Central necrosis and a thin rim of lymphocytes

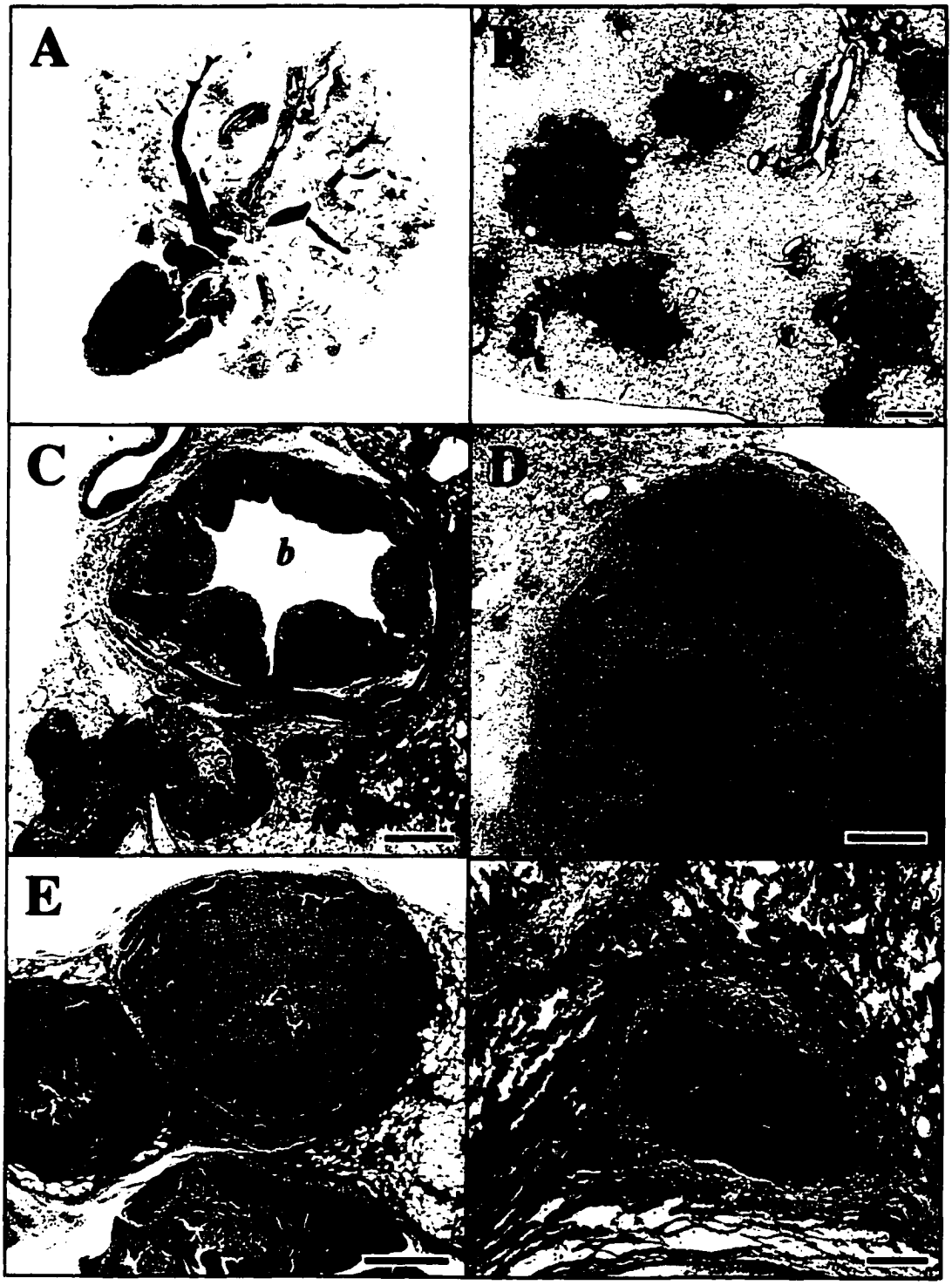

Figure 5.2
Representative low magnification photomicrographs of plumonary tuberculosis.
A. C57BL/6 Mouse: *Mus musculus,h* = heart. B. Hartley guinea pig: *Cavia porcellus* C. European Badger: *Meles meles*, *b*= bronchi, * =*sub*mucosa. D. Brushtail Possum: *Trichosurus vulpecula*. E. Holstein cow: *Bos taurus*. F. Human: *Homo sapiens*.In each case, *c*=necrotic core. Bar = 100um.

Figure 5.3
Representative high magnification photomicrographs of plumonary tuberculosis
A. C57BL/6 Mouse: *Mus musculus*, arrow = lymphocytes. B. Hartley guinea pig: *Cavia porcellus*
C. European badger: *Meles meles*, *n* = neutrophils, arrow = lymphocytes, arrow head = hemosiderin laden macrophages. D. Bryshtail possum: *Trichosurus vulpecula* E. Holstein cow: *Bos taurus*, arrows = multinucleated giant cells (Langhans type). F. Human: *Homo sapiens*.
In each case, *c*=necrotic core. Bar = 100um.

Discussion

The array of immunomorphologic patterns of pulmonary tuberculosis seen in these different mammals is striking. Any definitive statements on pathogenesis and hence epidemiology, however, is extremely difficult with such a limited data set. Also, the differences in the routes of infection and the strain and dose of bacilli used will affect the outcome (4) Nevertheless, it is worth considering a few points further.

The badger typically has a dramatic granulomatous bronchitis with the lumen of many of the larger airways filled with necrotic suppurative debris. This was a feature that was unique to the badger lesions, however, the author has noted similar lesions in the lungs of a tuberculous Asian elephant. Francis showed that a bronchogenic tuberculosis could be produced by intratracheal infection of dogs (4). It may represent a particularly florid expansion or infection of broncho-associated lymphoid tissue or a correlate of the extension of infection along lymphatic vessels as previously observed in C57BL/6 mice. It is possible that the bronchial lesions seed the parenchyma. A controlled time-course study would help resolve this issue. Whether these lesions result in increased release of bacilli as aerosol or sputum should also be investigated. In addition, the parenchymal granulomas of badgers had a morphology similar in some regards to those seen in C57BL/6 mice; particularly, the scattered aggregates of lymphocytes within the accumulation of epithelioid macrophages and limited necrosis. The arrangement of lymphocytes close to macrophages may allow for greater macrophage activation and hence mycobacterial killing (8). Could the badger represent an animal that is able to control bacterial proliferation and have a relatively prolonged disease time course?

Perhaps then it may only present a threat to cattle in chronic stages of disease when lesions might be degenerating.

The possum and cow lesions had similarities to those found in the laboratory guinea pig. In particular, the unitized, targetoid, expansile morphology with a variably thick fibrous capsule and prominent central necrosis. Along with these features, the accumulation of lymphocytes either around the margin of the lesion or diffusely scattered around the necrotic areas find similarities in the human lesions. Is it possible then that the possum and the cow have a reduced ability to control bacterial growth as is seen in the guinea pig, and the disease course is somewhat short? Perhaps the possum represents a greater relative threat to the cow than the badger. The development of giant cells and fibrosis are often considered to be correlated with resistance. In these studies it is not possible to comment on resistance, but it was interesting to note the paucity of giant cells in all species apart from the cattle.

It is interesting that in the model proposed by Francis (4) guinea pigs, cattle and humans are found in the two groups representing the most susceptible species and mice in the relatively resistant species. On the strength of the histopathological data in this study possums could be placed with cattle and badgers with mice. Francis concluded that all the main features of human tuberculosis could be reproduced in the guinea pig, and because of its convenience it is the animal of choice in studies on the pathology, and except for preliminary screening tests, the chemotherapy of tuberculosis.

The foregoing results are indeed interesting, but care should be taken not to over interpret. There are many factors that to influence tuberculosis pathogenesis, however, the novel appreciation of lymphocyte arrangement and overall morphology should be considered in any future pathological study.

Acknowledgements

The author wishes to graciously thank Drs E. Gormley and D. Collins for the visit to the Dublin University Veterinary School, the involvement in the Badger vaccine project and the supply of gross images. The author also extends his sincere thanks to Drs B. Buddle and B. Vesosky for the supply of possum and cattle tissue and images, and to Drs Shim and Lee from the Asan Medical Center, Soeul South Korea, for the supply of human images.

References

1. **Barlow, N. D.** 1994. Bovine tuberculosis in New Zealand: epidemiology and models. Trends Microbiol. **2:**119-24.

2. **Buddle, B. M., M. A. Skinner, and M. A. Chambers.** 2000. Immunological approaches to the control of tuberculosis in wildlife reservoirs. Vet Immunol Immunopathol. **74:**1-16.

3. **Cosivi, O., J. M. Grange, C. J. Daborn, M. C. Raviglione, T. Fujikura, D. Cousins, R. A. Robinson, H. F. Huchzermeyer, I. de Kantor, and F. X. Meslin.** 1998. Zoonotic tuberculosis due to *Mycobacterium bovis* in developing countries. Emerg Infect Dis. **4:**59-70.

4. **Francis, J.** 1958. Tuberculosis in Animals and Man: A study in Comparative Pathology. Cassell and co., London, England.

5. **Karlson, A. G.** 1960. Tubrculosis caused by human, bovine and avian tubercle bacilli in various animals. Proc. U.S. Livestock Sanitary Assoc. **64:**194-201.

6. **Masood, E.** 1998. Outcry as 'scientific' badger cull is launched to target TB. Nature. **394:**821.

7. **Moda, G., C. J. Daborn, J. M. Grange, and O. Cosivi.** 1996. The zoonotic importance of *Mycobacterium bovis*. Tuber Lung Dis. **77:**103-8.

8. **Orme, I. M.** 1998. The immunopathogenesis of tuberculosis: a new working hypothesis. Trends Microbiol. **6:**94-7.

9. **Rothel, J. S., S. L. Jones, L. A. Corner, J. C. Cox, and P. R. Wood.** 1990. A sandwich enzyme immunoassay for bovine interferon-gamma and its use for the detection of tuberculosis in cattle. Aust Vet J. **67:**134-7.

10. **Wedlock, D. N., B. Vesosky, M. A. Skinner, G. W. de Lisle, I. M. Orme, and B. M. Buddle.** 2000. Vaccination of cattle with *Mycobacterium bovis* culture filtrate proteins and interleukin-2 for protection against bovine tuberculosis. Infect Immun. **68:**5809-15.

Chapter Six

Conclusions

In these studies, I have shown that the specific arrangement and number of leukocyte subsets within pulmonary tuberculosis granulomas, and the overall morphology of the lesion, can differ markedly both within and between individual mammalian species. I would contend, therefore, that both factors dramatically influence disease progression.

Granulomagenesis is obviously a highly complex multilayered phenomenon that cannot be fully appreciated at this time. Nevertheless, the results of this work suggests novel hypotheses which taken together may allow for further dissection of the immunopathology of tuberculosis in the 'arrest and reactivate' and 'progressive' disease states of man I have discussed above.

Figure 6.1 is a working schematic of pulmonary granulomagenesis that has been developed principally from these mouse and guinea pig studies. It reflects the important immunopathology and highlights the perceived species differences. The letters (a) to (g) define key events where there are known species differences, and the arrows indicate possible variations on the theme in the associated box. The blue and purple text refers to the mouse and guinea pig models respectively. The asterisks define areas in which important information is lacking.

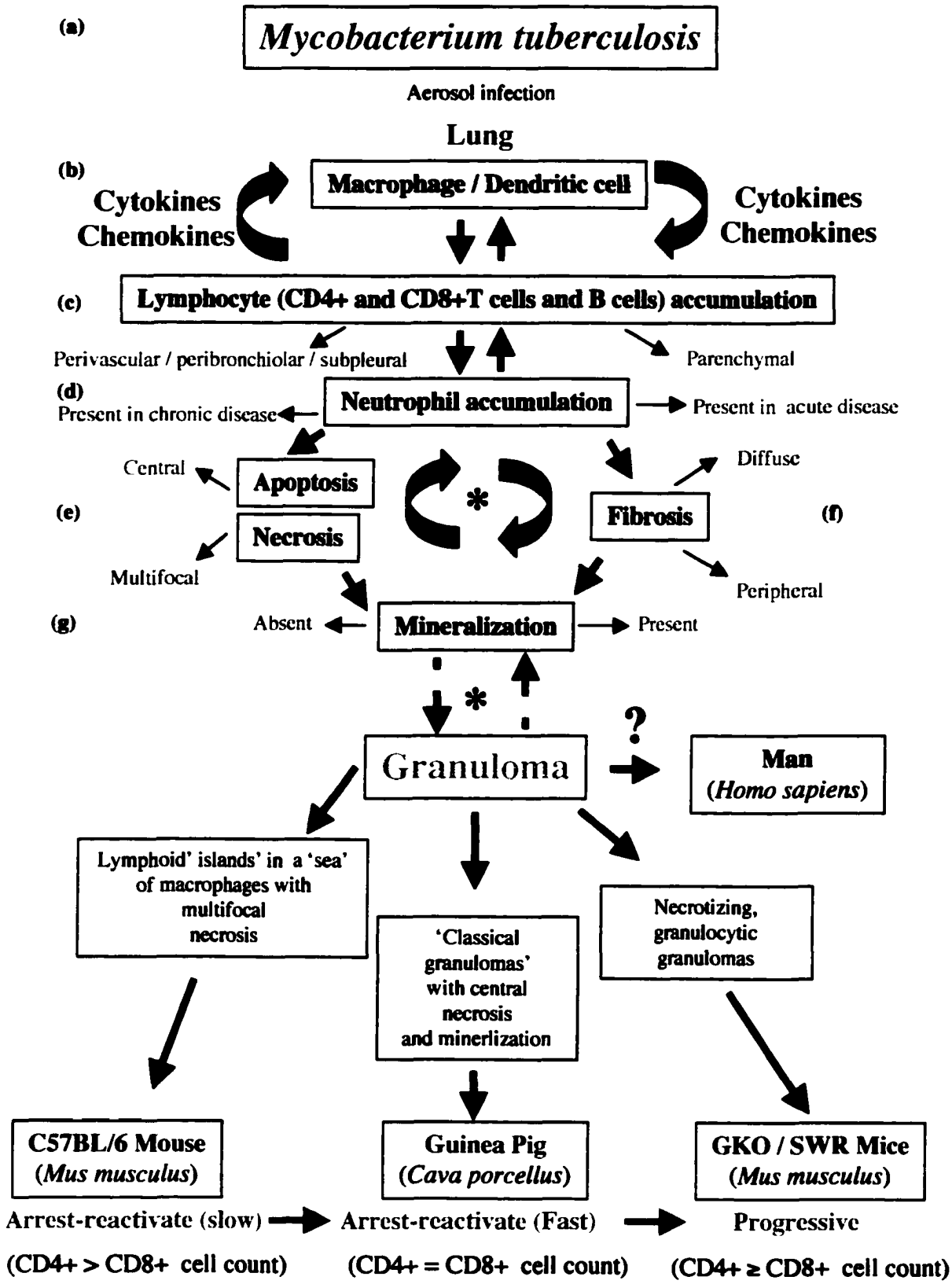

Figure 6.1 Granulomagenesis schematic. * Interplay of multiple factors. ? = Still to be fully defined

After aerosol infection (a) with *M.tuberculosis* and the phagocytosis of bacilli by alveolar macrophages and/or dendritic cells (b), there is an elaborate cascade of cytokines and chemokines that drives the recruitment, activation and proliferation of immune cells. The accumulation of lymphocytes (c), in or around the lesions is an attempt to activate the epithelioid macrophages to kill the bacilli. In our animal models this is not completely effective and bacterial numbers start to rise.

In the C57BL/6 mouse, containment of bacterial growth at a stationary level was correlated with a differential, selective distribution of $CD4^+$ and $CD8^+$ T cells within the multifocal lymphocyte aggregates of the granuloma. $CD4^+$ T cells were always found in greater numbers than $CD8^+$ T cells, and the latter were at times marginalized in these foci. In these positions the $CD4^+$ T cells may be important in generating a high focus of IFN-γ or possibly interacting with the many B cells to promote/control their proliferation. $CD8^+$ T cells on the other hand may be acting to sample antigens presented by the apposing macrophages and kill infected cells. This arrangement was consistent through chronic disease, when the granuloma had a large subpleural component, having developed from perivascular and peribronchiolar sites. The granuloma fraction rose slowly from a low level throughout the course of the disease until near death. In contrast, the Guinea pig also contained bacterial growth at a stationary level and had a similar number of $CD4^+$ and $CD8^+$T cells within granulomas. The lesions were of the 'classic granuloma' form with a distinct ring of lymphocytes, typically arising within the parenchyma, and the granuloma fraction increased relatively rapidly throughout the much shorter time course of disease. From this I suggest that guinea pigs do have an immunological mechanism to protect themselves from *M.tuberculosis,* but it is not as

effective as that in the C57BL/6 mice. In short, a similar number of $CD4^+$ and $CD8^+$ T cells in a targetoid, parenchymal granuloma is a deficient way to fight the infection. Or, to emphasize the lymphocyte role, the balance in T cell subset numbers and their specific locale, influences granuloma development and disease progression.

The lymphocyte arrangement in the badger granulomas was akin to that of the C57BL/6 mouse, whereas those of possum, cow and man were more akin to those of the guinea pig. Although admittedly a gross oversimplification, it will be interesting to see in the future whether the arrangement of $CD4^+$ and $CD8^+$ T cells in the granulomas from these wild and farm animals have comparable arrangements.

In the SWR and GKO mice, there was either limited or no halt in bacterial growth in the lung, with a concomitant rise in granuloma fraction. It is well known that the absence of IFN-γ results in a highly destructive, necrotizing granuloma (5, 8). The SWR mice demonstrate that a low percentage of proliferating, and IFNγ producing $CD4^+$ T cells, is also a component of severe extensive pneumonia. I note that this phenomena is well documented in the human AIDS patient (10). The SWR mice also had a low number of $CD4^+$ and $CD8^+$ memory cells at the time when C57BL/6 mice are able to contain bacterial growth, suggesting that SWR mice have reduced T cell antigen recognition or impaired transition to the memory phenotype.

One theory that has been previously proposed is that the arrangement of lymphocytes affects the cytokine gradients within the lesions (12). Therefore, in the guinea pig, with

lymphocytes arranged in a distinct mantle, the macrophages in the center of the granuloma are less likely to become activated compared to more peripherally located cells and so eventually degenerate. In contrast the multiple small islands of lymphocytes in the C57BL/6 mouse results in a more uniform cytokine distribution, so it is more likely that more macrophages are suitably activated.

This theory therefore implies that the ability of an animal to control infection is a reflection of the ability to focus lymphocytes within the centers of the infected areas of the lungs during the early course of the disease. Explanations for this scenario include differential expression of enzymes by T cells that allow them to move through the extracellular matrix, differential T cell chemokine expression and adhesion molecule expression, and differential levels of T cell proliferation within the lesion. It may also be the case that although the T cells are present in the guinea pig, they are not as effective at macrophage activation as those in the C57BL/6 granuloma. Also, by extension, animals that have macrophage dominated lesions die more rapidly from tuberculosis. This was seen with the SWR mice and has been reported with other mouse strains such as DBA/2 and CBA/J (15). Similarly, a prominence of macrophages early in the guinea pig lesions may be another reflection of an ineffective imbalance between innate and acquired immune mechanisms.

The phenotype and location of the T lymphocytes in the granuloma is clearly important to pathogenesis but one must also consider possible roles for the CD45R/B220$^+$ B lymphocytes, macrophages, neutrophils, necrosis and fibrosis. It is perhaps purely

academic to consider them in isolation, rather than as an integrated response, and this is further complicated by the fact that there are important differences in each case.

The prominent clustered arrangement of a significant number of CD45R/B220^{+} lymphocytes in the granulomas of all the mouse strains we examined suggests B cell proliferation and by inference a possible role in pathogenesis. Cells morphologically consistent with plasma cells were found most often at perivascular sites in chronic lesions, suggesting that immunoglobulin production may have been taking place. The role of antibodies in mice however, remains equivocal (2, 3, 14). In the guinea pig, we also observed clusters of cells positive for a Pan B cell marker, within granulomas. It is possible that the antibodies play a role in complement fixation during granulomagenesis. C5 deficient mice for example have recently been shown to have decreased ability to control *M.tuberculosis* growth in the lungs and increased pathology compared to controls (1).

Neutrophils (d) were prominent from a very early stage in the guinea pig granulomas but detected relatively late in the C57BL/6 granulomas, usually alongside areas of necrosis rather than apoptosis (e). In the guinea pig the presence of neutrophils precedes necrosis and indeed may drive the very early granuloma degeneration. This is in contrast to the long held theory of Dannenberg who has suggested an active mechanism based on DTH (6). However, we feel that DTH serves to mediate the attraction of monocytes from the blood into the local site of inflammation, rather than necrosis per se.

The role of apoptosis in granuloma development remains to be determined. In these studies we saw little evidence of apoptosis in the guinea pigs, but there was a suggestion that SWR mice exhibited more than C57BL/6 mice, and GKO mice in turn exhibited more than both of them. Klingler and colleagues have demonstrated that apoptosis associated with tuberculosis is mediated through a downregulation of bcl-2, an inhibitor of programmed cell death (9). Molloy and coworkers have shown that apoptosis of macrophages results in reduced viability of mycobacteria contained within (11). A very complex system thus governs cell death. Further study detecting specific apoptotic markers, such as caspases is warranted (13).

In the GKO mouse, neutrophils and eosinophils were present in the lesions very early, and in the SWR mice also, indicating that the presence of polymorphs was a relatively early phenomenon in mice unable to contain bacterial growth. Both of these mice strains should be considered as examples of the 'progressive' pathology in man. The early influence of neutrophils (and or eosinophils) may thus signal a disease process that will be more rapid and ultimately destructive to the lung tissue. They may by themselves mediate destructive changes through release of their cytoplasmic granules, or, they may interfere with macrophage activation and produce an environment which promotes bacterial growth. In man, the presence of neutrophils is also thought to be an early phenomenon, but we do not know the relative amounts in the individual lesions (1)

The production and deposition of collagen (f) is a process that demands more attention in granulomagenesis. The growing notion of fibroblasts and other stromal cells being

actively involved in the immune response (4), rather than simply responding as repair/healing elements, may become a very interesting issue for tuberculosis pathogenesis. The guinea pig and GKO mice produced granulomas that had distinct fibrous capsules. This was also present in the cattle and possum lesions and, to a lesser extent in man. This may simply reflect attemptive repair mechanisms and the instruction to 'wall off' the infection, but why is it not present in the C57BL/6 mouse, the SWR mouse and the badger? It may again reflect the presence of and position of certain lymphocyte phenotypes and the secretion of particular fibrinogenic cytokines or the speed with which the lesion develops.

In some mammals, the chronic lesion mineralizes (g) and in others, including man, it will liquefy and then ultimately cavitate. Liquefaction and cavitation were not observed in any of these studies however, mineralization was present in guinea pig and bovine lesions, was less significant in human and possum lesions and was not observed in the other species. The factors that govern these processes are still poorly understood. It could be hypothesized that the presence of these lesions is indicative of 'progressive', ultimately fatal disease.

In Figure 6.1, one of the asterisks is surrounded by neutrophil accumulation, apoptosis / necrosis, fibrosis and mineralization. The relative temporal and spatial contribution of these along with the lymphocyte accumulation to the granuloma formation is ultimately still unknown. Nevertheless, these studies have shown that with a granuloma made up of ($CD4^+$ numbers >$CD8^+$) lymphocyte 'islands' in a 'sea' of macrophages with multifocal

necrosis, arrest of bacteria growth is maintained for a relatively long period of time. In a 'classic granuloma' however, with an outer mantle of lymphocytes ($CD4^+$ numbers=$CD8^+$), central necrosis and mineralization, arrest of bacterial growth is maintained for only a relatively short time. With a rapidly growing, pyogenic, necrotizing granuloma where all lymphocyte subsets ($CD4^+$numbers≥$CD8^+$) are peripheralized, progression of disease will be rapid.

Where man fits in to this is still a matter of great debate. It is clear that humans can behave differently from the mouse and the guinea pig when confronted with *M.tuberculosis.* Infected humans present with a variety of granuloma forms, reflecting different immunopathological scenarios. It is thought that most humans cure the infection, but no studies to date have determined the number of bacilli in the lungs of infected human over time. Clearly the number of bacilli and inherent virulence factors are key factors in driving pathogenesis, but how they each relate to granulomagenesis remains to be seen. More information is required to define the actions of cytokines on granuloma formation and collagen metabolism on a molecular basis. Furthermore, it is easy to anticipate that the development of potential immunosuppressive strategies to inhibit cytokine activity will be a major challenge to researchers involved in the clinical management of patients.

I believe that studies on the pathogenesis of pulmonary tuberculosis that could follow my present work should concentrate on the following areas:

1. An investigation into the antigen specificity of the T cells within the granuloma
2. An investigation of the cytokine melieu in the developing granuloma
3. A stereological investigation into the progression of tuberculosis in these animals models
4. How vaccination alters the temporal and spatial arrangement of important lymphocyte subsets.

Increased attention to this disease and the integration of animal models and human studies has afforded us a greater understanding of tuberculosis and the steps necessary to combat this infection. The pace of this research must be maintained if we are to realize an effective vaccine in the next decade.

Dubos: from 'The White Plague: Tuberculosis, Man and Society', 1952 (7)

"Elucidation of the mechanisms of tuberculosis disease will long continue to require analysis by the methods of medical sciences. And the case of the stricken tuberculosis patient calls upon all the resources of medical practice. But the complete control of tuberculosis in society goes beyond medicine in its limited sense. It is a problem in social technology."

References

1. **Actor, J. K., E. Breij, R. A. Wetsel, H. Hoffmann, R. L. Hunter, Jr., and C. Jagannath.** 2001. A role for complement C5 in organism containment and granulomatous response during murine tuberculosis. Scand J Immunol. **53:**464-74.

2. **Bosio, C. M., and K. L. Elkins.** 2001. Susceptibility to secondary *Francisella tularensis* live vaccine strain infection in B-cell-deficient mice is associated with neutrophilia but not with defects in specific T-cell-mediated immunity. Infect Immun. **69:**194-203.

3. **Bosio, C. M., D. Gardner, and K. L. Elkins.** 2000. Infection of B cell-deficient mice with CDC 1551, a clinical isolate of *Mycobacterium tuberculosis*: delay in dissemination and development of lung pathology. J Immunol. **164:**6417-25.

4. **Buckley, C. D., D. Pilling, J. M. Lord, A. N. Akbar, D. Scheel-Toellner, and M. Salmon.** 2001. Fibroblasts regulate the switch from acute resolving to chronic persistent inflammation. Trends Immunol. **22:**199-204.

5. **Cooper, A. M., D. K. Dalton, T. A. Stewart, J. P. Griffin, D. G. Russell, and I. M. Orme.** 1993. Disseminated tuberculosis in interferon gamma gene-disrupted mice. J Exp Med. **178:**2243-7.

6. **Dannenberg, A. M., Jr.** 1993. Immunopathogenesis of pulmonary tuberculosis. Hosp Pract (Off Ed). **28:**51-8.

7. **Dubos, R. a. D., J.** 1952. Tuberculosis, Man, and Society: The Whte Plague. Little, Brown and Co, Boston.

8. **Flynn, J. L., J. Chan, K. J. Triebold, D. K. Dalton, T. A. Stewart, and B. R. Bloom.** 1993. An essential role for interferon gamma in resistance to *Mycobacterium tuberculosis* infection. J Exp Med. **178:**2249-54.

9. **Klingler, K., K. M. Tchou-Wong, O. Brandli, C. Aston, R. Kim, C. Chi, and W. N. Rom.** 1997. Effects of mycobacteria on regulation of apoptosis in mononuclear phagocytes. Infect Immun. **65:**5272-8.

10. **Margolick, J. B., and A. D. Donnenberg.** 1997. T-cell homeostasis in HIV-1 infection. Semin Immunol. **9:**381-8.

11. **Molloy, A., P. Laochumroonvorapong, and G. Kaplan.** 1994. Apoptosis, but not necrosis, of infected monocytes is coupled with killing of intracellular Bacillus Calmette-Guerin. J Exp Med. **180:**1499-1509.

12. **Orme, I. M.** 1998. The immunopathogenesis of tuberculosis: a new working hypothesis. Trends Microbiol. **6:**94-7.

13. **Stadelmann, C., and H. Lassmann.** 2000. Detection of apoptosis in tissue sections. Cell Tissue Res. **301:**19-31.

14. **Turner, J., A. A. Frank, J. V. Brooks, M. Gonzalez-Juarrero, and I. M. Orme.** 2001. The progression of chronic tuberculosis in the mouse does not require the participation of B lymphocytes or interleukin-4. Exp Gerontol. **36:**537-45.

15. **Turner, J., M. Gonzalez-Juarrero, B. M. Saunders, J. V. Brooks, P. Marietta, D. L. Ellis, A. A. Frank, A. M. Cooper, and I. M. Orme.** 2001. Immunological basis for reactivation of tuberculosis in mice. Infect Immun. **69:**3264-70.

Appendices

Appendix 1

PUBLICATIONS

Part of the work described in this dissertation has resulted in the following publications:

1. **Sousa, A. O., R. J. Mazzaccaro, R. G. Russell, F. K. Lee, O. C. Turner, S. Hong, L. Van Kaer, and B. R. Bloom.** 2000. Relative contributions of distinct MHC class I-dependent cell populations in protection to tuberculosis infection in mice. Proc Natl Acad Sci U S A. **97:**4204-8.

2. **Turner, O. C., A. D. Roberts, A. A. Frank, S. W. Phalen, D. M. McMurray, J. Content, O. Denis, S. D'Souza, A. Tanghe, K. Huygen, and I. M. Orme.** 2000. Lack of protection in mice and necrotizing bronchointerstitial pneumonia with bronchiolitis in guinea pigs immunized with vaccines directed against the hsp60 molecule of *Mycobacterium tuberculosis*. Infect Immun. **68:**3674-9.

3. **Gonzalez-Juarrero, M., O. C. Turner, J. Turner, P. Marietta, J. V. Brooks, and I. M. Orme.** 2001. Temporal and spatial arrangement of lymphocytes within lung granulomas induced by aerosol infection with *Mycobacterium tuberculosis*. Infect Immun. **69:**1722-8

4. **Turner, O. C., Sugawara, H. Yamada, B. Cummings, and I. M. Orme.** 2001. Crystalloid inclusions in the cytoplasm of alveolar macrophages of the SwR/J mouse. A possible cause of susceptibility to mycobacterium tuberculosis? J Submicrosc Cytol Pathol. **33:**217-9.